MATHEMATICAL MODELLING OF CHLORIDE INGRESS INTO CONCRETE AND ELECTROCHEMATICAL CHLORIDE REMOVAL FROM CONCRETE

Yu Wang, BEng, MSc

Doctor of Philosophy

ASTON UNIVERSITY IN BIRMINGHAM

March 2001

Aston University in Birmingham

MATHEMATICAL MODELLING OF CHLORIDE INGRESS INTO CONCRETE AND ELECTROCHEMATICAL CHLORIDE REMOVAL FROM CONCRETE

Yu Wang, BEng, MSc

Thesis submitted for the degree of Doctor of Philosophy

2001

ABSTRACT

This thesis presents a comprehensive mathematical model for simulating the transport behaviour of ions in porous media, which is then applied to predict the mass transport associated with chloride ingress into concrete or hydrated cement paste and electrochemical chloride removal from concrete. Compared with the other previous work, this study proposes an improvement for the mathematical governing equation, which includes most of the main factors affecting the two processes.

Numerical results are compared with experimental measurements. Effects of the degree of saturation of the concrete, ionic interaction, chloride binding on the process of chloride ingress and effects of externally applied current density, treating period, as well as the chloride binding on the effectiveness and efficiency of electrochemical chloride removal are discussed.

Chloride binding has a significant influence on the chloride distribution in the chloride ingress into concrete and electrochemical chloride removal from concrete processes. In the view of that, a special investigation is carried on the issue about the model of chloride binding.

Standard finite element methods are used to solve the mathematical governing equation. In the case of electrochemical chloride removal, however, the standard finite element methods have a limitation, which only can be successfully used to analyse the treatment with constant current densities on the surfaces of cathode and anode. For the treatment having a constant electrical potential gradient between cathode and anode, the standard finite element methods cannot give out a stable solution as the Peclet number is greater than 1 near the electrodes. In order to facilitate the use of the FE programme developed, a pre- and a postprocessor are also developed. These processors have a friendly, interactive graphic user interface, which makes the programme easily to be handled.

Key Words: Chloride Induced Corrosion, Concrete Structure, Saturation of Porous Material, Ionic Transport, FEM.

Dedicated to

My father

My mother in ground

My wife

My hometown, Chongqing, P.R. China

Papers completed in the period of study:

1. A Two-dimensional Model Of Electrochemical Chloride Removal From Concrete

   Wang, Y., Li, L.Y. and Page, C.L., *Computational Materials Science*, Vol. 20, No. 2, 2001, pp. 196-212.

2. Efficiency Investigation Of Chloride Removal From Concrete By Using An Electrochemical Method

   Wang, Y., Li, L.Y. and Page, C.L., Concrete Communication Conference 2000, *The 10th BCA Annual Conference on High Education and The Concrete Industry*, 29-30 June 2000, Birmingham University, UK

3. An Interactive Software For Finite Element Analysis Of Ionic Transport In Electrolyte Solutions

   Wang, Y., Li, L.Y. and Page, C.L., *199th Meeting of The Electrochemical Society*, Washington, DC, 25-31 March 2001

4. Numerical Analysis Of The Ionic Transference Numbers In The Process Of Electrochemical Chloride Removal

   Wang, Y., Li, L.Y. and Page, C.L., Paper prepared for *Cement and Concrete Research*

5. Mathematical Modelling Of Chloride Ingress Into Concrete From A Saline Environment With The Effects Of Ionic Coupling And Capillary Suction Of Solution

   Wang, Y., Li, L.Y. and Page, C.L., Paper prepared for *ACI Materials Journal*

6. A Chloride Binding Relationship For The Process Of Electrochemical Chloride Removal From Concrete

   Wang, Y., Li, L.Y. and Page, C.L., Paper prepared for publication

ACKNOWLEDGEMENTS

The author is deeply indebted to Dr. L.Y. Li and Professor C.L. Page, under whose supervision this research project was conducted, and whose knowledge, expertise, guidance and support are greatly appreciated. Special appreciations are to Dr. Li's guidance on mathematical modelling and Prof. C.L. Page's guidance on the principles of corrosion and chemical reaction theory. The author believes that it is impossible to complete this study so smoothly without the help from them.

Thanks also to the technical staff, Robert Poole, for his assistance on the computer work.

I would like to thank my friends and colleagues, Dr. L.F. Lui, Dr. Y.D. Yuang, Bahjat Khalafallah, C.Y. Wu, and Dr. R.T. Tenchev, for their encouragements, stimulating discussions, light chat, creation of a friendly working environment during the course of this research and all the other helps from them.

Finally, I would like to say a big 'thank you' to my wife for her understanding and support on my pursuing my objectives for many years.

The study is financed by the Oversea Research Scheme of the CVCP and the Department of Civil Engineering, Aston University.

CONTENTS

PAGE

ABSTRACT 2
ACKNOWLEDGEMENTS 5
CONTENTS 6
LIST OF TABLES 10
LIST OF FIGURES 11
NOMENCLATURE 17

CHAPTER 1 INTRODUCTION

1.1 BACKGROUND OF THE PROJECT 19
1.2 PURPOSE OF THE STUDY 21
1.3 LAYOUT OF THE THESIS 22

CHAPTER 2 LITERATURE REVIEW

2.1 INTRODUCTION 23
2.2 PRINCIPLES OF CORROSION 23
2.2.1 Thermodynamics Of Corrosion 23
2.2.2 Electrochemical Kinetics Of Corrosion 26
2.2.3 Passivity 26
2.3 MECHANISMS OF STEEL CORROSION IN CONCRETE 28
2.3.1 Concrete Materials 28
2.3.2 Aggregates, Admixtures And Pore Structure 30
2.3.3 Pore Solution Phase Composition Of Cement Materials 31
2.3.4 The Corrosion Of Steel In Concrete 32
2.4 THE ROLE OF CHLORIDE IN THE CORROSION OF STEEL IN CONCRETE. 34
2.4.1 Effect On Pitting Initiation 34
2.4.2 Effect On The Interface Of Passive Film/Solution 35
2.4.3 Effect On Passive Film 36
2.4.4 Effect On Steel (Propagation Of Pitting) 36

2.4.5 Threshold Chloride Concentrations In Concrete 37
2.5 THE TRANSPORT OF CHLORIDE IONS IN CONCRETE 38
2.5.1 Transport Mechanisms 39
2.5.2 Chloride Binding 39
2.6 PREVENTION AND REHABILITATION TECHNIQUES FOR CHLORIDE INDUCED CORROSION 42
2.6.1 Concrete Modification 42
2.6.2 Surface Treatment 43
2.6.3 Patch Repair 44
2.6.4 Cathodic Protection 45
2.6.5 Electrochemical Chloride Removal 46
2.7 MODELLING OF CHLORIDE TRANSPORT IN CONCRETE 48
2.7.1 Modelling Of Chloride Ingress Into Concrete 48
2.7.2 Diffusion Coefficient 53
2.7.3 Chloride Binding Isotherm 54
2.7.4 Modelling Of Electrochemical Chloride Removal Process 58

CHAPTER 3 MATHEMATICAL MODELLING OF IONIC TRANSPORT IN CONCRETE

3.1 INTRODUCTION 60
3.2 MATHEMATICAL MODEL OF IONIC TRANSPORT IN ELECTROLYTE 60
3.3 MATHEMATICAL MODEL IN POROUS MEDIA 63
3.4 FINITE ELEMENT ANALYSIS 64
3.5 MODELLING OF ECR 67
3.6 DISCUSIONS 71

CHAPTER 4 MODELLING OF CHLORIDE INGRESS INTO CONCRETE FROM A SALINE ENVIRONMENT

4.1 INTRODUCTION 72
4.2 THE PORE STRUCTURE OF PORTLAND CEMENT AND ITS EFFECTS ON MASS TRANSPORT PROPERTIES 73

4.3 THE THEORY OF WATER TRANSPORT IN POROUS MATERIALS 73
4.4 MODELLING OF CHLORIDE INGRESS INTO CONCRETE 76
4.5 RESULTS AND DISSUSIONS 77
4.6 CONCLUSIONS 80

CHAPTER 5 IONIC REDISTRIBUTION IN THE PROCESS OF ECR

5.1 INTRODUCTION 95
5.2 ONE-DIMENSIONAL MODELLING OF ECR 95
5.2.1 Experiment Simulated 95
5.2.2 Results And Discussions 97
5.3 TWO-DIMENSIONAL MODELLING OF ECR 98
5.3.1 Cases Studied 98
5.3.2 Numerical Results Of The Current Density Distribution 99
5.3.3 Numerical Results Of The Ionic Redistribution 100
5.4 CONCLUSIONS 102

CHAPTER 6 EFFECTIVENESS AND EFFICIENCY INVESTIGATIONS OF ECR

6.1 INTRODUCTION 141
6.2 CASE STUDIES 141
6.3 RESULTS AND DISCUSIONS 142
6.4 CONCLUSIONS 144

CHAPTER 7 CHLORIDE BINDING RELATIONSHIPS

7.1 INTRODUCTION 159
7.2 A NEW CHLORIDE BINDING RELATIONSHIP 161
7.3 MODELLING OF THE EXPERIMENT OF ECR 165
7.3.1 The Experiment 165
7.3.2 Results And Discussions 165

7.4 CONCLUSIONS 167

CHAPTER 8 IONIC TRANSFERENCE NUMBERS IN THE PROCESS OF ECR

8.1 INTRODUCTION 176
8.2 THE FINITE ELEMENT ANALYSIS OF IONIC TRANSFERENCE NUMBERS 177
8.3 RESULTS AND DISCUSSIONS 178
8.4 CONCLUSIONS 181

CHAPTER 9 COMPUTER PROGRAM

9.1 INTRODUCTION 192
9.2 PROGRAM -- FEACER 193
9.3 FUNCTIONS OF THE INTERACTIVE SOFTWARE 196
9.4 CONCLUSIONS 209

CHAPTER 10 GENERAL CONCLUSIONS AND FURTHER WORK

10.1 GENERAL CONCLUSIONS 210
10.2 FURTHER WORK IN DEVELOPMENT 212

REFERENCES 214

LIST OF TABLES

Table.4.1 Parameters and initial data of specimen 81
Table 5.1 Initial concentrations and diffusion coefficients 103
Table 6.1 Initial concentrations and diffusion coefficients 145

LIST OF FIGURES

Fig. 2.1 Hemholtz Plane 24

Fig. 2.2 Schematic active-passive polarisation behaviour 27

Fig. 2.3 Principal hydration reactions of Portland cement minerals 29

Fig. 2.4 Hydroxyl ion concentration ion pore solution of Portland cement pastes of w/c:0.5, cured for 28 days 31

Fig. 2.5 The corrosion reactions on steel 33

Fig. 2.6 Schematic determination of critical pitting potential, E_{pit}, from anodic polarization 35

Fig. 2.7 Schematic of corrosion processes occurring at an active growing pit in iron. 38

Fig. 2.8 Chloride binding capacity of different types of cement 41

Fig. 2.9 Principle of electrochemical chloride extraction 47

Fig. 3.1 Co-ordinates of capillary 63

Fig. 4.1 The calculated percentile volumes of different components in fully hydrated Portland cement pastes prepared with w/c ratio of 0.5 (left) and 0.3 (right) .. 82

Fig. 4.2 Relation between water permeability and w/c for mature hydrated cement pastes 82

Fig. 4.3 Relation between water permeability and curing time hydrated cement pastes (w/c: 0.7) 83

Fig. 4.4 The variation of hydraulic diffusivity with saturation 83

Fig. 4.5 Saturation of pore structure and ionic concentration profiles after 5 minutes exposure to a saline solution ($\theta_0 = 0.8$, $\tau = 1.9$) 84

Fig. 4.6 Ionic concentration profiles after 10 minutes exposure to a saline solution ($\theta_0 = 1.0$, $\tau = 1.9$) 85

Fig. 4.7a Ionic concentration profiles after 100 days exposure to a saline solution ($\theta_0 = 1.0$, $\tau = 1.9$) 86

Fig. 4.7b Total chloride concentration profiles after 100 days exposure to a saline solution ($\theta_0 = 1.0$, $\tau = 1.9$) 87

Fig. 4.7c Comparison of relative errors ($\theta_0 = 1.0$, $\tau = 1.9$) 88

Fig. 4.8a Ionic concentration profiles after 100 days exposure to a saline solution ($\nabla\phi \neq 0$, $\tau = 1.9$) 89
Fig. 4.8b Total chloride concentration profiles after 100 days exposure to a saline solution ($\nabla\phi \neq 0$, $\tau = 1.9$) 90
Fig. 4.8c Comparison of relative errors ($\nabla\phi \neq 0$, $\tau = 1.9$) 91
Fig. 4.9a Chloride concentration profiles predicted by three models 92
Fig. 4.9b Comparison of total chloride concentration profiles 93
Fig. 4.9c Comparison of relative errors in the predictions of three models 94

Fig. 5.1 Arrangement for galvanostatic polarization 103
Fig. 5.2a Ionic concentration profiles in pore solution of cement paste with 1% chloride addition ($I = 0.005$ A/m^2) 104
Fig. 5.2b Ionic concentration profiles in pore solution of cement paste with 1% chloride addition ($I = 0.005$ A/m^2) 105
Fig. 5.3a Ionic concentration profiles in pore solution of cement paste with 1% chloride addition ($I = 1$ A/m^2) 106
Fig. 5.3b Ionic concentration profiles in pore solution of cement paste with 1% chloride addition ($I = 1$ A/m^2) 107
Fig. 5.4a Ionic concentration profiles in pore solution of cement paste with 1% chloride addition ($I = 5$ A/m^2) 108
Fig. 5.4b Ionic concentration profiles in pore solution of cement paste with 1% chloride addition ($I = 5$ A/m^2) 109
Fig. 5.5a Ionic concentration profiles without the consideration of chloride binding ($I = 0.005$ A/m^2) 110
Fig. 5.5b Ionic concentration profiles without the consideration of chloride binding ($I = 0.005$ A/m^2) 111
Fig. 5.6a Ionic concentration profiles without the consideration of chloride binding ($I = 1$ A/m^2) 112
Fig. 5.6b Ionic concentration profiles without the consideration of chloride binding ($I = 1$ A/m^2) 113
Fig. 5.7a Ionic concentration profiles without the consideration of chloride binding ($I = 5$ A/m^2) 114

Fig. 5.7b Ionic concentration profiles without the consideration of chloride binding (I = 5 A/m^2) 115
Fig. 5.8 Two-dimensional cases studied 116
Fig. 5.9 Distributions of potential function ψ and the distribution of their corresponding current densities in case 1 and case 2 117
Fig. 5.10a Ionic concentration profiles after 4 weeks at I = 0.001 A/m^2 in case one 118
Fig. 5.10b Ionic concentration profiles after 8 weeks at I = 0.001 A/m^2 in case one 119
Fig. 5.10c Ionic concentration profiles after 12 weeks for I = 0.001 A/m^2 in case one. 120
Fig. 5.11a Ionic concentration profiles after 4 weeks at I = 0.001 A/m^2 in case two 121
Fig. 5.11b Ionic concentration profiles after 8 weeks at I = 0.001 A/m^2 in case two 122
Fig. 5.11c Ionic concentration profiles after 12 weeks for I = 0.001 A/m^2 in case two. 123
Fig. 5.12a Ionic concentration profiles after 4 weeks at I = 3 A/m^2 in case one 124
Fig. 5.12b Ionic concentration profiles after 8 weeks at I = 3 A/m^2 in case one 125
Fig. 5.12c Ionic concentration profiles after 12 weeks for I = 3 A/m^2 in case one 126
Fig. 5.13a Ionic concentration profiles after 4 weeks at I = 3 A/m^2 in case two 127
Fig. 5.13b Ionic concentration profiles after 8 weeks at I = 3 A/m^2 in case two 128
Fig. 5.13c Ionic concentration profiles after 12 weeks for I = 3 A/m^2 in case two 129
Fig. 5.14a Ionic concentration profiles after 4 weeks at I = 5 A/m^2 in case one 130
Fig. 5.14b Ionic concentration profiles after 8 weeks at I = 5 A/m^2 in case one 131
Fig. 5.14c Ionic concentration profiles after 12 weeks for I = 5 A/m^2 in case one 132
Fig. 5.15a Ionic concentration profiles after 4 weeks at I = 5 A/m^2 in case two 133
Fig. 5.15b Ionic concentration profiles after 8 weeks at I = 5 A/m^2 in case two 134
Fig. 5.15c Ionic concentration profiles after 12 weeks for I = 5 A/m^2 in case two 135
Fig. 5.16 Distributions of free chloride concentrations and pH values in pore solution at the steel surface after 12 weeks in case one 136
Fig. 5.17 Distributions of free chloride concentrations and pH values in pore solution at the steel surface after 12 weeks in case two 137
Fig. 5.18 The variation of average ionic concentrations at the surface of steel cathode in case two subjected to 5 A/m^2 current density 138
Fig. 5.19 The comparison of the chloride removal effectiveness and efficiency at different current densities in two cases 139
Fig. 5.20 The average chloride removed by a unit current per week 140

Fig. 6.1 Case one: all of the reinforcements are connected to a galvanostat.....146
Fig. 6.2 Case two: every steel is connected to its own galvanostat.....146
Fig. 6.3 Case three: each deepest embedded steel is connected to its own galvanostat146
Fig. 6.4 Current density distributions in the three cases 147
Fig. 6.5a Ionic concentration profiles after 4 weeks in case one 148
Fig. 6.5b Ionic concentration profiles after 8 weeks in case one 149
Fig. 6.5c Ionic concentration profiles after 12 weeks in case one 150
Fig. 6.6a Ionic concentration profiles after 4 weeks in case two 151
Fig. 6.6b Ionic concentration profiles after 8 weeks in case two 152
Fig. 6.6c Ionic concentration profiles after 12 weeks in case two 153
Fig. 6.7a Ionic concentration profiles after 4 weeks in case three 154
Fig. 6.7b Ionic concentration profiles after 8 weeks in case three 155
Fig. 6.7c Ionic concentration profiles after 12 weeks in case three 156
Fig. 6.8 Comparison of the effectivenesses of ECR 157
Fig. 6.9 Comparison of the efficiencies of ECR 157
Fig. 6.10 Average chloride concentration at the steel surface for case two 158

Fig. 7.1a Predicted ionic concentration profiles for the experiment of Bertolini et al. (I = 0.005 A/m^2) 168
Fig. 7.1b Predicted ionic concentration profiles for the experiment of Bertolini et al. (I = 0.005 A/m^2) 169
Fig. 7.2a Predicted ionic concentration profiles for the experiment of Bertolini et al. (I = 1 A/m^2) 170
Fig. 7.2b Predicted ionic concentration profiles for the experiment of Bertolini et al. (I = 1 A/m^2) 171
Fig. 7.3 Predicted total chloride content for the experiment of Bertilini et al. (I =1 A/m^2).....172
Fig. 7.4a Predicted ionic concentration profiles for the experiment of Bertolini et al. (I = 5 A/m^2) 173
Fig. 7.4b Predicted ionic concentration profiles for the experiment of Bertolini et al. (I = 5 A/m^2) 174
Fig. 7.5 Predicted total chloride content for the experiment of Bertilini et al. (I = 5 A/m^2).....175

Fig. 8.1a Distribution of ionic transference numbers with the effect of chloride binding (I = 1 A/m^2)....183
Fig. 8.1b Variation of chloride transference number according to the ionic concentrations with the effect of chloride binding (I = 1 A/m^2)....184
Fig. 8.2a Distribution of ionic transference numbers with the effect of chloride binding (I = 5 A/m^2)....185
Fig. 8.2b Variation of chloride transference number according to the ionic concentrations with the effect of chloride binding (I = 5 A/m^2)....186
Fig. 8.3 Variation of chloride transference number according to the *Cl/OH* ratio....187
Fig. 8.4a Distribution of ionic transference numbers without the effect of chloride binding (I = 1 A/m^2)....188
Fig. 8.4b Variation of chloride transference number according to the ionic concentrations without the effect of chloride binding (I = 1 A/m^2)....189
Fig. 8.5a Distribution of ionic transference numbers without the effect of chloride binding (I = 5 A/m^2)....190
Fig. 8.5b Variation of chloride transference number according to the ionic concentrations without the effect of chloride binding (I = 5 A/m^2)....191

Fig. 9.1 Structure and flow-chart of FEAECR....194
Fig. 9.2 Structure and flow-chart of ECRPRO....195
Fig. 9.3 FEA software for ionic transport in electrolyte solution....197
Fig. 9.4 Structure and flowchart of the software....197
Fig. 9.5 Main window....198
Fig. 9.6 Window for editing axes....198
Fig. 9.7 Submenu under the menu of Mesh generation....199
Fig. 9.8 Drawing structure....200
Fig. 9.9 The dialog box for defining line....200
Fig. 9.10 Dialog box for defining arc....201
Fig. 9.11 Defined structure....201
Fig. 9.12 Mesh generated....202
Fig. 9.13 Submenu under the menu of Apply electric field....203
Fig. 9.14 Define boundary for solving Laplace equation....203

Fig. 9.15 Subwindow for displaying the potential function 204
Fig. 9.16 Subwindow for displaying the current density distribution 204
Fig. 9.17 Submenu under the menu of Finite element analysis 205
Fig. 9.18 Subwindow for data input 205
Fig. 9.19 Dialog box for defining boundary condition 206
Fig. 9.20 Subwindow for displaying the results at a defined time interval in the process of computation 206
Fig. 9.21 Submenu under the menu of Result data 207
Fig. 9.22 Result displaying window 207
Fig. 9.23 Result display of chloride concentration distribution 208
Fig. 9.24 Result display of pH variation 208

NOMENCLATURE

C_i	Ionic concentration in solution
D_i	Ionic diffusion coefficient
D_w	Hydraulic diffusivity
E	Electrochemical potential
F	Faraday's constant
G	Free energy
I	Current density
i	Subscript means species
J_i	Ionic flux
k	Hydraulic conductivity
k_f	Rate constant for forward reaction
k_r	Rate constant for backward reaction
K	Thermodynamic equilibrium constant
n	Total number of ionic species
q	Water flow velocity
R	Gas constant
R_i	Rate of homogeneous ionic production
R_i'	Rate of heterogeneous ionic production
S_i	Concentration of the released bound ions in solution
t	Time
t_i	Ionic transference number
$\mathbf{v}$	Velocity of bulk solution
V	Volume of bulk solution
w	Content of the porous water in which ions transport
z_i	Ionic charge number
ϕ	electrostatic potential
ε	Porosity of pore structure
ψ	Capillary potential
φ	Potential function
α	Experimental constant for Langmuir isotherm

β Experimental constant for Langmuir isotherm

θ Saturation of pore structure or water content in the pore

τ Tortuosity of pore structure

CHAPTER 1

INTRODUCTION

1.1 BACKGROUND OF THE PROJECT

Reinforced concrete is widely used throughout the world as a major material of the infrastructure. For a long time, the reinforcements in concrete were thought to be well separated from their environments since the concrete cover provides a physical barrier to many aggressive agents, which have the possibility to attack the reinforcements. Because of this, it had been widely assumed that reinforced concrete was an inherently durable material, even when produced with scant regard for quality control and exposed to environments that would be regarded as highly corrosive to steel [Page, 1998b].

In the recent decades, however, the above conception has changed as the result of unscheduled maintenance problems that have afflicted reinforced concrete structures in many countries [Page, 1998b; Walker, 1997; Subramnian and Wheat, 1989; AI-Bahar et al., 1998]. For example, in the UK, the repair, refurbishment and maintenance of existing structures have become a significant part of the total cost of the construction. Excluding land costs, the total UK cost of construction in 1986 was estimated at approximately 31 billion pounds and repair, refurbishment and maintenance had accounted for about 14 billion pounds (45% of the total cost of construction). In 1988, it is estimated that the cost of repairing decayed concrete structures was probably of 1 billion pounds [Shaw, 1993]. In North America the estimated cost of restoration of structures is in the order of 10 billion dollars [Hansson and Hasson, 1993]. Same problem has also been found in Europe and worse situation is found in Middle East as the result of more severe environmental conditions there [Society for the Cathodic Protection of Reinforced Concrete, Report, 1995].

With respect to these problems, detailed investigations have revealed that one of the major causes for the deterioration of concrete structures is the corrosion of the

reinforcement [Gonda, 1970; Fraczek, 1987; Page, et al., 1996; Hobbs, 1998], which, because of the substantial volume increase that accompanies the transformation of iron to rust, always exerts expansive tensile stress on the concrete cover and can finally lead to cracking, delamination and spalling of the cover concrete. Therefore, knowledge on how to stop corrosion from occurring is valuable and will contribute to the world needs.

Now, it is widely recognized that the penetration of chloride ions is the most common initiating mechanism for the corrosion of the reinforcement in concrete [Kitowski and Wheat, 1997]. Once a sufficient quantity of chloride ion has accumulated around the embedded steel, pitting corrosion of the metal is liable to occur unless the environmental conditions are strongly anaerobic [Page and Treadaway, 1982]. Based on this understanding, it is therefore desirable to develop methods which can simulate the chloride ingress process and predict the chloride concentration profiles accurately to help to assess the service condition of a concrete structure. On the other hand methods to repair the contaminated structure or prevent new reinforced concrete structures from chloride attack are needed as well.

In general, for a chloride contaminated structure, conventional repair methods are to remove chloride laden concrete followed by application of fresh, chloride-free, concrete. Recently, however, considerable progress has been made in the development of electrochemical methods for the protection and repair of reinforced concrete structures that are exposed to deterioration due to the chloride-induced corrosion. One of such techniques is Cathodic Protection (CP) which is to apply a small current density through the concrete (normally less than 20 mA/m^2) between the reinforcing steel and an extended anode. There is a practical disadvantage of cathodic protection because of the need to monitor and maintain the system throughout the remaining service life of the structure concerned. As an alternative, Electrochemical Chloride Removal (ECR), which also is referred as desalination or Electrochemical Chloride Extraction (ECE), has therefore been developed in recent years to extract chloride ions out of chloride-contaminated concrete structures [Tritthart, 1996] Similiar as CP, but ECR applies a relatively large cathodic current density (typically averaging about 1 A/m^2, but locally exceeding this because of non-uniform current distribution) to the reinforcing steel. The applied higher cathodic current density will force chloride ions to migrate out of the

concrete. The treatment of ECR is normally taken in a short period, such as few weeks [Bertolini, et al., 1996].

For the ECR process, an important issue is to understand how the choride ions within concrete move under the influence of the externally applied electrical field. Investigations on the ionic concentration profiles in the process, on the effectiveness and efficiency of chloride removal corresponding to the current density applied and on the treating time have been carried out. There are also concerns over possible side effects of this technique on the concrete structures, owing to the nature of electrochemical and transport process involved [Page, 1992; Page and Yu, 1995].

1.2 PURPOSE OF THE STUDY

Whether to assess the serviceability of a concrete structure under the risk of chloride attack or to investigate the effectiveness of the ECR process, the chloride redistribution in concrete is what is of most concerned. Because computer modelling is a promising technique and is able to give an economical analysis and an immediate assessment for such problem, the development of a mathematical model describing chloride transport in concrete and using numerical analysing methods to obtain results from the model is of a great practical significance. This is the main objective of this study. In this study, a comprehensive mathematical model is developed to simulate the transport behaviour of ions in porous media. This model is then used to model the processes of chloride ingress into concrete and the electrochemical chloride removal from concrete. The accuracy of the predictions for a process of chloride ingress into concrete from a saline environment and on the ionic redistributions in the process of ECR are also investigated. Lastly the influences of current densities applied and treating time on the effectiveness and efficiency of ECR are discussed.

In addition to the numerical model, a user friendly, interactive graphic user interface is also developed. The software package developed can be easily handled by users with a little knowledge of finite element analysis (FEA).

1.3 LAYOUT OF THE THESIS

The main content of this thesis is divided into ten chapters. Chapter 1 is the introduction, in which the background of the project, the significance and the purpose of the study are introduced. Chapter 2 is the literature review, which goes over the fundamental theory about metallic corrosion, the characteristics of concrete material, the role of chloride ions in corrosion of reinforcement in concrete, the current repairing methods for the chloride induced corrosion and the development of research on the mathematical modelling of chloride transport in concrete. In Chapter 3, a comprehensive mathematical model, which describes the ionic transport in porous media, is presented. The mathematical governing equations are solved using a standard finite element method. In Chapter 4, the proposed mathematical model is used to simulate the process of chloride ingress into concrete from a saline environment. Numerical results are compared with experimental results. In Chapter 5, the mathematical model is used to simulate the process of ECR. Firstly the model is used to simulate a one-dimensional experiment in order to validate the model developed. In the second part, the model is extended to two-dimensional modelling, where two cases were studied. In Chapter 6, the convenience of two-dimensional modelling is exploited to evaluate the effect of the configuration of the reinforcements on the effectiveness and efficiency of the ECR process. Chapter 7 focuses on the chloride binding isotherm, in which a new isotherm based on chemical reaction kinetics is proposed. Chapter 8 is on the numerical analysis of ionic transference numbers in which the chloride transference number is used to indicate the efficiency of the ECR process. Chapter 9 introduces the finite element program and the interactive software developed. The functions of the software are also presented. Finally in Chapter 10, general conclusions drawn from the study and further work in development.

CHAPTER 2

LITERATURE REVIEW

2.1 INTRODUCTION

Metallic corrosion is the result of chemical reactions between a metal or metal alloy and its environment where the typical characteristic is aqueous. The aqueous medium is required as the carrier for ions that allow corrosion current to flow between anodic and cathodic sites on the metal surface, therefore the process is electrochemical in nature [Jones, 1996; Page, 1998c] and the aqueous medium is called an electrolyte.

Even though the procedure for the construction of reinforced concrete structures is bound by codes of practice and technical rules, deterioration due to corrosion of reinforcement is escalating. By now, chloride ions have been ascertained as one of the main reasons for the corrosion of reinforcement. Because of this, the mechanisms of the chloride induced corrosion, the process of chloride transport in concrete as well as the remedial and preventative methods have aroused more and more interest in researchers in the recent decades. Significant progress has been made in this field.

2.2 PRINCIPLES OF CORROSION

2.2.1 Thermodynamics Of Corrosion [Jones, 1996]

A conducting metal containing mobile electrons forms a complex interface in contact with its surrounding aqueous medium. Under such condition the un-symmetrical polar H_2O molecules ($\overset{O}{\underset{H}{\diagup\diagdown}}\overset{}{H}$) are attracted to the conductive surface, forming an oriented solvent layer, which prevents close approach of other charged species ions in bulk solution. Charged ions in solution also attract their own sheath of polar water-solvent molecules, which further insulate them from the conducting metal surface. The plane of

the closest approach of positively charged cations to the negatively charged metal surface is often referred as the outer Hemholtz Plane, as indicated in Fig. 2.1. The Hemholtz Plane is an interfacial structure of separated charge commonly referred to as the electrical double layer, which behaves experimentally much like a charged capacitor (Fig. 2.1).

Fig. 2.1 Hemholtz Plane [Jones, 1996]

For a reaction of corrosion, such as Eq. (2.1), the corrosion of zinc in a solution of hydrochloric acid in water, there is a change of free energy, normally expressed as ΔG. If ΔG is negative, which means the reaction products having a lower free energy than the reactants, the reaction will proceed spontaneously. When the reaction arrives at a reversible equilibrium state, an electrochemical potential, E, is regarded to relate with

the equilibrium state of the reaction. A fundamental relationship associates the potential, E, with the change of free energy, ΔG, in the form of Eq. (2.2),

$$Zn + 2HCl \rightarrow ZnCl_2 + H_2 \tag{2.1}$$

$$\Delta G = -nFE \tag{2.2}$$

where n is the number of electrons (or equivalents) exchanged in the reaction, F is the Faraday's constant, the negative (-) is included to conform to the convention that a positive potential results in a negative free energy change for spontaneous reactions.

To predict the spontaneous direction of an electrochemical reaction, the reaction may be separated into its composite half-cell reactions. For example, the reaction Eq. (2.1) can be separated into two half-cell reactions, the anodic reaction Eq. (2.3) and cathodic reaction Eq. (2.4).

$$Zn \rightarrow Zn^{2+} + 2e^- \tag{2.3}$$

$$2H^+ + 2e^- \rightarrow H_2 \tag{2.4}$$

It is expected that the two half-cell reactions also have their own free energy changes and corresponding potentials, which are expressed as e_a and e_c, respectively. The algebraic sum of the two potentials is equal to E, i.e. $E = e_a + e_c$.

The spontaneous direction may be derived conventionally from the algebraic sum of the half-cell potentials. A positive E corresponds to a negative free energy change, which indicates that the reaction is spontaneous.

2.2.2 Electrochemical Kinetics Of Corrosion

Corrosion is thermodynamically possible under most environmental conditions. For the study of corrosion, another important objective is to know how fast corrosion occurs or how much the corrosion rate is.

For an electrochemical reaction, which either produces or consumes electrons, the rate of electrons flowing to or from a reacting interface is a measure of the reaction rate. Electron flow is conveniently measured as current, I. The relationship between I and the mass reacted, m, follows the Faraday's law:

$$m = \frac{I \cdot t \cdot a}{n \cdot F} \tag{2.5}$$

where F is the Faraday's constant, n is the number of the equivalents exchanged, a is the atomic weight of the reacting species and t is time.

If divide both sides of equation (2.5) with time t and the surface area A, we can get the corrosion rate, r:

$$r = \frac{m}{t \cdot A} = \frac{i \cdot a}{n \cdot F} \tag{2.6}$$

where $i = I/A$ is the current density. Equation (2.6) indicates that the corrosion rate can be defined as the mass loss per unit area per unit time.

2.2.3 Passivity

For many metals, including iron, the corrosion rate decreases above some critical potential, such as E_{pp} shown in Fig. 2.2. This corrosion resistance above E_{pp} is called as passivity. Below E_{pp} the metal corrodes at a relative high rate in an active state, but above E_{pp}, the passive corrosion rates are very low. A reduction of 10^3 to 10^6 times below the corrosion rate in active state is not unusual.

Investigations have revealed that passivity is caused by formation of a thin, protective, hydrated oxide corrosion-product surface film, which acts as a barrier to corrosion reactions. Whether a metal exists in the passive state above E_{pp} or in the active state below E_{pp} depends on the potential or oxidising power of the solution that the metal contacts. In view of this, passivity can be defined as a condition of corrosion resistance due to formation of thin surface films under oxidising conditions.

Fig. 2.2 Schematic active-passive polarisation behaviour [Jones, 1996]

The composition, structure and even the thickness of a passive film are in fact extremely difficult to determine. For iron, a favoured structure explanation is that an inner layer of Fe_3O_4 under an outer layer of γ-Fe_2O_3 or $FeOOH$ [Jones, 1996]. A passive film may form by a direct electrochemical reaction, such as

$$Fe + 2H_2O \rightarrow Fe(OH)_2 + 2H^+ + 2e^- \qquad (2.7)$$

But the assumed certain stable phase, $Fe(OH)_2$, may or may not be attained eventually in the film structure. Elmiligy et al. [1975] assumed a series of anodic reactions for iron:

$$Fe + H_2O \rightarrow (FeOH)_{ad} + H^+ + e^- \quad (2.8a)$$

$$(FeOH)_{ad} \rightarrow (FeO)_{ad} + H^+ + e^- \quad (2.8b)$$

$$(FeO)_{ad} + H_2O \rightarrow (FeOOH)_{ad} + H^+ + e^- \quad (2.8c)$$

where subscript '*ad*' denotes an adsorbed complex. Adsorption seems likely in the early stages of the film formation and growth. Even through *FeOOH* formed by these dissolution and re-precipitation is not generally as tenacious and protective as oxides formed by oxidation, the corrosion rate is reduced substantially as the passive film begins to form.

2.3 MECHANISMS OF STEEL CORROSION IN CONCRETE

2.3.1 Concrete Materials

Concrete is a composite material, made by mixing graded aggregates with a hydraulic cement (usually a Portland cement or a blended cement which includes a combination of cementitious materials) and water in proportions that are varied to suit different applications. In addition to these basic ingredients, small quantities of chemical admixtures are sometimes included to modify specific properties of the concrete in its fresh or hardened state. Provided that the constituent materials used are all of normally specified purity and physical characteristics, it is the cement paste fraction (i.e. the continuous matrix made up of cement particles, water and their reaction products) that has the predominant influence on the properties of concrete [Page, 1998a].

Since the mid-19th century Portland cements, made by fusing limestone and clay to form a clinker and grinding the product with small quantities of gypsum (a retarder of early hydration, which would otherwise be excessively rapid causing a 'flash set' on mixing the cement with water), have been used for the vast bulk of concrete production worldwide. An ordinary Portland cement might typically have a composition, 50-60%

C_3S (Tri-calcium silicate, $3CaO.SiO_2$), 10-25% C_2S (Di-calcium silicate, $2CaO.SiO_2$), 10% C_3A (Tri-calcium aluminate, $3CaO.Al_2O_3$), 10% C_4AF (Tetra-calcium alumino-ferrite, $4CaO.Al_2O_3.Fe_2O_3$) and 5-10% other minor components, such as gypsum ($CaSO_4.2H_2O$) and alkalis (Na_2O and K_2O).

Fig. 2.3 Principal hydration reactions of Portland cement minerals [Page, 1998a]

When Portland cement is mixed with water at normal ambient temperature, the four major cement materials gradually undergo a complex sequence of exothermic hydration reactions that result in setting and hardening of the initially fluid paste. Some of these reactions proceed rapidly over the first few days but others may continue for years if necessary moisture remains available. A simplified representation of the main reactions and the relative volumes of their hydration products in fully hydrated cement are shown in Fig. 2.3 [Page, 1998a]. The most important reactions are those of the C_3S and C_2S, which have widely different reaction rates but form similar products. These are Calcium Silicate Hydrate gel (CSH), a rigid network of colloidal particles (sub-micrometer sized) of poorly defined structure, and calcium hydroxide (portlandite) in the form of larger hexagonal crystals. CSH occupies about 60% of the volume of a fully hydrated cement paste and constitutes the main binding material in hardened cement, whilst the portlandite contributes about a further 20% of the volume. The remainder comprises various calcium sulphoaluminate and aluminoferrite hydrates, which are the products of

hydration of the C_3A and C_4AF phases and gypsum; these include the crystalline hydrates, ettringite ($C_3A.3CaSO_4.32H_2O$) formed in the early stages of hydration and the monosulphate phase ($C_3A.CaSO_4.12H_2O$) to which it later transforms.

2.3.2 Aggregates, Admixtures And Pore Structure

The primary functions of aggregates in normal density structural concrete are to provide a relatively cheap space-filler, which reduces the volume of more expensive cement required per unit volume of the concrete and restrains the dimensional instability (creep, thermal and moisture movements) of the cement matrix. It follows that aggregates should be mechanically sound, chemically and physically stable and free from significant quantities of harmful impurities. Methods for assessing these characteristics are generally well documented [Neville, 1995].

Admixtures are chemicals that are added to concrete immediately before or during mixing in quantities no longer than 5% by mass of cement for the purpose of modifying some property or properties of the material in its fresh or hardened state. Many different types of admixture are available and their use has increased greatly in recent years [Neville, 1995]. Details of admixtures may also be found in other sources [Rixom and Mailvaganam, 1986 and Hewlett, 1988].

Even after prolonged hydration, hardened cement paste contains pore of varied dimensions, ranging from 'gel pores' (of the order of nm in width) through 'Capillary pores' (generally greater than 10 nm in width) to discrete macroscopic voids associated with incomplete compaction (of the order of mm in size). The larger capillary pores (>30 nm) are of particular importance with respect to the durability of concrete since they provide the major interconnected pathways along which aggressive substances may most readily penetrate the cement matrix from the environment.

2.3.3 Pore Solution Phase Composition Of Cement Materials

Since many of the most important degradation processes that affect reinforced concrete are ones that depend on the presence of an aqueous solution phase within the pores of the material, it is clear of importance to obtain an understanding of the main compositional features of this liquid [Longuet, et al., 1973; Canham, et al., 1987, Page, 1998c].

Fig. 2.4 Hydroxyl ion concentration in pore solution of Portland cement pastes of w/c: 0.5, cured for 28 days (except where otherwise stated) [Page, 1998c]

Results of studies have shown that the pore solution present in Portland cement pastes or concretes, cured at ordinary temperatures becomes essentially a mixed solution of *NaOH* and *KOH* with only low concentrations of other dissolved ions (Ca^{2+}, SO_4^{2-}, etc) [Barneyback and Diamond, 1981]. This happens during early stages of cement hydration and the concentration of alkalis in the liquid changes little after the first few days of curing, being determined mainly by the equivalent Na_2O content of the cement ($\%Na_2O+0.659\%K_2O$) as shown in Fig. 2.4 [Nixon and Page, 1987].

As a generalization, the pore liquid phase in concrete made from most common cements may be regarded as an alkaline solution with a pH value that is normally in the range of 13-14. This is fortunate insofar as the performance of embedded reinforcing steel is concerned because it provides an environment in which corrosion of the metal is inhibited, but it may cause problems for materials that are unstable in alkaline media, e.g. aluminium, glasses and certain types of aggregate.

2.3.4 The Corrosion Of Steel In Concrete

The alkaline condition in concrete leads to a 'passive' film forming on the reinforcing steel surface [Arup, 1983; Crane, 1983]. Once the passive layer breaks down, the areas of rust will start appearing on the steel surface. When steel in concrete corrodes, it dissolves in the pore water and gives up electrons to take an anodic reaction, such as:

$$Fe \rightarrow Fe^{2+} + 2e^{-}. \tag{2.9}$$

The two electrons ($2e^{-}$) created in the anodic reaction must be consumed elsewhere on the steel surface to preserve electrical neutrality. So another chemical reaction will take place to consume the electrons. It is a cathodic reaction, which consumes water and oxygen:

$$2e^{-} + H_2O + \frac{1}{2}O_2 \rightarrow 2OH^{-} \tag{2.10}$$

It should be noted that water and oxygen are necessary at the cathode for corrosion occurrence.

The above anodic and cathodic reactions are only the first step in the process of creating rust. If the reaction just processes to this step, the ferrous ions (Fe^{2+}) will combine with the hydroxyl ions (OH^{-}) to form soluble ferrous hydroxide as in Eq. (2.11), which can dissolve into the pore solution.

$$Fe^{2+} + 2OH^- \rightarrow Fe(OH)_2 \text{ (Ferrous hydroxide)} \quad (2.11)$$

At such situation, the cracking and spalling of the concrete are impossible to take place. In reality, however, with the presence of sufficient oxygen, the product $Fe(OH)_2$ can be further oxidized to form insoluble hydrated red rust. The process can be expressed in several ways. One is shown below where ferrous hydroxide becomes ferric hydroxide then further becomes hydrated ferric oxide (rust).

$$4Fe(OH)_2 + O_2 + 2H_2O \rightarrow 4Fe(OH)_3 \text{ (Ferric Hydroxide)} \quad (2.12)$$

$$2Fe(OH)_3 \rightarrow Fe_2O_3 \cdot 2H_2O + H_2O \text{ (Hydrated Ferric Oxide, Rust)} \quad (2.13)$$

The full corrosion process is illustrated in Fig. 2.5.

Fig 2.5 Corrosion reactions on steel [Broomfield, 1997]

Un-hydrated ferric oxide, Fe_2O_3 has volume of about twice that of the steel it replaces when fully densified. When it becomes hydrated, it swells even more and becomes porous. This means that its volume increase at the steel/concrete interface is two to ten times, which could lead the concrete to crack and spall.

Corrosion of steel in concrete generally starts with the formation of pits which increase in number, expand and join up leading to the generalized corrosion usually seen on reinforcing bar. The principle of pit formation is fairly simple. At some suitable sites on the steel surface (often thought to be a void in the cement paste or a sulphide inclusion in steel), where the passive film is more vulnerable to attack and positive electrochemical potential attracts chloride ions, corrosion is initiated and acids are formed. The formed acids may be hydrogen sulphide from the sulphide (MnS) inclusion in concrete and *HCl* from the chloride ions if they present.

2.4 THE ROLE OF CHLORIDE IN THE CORROSION OF STEEL IN CONCRETE

A number of researches [Hausmann, 1967; Ganda, 1970; Holden, et al., 1985; Gibson, 1987; Al-Amoudi, et al, 1994; Allam, et al., 1997; Gonzalez, et al., 1998] have shown that the chloride ions in concrete have a negative effect to the passive film on the steel surface. Unlike carbonation, which causes overall drop in pH of pore solution [Al-Khaiat and Hague, 1997], the chloride ions act as catalysts to corrosion, when there is sufficient concentration at the steel bar surface, to break down the passive film and to allow the corrosion process to proceed quickly. Chloride ions have effects on several aspects of the corrosion of reinforcing steel in concrete. In the following sections, some discussions will be given about these effects.

2.4.1 Effect On Pitting Initiation

Pitting will initiate at a critical pitting potential, E_{pit}, which is used as a measure of resistance to pitting corrosion as shown schematically in Fig. 2.6. The presence of chloride in solution decreases the passive potential range and increases current densities and corrosion rates at all potentials. Obviously, the higher the E_{pit}, the more resistant the metal or alloy to pitting. Pit initiates above E_{pit} when the potential (i.e. corrosion potential) is established chemically by a dissolved oxidant.

Fig. 2.6 Schematic determination of critical pitting potential, E_{pit}, from anodic polarization
[Jones, 1996]

2.4.2 Effect On The Interface Of Passive Film/Solution

At this moment, the actual mechanism of pit initiation at E_{pit} is not well understood, but considerable experiments have revealed that relatively more chloride salt accumulates on metal surface compared with other anions of acid in solution [Jones, 1996] at potential even below E_{pit}. It means that chloride ions must be fairly strongly bound or absorbed by metal surface, probably the results of the electrostatic attraction between the positively charged surface and the negatively charged chloride ions and relatively much stronger mobility in solution and aggressivity in pitting of chloride ions. So a high-chloride, low-pH microenvironment may be developed at the interface of steel/solution, where a hydrolysis reaction induced by chloride ions directly reduces the alkalinity in pore solution, that perhaps finally results in the depassivation of the passive film of steel. The hydrolysis reaction may be exemplified as:

$$Fe^{2+} + 2H_2O + 2Cl^- \rightarrow Fe(OH)_2 + 2HCl \qquad (2.14)$$

$Fe(OH)_2$ is a weak base and HCl is a strong acid, leading to the suggested low pH.

2.4.3 Effect On Passive Film

However, the depassivation does not necessarily occur through a direct reduction of the alkalinity in pore solution by the chloride-induced reaction. Some researchers now believe that the chloride ions also act directly by migrating through the passive film [Sharland, 1987]. It seems widely accepted that the penetration process proceeds by the adsorption of anions at the film/solution interface and the adsorbed anions push one another thus leading the oxide to which they are strongly attached to be pushed apart. Any crack or split in the film, so produced, gets further anion adsorbed on to its sides and the process is progressive. This theory was firstly proposed by Hoar et al. [1965] and Hoar and Jacob [1967]. The actual mechanism of migration, however, is not well understood. Ogura and Ohama [1981] suggested that nucleation sites are related to microscopic inclusion and grain boundaries on the metal surface. Other theories include the effects of the chloride ion concentration [Manfore and Verbeck, 1960 and Uhlig, 1971] and localized concentrations of lower pH at film/solution interface due to reduction of the iron oxide film.

2.4.4 Effect On Steel (Propagation Of Pitting)

When reaching the iron substrate, chloride ions will act as a catalyst for the oxidation of the iron by taking an active part in reaction. They oxidise the iron to form the complex ions, $FeCl^{3-}$, $FeCl_6^{4-}$ or $FeCl_6^{3-}$, and draw these unstable ions into solution, where they will react with available hydroxyl ions to form Ferrous hydroxide, $Fe(OH)_2$. These reactions release the chloride ions back into solution and further consume more hydroxyl ions, as seen in the following reaction processes:

$$2Fe + 6Cl^- \rightarrow 2FeCl_3^- + 4e^- \qquad (2.15)$$

$$Fe + 6Cl^- \rightarrow FeCl_6^{4-} + 2e^- \quad (2.16)$$

$$Fe + 6Cl^- \rightarrow FeCl_6^{3-} + 3e^- \quad (2.17)$$

The above reactions are followed by:

$$FeCl_3^- + 2OH^- \rightarrow Fe(OH)_2 + 3Cl^- \quad (2.18)$$

$$FeCl_6^{3-} + 2OH^- \rightarrow Fe(OH)_2 + 6Cl^- \quad (2.19)$$

The electrons released by the oxidation reactions (2.15)-(2.17) flow through the steel to the cathode sites. This process would result in a reduction in pH to the points of corrosion initiation. This probably accounts for the process of pitting corrosion. The lowered pH at these sites contributes to the continual breakdown of passive oxide film [Ritter and Rodriguez, 1982].

Fig. 2.7 serves as a simple model for the pitting of iron in a slightly alkaline chloride solution. An insoluble cap of $Fe(OH)_3$, the corrosion product, collects at the pit mouth when Fe^{2+} diffuses out of the acid pit interior to exterior, where it is oxidised to Fe^{3+}. The cap impedes easy escape of Fe^{2+}, but is sufficiently porous to permit the migration of chloride ions into the pit, thereby sustaining a high acid chloride concentration in the pit. As a result, anodic polarization of the pit interior will occur by coupling to the exterior passive cathode sites where cathodic reduction of a dissolved oxidant such as oxygen will consume the electrons liberated by the anodic pit reaction.

2.4.5 Threshold Chloride Concentrations In Concrete

Because the tricalcium aluminate, C_3A, content in Portland cement is usually large enough to combine with a significant amount of chloride ions by forming an insoluble calcium chloroaluminate, large quantities of chloride ions appear to be immobilized. Now the prevailing theory is that the immobilized chloride has little effect on the steel corrosion. Experiments show that only when the chloride concentration reaches a

critical level, the steel could be deprived of its passivity [Glass and Buenfeld, 1997]. So it is obviously needed to define a limit of chloride content that can be tolerated without the danger of imminent corrosion. Detailed discussions about the threshold chloride concentration in concrete can be found in literature [Hausmann, 1967; Page, 1975; Page and Treadanay, 1982; Tritthart, 1990; Kayyali and Haque, 1995; Hussain, et al., 1996; Glass and Buenfeld, 1997].

Fig. 2.7 Schematic of corrosion processes occurring at an active growing pit in iron [Jones, 1996]

2.5 THE TRANSPORT OF CHLORIDE IONS IN CONCRETE

Because the corrosion of steel in concrete can be induced by the presence of chloride ions, the chloride transport in concrete is important with regard to the durability of reinforced concrete structures. Questions about how long it takes for chloride ions from the environment to penetrate into concrete and reach the reinforcement at a critical concentration or how much chloride ions can be extracted away from reinforcement or out of concrete in an electrochemical treatment has attracted many researches [Page et al., 1981; Page and Vennesland, 1983; Arya and Newman, 1990; Streicher and Alexander; 1995; Tang, 1996a; Nillson et al., 1996; Stoop and Polder, 1996].

2.5.1 Transport Mechanisms

The process of chloride transport in concrete is rather complicated. It may involve several mechanisms, such as diffusion, migration and convection with flowing water, which are accompanied by physical and chemical reactions.

Diffusion is defined as the substance movement due to the concentration gradient, or more strictly speaking, due to the chemical potential difference. In concrete, only free ions in pore solution are regarded to be able to diffuse [Tang, 1996a].

Migration is defined as the movement of charged substance under the influence of an electrical field. Similar to the diffusion, only free ions in pore solution are able to migrate.

Convection is defined as the solute movement due to the flow of bulk solution. For the chloride transport in concrete, it may be caused by:

- Hydraulic flow of pore solution due to gradient of pressure. For example, the new coastal construction suffers the ingress of seawater.
- Capillary suction of pore solution in an unsaturated pore structure due to the surface tension of the pore walls.
- Moisture flow and evaporation due to the gradient of vapour pressure.

At present, it is very difficult to quantify the influences of all of the above mechanisms on the chloride transport process. Therefore, some simplifications have to be made in the analysis model.

2.5.2 Chloride Binding

It is the free chloride ions in pore solution that can move from one place to another place and have the possibility to destroy the passive film on the surface of steel bar in concrete and to initiate corrosion. When free chloride ions in environments penetrate into concrete, some of these ions will be physically and chemically absorbed by the

products in concrete. This is called chloride binding [Tang, 1996a; Magnat and Molloy, 1995]. The bound chloride, of course, cannot reach the surface of reinforcement. This binding effect, therefore, has the ability to retard the transport process of free chloride ions.

Results of studies have shown that the cement component responsible for the major part of the chloride binding is tricalcium aluminate, C_3A [Hewlett, 1997], which reacts with chloride ions to form chloroaluminates, the known forms of which are:

$3CaO{\cdot}Al_2O_3{\cdot}CaCl_2{\cdot}10H_2O$ Monochloraluminate hydrate (also known as Friedel's salt)

$3CaO{\cdot}Al_2O_3{\cdot}3CaCl_2{\cdot}32H_2O$ Trichloraluminate hydrate

The extent to which will occur will depend on the C_3A content and gypsum ($CaSO_4$) content, because the C_3A will react preferentially with the sulphites as oppose to the chloride

For ordinary portland cement mixes, the chloride binding increases with increasing the value of water to cement (w/c) ratio. This is probably due to the greater porosity and permeability of the higher w/c ratio paste allowing greater access of chloride ions to C_3A.

Factors, including cement type, alkalinity and temperature, which may affect the chloride binding, were discussed by Tang [1996a]. A brief description of these factors is presented in the following.

(1) Cement Type

The total content of alumina and iron oxide in cement dominates chemical binding, whereas the fineness of hydration gel dominates physical binding. Fly ash cement containing higher amount of alumina and iron oxide reveals a higher chemical binding capacity and slag cement favouring the formation of finer hydrated products reveals a higher physical binding capacity. From Fig. 2.8 it can be seen that the difference in

binding capacity between different types of cement appears at low free chloride concentrations.

Fig. 2.8 Chloride binding capacity of different types of cement [Tang, 1996a]

(2) Alkalinity

Many researchers [Tritthart, 1989; Byfors, 1990; Page et al., 1991] have found that the hydroxide concentration in pore solution has a significant influence on chloride binding. The general tendency is that the higher the hydroxide concentration the less chloride will be bound, because there exists competition between hydroxide and chloride ions for adsorption sites.

(3) Temperature

For physical adsorption, an elevated temperature increases the thermal vibration of adsorbents. Although an elevated temperature also increases the rate of chemical reaction, it may increase the solubility of reaction products as well. Therefore both physical adsorption and chemical reaction tend to decrease chloride binding at an elevated temperature.

Although plenty of data measured by different methods and expressed in different ways have been published until now, it is difficult to use these data for a quantitative analysis about the effects of these factors on chloride binding.

2.6 PREVENTION AND REHABILITATION TECHNIQUES FOR CHLORIDE INDUCED CORROSION

As discussed in section 2.4, chloride in concrete can induce reinforcement corrosion, which finally results in the deterioration of the concrete structure. Even though prudent measures are always taken during the design of a structure to prevent or to reduce the risk of corrosion of the reinforcement, chloride may be introduced into concrete through several ways, such as being added as an admixture or accelerator in the concrete as well as being mixed into concrete with contaminated water and aggregates being used. Another important mode of the introduction is by penetration from the environment, such as in the case of structures being exposed to a marine environment or being contaminated by de-icing salts in the winter.

In practice, the prevention methods for chloride-induced corrosion are normally concrete modification, reinforcing steel modification and cathodic protection. The rehabilitation methods are patch repair or removal of chloride contaminated concrete, cathodic protection and electrochemical chloride removal. Ismail [1998] gave a comprehensive review of these methods and analysed the possible work in the area of electrochemical chloride removal. From his work a clear outline is obtained as the follows.

2.6.1 Concrete Modification

(1) Quality, Cover and Water/Cement Ratio

By following the design codes in design and notes in practice, which correspond to the related environmental conditions, a concrete structure normally can sustain a long of life

in good quality state. Concrete cover should be adequate and uniform throughout the structure. The water/cement ratio is an important parameter that should be kept within the specification and be as low as possible. Besides these, compacting should be carried out in a proper way to ensure good compaction and to avoid segregation.

(2) Decreasing Permeability of Concrete

The basic first step approach to control the permeability of concrete should be in the mix design and in the placement of the concrete. The other approaches can be divided into either being applied during construction of the structure, such as the use of latex modified concrete or after the structure has undergone some service life, such as the use of extremely low water/cement ratio overlay material or a top coat. Both of these techniques are useful in slowing down the ingress of chloride as well as oxygen [Strecker, 1987]

(3) Reinforcing Steel Modification

The modification of the coatings of reinforcement is a normal method used in practical engineering. The most common applications are coatings with fusion bonded epoxy and galvanised coatings. Special site precautions must be taken on both of these methods at the time of constructing the cages. The bend radii of the bar should be within the prescribed limits. However both these techniques have problems, zinc corrodes over time and is only expected to be passive at a pH below about 12.5. It tends to dissolve as the pH increases above this level. Epoxy coating has been reported to debond from the reinforcing bar, even in zones where corrosion did not occur. This happens particularly on structures exposed to sub-tropical marine environments [Smith et al., 1993]. Stainless steel and bronze could also be used, but the high cost implied has made them impractical.

2.6.2 Surface Treatment

Surface coating can be applied for newly built structures. For concrete already showing signs of deterioration with enough salt present at the reinforcement, the application of

surface coating is considered to be too late and is unlikely to prevent further deterioration. Surface coating only has the advantages in (1) increasing the resistance of concrete to chloride penetration; (2) increasing the resistance of the concrete to carbon dioxide penetration; (3) reducing the moisture content of the concrete.

Waterproof is important for the coating material since chloride always ingresses as a dissolved salt in the water. Any coating, therefore, that can form a coherent waterproof barrier is able to reduce penetration of salty water into the concrete. For example, Epoxy, Methy methacrylate, Moist-cured urethane and Alkyl-alkoxy are all suitable for a saline environment [Mallet, 1994].

It is important to note that the building up of water-vapour pressure behind the coatings can cause the coatings to peel off unless the adhesion to the surface is very good. It is possible to overcome or reduce this problem by using a priming coating which penetrates into the surface of the concrete, but the water in the surface pores can reduce the degree of impregnation. The water therefore has to be first displaced by heating or soaking with impregnants.

2.6.3 Patch Repair

This method is to remove the cracked, spalled or delaminated concrete, then expose the corroded steel bar and clean it or further strengthen it with extra steel if needed. The removed concrete is then replaced with either new concrete or repair mortar. In order to prevent further contamination, the new surface is often coated with a surface coating. This method may appear easy and cheap but unless all the significantly contaminated material is removed even in regions remote from the active corrosion area, corrosion will be initiated again in the area around the repair [Thompson, 1989]. This is because initially, the anodic zone sacrificially protects the surrounding areas, which contain smaller amounts of chloride. Once fresh non-contaminated material replaces the contaminated area, this protection is removed and the surrounding areas become the new anodes. This incipient anode formation can be avoided if most of the chloride-contaminated concrete is removed, a process which inevitably raises the cost. This

method also requires the structure to be assessed periodically for loading bearing capacity and safety, hence it is not always the most economical.

2.6.4 Cathodic Protection

Cathodic Protection (CP) was first employed to suppress the corrosion of a British ship hull by Davy in 1824. Since then it had been used in situations such as buried pipelines, submerged coastal and offshore structures. Its first application above the ground was on a bridge deck concrete structure by the California Department of Transportation in 1973 [Stratful, 1974].

Because the basic mechanism of corrosion is the development of anodic and cathodic sites, CP is to impede the development by providing electrons from an external source, such as a DC power supply, via an external anode installed at the surface of concrete. The flow of electrons between the anode and the steel bar turns the corroded sites into cathodes. Hence corrosion is suppressed. The name called for this process is 'impressed current cathodic protection system'.

Various control criteria for cathodic protection were suggested including of the achieving sufficiently negative steel potentials in the range of -650mV to -1135mV [Mallet, 1994]. However, the difficulty in measuring absolute potential and the worry of overprotection on some parts of the structures because of differences in concrete resistivity has made this criterion inappropriate. The most widely accepted criterion is now based on a potential shift of 100mV to 150mV [Broomfield, 1997]. The current density applied normally is between 5 to 20 mA/m^2 at about 2 to 10 volts for each square metre of concrete surface, so a power of 100 watts should be needed to protect 2,500 m^2 to 10,000 m^2 of concrete surface [Society for The Cathodic Protection of Reinforced Concrete, 1995].

Cathodic protection was shown to be a successful option for repair [Boam, 1989] for which the only concern raised is about the continuous maintenance of the system, which is difficult and costly. Cathodic protection can be used either as a repair technique or can be installed on a new construction to prevent corrosion from occurring.

Another form of cathodic protection, which is cheaper to be installed and to be maintained, is by connecting the steel reinforcement to a metal which is higher in the electrochemical series of metals than steel, such as magnesium, aluminium and zinc. This metal gradually dissolves over a period when it is connected to the steel reinforcement. This kind of mechanism is termed as 'sacrificial anode system'.

2.6.5 Electrochemical Chloride Removal

Electrochemical Chloride Removal (ECR), which sometime is called Desalination or Electrochemical Chloride Extraction (ECE), is similar to CP except that a higher direct current (DC) density is applied between the reinforcing steel and a temporary anode/electrolyte system which is attached to the exterior surface of the concrete, for a limited period. Under the action of the electrical field, the negatively charged chloride ions will move along the current flow lines from the reinforcement which acts as the cathode, towards the external anode where they are collected. The schematic process of ECR is shown in Fig. 2.9.

The speed of ionic migration in concrete depends very much on the size of pores, as well as their geometry and distribution, which are related to w/c ratio, compaction, curing and type of concrete. It is this variation in the microstructure of the cement matrix that results in a different speed of chloride extraction from case to case.

In the view of the above principle, to design an ECR system reference to the electrical resistance between the surface of the concrete and the reinforcement as well as the resistance on the surface itself is very important. This is to ensure that a relatively equal level of chloride is removed from all areas of the concrete because the current will flow through the path of lowest resistance. It is a mistake to think that the resistivity of surface and the cover depth of the concrete are uniform since local damage to the integrity of reinforced concrete could result and leave significant amounts of chloride still present in the adjoining areas. This is because the total resistance between the concrete surface and reinforcement is lower in the corroding zone. Hence the corroding zone will receive a greater percentage of current. Marine structures are a clear example

of the situations where the resistivity can be significantly different, varying from low in the tidal zones to medium and to high in the atmospheric zone. Considering these factors, a structure would need to be divided into zones to enable different levels of treatment to be set [Collins and Farinha, 1991; Polder and Hondel, 1992].

For ECR, the most frequently used external electrolytes are calcium hydroxide, sodium borate, sodium hydroxide and tap water. When an alkaline solution is used, OH^- ions that present at the anode are converted into oxygen and water molecules. Hence the pH of electrolyte decreases. Water, however, decomposes at the anode and oxygen gas and hydrogen ions are formed. The pH of the electrolyte should be kept above 7 to avoid the formation of chlorine gas that is a health hazard and an acidic electrolyte could also etch the concrete. A detailed description for this process will be presented in Chapter 3.

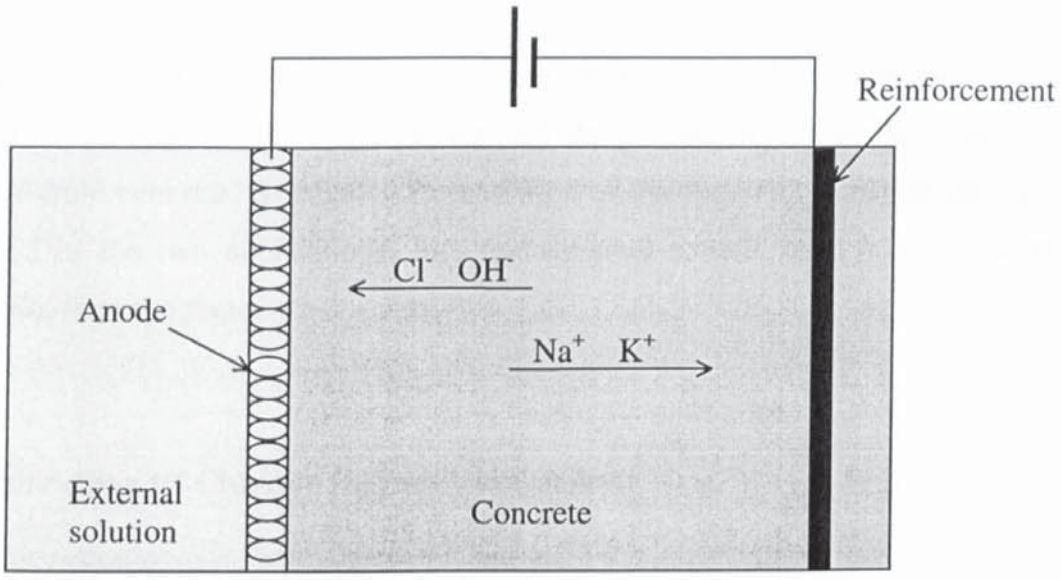

Fig 2.9 Principle of electrochemical chloride extraction

A proprietary system for ECR treatment was developed in Norway [Broomfield, 1997]. This treatment used shredded paper and water sprayed onto the surface to form a wet 'papier mache'. A mesh anode is fixed to the surface on wooden batons before another layer of wet 'papier mache' is applied. Steel mesh has been tried but is not very popular because it can be consumed during treatment and strains the concrete surface. The current is applied for a desired length of time. When the treatment is complete, the current is switched off and the anode system is removed. The treated surface is cleaned and a surface coating is applied, if necessary, to avoid further ingress of chloride.

So far ECR has been used successfully in many countries of the world with applications varying from quays, office buildings, road bridges, car parks, housing and industrial plants [Miller, 1994]. Experimental investigations on the factors affecting the effectiveness and efficiency of the chloride removal, possible re-initiation of corrosion and effects on chemical and mechanical properties of concrete have been reported [Bertolini et al., 1996; Ismail, 1998]. In addition to the experimental studies, mathematical modelling has also been developed [Yu and Page, 1996]. Especially in recent years, computer modelling of ECR has been reported widely [Li and Page, 1998a, 1998b, 2000; Sa'id-Shawqi, 1998; Hassanein, et al. 1998].

2.7 MODELLING OF CHLORIDE TRANSPORT IN CONCRETE

In the past decade, computer modelling has been used in the investigations of the process of chloride ingress into concrete and the process of electrochemical chloride removal from concrete. Because of the variation of the dominant transport mechanisms involved in the two applications, the mathematical models used have some major difference between them.

2.7.1 Modelling Of Chloride Ingress Into Concrete

For the application of chloride ingress into concrete from a saline environment, diffusion is normally regarded as the decisive mechanism. If the solution convection caused by the in-saturation of the concrete is ignored and the ions are regarded as uncharged diffusants, we can use Fick's first law to model the process. Fick's first law assumes that concentration gradient is the driving force of the transport of diffusants and has the following form for one-dimensional problems:

$$J_d = -D\frac{\partial C}{\partial x} \tag{2.20}$$

where J_d is the flux, D is the diffusion coefficient and C is the concentration of diffusant.

Based on Fick's first law, Tang and Nilsson [Tang and Nilsson, 1996b] proposed a mathematical model to predict the penetration of chloride into concrete. Their model consists of two main processes: (1) simulating free chloride penetration through the pore solution in concrete, and (2) calculating the distribution of the total chloride content in concrete.

For the first process, the quantity of the diffused free chloride is calculated by using the following equation:

$$\Delta q_{i,j}(diff) = A_{i,j}(diff) \cdot D_{i,j} \frac{C_{i-1,j-1} - 2C_{i,j-1} + C_{i+1,j-1}}{\Delta x} \Delta t_j \tag{2.21}$$

where subscripts i and j denote the depth position and time step, respectively, $\Delta q_{i,j}(diff)$ is the amount of free chloride diffusing through the area A(diff) at position x_i in a time interval Δt, D is the chloride diffusion coefficient in concrete, which is a function of temperature, depth of ingress and pore structure, C is the free chloride concentration in concrete, x is the coordinate and $\Delta x = x_{i+1} - x_i$.

The concentration C is dependent on the quantity of total chlorides, chloride binding isotherm, which is a function of the concentration C, and water content in concrete. For the second process, the total quantity of chlorides Q (total) becomes:

$$Q_{i,j}(total) = Q_{i,j-1}(total) + \Delta q_{i,j}(diff) \tag{2.22}$$

the new free chloride concentration $C_{i,j}$ can be determined by solving the following equation:

$$Q_{i,j}(total) = C_{i,j} \cdot w_{si,j} + Q_{i,j}(bound) \tag{2.23}$$

where w_s is the water content in concrete, and Q (bound) is the quantity of bound chloride, which is a function of $C_{i,j}$ and is described by the modified BET (Brunauer-Emmett-Teller) binding isotherm.

Atkinson and Nickerson [1984], based on the research of Page et al. [1981], assumed that diffusion only takes place in the aqueous phase and that any ions adsorbed to the solid phases can only move by desorption into the pore solution with which they are in equilibrium. The diffusion process was also described with Fick's first law:

$$J_x = -D_p \frac{dC_l}{dx} \tag{2.24}$$

where J_x is the flux per unit cross-section area of the pore liquid rather than per unit area of the porous medium. D_p is the diffusion coefficient for the diffusion within the pore solution. C_l is the free ion concentration in liquid. If it is in a free liquid phase, the ionic diffusion coefficient is D_f which could be measured with the method of $J_f = -D_f \frac{dC_l}{dx}$ in the free liquid phase. D_p can then be calculated as follows:

$$D_p = D_f \frac{\delta}{\tau^2} \tag{2.25}$$

where δ is the constrictivity and τ is the tortuosity. Both of them are related to the structure of porous media.

For convenience, the ionic diffusion flux is expressed in the term of the average flux per unit area of a porous medium rather than the porous solution:

$$J_x = -D_i \frac{dC_l}{dx} \tag{2.26}$$

$$D_i = D_f \frac{\varepsilon \cdot \delta}{\tau^2} \tag{2.27}$$

where ε is the volume fraction of porosity. The quantity $\varepsilon\delta/\tau^2$ is known as the diffusibility of the porous medium. Furthermore, replacing C_l with C, the average concentration in the medium would yield:

$$J_x = -D_a \frac{dC}{dx} \tag{2.28}$$

where $C = \varepsilon C_l + (1-\varepsilon)C_b$, C_b is the concentration of adsorbed species in solid. By introducing other parameters, the volumetric distribution coefficient $\gamma = C_b/C_l$ and $\alpha = \varepsilon + (1-\varepsilon)\gamma$, D_a can be expressed as:

$$D_a = D_f \frac{\delta}{\tau^2}\frac{\varepsilon}{\alpha}. \tag{2.29}$$

Based on the above mathematical model, the experiments performed by Atkinson and Nickerson [1984] proved Page et al.'s [1981] observation that the diffusion of ions in water-saturated cement paste is a strong function (approximately exponential) of the water/cement ratio at fabrication. Obviously, the effect of interaction between species was not considered in this model.

Utilising Fick's first law to determine the profile of chloride concentration in concrete, it is necessary to know flux, J, which is easily measured at steady state. This is why the Fick's first law is normally used in steady state diffusion analysis.

When consider mass conservation, it is required that at any point along the diffusion path the difference between the quantity of ions diffusing inwards and outwards should balance the change in total quantity of free and bound ions present. For unidirectional diffusion in homogeneous cement paste or concrete this may be expressed by the following equation [Sergi et al., 1992]:

$$\frac{1}{w}\frac{\partial M}{\partial t} = \frac{\partial C_i}{\partial t} + \frac{1}{w}\frac{\partial S_i}{\partial t} = -\frac{1}{\varepsilon}\frac{\partial J_i}{\partial x} \tag{2.30}$$

where w is the water content in which diffusion occurs, expressed as per unit weight of cement or concrete (g water/g cement or g concrete), M is the quantity of total ions in mmole/g cement or mmole/g concrete, C_i is the free ions concentration of species, i, in pore solution (mole/l), S_i is the quantity of bound ions in mmole/g cement or mmole/g concrete, t is time in second, x is distance in cm, J_i is the ions flux in bulk paste in mmole/cm^2/s, ε is volume fraction of the water in which diffusion occurs, expressed in per unit volume of bulk paste or concrete.

Substituting Fick's first law which is expressed as:

$$J_i = -\varepsilon D_i \frac{\partial C_i}{\partial x} \tag{2.31}$$

into Eq. (2.30) yields:

$$\frac{\partial C_i}{\partial t} + \frac{1}{w}\frac{\partial S_i}{\partial t} = D_i \frac{\partial^2 C_i}{\partial x^2}. \tag{2.32}$$

where D_i is the diffusion coefficient which was regarded as a constant.

When the quantity of bound ions is expressed as a function of free ions concentration in solution, Eq. (2.32) can be simplified as Fick's second law:

$$\frac{\partial C_i}{\partial t} = D_i^* \frac{\partial^2 C_i}{\partial x^2} \tag{2.33}$$

$$D_i^* = \frac{D_i}{\left(1 + \frac{1}{w}\frac{\partial S_i}{\partial C_i}\right)} \tag{2.34}$$

where D_i^* is the apparent diffusion coefficient in cm^2/s.

Sergi et al. [1992] made use of Fick's second law to simulate a one-dimensional chloride ingress experiment. They interpolated the experimental results of chloride and

hydroxyl profiles in concrete and obtained the two ions' diffusivity in the diffusion process. Since chloride binding is a relatively fast process compared with its diffusion [Pereira and Hegedus, 1984], a Langmuir adsorption isotherm can be used to approximate the instantaneous relationship between bound and free chlorides. This isotherm yields the following form of apparent chloride diffusion coefficient:

$$D_i^* = \frac{D_i}{\left(1+\frac{\alpha}{w(1+\beta C_i)^2}\right)} \tag{2.35}$$

where α and β are empirical constants.

Berke and Hick [1994] also utilized Fick's second law to predict the chloride profiles in concrete. In their work the diffusivity D was expressed as a function of temperature:

$$D_2 = D_1\left(\frac{T_2}{T_1}\right)\exp\left[k\left(\frac{1}{T_1}-\frac{1}{T_2}\right)\right] \tag{2.36}$$

where k is the activation energy for a molecule to escape to a vacant site in the fluid divided by gas constant. T is temperature

Because Fick's second law is defined by considering the mass conservation in a controlled volume at any moment, it is applicable to any non-steady state processes.

2.7.2 Diffusion Coefficient

Diffusion coefficient is a key parameter in the diffusion modelling. Because the diffusion of chloride ions within the pore solution of hardened concrete and related media is a complex process, which involves such as electrostatic coupling of various ions in the pore solution, ion/pore surface interactions, osmotic effects and partition, it is obvious that no single test method can provide adequate information to allow an accurate prediction for diffusion rates for a variety of conditions of exposure and

materials. It is normally accepted to use steady state diffusion measurements, which are obtained from well-characterised specimens, as a means of studying the effects of several factors that influence chloride diffusion in cementitious materials [Page and Ngala, 1995].

A considerable effort has been made to determine the diffusion coefficient of chloride's transport in concrete. The widely used method for measuring diffusion coefficient uses a diaphragm cell. Normally for steady state diffusion experiments, Fick's first law is adopted to determine the diffusion coefficient. The chloride diffusivity obtained in such a way is called 'effective diffusivity', D_{eff}, which is a constant. For measuring chloride diffusivity in non-steady state diffusion process, for which the Fick's second law is adopted, the chloride diffusivity is referred as 'apparent diffusivity', D_{app}. From the previous section, it can be seen that the apparent diffusivity is not a constant, but is related to the local free chloride concentration and bound chloride produced. The determination of the chloride diffusion coefficient is a rather complex problem, which is beyond this study, further information can be found in literature such as [Dhir, et al., 1990 and 1998; Tang and Nilsson, 1992; Zhang and Gjorv, 1994 and 1995].

2.7.3 Chloride Binding Isotherm

The effect of chloride binding will retard the rate of chloride ion transport in concrete, since the amount of free chloride in pore solution is reduced [Martin-Perez, et al., 2000]. In literature, the term 'Chloride Binding Isotherm' is usually used to describe the quantitative relationship between bound (or total) chloride and free chloride at a constant temperature. Many models have been suggested in the literature. Some representatives are given here.

Tuutti [1982] suggested a simple linear relationship:

$$C_b = \alpha \cdot C \tag{2.37}$$

where C_b is the concentration of bound chloride ions, C is the concentration of free chloride ions, and α is a constant. The experimental data reported by others do not fit the above over-simplified equation. Arya and Newman [1990] proposed a linear relationship with an intercept on the axis for bound and total chloride:

$$C_b = \alpha \cdot C_t + \beta \tag{2.38}$$

where β is the intercept constant. Although the equation fits their experimental data fairly well, it cannot explain the physical meaning of $C_b = \beta$ at $C_t = 0$, specially when considering the external chloride penetration. For instance, if a chloride-free concrete is exposed to a chloride-free solution, the concentration of the bound or total chloride should not be β, but zero. Therefore the equation is not applicable at low free chloride concentrations, where the experimental data remarkably diverge from linearity, as pointed out by Mangat and Molloy [1995].

In fact, the linear relationship works only in a limited range of free chloride concentration. In most cases the relationship between bound and free chlorides is non-linear. Pereira and Hegedus [1984] and Sergi, et al. [1992] suggested that chloride binding is a relatively fast process in comparison with diffusion and therefore an instantaneous relationship between bound and free chloride may be approximated by the Langmuir adsorption isotherm, which can be expressed as:

$$S_a = \frac{\alpha C_a}{1 + \beta C_a} \tag{2.39}$$

where α and β are empirical constants.

Tang and Nilsson [1993] found that the chloride binding capacity for concrete strongly depends on the water-cement ratio and the addition of aggregate. They thought that the relationship between the bound chloride and free chloride can be described by Langmuir isotherm at low free chloride concentrations ($\leq$ 0.05 mole/l), but by Freundlich isotherm at high free chloride concentration (0.01-1 mole/l) as the following:

$$C_b = \alpha \cdot C^{\beta} \tag{2.40}$$

or

$$\log C_b = \beta \log C + \log \alpha \tag{2.41}$$

where α and β are the absorption constants, which are purely empirical coefficients without physical meaning.

In 1990, Xu, according to Tang [1996a], proposed a modified BET equation to describe chloride binding. The BET multi-layer adsorption theory has widely been used in many fields for the determination of surface specific area. Tang and Nilsson [1996a] reviewed and utilized this theory. The most usual form of the BET equation is:

$$\frac{S}{S_m} = \frac{\alpha \cdot x}{(1-x)[1+(\alpha-1)x]} \tag{2.42}$$

where S is the amount of the absorbed absorbate, S_m is the monolayer adsorption capacity, α is the adsorption constant, $x = p/p_s$, where p is the vapour pressure of the absorbate and p_s is the saturation vapour pressure of the absorbate.

The BET theory is originally developed for gas adsorption. The adsorption constant α is related to the difference between the adsorption energy at the first layer and those at the second or higher layers. The original derivation of the BET equation assumed that the adsorption energy at the second layer is the same as that at the higher layers and is equal to the heat of liquefaction, that is:

$$\alpha \propto \exp\left(\frac{E_1 - E_2}{RT}\right) \quad \text{and} \quad E_2 = E_3 = \cdots = E_n = H_1$$

where E_1 is the adsorption energy at the layer as designated by the subscript, H_1 is the heat of liquefaction. The problem of the original BET theory is that when $x \rightarrow 1$, the adsorption becomes infinite. To avoid this infinite adsorption, Brunauer et al. [1969]

introduced a parameter $k < 1$, so that, $x = k\frac{p}{p_s}$ in the previous BET equation (2-42). This treatment was based on the fact that even at the saturation vapour pressure the number of adsorption layer is still limited, since in the original derivation x is defined as the ratio of the adsorbed fraction at the first layer to that at the second layer. A very small value of k implies a very small number of adsorption layers. Therefore, this treatment seems contrary to the original assumption of multi-layer adsorption, where the number of adsorption layers tends to the infinite. Xu tried another approach by assuming that the adsorption energy at the second layer is not equal to those at the third or higher layers, that is $E_2 \neq E_3$ and $E_3 = E_4 = \cdots = E_n = H_1$ and derived the following modified equation:

$$\frac{S}{S_m} = \frac{\alpha x\left[1-(1-\beta)(1-\beta x)^2\right]}{\beta(1-\beta x)\left[1-\beta x+\alpha x(1-\beta x+x)\right]} \tag{2.43}$$

where $\beta \propto \exp\left(\frac{H_1 - E_2}{RT}\right)$ which is related to the difference between the adsorption energy at the second layer and one at the third or higher layers. Tang and Nilsson [1996a] applied the equation (2.42) to the chloride binding isotherm by assuming $x = C/C_s$, where C is the free chloride concentration and C_s is the concentration in a saturated solution. They also found that when the bound chloride is expressed in terms of the weight of hydration gel, the influence of water-cement rations and aggregate content could be eliminated. So in their discussion the unit based on the weight of cement was used instead.

Wee et al. [1997] considered the chemical binding and physical adsorption of Cl^- with the following relationship between adsorption S and free chloride concentration:

$$S = \frac{\alpha\left(\frac{C}{\rho_0}\right)^{\beta}\exp\left(-\frac{\gamma}{t^*}\right)}{100} \tag{2.44}$$

where α, β and γ are the constants related to materials and water/cement ratios, t^* is the exposure periods (weeks), ρ_c is the cement content (g/m^3).

In their mathematical modelling for the process of electrochemical chloride removal, Hassanein et al. [1998] and Glass et al. [1998] proposed that the reaction of free chloride with binding sites (b) to give bound chloride (bCl) may be described by:

$$Cl^- + b \leftrightarrow bCl\,. \tag{2.45}$$

For this reaction, they approximated the rate of bound chloride release by using a linear function as following:

$$\frac{\partial S}{\partial t} = -k_r S \tag{2.46}$$

where k_r is the rate constant; S is the mass of ion bound by the solid porous material and is expressed relative to the mass of sample which have a water filled porosity of ε volume fraction and ρ_s density.

2.7.4 Modelling Of Electrochemical Chloride Removal Process

In the application of ECR process, the mathematical model used needs to consider not only diffusion process but also migration caused by the applied electrical field. Recognising this, Nernst-Planck equation has been adopted to determine the flux [Yu and Page, 1996]. In the past decade, the application of Nernst-Planck equation on the modelling of ECR process is not completely in an agreement. A simple model which does not consider the effect of ionic interaction was adopted by many researchers [Tang, 1996a; Sa'id-Shawqi, 1998; Hassanein et al., 1998; 1999]. In these works, in order to simplify the analysis it was assumed that the local electrical field does not vary during treatment. It was also assumed that the chloride ion diffusion coefficient in concrete remains constant during the process. With these assumptions, the mass conservation based on the Nernst-Planck equation can be solved using the finite difference methods.

In reality, however, because of the electrostatic interaction between ions, the change of ions content in concrete during ECR treatment should result in the variation of the local electrical field in concrete from time to time. Yu and Page [1996] proposed the simulation of multicomponent ionic migration in concrete associated with ECR by considering the effect of ionic interaction. In their work, the ionic diffusion coefficients in pore solution were used and were assumed as constants in a dilute solution. The boundary condition at steel cathodes was assumed to be that only hydroxyl ions are generated there due to the electrochemical reactions, which otherwise has no effect on the ionic migration process. This is equivalent to the assumption that the system is set up such that at cathodes the hydroxyl ions have a flux equivalent to the externally applied current density but all the other ions there have zero flux. The results of their calculation are in qualitative but not in quantitative agreement with those observed experimentally. The quantitative disagreement was assumed to be caused by the neglect of the effect of ionic binding/desorption.

Li and Page [1997a; 1997b; 1998a] further developed the above work by dealing with the electrostatic coupling of ions in a multi-component pore electrolyte and by considering the chloride binding with or the desorption from the pore surfaces. They also took into account of the compositional changes occuring within a finite volume of external electrolyte (saturated $Ca(OH)_2$ solution initially) in contact with the anode. Under the condition of galvanostatic (i.e. the treating current density is constant), the governing equation is solved for each ionic species using the finite element method. Li and Page [1998b] also investigated the effect of ionic concentrations on the ionic diffusion and migration in concentrated solutions. Li and Page only used this model to analyse a one-dimensional problem. In this thesis, the mathematical model used by Li and Page is developed to analyse the ECR process in two-dimension. In addition to that the ionic convection with the pore solution is also considered into the model. This comprehensive model is used to simulate the chloride ingress into concrete from a saline environment and the results are compared with that from other models.

CHAPTER 3

MATHEMATICAL MODELLING OF IONIC TRANSPORT IN CONCRETE

3.1 INTRODUCTION

As reviewed in Chapter 2, chloride transport in concrete is a complex phenomenon involving the diffusion of ions in the solution due to concentration gradient, migration caused by an externally applied current and the interactions of dissociated ions. In addition, ionic convection along with bulk solution, caused by pressure gradient and hydration suction [Nagesh and Bishwajit, 1998], also exists in unsaturated concrete structures. The hydration suction is a capillary transport of solution due to unbalanced surface tension forces between fluid and fluid, and fluid and pore surface [Martys and Ferraris, 1997; Puyate and Lawrence, 1999]. The unbalanced surface tension force between fluid and pore surface will cause the fluid to be adsorbed on or desorbed from the concrete matrix. This chapter presents a mathematical model, which takes all of these major factors into account and describes the transport of ions in porous media. The model can be used to simulate not only the chloride ingress into concrete from a saline environment and the electrochemical chloride removal from concrete, but also the general ionic transport in electrolyte solution. Finally the governing equation is solved using the finite element method.

3.2 MATHEMATICAL MODEL OF IONIC TRANSPORT IN ELECTROLYTE

If the pore solution in concrete is assumed to be an ideal dilute electrolyte, the ionic transport of each dissolved species can be defined by using the following mass transfer equation [Newman, 1973; Jacobs and Probstein, 1996]:

$$J_i = -z_i D_i (\frac{F}{RT} \nabla \phi) C_i - D_i \nabla C_i + C_i \mathbf{v} \tag{3.1}$$

where J_i is the flux of species i, z_i is the charge number, F is the Faraday's constant, D_i is the diffusion coefficient, C_i is the concentration, ϕ is the electrostatic potential and $\mathbf{v}$ is the velocity of bulk solution. ∇ and $\mathbf{v}$ are defined in natural coordinate system.

Eq. (3.1) is also called the Nernst-Planck equation [Shapiro, et al., 1989]. The three terms on the right-hand side of the equation represent the three mechanisms of the mass transfer:

- Migration of a charged species in an electrical field
- Ionic diffusion due to a concentration gradient
- Convection of ions along with bulk solution

According to the mass conservation of a species, we have the following equation:

$$\frac{\partial C_i}{\partial t} = -\nabla J_i + R_i \tag{3.2}$$

where t is the time and R_i is the rate of homogeneous production of the species.

Substituting Eq. (3.1) into Eq. (3.2) yields:

$$\frac{\partial C_i}{\partial t} = z_i \frac{F}{RT} \nabla (D_i C_i \nabla \phi) + \nabla (D_i \nabla C_i) - \nabla (C_i \mathbf{v}) + R_i \tag{3.3}$$

In order to determine $\nabla \phi$, the current density due to the motion of charged ions in the electrolyte is introduced:

$$I = F \sum_i^n z_i J_i \tag{3.4}$$

where I is the current density, n is total number of the species in the electrolyte.

Substituting Eq. (3.1) into Eq. (3.4) yields:

$$\frac{F}{RT}\nabla\phi = -\frac{\frac{I}{F}+\sum_{i}^{n} z_i D_i \nabla C_i}{\sum_{i}^{n} z_i^2 D_i C_i} \tag{3.5}$$

If the velocity of bulk solution is known, Eqs. (3.5) and (3.3) fully describe the transport behaviour of ions in an ideal electrolyte, from which the gradient of electrostatic potential and the concentration profile of each ionic species can be determined for a given current density.

In two-dimensional modelling, in order to determine the components of current density, I_x and I_y, the condition of local electroneutrality is used:

$$\sum_{i}^{n} z_i C_i = 0 \quad \text{and} \quad \sum_{i}^{n} z_i \frac{\partial C_i}{\partial t} = 0 \tag{3.6}$$

Substituting Eq. (3.2) into (3.6) and noting that $\sum_{i}^{n} z_i C_i \mathrm{v} = 0$ and $\sum_{i}^{n} z_i R_i = 0$ [Newman, 1973], we have

$$\nabla I = 0 \tag{3.7}$$

From Eq. (3.7), the components of current density in x and y directions can be determined by solving the following Laplace Equation:

$$\nabla^2\psi = \frac{\partial^2\psi}{\partial x^2} + \frac{\partial^2\psi}{\partial y^2} = 0 \tag{3.8}$$

where $I_x = \frac{\partial\psi}{\partial x}$ and $I_y = \frac{\partial\psi}{\partial y}$, ψ is a potential function.

3.3 MATHEMATICAL MODEL IN POROUS MEDIA

When applying the above model to predict the ionic transport in porous media, one has to consider the influence of tortuosity and porosity of the pore structure, the saturation of the pore structure and adsorption or desorption of ions at the interface between the liquid and solid phase. When these factors are taken into account, Eqs. (3.3) and (3.5) become:

$$\tau^2 \frac{\partial}{\partial t}(C_i\theta + S_i\theta) = z_i \nabla\left[D_i \left(\frac{F}{RT} \nabla\phi \right) C_i\theta \right] + \nabla(D_i \nabla(C_i\theta)) - \tau\nabla(C_i\theta v) \qquad (3.9)$$

$$\frac{F}{RT}\nabla\phi = -\frac{\frac{\pi I}{F\varepsilon^{3/2}} + \sum_i^n z_i D_i \nabla(C_i\theta)}{\sum_i^n z_i^2 D_i C_i \theta} \qquad (3.10)$$

where τ is the tortuosity of pore structure, which is defined by the relation between the natural coordinate of the circular capillary l and the porous medium coordinate x as dx/dl =1/τ (see Fig. 3.1), ε is the volume fraction of porosity, θ is the water content of the pore structure, which is expressed as the volume fraction saturated at time t, and S_i is the concentration of the released bound ions of species i in solution, which normally is expressed as a function of C_i i.e., $S_i\theta = f(C_i\theta)$. A detailed discussion about θ will be presented in the next chapter. ∇ is defined in x-y coordinate system.

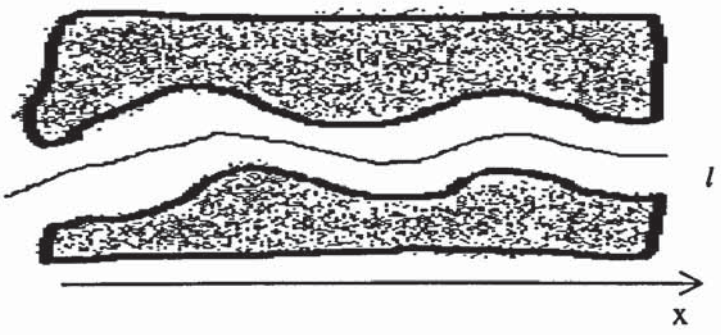

Fig. 3.1 Co-ordinates of capillary

3.4 FINITE ELEMENT ANALYSIS

Eqs. (3.9) and (3.10) are the transient non-linear convection-diffusion equations with variable coefficients, which can be solved numerically by using finite element methods. The two-dimensional linear-order Galerkin formulation is applied to Eq. (3.9) with the local approximations of the form:

$$C_i(x,y,t)\theta(x,y,t)=\sum_j^4 N_j(x,y)(C_i\theta)^j = N\{(C_i\theta)^j\} \tag{3.11}$$

where $N=[N_1,N_2,N_3,N_4]$ is the shape function matrix for four-node elements, j denotes the nodal number of an element, and $\{(C_i\theta)^j\}=[(C_i\theta)^1,(C_i\theta)^2,(C_i\theta)^3,(C_i\theta)^4]^T$ is the nodal concentration vector of species i, equivalent to a saturated state. The release rate of bound ions can be expressed as a function of the rate of free ions as follows,

$$\frac{\partial(S_i\theta)}{\partial t}=\frac{\partial(S_i\theta)}{\partial(C_i\theta)}\frac{\partial(C_i\theta)}{\partial t}=\lambda(C_i\theta)\frac{\partial(C_i\theta)}{\partial t} \tag{3.12}$$

where λ is the relation-function between the concentration rates of free and bound ions. Substituting Eqs. (3.11) and (3.12) into (3.9), and weighting the residual with N_j, it yields the following element matrix equation:

$$(M_i^s+M_i^c)\left\{\frac{\partial(C_i\theta)}{\partial t}\right\}=(K_i^d+K_i^m)\{(C_i\theta)\}-J_i^b \tag{3.13}$$

in which

$$M_i^s=\int_\Omega\left[\lambda(C_i\theta)N^TN\right]dxdy$$

$$M_i^c=\int_\Omega(N^TN)dxdy$$

$$K_i^d = -\int_{\Omega} D_i \left(\frac{\partial N^T}{\partial x}\frac{\partial N}{\partial x} + \frac{\partial N^T}{\partial y}\frac{\partial N}{\partial y} \right) dxdy$$

$$K_i^m = -\int_{\Omega} \left[\frac{\partial N^T}{\partial x}\left(z_i D_i \frac{F}{RT}\frac{\partial \phi}{\partial x} - \tau^2 \mathrm{v}_x \right) N + \frac{\partial N^T}{\partial y}\left(z_i D_i \frac{F}{RT}\frac{\partial \phi}{\partial y} - \tau^2 \mathrm{v}_y \right) N \right] dxdy$$

J_i^b = the flux vector at element boundaries

The components of the gradient of electrostatic potential can be calculated in terms of Eq. (3.10),

$$\frac{F}{RT}\frac{\partial \phi}{\partial x} = -\frac{\frac{\tau I_x}{F\varepsilon^{2/3}} + \sum_{i=1}^{n} z_i D_i \frac{\partial N}{\partial x}\left\{(C_i\theta)^j\right\}}{\sum_{i=1}^{n} z_i^2 D_i N\left\{(C_i\theta)^j\right\}} \tag{3.14}$$

$$\frac{F}{RT}\frac{\partial \phi}{\partial y} = -\frac{\frac{\tau I_y}{F\varepsilon^{2/3}} + \sum_{i=1}^{n} z_i D_i \frac{\partial N}{\partial y}\left\{(C_i\theta)^j\right\}}{\sum_{i=1}^{n} z_i^2 D_i N\left\{(C_i\theta)^j\right\}} \tag{3.15}$$

For transient problem, the time derivative can be approximated by the backward difference method [See e.g. Heinrich and Pepper, 1999]:

$$\frac{\partial}{\partial t}(C_i\theta)^{t_\theta} = \frac{(C_i\theta)^{n+1} - (C_i\theta)^n}{\Delta t} \tag{3.16}$$

where $(C_i\theta)^n = C_i(x,y,t_n)\theta(x,y,t_n)$ denotes the value of the dependent variable at time $t = t_n$, Δt is the time step increment, and $t_{n+1} = t_n + \Delta t$.

The corresponding $(C_i\theta)^{t_\theta}$ at the same time is then defined by:

$$(C_i\theta)^{t_\theta} = \Theta(C_i\theta)^{n+1} + (1-\Theta)(C_i\theta)^n \tag{3.17}$$

where Θ is normally specified to be a value between 0 and 1.

Substituting Eqs. (3.16) and (3.17) into (3.13) and setting Θ=1/2 (Crank-Nicolson method) [Zienkiewicz and Taylor, 1991], we obtain:

$$\left[\frac{(M_i^S + M_i^C)^{n+1} + (M_i^S + M_i^C)^n}{\Delta t} - \left(K_i^d + K_i^m\right)^{n+1}\right]\left\{C_i\,\theta\right\}^{n+1} =$$

$$\left[\frac{(M_i^S + M_i^C)^{n+1} + (M_i^S + M_i^C)^n}{\Delta t} + \left(K_i^d + K_i^m\right)^n\right]\left\{C_i\,\theta\right\}^n - \left(J_i^b\right)^{n+1} - \left(J_i^b\right)^n \tag{3.18}$$

By defining two new matrices as the modified conductivity matrix K^* and the modified external flow vector Q^*, the solution to Eq. (3.13) becomes the solution of the set of linear equations:

$$K^*\left\{C_i\,\theta\right\}^{n+1} = Q^* \tag{3.19}$$

Both K^* and Q^* are the functions of ionic concentrations, C_i, and material saturation, θ. There are two basic approaches that can be used in solving this problem:

1. Use the ionic concentration distribution from the previous time step, t_n, to calculate K^* and Q^* and thus solve Eq. (3.19) directly, or

2. Use an iterative solution technique that allows K^* and Q^* to be continually revised on the basis of the converging solution.

The program developed contains the option of either solving the entire problem directly or iteratively.

3.5 MODELLING OF ECR PROCESS

When applying the above mathematical model to analyse the process of ECR, specific consideration is needed on the boundary. During ECR process, chemical reactions take place at electrodes, which can be expressed by:

- At cathode

$$\frac{1}{2}O_2 + H_2O + 2e^- \rightarrow 2OH^- \tag{3.20}$$

$$2H_2O + 2e^- \rightarrow H_2 + 2OH^- \tag{3.21}$$

$$Fe^{3+} + e^- \rightarrow Fe^{2+} \tag{3.22}$$

Reaction (3.20), requires oxygen to form OH^- ions. If not enough oxygen is present to the reaction because of the slow diffusion of oxygen from outside, this reaction can be neglected and therefore the reaction (3.21) becomes dominant.

When an external current is applied, the corrosion reaction:

$$Fe^{2+} + 2H_2O \rightarrow Fe(OH)_2 + 2H^+ \tag{3.23}$$

may be retarded. OH^- ions production will decrease [Andrade et al., 1995] and the reaction (3.22) may proceed at some level.

- At anode

$$2OH^- \rightarrow \frac{1}{2}O_2 + H_2O + 2e^- \tag{3.24}$$

$$H_2O \rightarrow \frac{1}{2}O_2 + 2H^+ + 2e^- \tag{3.25}$$

$$2Cl^- \rightarrow Cl_2 + 2e^- \tag{3.26}$$

The reaction (3.25) indicates that electrolysis of water happens at anode as well. The produced H^+ ions should migrate towards the cathode and meet with OH^- and Cl^- ions moving in the opposite direction. OH^- ions are neutralised by H^+ ions to form water, and hydrochloric acid is formed with Cl^- ions. According to the reaction (3.26), Cl^- ions arriving at anode are discharged and form chlorine gas.

Both the acidification of the electrolyte and the formation of chlorine gas are often regarded as undesirable. An electrolyte that has turned acidic may attack the concrete, and chlorine gas is very toxic and thus hazardous to health. The use of an alkaline electrolyte, such as a saturated $Ca(OH)_2$ solution or a sodium borate solution, can prevent the acid attack and the development of chlorine gas [Mietz, 1999]. At pH-values above 7 practically no chlorine gas is formed because the reaction (3.24) is easier to take place.

Besides the reactions at the boundary, chemical reactions also take place in the concrete. Damidot and Glasser [1993] investigated the CaO-Al_2O_3-$CaSO_4$-H_2O system at 25°C with calculations on the equilibrium solubility surfaces of AH_3, $C_3AH_6CHC_6AS_3H_x$, and gypsum ($CaSO_4.H_2O$). To simplify the calculation, they did not consider the detail specification of the concrete and took the following assumptions:

1. H^+ can be neglected with respect to OH^-, due to the generally high pH value of the system;

2. Ca^{2+} is the only ion calcium containing species in solution;

3. SO_4^{2-} is the only ion sulphate containing species in solution;

4. $Al(OH)_4^-$ is the only ion aluminium containing species in solution;

Therefore the electrical balance of the solution can be written by using four master species in chloride-contaminated concrete:

$$2[Ca^{2+}]=[Al(OH)_4^-]+[OH^-]+[Cl^-]+2[SO_4^{2-}] \tag{3.27}$$

They calculated the values of the solubility products from experimental data with respect to the four master species except chloride for ettringite, monosulphoaluminate, hydrogarnet, calcium hydroxide, gypsum and gibbsite:

1) ettringite ($C_6AS_3H_{32}$)

$$3CaO\cdot Al_2O_3\cdot 3CaSO_4\cdot 32H_2O=6Ca^{2+}+2Al(OH)_4^-+3SO_4^{2-}+4OH^-+26H_2O \tag{3.28}$$

$$K_1=(Ca^{2+})^6(Al(OH)_4^-)^2(SO_4^{2-})^3(OH^-)^4=2.8\times10^{-45} \tag{3.29}$$

2) monosulphoaluminate (C_4ASH_{12})

$$3CaO\cdot Al_2O_3\cdot CaSO_4\cdot 12H_2O=4Ca^{2+}+2Al(OH)_4^-+SO_4^{2-}+4OH^-+6H_2O \tag{3.30}$$

$$K_2=(Ca^{2+})^4(Al(OH)_4^-)^2(SO_4^{2-})\ (OH^-)^4=3.71\times10^{-30} \tag{3.31}$$

3) hydrogarnet (C_3AH_6)

$$3CaO\cdot Al_2O_3\cdot 6H_2O=3Ca^{2+}+2Al(OH)_4^-+4OH^- \tag{3.32}$$

$$K_3=(Ca^{2+})^3(Al(OH)_4^-)^2(OH^-)^4=2.91\times10^{-23} \tag{3.33}$$

4) calcium hydroxide ($Ca(OH)_2$)

$$Ca(OH)_2=Ca^{2+}+2OH^- \tag{3.34}$$

$$K_4 = (Ca^{2+})(OH^-)^2 = 8.9\times10^{-6} \tag{3.35}$$

5) gibbsite (AH_3)

$$Al(OH)_3 + OH^- = Al(OH)_4^- \tag{3.36}$$

$$K_5 = (Al(OH)_4^-)/(OH^-) = 3.99\times10^{-2} \tag{3.37}$$

6) gypsum ($CaSO_4 \cdot 2H_2O$)

$$CaSO_4 \cdot 2H_2O = Ca^{2+} + SO_4^{2-} + 2H_2O \tag{3.38}$$

$$K_6 = (Ca^{2+})(SO_4^{2-}) = 3.72\times10^{-5} \tag{3.39}$$

The CaO-Al_2O_3-$CaSO_4$-H_2O system in the presence of Na_2O was also studied by Damidot and Glasser [1993]. For sodium concentration that does not exceed 1M/l, no new component is added into the system, since AH_3, C_3AH_6, gypsum and CH are known to be stable in *NaOH* solution. Ettringite also seems to be stable. So only the electrical balance and the ionic strength equations are different from the case without alkali:

$$2[Ca^{2+}] + [Na^+] = [Al(OH)_4^-] + [OH^-] + [Cl^-] + 2[SO_4^{2-}] \tag{3.40}$$

Basing on the experimental result, Bertolini et al. [1996] developed an approximately linear relationship between the logarithm of sulphate concentration in mmole/l and the solution pH value with a slope close to 2. The three equilibrium reactions, (3.28), (3.30) and (3.34), they considered yield:

$$[SO_4^{2-}] = K_1^{1/3} K_2^{-1/3} K_3^{-1} [OH^-]^2 \tag{3.41}$$

whence

$$\log[SO_4^{2-}] = 2\text{pH} + \log(K_1^{1/3} K_2^{-1/3} K_3^{-1} K_w^2) \tag{3.42}$$

where K_w is the ionic product of water.

From the above experimental investigations, it can be seen that due to the generally high pH value of pore solution, the concentrations of SO_4^{2-} and $Al(OH)_4^-$ are very low and may be neglected. In the process of ECR, only negative ions in the concrete are extracted out from the concrete. Since the transport of ions is much quicker in the external aqueous electrolyte than in the concrete, the concentration of each ionic species in the external electrolyte can be assumed to be uniform and only consider the solubility equilibrium of $Ca(OH)_2$ [Li and Page, 1998a]:

$$C_{Ca} \cdot C_{OH}^2 = K_4 \tag{3.43}$$

3.6 DISCUSSIONS

By introducing the tortuosity, porosity and saturation of the pore structure, the basic principles of the ionic transport in electrolyte can be used to simulate the ionic transport in a porous medium. As an application, it can be used to simulate chloride ingress into concrete from a saline environment and the electrochemical chloride removal from concrete.

The proposed model has considered most of the factors involved in the two processes. However, the ionic diffusion coefficients, which are normally dependent on the ionic concentrations and the saturation of the pore structure [Nagesh and Bishwajit, 1998], are not discussed because of their complexity. Under the assumption of ideal dilute solution, they can be treated as constants [Li and Page, 2000]. The influence of ionic concentrations on the flow of bulk solution is also neglected.

CHAPTER 4

MODELLING OF CHLORIDE INGRESS INTO CONCRETE FROM A SALINE ENVIRONMENT

4.1 INTRODUCTION

As mentioned in Chapter 1, the corrosion of reinforcing steel in concrete due to chloride ingress is one of the main causes of the deterioration of reinforced concrete structures, particularly in marine environments. It is therefore desirable to develop methods, which can be used to simulate the chloride ingress process and predict the chloride concentration profiles more accurately to help to access the service condition for reinforced concrete structures. In the past decades, both physical and computer modelling have been adopted to investigate the process of chloride ingress [Sergi, et al, 1992; Mangat and Molloy, 1994a and b; Tang, 1996b; Wee, et al, 1997; Onyejekwe and Reddy, 2000]. As reviewed in Chapter 2, most researchers used Fick's second law to model the ingress of chloride ions in concrete.

In reality, however, the contaminating solution containing chloride, such as seawater, is a mixture having various dissociated charged ions. In addition, as the pore structure of concrete is normally partially saturated, the chloride ingress may be affected by the hydraulic suction. Consequently, the process of chloride ingress into concrete is rather complicated. This chapter presents the numerical modelling results for the process of chloride ingress into concrete using the mathematical model described in the previous chapter. The results are compared with those obtained from other models and experiments.

4.2 THE PORE STRUCTURE OF PORTLAND CEMENT AND ITS EFFECTS ON IONIC MASS TRANSPORT

Hardened cement paste contains pore of various dimensions, ranging from 'gel pore' (of the order of nm in width) through 'capillary pores' (generally greater than 10 nm in width) to discrete macroscopic voids associated with incomplete compaction (of the order of mm in size). Models of the pore structure are reviewed in references such as Taylor, 1990 and Neville, 1995. Normally, Portland cement requires 40% of its own weight of water to hydrate. Of this, 25% is required for chemical reactions, which is non-evaporable, and undergoes shrinkage equivalent to 25% of the water volume. The other 15% water, known as gel water, is adsorbed onto the internal surfaces of the CSH gel and is evaporable under extreme conditions. The shrinkage of the CSH gel causes voids, known as capillary voids, which, dependent on conditions, may or may not form a connected network. Excessive water not required for hydration will occupy these capillary voids, which is normally regarded as the pore solution. On the other hand, if there is insufficient water un-reacted cement would remain [Bohris et al., 1998] (Fig. 4.1). The larger capillary pores (> 30 nm) are of particular importance with respect to the durability of concrete since they provide the major interconnected pathways along which aggressive substance may most readily penetrate the cement matrix from the environment.

In general, the overall porosity and proportion of capillary pores in hardened cement pastes (or concretes) decrease as the water/cement ratio (w/c) is reduced and as the degree of hydration is increased. These effects are reflected in the mechanical and physical properties of the material. To achieve high strength and, more importantly for durability, low permeability (Figs. 4.2 and 4.3), it is essential to minimise porosity by employing a mix of low w/c and ensuring that the material is cured for an adequate period in a moist environment [Power et al., 1954].

4.3 THE THEORY OF WATER TRANSPORT IN POROUS MATERIALS

By neglecting the effect of the ionic concentration on the bulk solution, when utilising the mathematical model described in Chapter 3 to simulate outer solution ingress into

unsaturated concrete, it can be simplified as water ingress. In literature, water flowing though a porous material can be caused by two factors: pressure gradient and capillary forces. The latter also is called wick action. For the first one, the process can be described mathematically by Darcy's Law [See e.g.Wang and Anderson, 1982; Probstein, 1989], according to which the velocity of water transporting in the pore is proportional to the gradient of water head. In general, this theory has a good application in hydrology engineering. For the second process, however, Darcy's Law gives nothing about the driving force, considering the fact that the capillary suction rate depends on the degree of saturation of the porous medium. Unsaturated flow theory [Philip, 1969] developed a physical assumption for capillary flow in unsaturated materials, which embodies the idea of Darcian flow in a porous material in response to the capillary force arising from its own pore structure at all fractional saturations. According to the theory, the mathematical modelling of water transport in porous materials is expressed in the extended Darcy equation [Hall, 1989]:

$$q = k(\theta)F_c(\theta) \tag{4.1}$$

where q is the water flow velocity, k is the hydraulic conductivity and F_c is the capillary force. Both k and F_c are dependent on the water content, θ [Martys and Ferraris, 1997]. In addition, the capillary force is associated with the gradient of the capillary potential, ψ, i.e.

$$F_c = -\nabla\psi(\theta) \tag{4.2}$$

Substituting Eq. (4.2) into (4.1) yields

$$q = -D_w(\theta)\nabla\theta \tag{4.3}$$

in which

$$D_w(\theta) = k(\theta)\frac{d\psi}{d\theta} \tag{4.4}$$

is called the hydraulic diffusivity. In problems involving gravitational effects, ψ and k need to be considered as a function of these gravitational effects. From this point, it is obvious that this theory unites the two factors controlling the water transport in porous materials. The expression of D_w is not well defined for concrete materials. For soils, however, it has been suggested as [Hall, 1989]:

$$D_w = D_0 \exp(B\theta_r) \tag{4.5}$$

where D_0 and B are the empirical constants, θ_r is the normalized water content defined by:

$$\theta_r = (\theta - \theta_0)/(\theta_1 - \theta_0) \tag{4.6}$$

where θ_0 is the initial water content which, for dry materials, is almost equal to zero and θ_1 is the water content at wetted surface, which is regarded as 1 in a water reservoir.

Although, Eq. (4.5) was originally proposed for soils [Brutsaert, 1979], it has been recommended as a universal equation for other engineering materials if the parameter B is given different values [Hall, 1989].

Applying the condition of mass conservation to the pore structure, the transient water content at any location can be determined by:

$$\frac{d\theta}{dt} = -\nabla q \tag{4.7}$$

Substituting Eq. (4.3) into (4.7), we have:

$$\frac{d\theta}{dt} = -\nabla(D_w \nabla\theta) \tag{4.8}$$

The hydraulic diffusivity D_w as a function of θ can be obtained experimentally. For ordinary Portland cement the following form was reported by Hall [1989]:

$$D_w = 0.49\exp(6.55\theta_r) \text{ (in mm}^2\text{/min)} \quad (4.9)$$

Using Eqs. (4.8) and (4.9) to simulate water transport in concrete, it is not necessary to consider the effect of the water adsorption or desorpation in the pore surface, as this factor has been considered in the hydraulic diffusivity with Eq. (4.9). The equation defines that the diffusivity decreases with the decrease in degree ofI saturation as shown in Fig. 4.4. This relationship reveals the fact that the water, which is in direct contact with solid pore surface at any location, is almost completely adsorbed by the pore surface.

4.4. MODELLING OF CHLORIDE INGRESS INTO CONCRETE

The problem of chloride ingress into a concrete, studied experimentally by Sergi, et al. [1992] is simulated here. The concrete cylindrical specimen is a hardened OPC paste with water/cement ratio 0.5 and its one end was exposed to a 1 mol/l *NaCl* solution saturated with $Ca(OH)_2$ for 100 days. The parameters and initial data used in the simulation are given in Table. 4.1. Ionic diffusivities in solution are assumed to be constants.

Considering the non-linearity of the relationship between the free and bound chloride contents, bound chloride was approximated by the Langmuir adsorption isotherm. The values of $\alpha = 1.67$ and $\beta = 4.08$ (l/mol) were obtained by Sergi, et al. [1992]. The ratio of evaporable water to cement, w, is assumed as 0.3.

To solve the governing equations described in Chapter 3, the program employs a separated two-step method. First the convection equation (4.8) is solved. When the transient saturation is determined, the next step is to solve the ionic governing equations (3.9). The influence of ionic concentrations on the solution convection is neglected in this model.

4.5. RESULTS AND DISCUSSION

Fig. 4.5 shows the solution content profile and the effect of solution ingress on the ionic profiles at an earlier stage. Compared with Fig. 4.6, which does not consider the effect of solution ingress by assuming a saturated specimen, Fig. 4.5 shows that the velocities of sodium and chloride penetration increase significantly but the concentration of potassium near surface becomes very low. This is caused by the ionic convection with solution. Because of the significant increase of sodium and chloride adsorption, hydroxyl level becomes very high near the surface to maintain charge balance in solution. It can be expected that, with the time elapse, similar front of ionic concentration profiles will present at further depths. The ionic convection will not cease until the concrete becomes saturated. It also can be noted that the process of saturation of concrete is not synchronous with the ions ingress. The ionic ingress is much slower than the process of saturation. This result is in agreement with experimental observation that has shown that the chloride front moved into the concrete at a lower rate than the water in which chloride was dissolved [McCarter, et al. 1992].

Fig. 4.7 shows the influence of electrostatic interaction between the dissolved ions on the ionic profiles. Comparing them with the result without considering ionic interaction ($\nabla\phi = 0$ in Eq. (3.9)), it can be seen that the ionic interaction has an impelling effect on chloride ingress. The consideration of ionic interaction presents an improved prediction on free and total chloride profiles, which are closer to experimental results. In addition, the hydroxyl distribution in concrete is also greatly affected by the ionic interaction. A fairly good prediction for this is presented by the model, which considers ionic interaction. Fig. 4.7c compares the prediction errors of the two models. It shows that with the consideration of ionic interaction, the average relative error for free chloride

prediction is 0.36; for hydroxyl it is 0.3. If the ionic interaction is not considered, the average relative errors for free chloride is 0.56 and for hydroxyl is 0.37. It can be calculated that the prediction error decreases by 37.5% and 18.9% for chloride and hydroxyl, respectively, when the interaction of ionic species in solution is considered.

Fig. 4.8 shows the combined effect of capillary suction and ionic coupling on the ionic profiles in concrete after 100 days. It can be seen that the capillary suction has a significant effect on the final distribution of ionic concentrations. Due to the convection of pore solution the ingress depth of sodium and chloride increases. Compared with the result where the effect of capillary suction is neglected ($\theta = 1$ in Eq. (3.9)), the present model provides a fairly good prediction, which agrees very well with experimental data of both free and total chlorides. Fig 4.8c compares the prediction errors. It can be seen that the effect of capillary suction on chloride, potassium and sodium profiles is much greater than on hydroxyl profile. For chloride ions, the proposed model presents a 0.17 average relative error, which is 52.8% less than that the model that considers only the effect of ionic interaction.

From the above discussions, it can be seen that ionic interaction in solution and the capillary suction of solution in unsaturated concrete have significant influence on the chloride ingress. The proposed model presents a fairly good prediction for the process. In literature, Fick's second law has been widely used to predict the process of chloride ingress [Sergi, et al., 1992; Chatterji, 1995], in which all these effects (tortuosity, chloride adsorption, ionic interaction and capillary suction) are taken into account by modifying the diffusion coefficient. This is why the value of the diffusion coefficient, which is called as apparent chloride diffusivity, used for concrete is much lower than

that for dilute solutions. In some references, the effect of chloride adsorption was isolated and was considered separately [Sergi, et al., 1992; Wee, et al., 1997; Martin-Perez, et al., 2000]. In experiments, because of the variation of experimental conditions and concrete specimens, it leads the chloride diffusivity measured to be widely scattered [Yu and Page, 1991; Andrade, 1993; Dhir and Byars, 1993; Andrade, et al., 1994; Gjorv, et al., 1994; Ngala, et al., 1995; Bentz, et al., 1996; Ahmad, et al., 1997]. This will create difficulties in practical applications. In the proposed model, the ionic diffusivities are defined with respect to the pore solution, which is independent of the quality of concrete and the experimental conditions. The parameters used in the model such as tortuosity, porosity, initial saturation can be determined for a given material by using simple, standard experimental measurements and they have stable values [Sharif, el al., 1997]. The comparisons of the results from the proposed model and those from others are given in the following.

Figs. 4.9 shows the free and total chloride profiles predicted by using the proposed model, the Fick's second law, and the model considering only the effect of chloride adsorption [Sergi, et al. 1992], respectively. Fig. 4.9a shows that when the apparent chloride diffusivity is 1.35×10^{-11} (m^2/s), which is about 87% less than the diffusivity in dilute solution, a reasonable good prediction is provided by the Fick's second law. When the chloride diffusivity is 4.28×10^{-11} (m^2/s), which is about 58% less than the diffusivity in dilute solution, the model considering specifically the effect of chloride binding presents a very similar result as that of the proposed model. Figs. 4.9c show the comparison of the prediction errors in the three models. It can be seen that the average relative errors of the three models are very close, particularly those in the proposed model and the model considering only the effect of chloride binding are very close.

4.6. CONCLUSIONS

A comprehensive mathematical model has been used to simulate the process of chloride ions ingress into concrete from a saline environment. Compared with Fick's second law and another existing model, the present model has a distinct capacity to deal with the problem of chloride ingress from environments into unsaturated concrete structures. The numerical results of the model demonstrate that the initial bulk convection caused by the unsaturation of concrete and the ionic electrostatic interaction in the solution have significant influence on the chloride distribution profiles. The results also confirm that the chloride adsorption by solid phase has an important influence on the ionic distribution in concrete. Mathematical model, which considers the adsorption specifically but incorporates other influences into chloride diffusion coefficient, also can provide good results.

Compared with other models, the proposed model not only has presented a fairly good result, but also has made itself applicable to different cases with unified ionic diffusivities. This can make the model more standard because it considers the influence factors on the process specifically and the parameters introduced are directly related to the concrete quality and condition, which can be easily determined by standard experimental measurements.

Table 4.1 Parameters and initial data of specimen

	K	*Na*	*Cl*	*OH*	*Ca*
Ionic Diffusion Coefficients in solution (m^2/s)	$3.9x10^{-11}$	$2.7x10^{-11}$	$1.02x10^{-10}$	$5.28x10^{-10}$	$1.6x10^{-11}$
Initial concentration (mol/m^3)	100	285	0.0	385	0.0
θ_0	0.8/1.0				
τ	1.9				
ε	0.11				
w	0.3				

Fig. 4.1 The calculated percentile volumes of different components in fully hydrated Portland cement pastes prepared with w/c ratio of 0.5 (left) and 0.3 (right) [Bohris et al., 1998]

Fig. 4.2 Relation between water permeability and w/c for mature hydrated cement pastes [Page, 1998a]

Fig. 4.3 Relation between water permeability and curing time hydrated cement pastes (w/c: 0.7) [Page, 1998a]

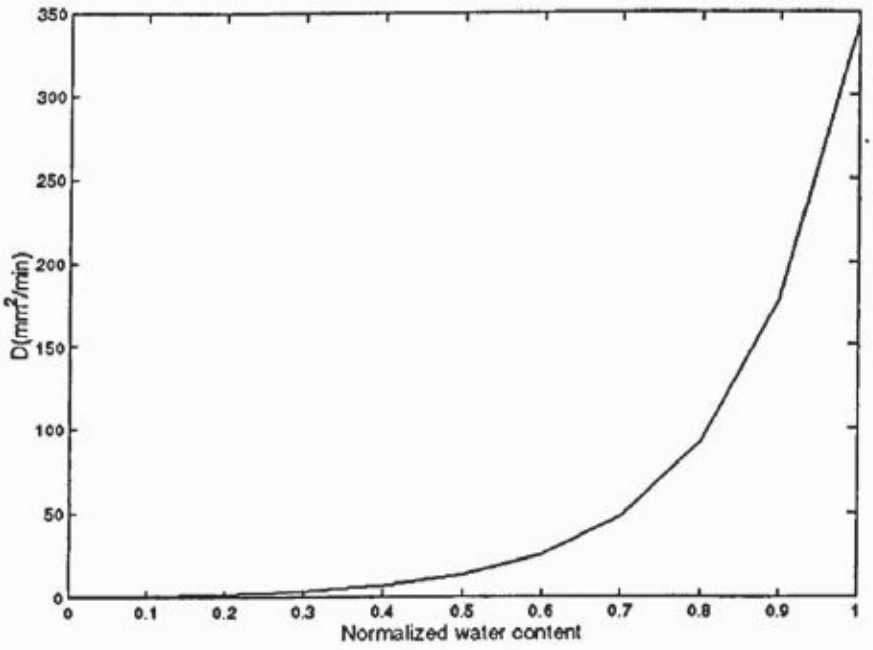

Fig. 4.4 The variation of hydraulic diffusivity with saturation

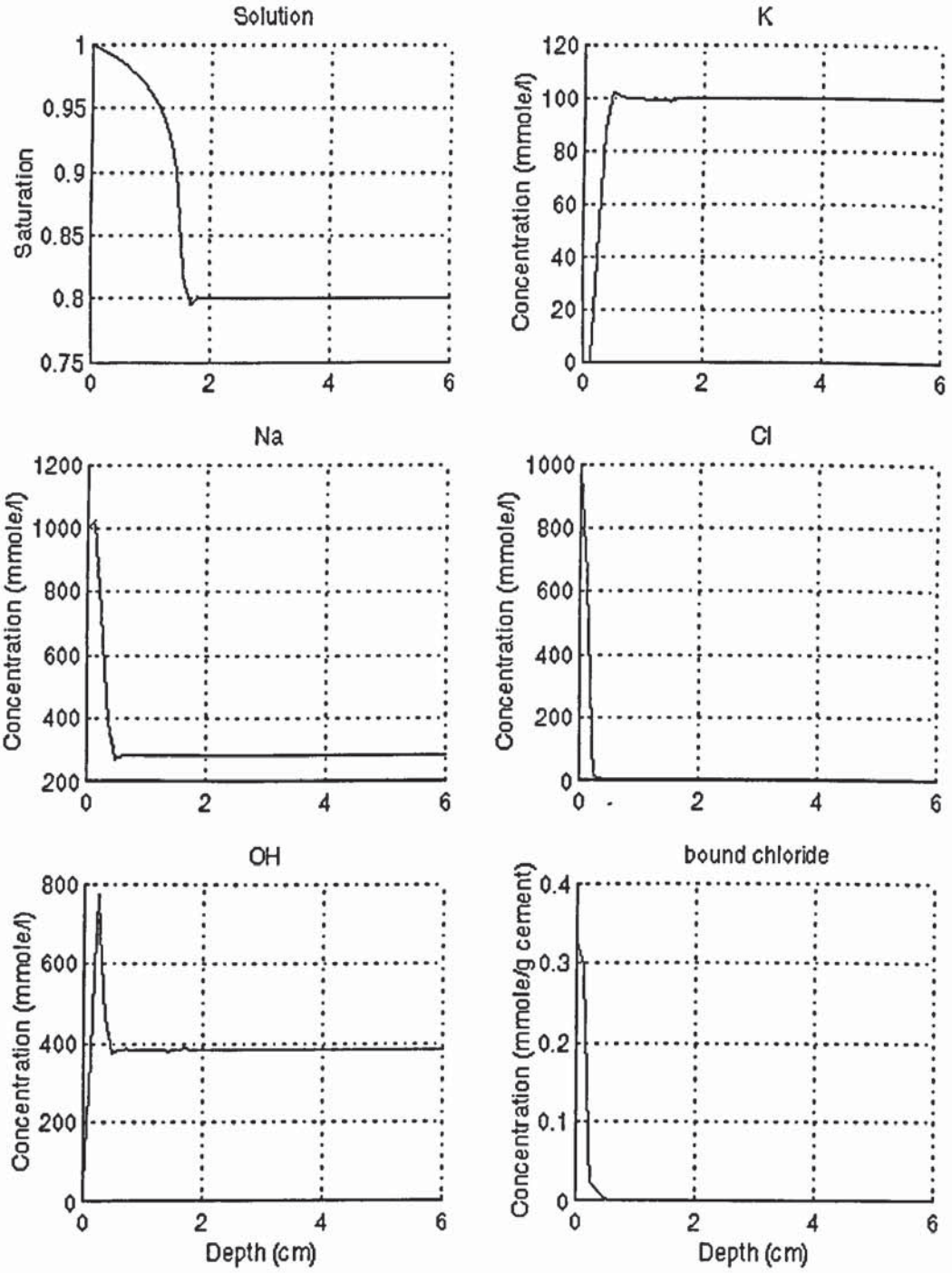

Fig. 4.5 Saturation of pore structure and ionic concentration profiles after 5 minutes exposure to a saline solution ($\theta_0 = 0.8$, $\tau = 1.9$)

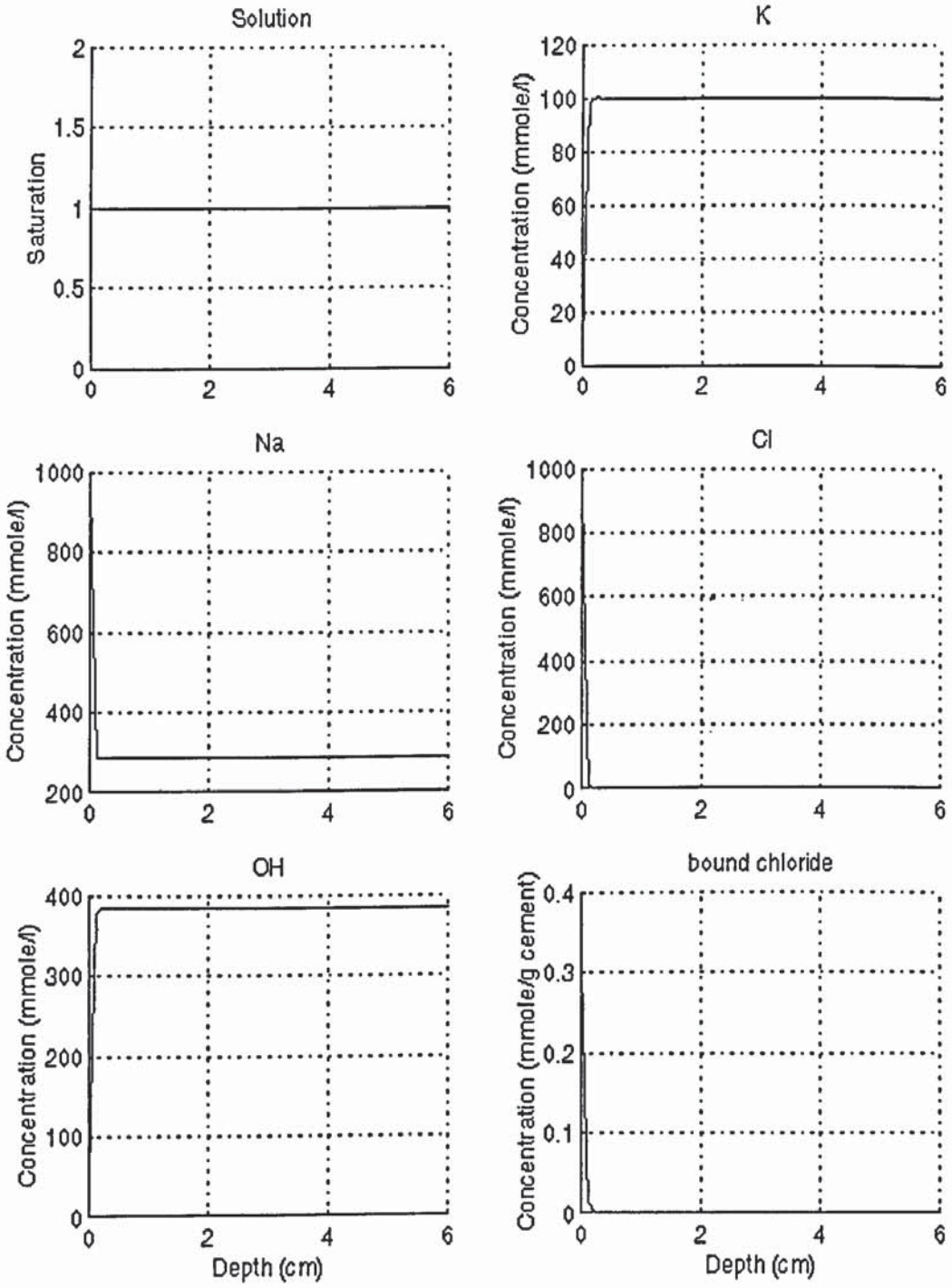

Fig. 4.6 Ionic concentration profiles after 10 minutes exposure to a saline solution

($\theta_0 = 1.0$, $\tau = 1.9$)

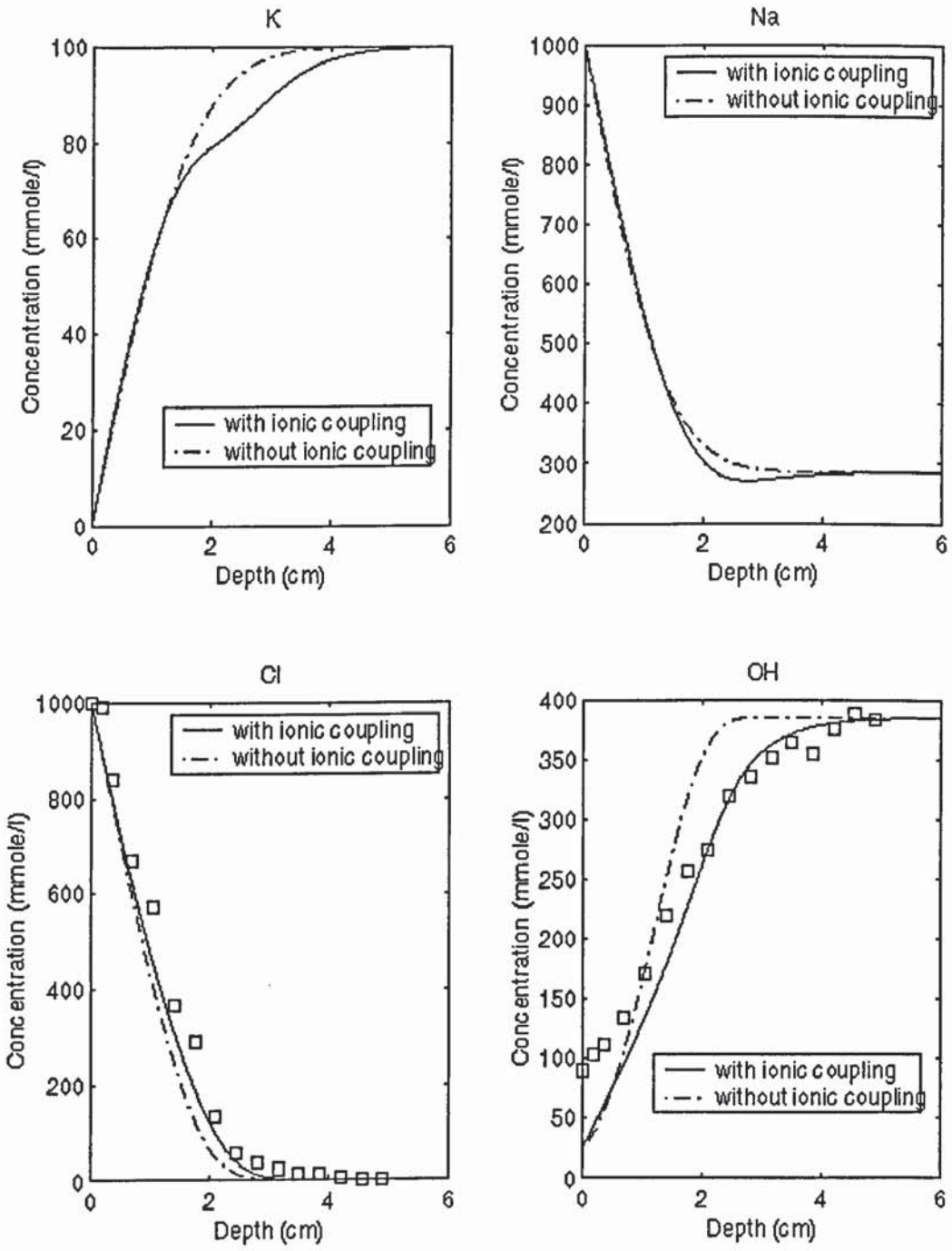

Fig. 4.7a Ionic concentration profiles after 100 days exposure to a saline solution

($\theta_0 = 1.0$, $\tau = 1.9$)

□ is the experimental data

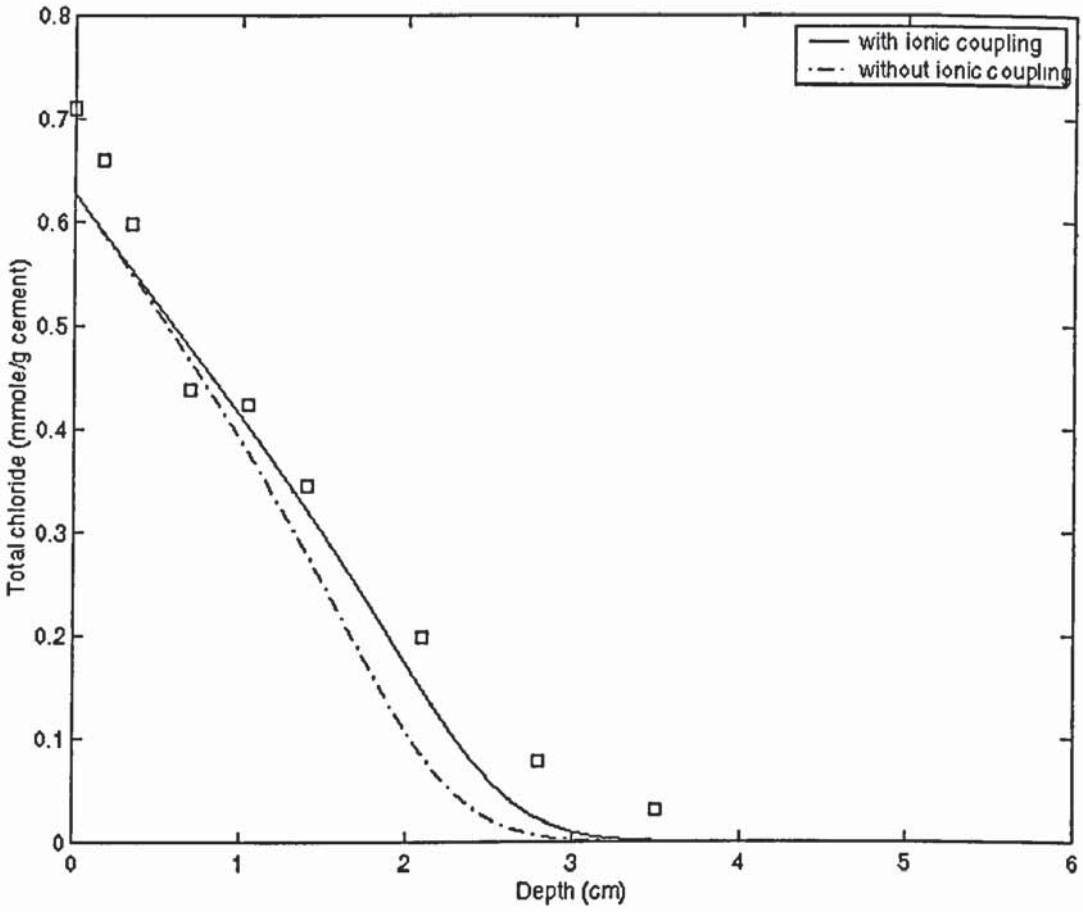

Fig. 4.7b Total chloride concentration profiles after 100 days exposure to a saline solution

($\theta_0 = 1.0$, $\tau = 1.9$)

□ is the experimental data

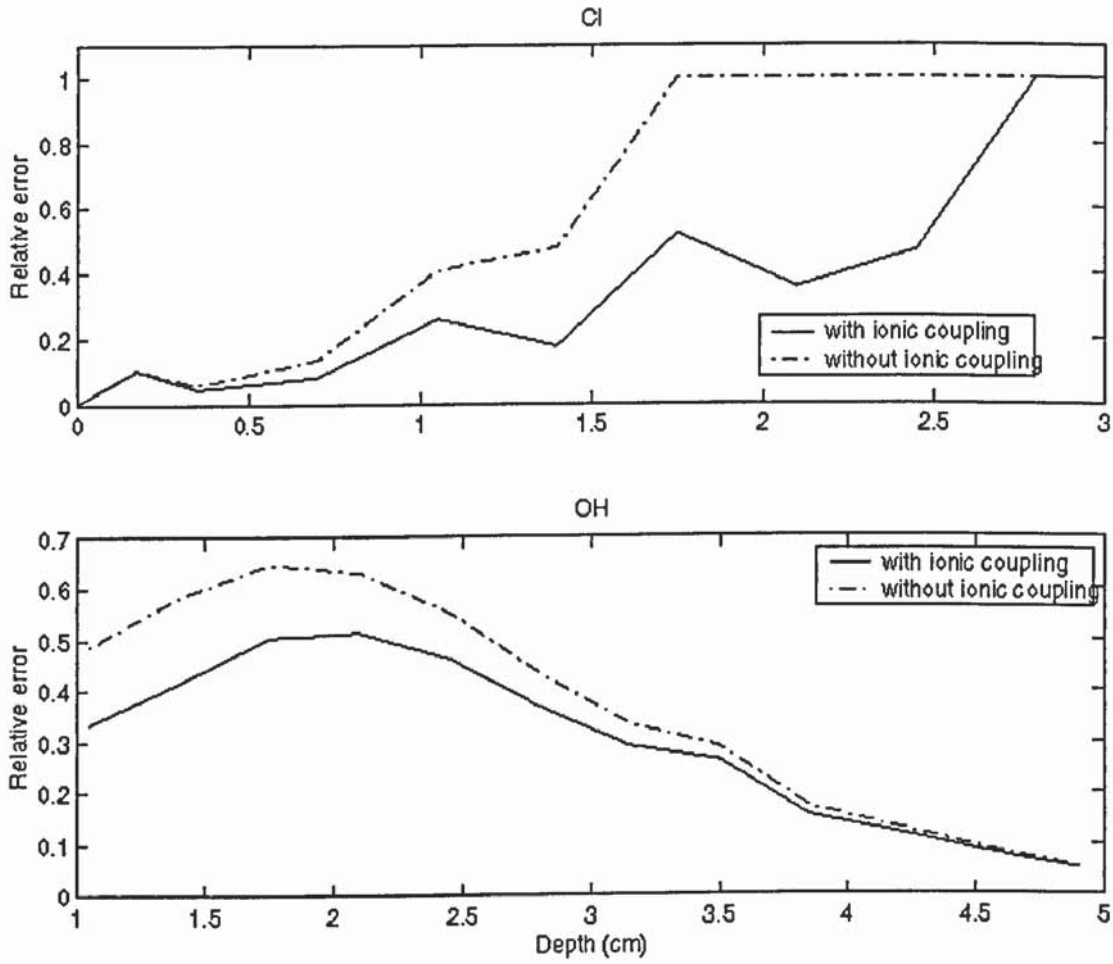

Fig. 4.7c Comparison of relative errors, which are defined as:

| Numerical data – Experimental data | / Experimental data

($\theta_0 = 1.0$, $\tau = 1.9$)

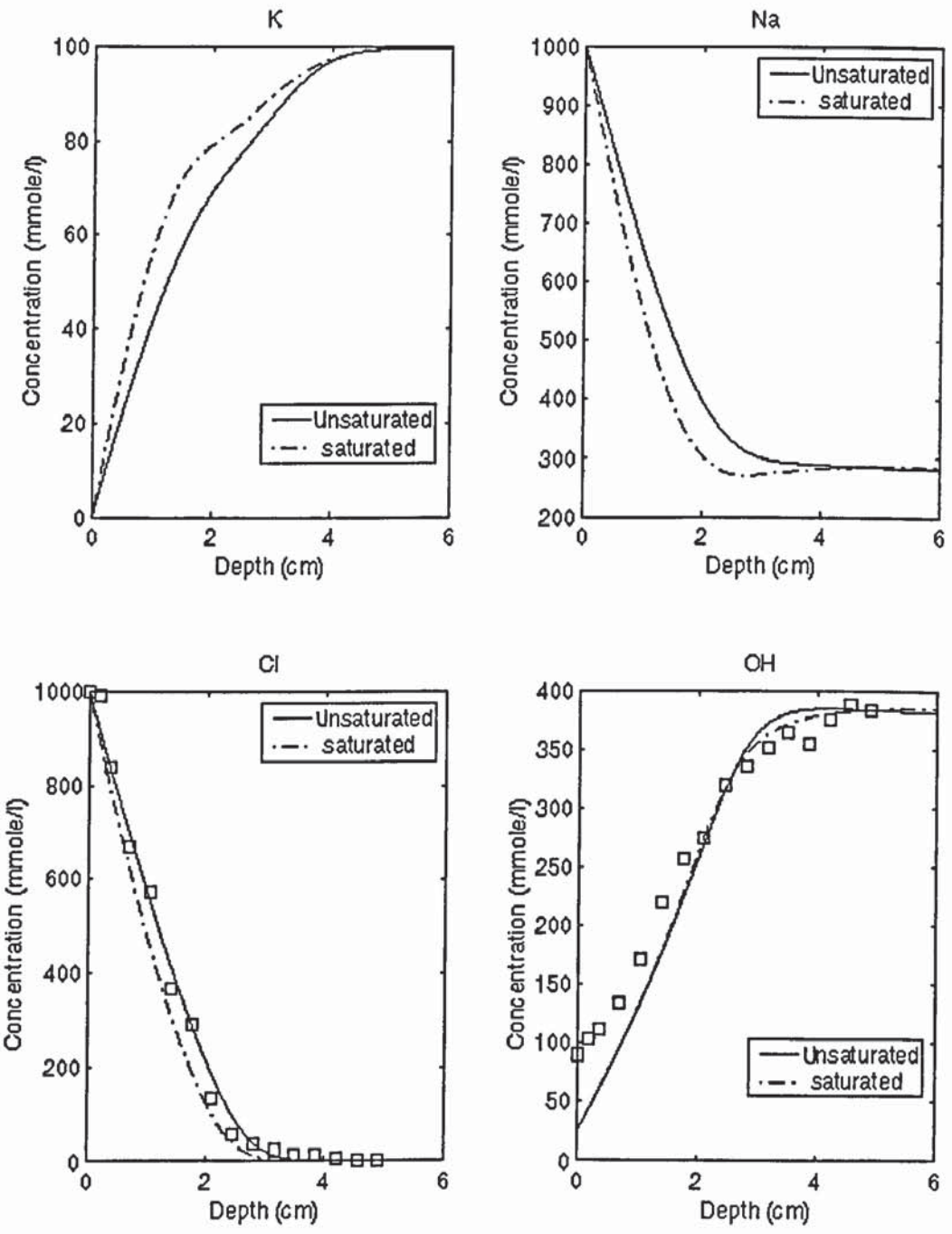

Fig. 4.8a Ionic concentration profiles after 100 days exposure to a saline solution

($\nabla\phi \neq 0$, $\tau = 1.9$)

□ is the experimental data

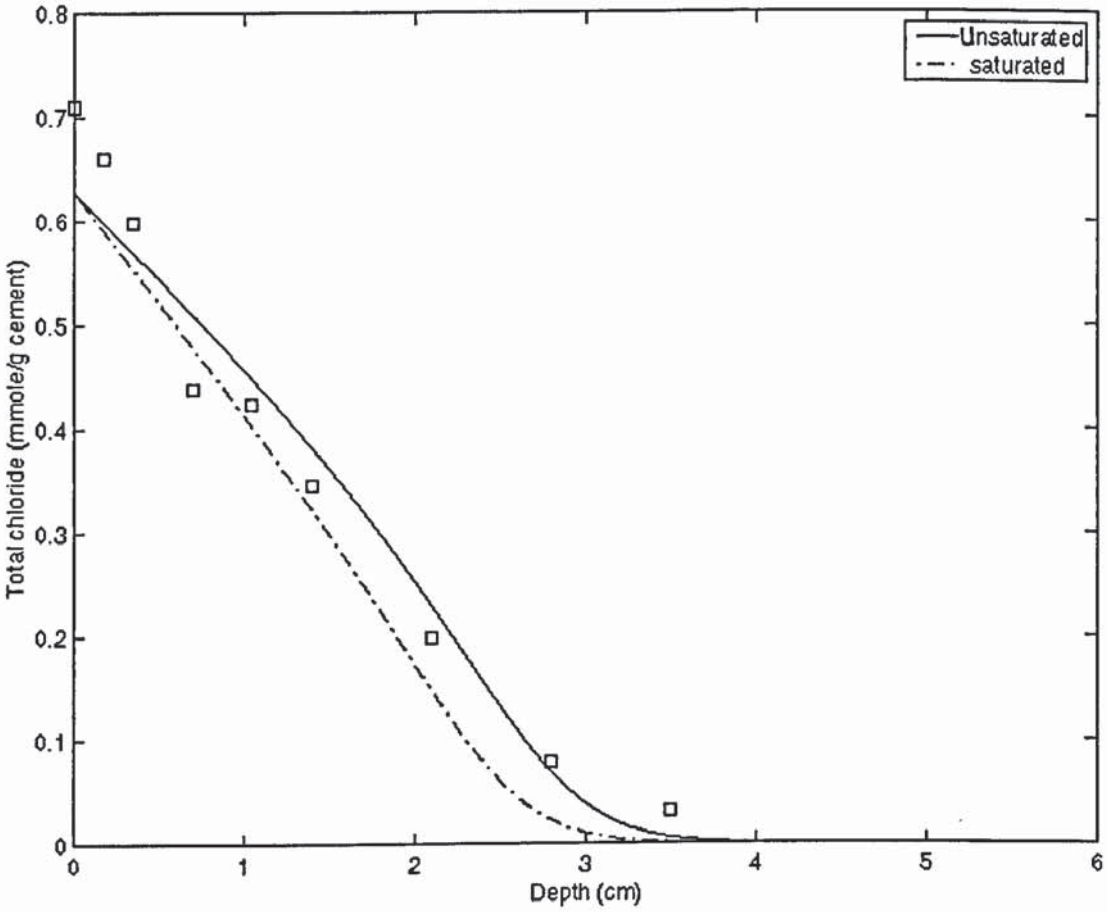

Fig. 4.8b Total chloride concentration profiles after 100 days exposure to a saline solution

($\nabla\phi \neq 0$, $\tau = 1.9$)

□ is the experimental data

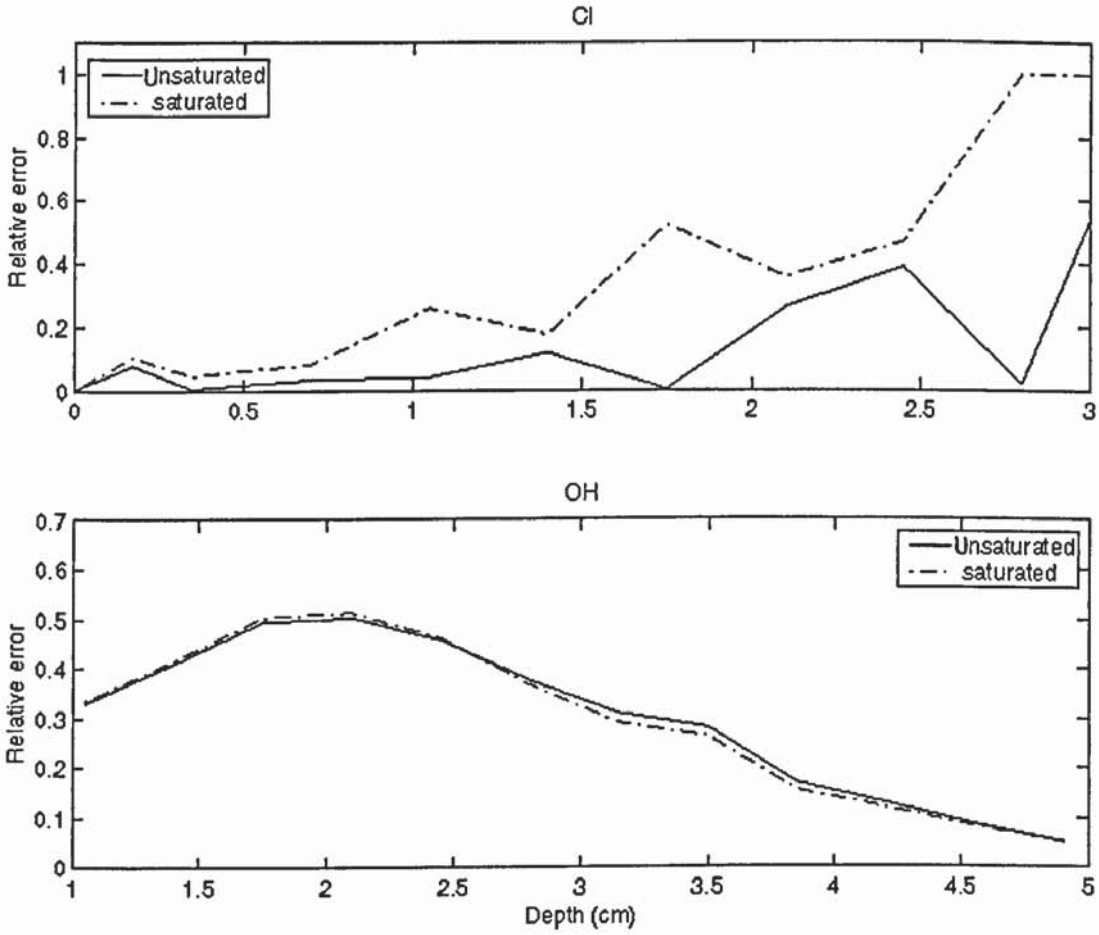

Fig. 4.8c Comparison of relative errors, which are defined as:

| numerical data – experimental data | / experimental data

($\nabla\phi \neq 0$, $\tau = 1.9$)

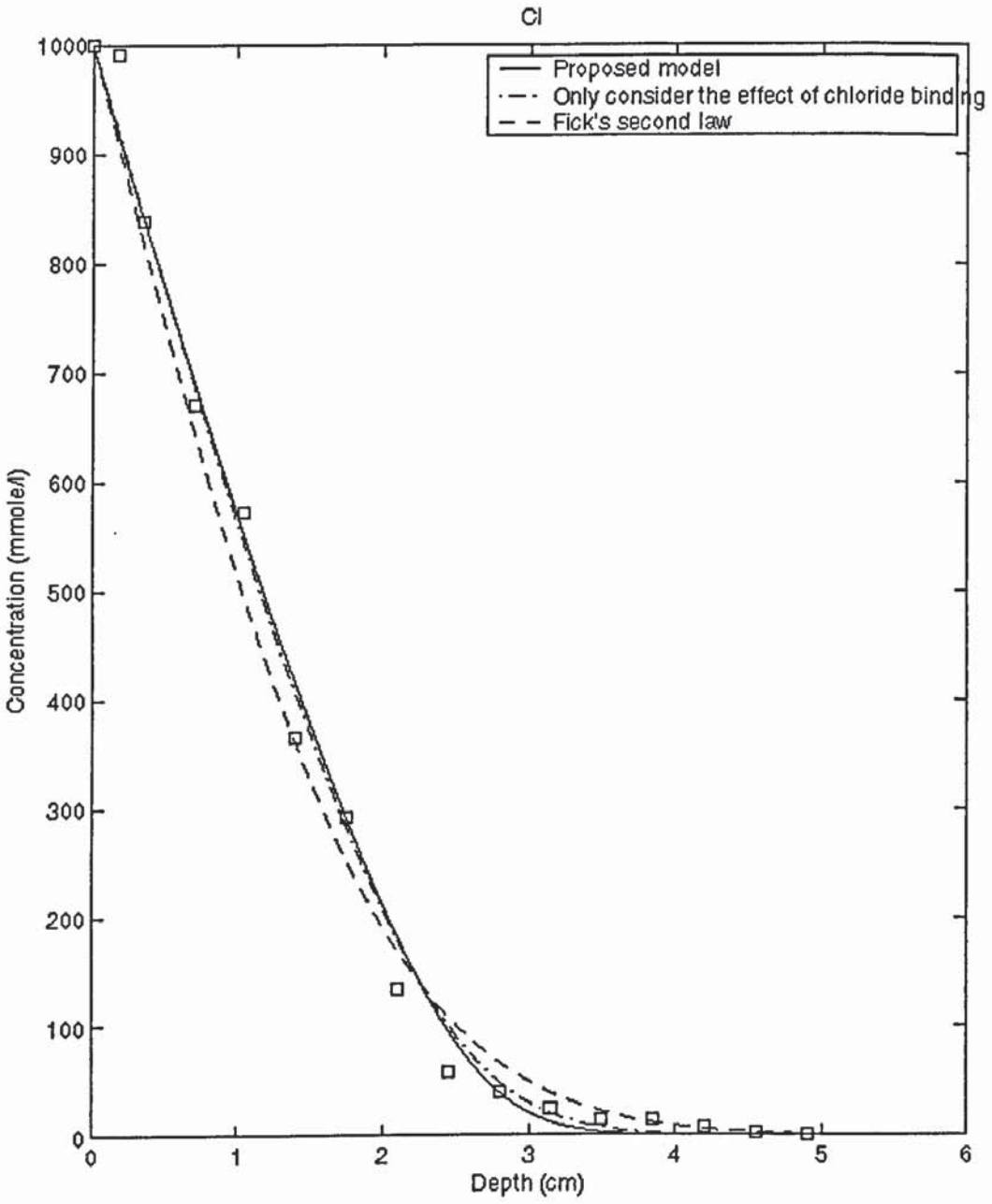

Fig. 4.9a chloride concentration profiles predicted by three models

□ is the experimental data

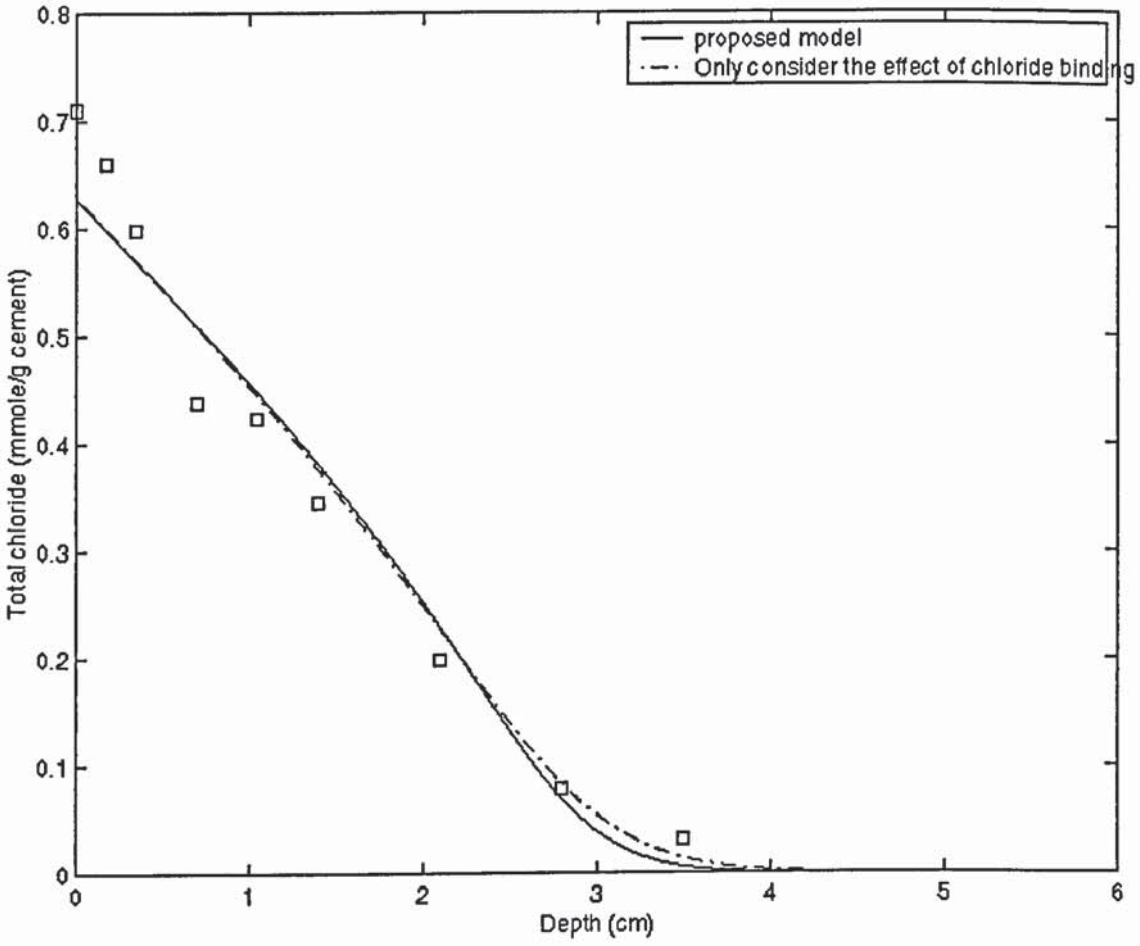

Fig. 4.9b Comparison of total chloride concentration profiles

□ is the experimental data

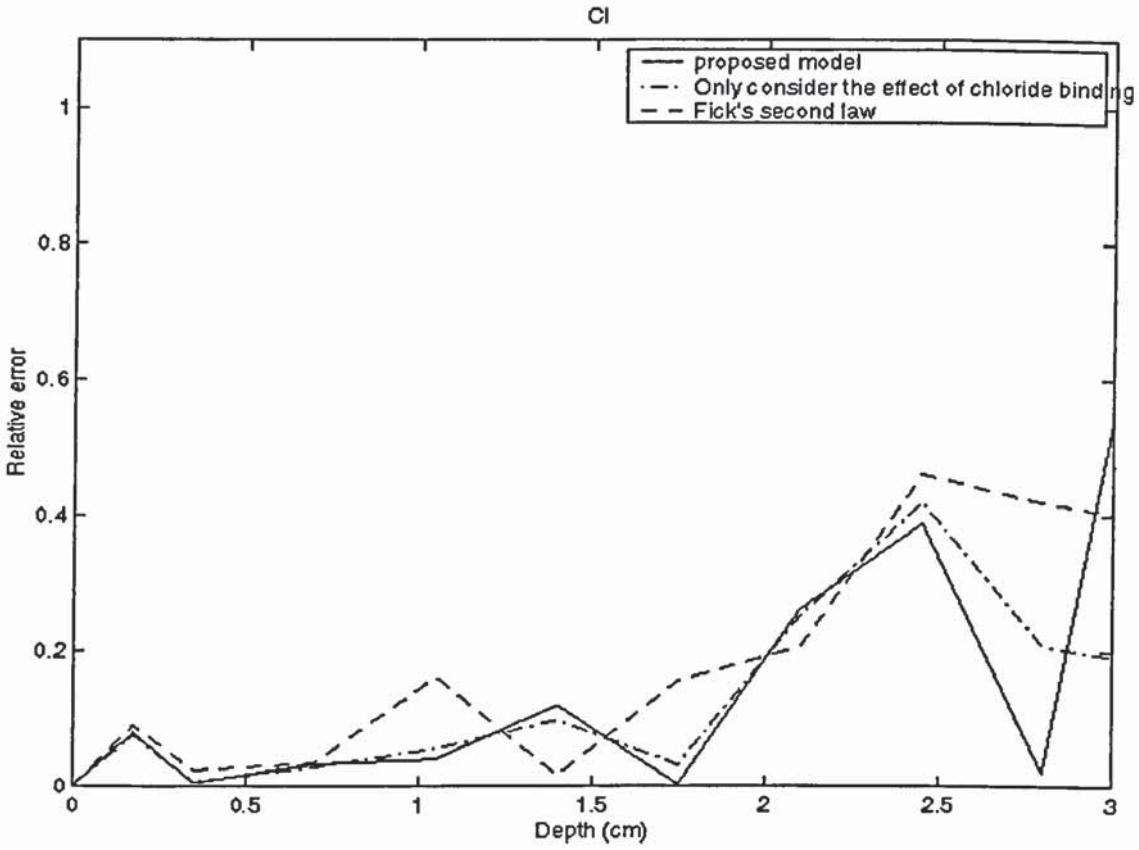

Fig. 4.9c Comparison of relative errors in the predictions of three models

CHAPTER 5

IONIC REDISTRIBUTION IN THE PROCESS OF ECR

5.1 INTRODUCTION

In this chapter, the model described in Chapter 3 is applied to simulate the process of chloride removal from concrete under the condition that a constant density D.C. current is applied through the reinforcing steel and an external anode placed in a suitable electrolyte at the surface of the concrete. The first example in this chapter is to test the model by comparing its predictions with the results of a one-dimensional experiment. After that a two-dimensional modelling is presented. The study is focused on the ionic redistributions during the process of ECR with different current densities and different periods. It is also evaluated that the effectiveness and efficiencies of ECR in removing chloride ions at different current densities and in different cases where the placement of external anode is different.

5.2 ONE-DIMENSIONAL MODELLING OF ECR

In order to validate the model, a one-dimensional problem that has been studied experimentally is simulated here. The comparison of numerical predictions with the experimental results is presented.

5.2.1 Experiment Simulated

To investigate the effects of the ECR process on reinforced concrete, an experiment of rectangular prism specimens of hydrated cement paste containing sodium chloride, subjected to electrolysis between centrally embedded steel cathode and an external anode of activated titanium was carried out by Bertolini et al. [1996]. Fig. 5.1 shows the

experimental arrangement. The specimens were made to contain evenly 1.0% chloride by mass of cement by adding *NaCl* to the mix water. The cathodic current densities were galvanostatically controlled at the values of 0.005, 1 and 5 A/m^2, respectively, while the durations of polarisation are 4, 8 and 12 weeks. The experimental results showed the changes of the ionic concentration profiles in the pore solution phase and changes of total chloride content with applied current densities and treatment durations. It was found that higher current densities not only caused the free and bound chloride content in specimens to decrease with time, but also produced major increase of alkali concentrations in the pore solution near the embedded steel.

The above experiment is simulated by using the developed finite element program FEAECR based on the mathematical model described in Chapter 3. Detailed information about the computer program will be presented in Chapter 9. In this study, the concrete specimens are considered to be saturated so that the ionic convection with the solution is neglected. The chemical species involved are assumed to be potassium, sodium, hydroxyl, chloride and calcium. Sulphide and other possible ionic species are not considered here because their concentrations are likely to be very low when compared to the all five ionic species listed. The parameters used in the simulation are assumed as $\tau = 2.0$, $\varepsilon = 0.11$, $w = 0.3$ (evaporable water content in concrete). The initial ionic concentrations are listed in Table. 5.1. Ionic diffusion coefficients in the solution are the same as those used in Chapter 4.

The relationship between free and bound chlorides is assumed to follow the Langmuir isotherm, in which $\alpha = 0.42$ and $\beta = 0.8$ (l/mol) are taken according to the experimental data [Li and Page, 2000].

During the process of ECR, chloride ions are transported out of the concrete and collected in the external electrolyte reservoir. For the case where the electrolyte reservoir is very large or the anode is flushed constantly with potable water, the boundary conditions at anode for determining ionic concentrations can be simplified to $C_i = C_{i0}$, where C_{i0} is the ionic concentration in the external solution. The boundary conditions on those where there is no anode and cathode are assumed to have zero flow for the current and zero fluxes for all ionic species.

5.2.2 Results And Discussions

Figs. 5.2-5.4 show the concentration distribution profiles of potassium, sodium, chloride, and hydroxyl ions within pore solution at three times when the specimens are subjected to current densities of 0.005, 1 and 5 A/m^2, respectively. The effect of the release of bound chloride in the solid phase of the concrete has been taken into account. The solid lines with symbols are the experimental results. The concentration profiles of calcium ions are not given here. This is partly because they can be calculated directly in terms of the electroneutrality condition or the solubility equilibrium condition and partly because they are significant only in the region close to the anode.

The results show that at the lowest current density, 0.005 A/m^2, the concentrations of all the ions have little variation with the distance away from the steel cathode except near the anode, where significant depletion of chloride and hydroxyl is observed. At a current density of 1 A/m^2, however, there is significant enhancement of the concentrations of sodium, potassium and hydroxyl ions in the vicinity of the steel cathode, particularly after the specimens have been polarized for 12 weeks. Concentrations of chloride ions are also reduced progressively over the length of the specimens. Polarization at the highest current density of 5 A/m^2 caused similar but much more pronounced changes than those observed at 1 A/m^2. The modelling results are in reasonable agreement with the experimentally measured data.

It may be seen from Figs. 5.3 and 5.4 that, in contrast with the two cations and hydroxyl ions, chloride ions have a lower concentration in the vicinity of the steel than in the other region. The effects of polarization time on the change of free chloride concentration are significant as shown in Fig. 5.4. Chloride concentration, particularly near the steel, tends to decrease with the increase of polarization time, indicating that dissolved chloride ions are removed from the pastes by the migration under the influence of driving force of applied electrical field. It can be noticed that during the first four weeks the chloride removal is rapid but in the later time, the chloride removal

becomes slow. This means that the efficiency of this process becomes lower after a certain time.

Figs. 5.5-5.7 show the numerical results without considering the effect of chloride binding. Comparing with the experimental results, it can be seen that the chloride content in solution is under estimated significantly in the case where a high current density of 5 A/m^2 is used and bound chloride release is neglected. It can also be seen that bound chloride release has much less influence on the concentration distribution profiles of potassium, sodium and hydroxyl than that of chloride. In reality, in the process of ECR, the bound chloride will be released into the pore solution as the requirement of the balance between free and bound chlorides. A detailed discussion on the mathematical model for the chloride binding is presented in Chapter 6.

5.3 TWO-DIMENSIONAL MODELLING OF ECR

In this section, we will investigate the two-dimensional ionic concentration redistribution in the process of ECR, which has a practical significance. As there are no experimental measurements available, only numerical predictions are presented. The discussion will still mainly focus on the influence of treating periods and current densities.

5.3.1 Cases Studied

Two cases in which a rectangular prism specimen of hydrated cement paste containing sodium chloride with a centrally embedded steel bar subjected to the treatment of ECR are investigated. In case one an external anode is placed on the one side of the paste (see Fig. 5.8a), while in second case, two external anodes are placed on both sides of the paste (see Fig. 5.8b). For convenience, the initial concentrations of all ionic species are assumed to be constants having the values shown in Table 5.1. Ionic diffusion coefficients in solution are the same as those used in Chapter 4. The other parameters used in the numerical study are assumed as that $w = 0.35$, $\alpha = 1.67$, and $\beta = 4.08$ (l/mol)

here [Li and Page, 1998a]. The treating current densities on the surface of the steel bar are assumed to be 0.001, 3, and 5 A/m^2, respectively.

For the two-dimensional modelling, the components of the gradient of electrostatic potential can be calculated in terms of Eq. (3.10), in which the current density components, I_x and I_y, need to be determined in advance. Because of the condition of electroneutrality, the current density satisfies the following equation:

$$\nabla \boldsymbol{I} = 0 \tag{3.7}$$

which is equivalent to solving the following Laplace equation:

$$\nabla^2 \varphi = \frac{\partial^2 \varphi}{\partial x^2} + \frac{\partial^2 \varphi}{\partial y^2} \tag{3.8}$$

where $I_x = \frac{\partial \varphi}{\partial x}$, $I_y = \frac{\partial \varphi}{\partial y}$, and φ is a potential function of the current density.

The boundary conditions at anode and cathode for determining the distribution of current density are defined by the condition of φ = constant under the assumption that no current flow between locations on the metal surface.

5.3.2 Numerical Results Of The Current Density Distribution

Fig. 5.9 shows the profiles of potential function, φ, and the distribution of their corresponding current densities in case one and case two corresponding to a current density 5 A/m^2, where arrows represent the directions of current and the length of arrows represent the magnitude of the current density at that position. Because the structure is symmetrical, only half of the structure is presented here. Similar results were found for the current densities of 0.001 and 3 A/m^2. The results show that in case one, the current densities behind the reinforcement are very small because the gradients of potential function there are also very small. This region, in reference [Hansson and

Hansson, 1993], is referred as 'stagnant' region in which the driving force for migration is negligibly small. Thus, chloride ions will not be easily driven out of this area as a result of the applied electrical field. In case two, a symmetrical current distribution is produced, so the 'stagnant' region is prevented.

It can be seen that the highest current density is at the surface of steel bar and that the current density distribution along the surface of steel bar is not even.

5.3.3 Numerical Results Of The Ionic Redistribution

Figs. 5.10 and 5.11 show the concentration profiles of each ionic species in pore solution in case one and case two, respectively, when the paste is subjected to a constant current density of 0.001 A/m^2 at the steel bar for four, eight and twelve weeks, respectively. A significant drop of ionic concentrations is observed near the anode. There is no obvious ionic concentration change in the region near the steel bar. Because the current density applied is so small, the removal of chloride is mainly caused by the diffusion due to the concentration gradient near the anode. This diffusion process is rather slow.

With the increase of the applied current density, the influence of the migration of the ionic transport increases. Figs. 5.12 - 5.13 show the ionic concentration profiles at four, eight and twelve weeks in case one and case two, respectively, when the paste is subjected to a constant current density of 3 A/m^2 at the steel cathode. It can be seen that chloride ions moved significantly away from the steel bar to the external anode, whereas potassium and sodium ions moved in the opposite way towards the steel bar. The concentration of chloride ions is reduced progressively in the vicinity of the steel bar with the time, where the chloride ions have a lower concentration than in other regions. In the same area, a significant enhancement of the concentrations of potassium, sodium and hydroxyl ions is observed. Compared with Fig. 5.13, Fig. 5.12 shows that the ionic concentrations in the region far behind the steel, the 'stagnant' region, have little change. In both cases, the chloride concentration profiles display a saddle shape, which is in agreement with the experimental observation [Sa'id-Shawgi, et al., 1998]. This saddle shape of chloride concentration profiles has a negative influence, which may

cause the re-migration and lead chloride back to the steel bar when the treatment stops. Figs. 5.14 - 5.15 show similar but more pronounced changes of ionic concentrations when the current density is increased to 5 A/m^2.

Figs. 5.16 and 5.17 show the distribution of free chloride concentrations and pH values of pore solution along the surface of steel bar after 12 weeks treatment in the above two cases. It can be seen that the level of free chloride concentration at the surface of steel bar is reduced when treating current density increases, while the level of pH value at the surface of steel bar increases. In case one, the distribution of free chloride concentration and the pH value along the surface of steel bar is not uniform. It can be seen that there are the lowest free chloride concentration and the highest pH value at the site closest to the external anode. But in case two, the distributions of free chloride and pH value are almost uniform along the surface of steel bar. It also can be seen that in both cases the average levels of free chloride concentration and pH value at the surface of steel bar are almost the same.

Fig. 5.18 shows the variation of the average ionic concentrations at the surface of steel bar during the process of ECR at the current density of 5 A/m^2 in case two. It clearly shows that, after four weeks, the rate of decrease of chloride concentration becomes very slow, but the concentration of hydroxyl still has a significant increase.

The effectiveness and efficiency of chloride removal may be assessed from Fig. 5.19, which shows the average chloride concentration left in the bulk pore solution and the average chloride removed at the end of each period of treatment with different current densities for the two cases. The results indicate that case two has a better chloride removal effectiveness and efficiency than case one for the same current density. In both cases, more chloride is removed in the earlier period, however, after a certain time, the efficiencies become lower. For both cases, the efficiency referring to time (week) will be enhanced with the increase of the treating current density. Fig. 5.20 compares the average chloride removed by a unit current in a week. It can be seen that case two has a better efficiency than case one. In both cases the efficiencies decrease with time. It also can be seen that, in both cases, the average chloride concentration removed by unit current in every week will decrease as treating current density increase.

5.4 CONCLUSIONS

From the studies conducted in this chapter, it can be seen that electrochemical chloride removal can be reasonably well simulated by the mathematical model described in Chapter 3. This model reveals that the chloride binding is a very important factor in the process of ECR and, if it is neglected, the content of chloride in pore solution will be highly underestimated.

It is found that the ECR process is capable of removing free and bound chloride quite effectively. A higher current density and a longer treating time will remove more chloride ions and generate a higher local alkalinity particularly in the region near the steel bar. However, this may result in an enhanced risk for alkali-aggregate reaction.

Two-dimensional modelling of the ECR process shows that the position of external anode plays an important role in the removal of chloride, because the position of external anode is directly related to the distribution of current density in concrete. The more expansive the distribution of current density is, the less is the 'stagnant' region. This will cause more chloride to be removed.

An un-symmetrical treatment will cause the distributions of free chloride concentration and the pH value of pore solution along the surface of steel bar not to be uniform. At the end of the ECR process, the chloride concentration profile in bulk solution has a saddle shape. This implies that there will be a re-migration of chloride back to the steel bar after the ECR process.

The position of external anode also influences the efficiency of the ECR process. Increasing the contacting area of external anode with concrete surface will enhance the efficiency of ECR. During the process of ECR, the efficiency of chloride removal will decrease with the treating time. The efficiency referring to the treating time will increase when the treating current density increases, but the efficiency referring to the unit electrical current will decrease when the treating current density increases.

Table 5.1. Initial concentrations and diffusion coefficients

	Potassium	Sodium	Chloride	Hydroxyl	Calcium
External solution (mol/l)	0.005	0.005	0.01	0.0252	0.0126
Pore solution (mol/l)	0.1	0.9	0.38	0.62	0.0

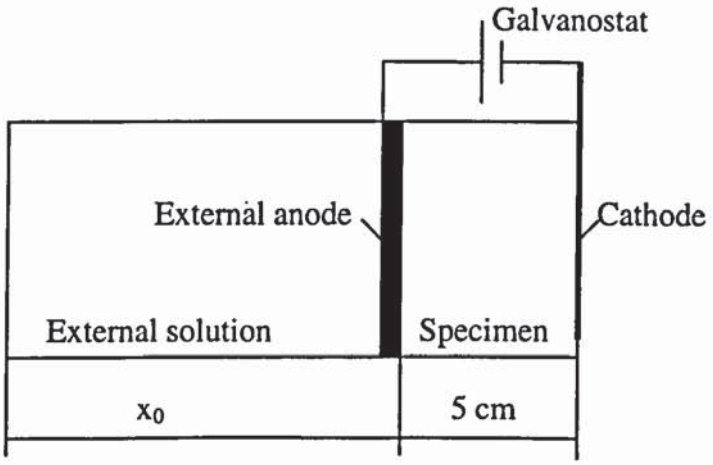

Fig. 5.1 Arrangement for galvanostatic polarization

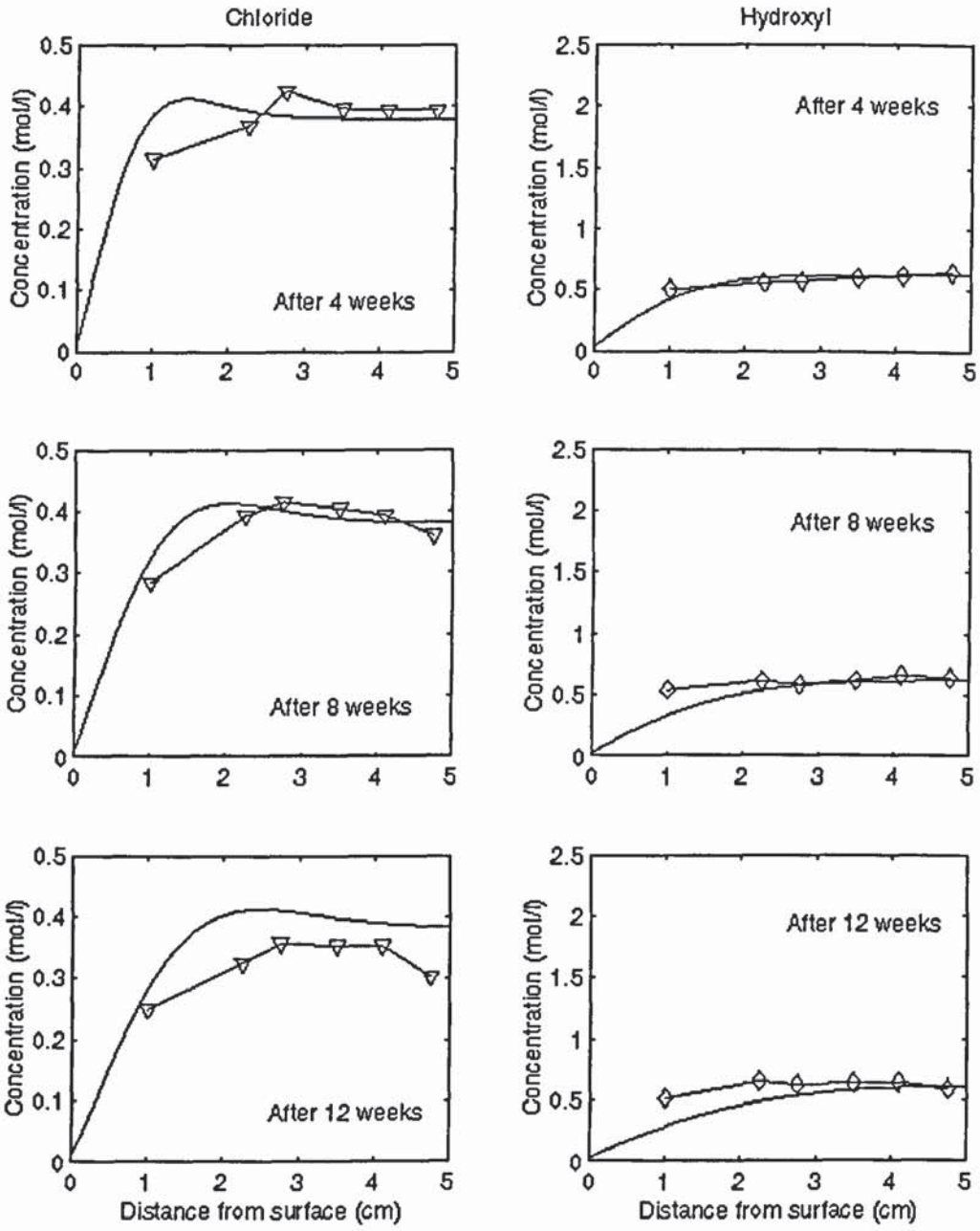

Fig. 5.2a Ionic concentration profiles in pore solution of cement paste with 1% chloride addition

($I = 0.005$ A/m^2)

–: numerical results, ∇: experimental results

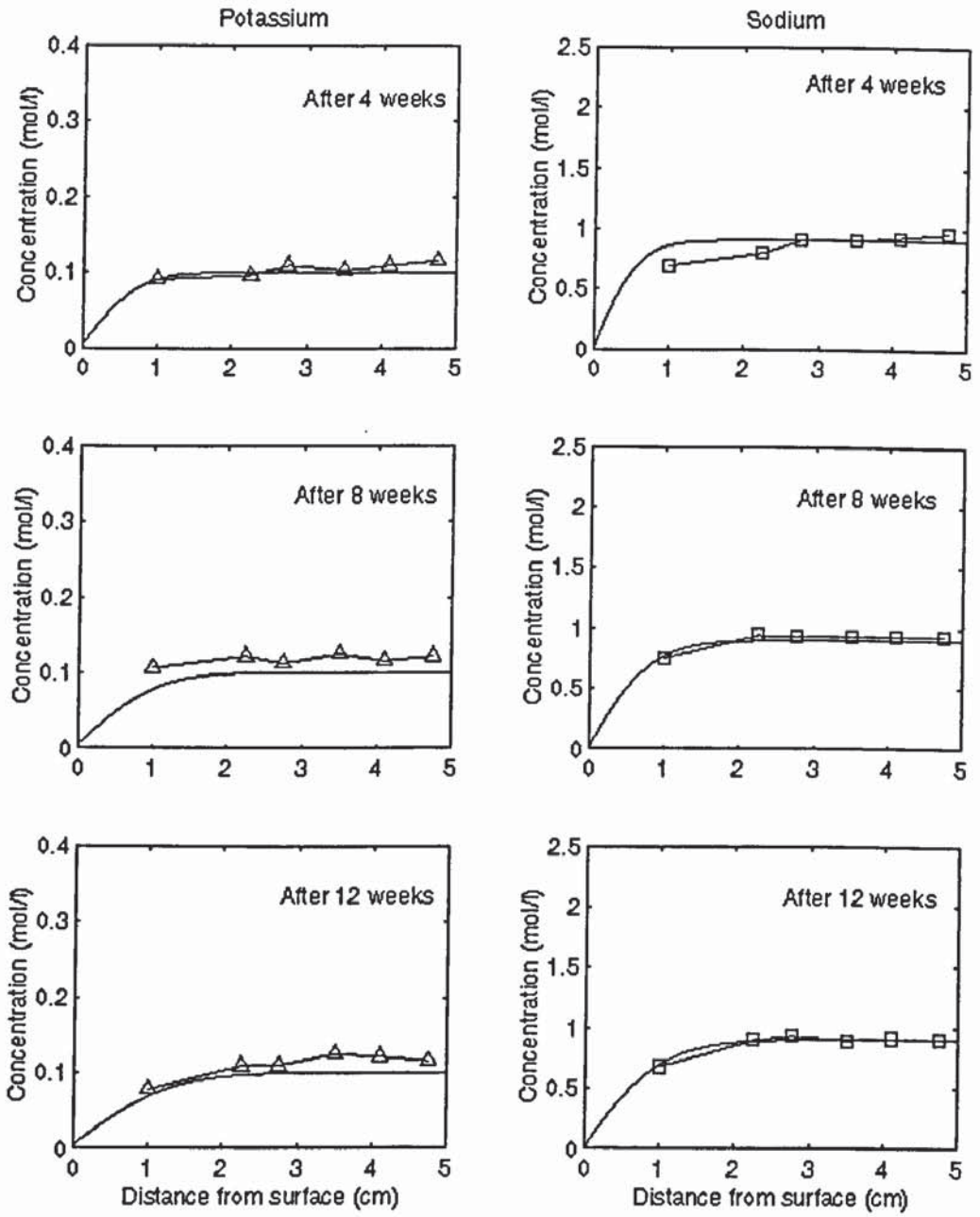

Fig. 5.2b Ionic concentration profiles in pore solution of cement paste with 1% chloride addition

($I = 0.005$ A/m^2)

–: numerical results, ∇ : experimental results

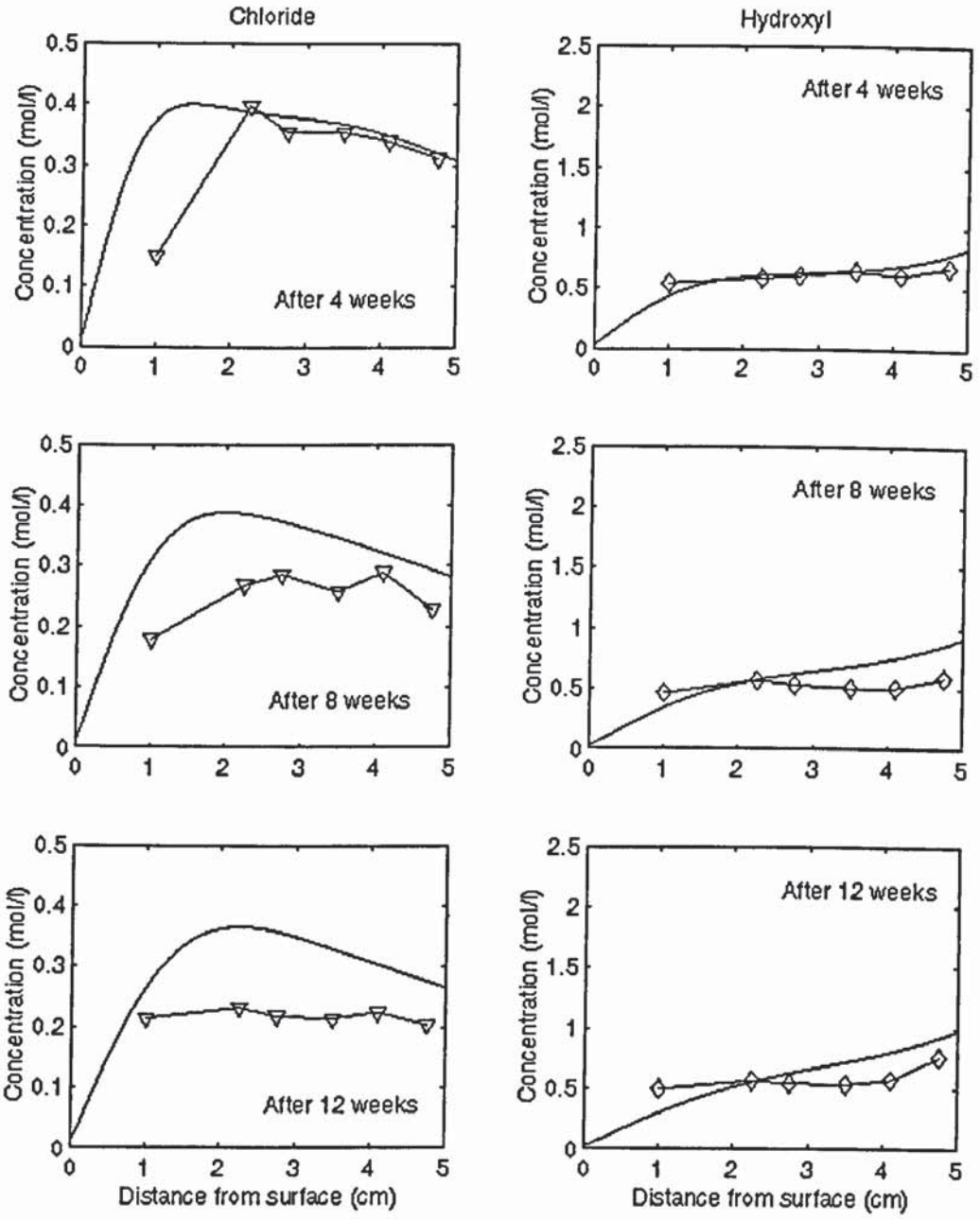

Fig. 5.3a Ionic concentration profiles in pore solution of cement paste with 1% chloride addition

($I = 1$ A/m^2)

–: numerical results, ∇ : experimental results

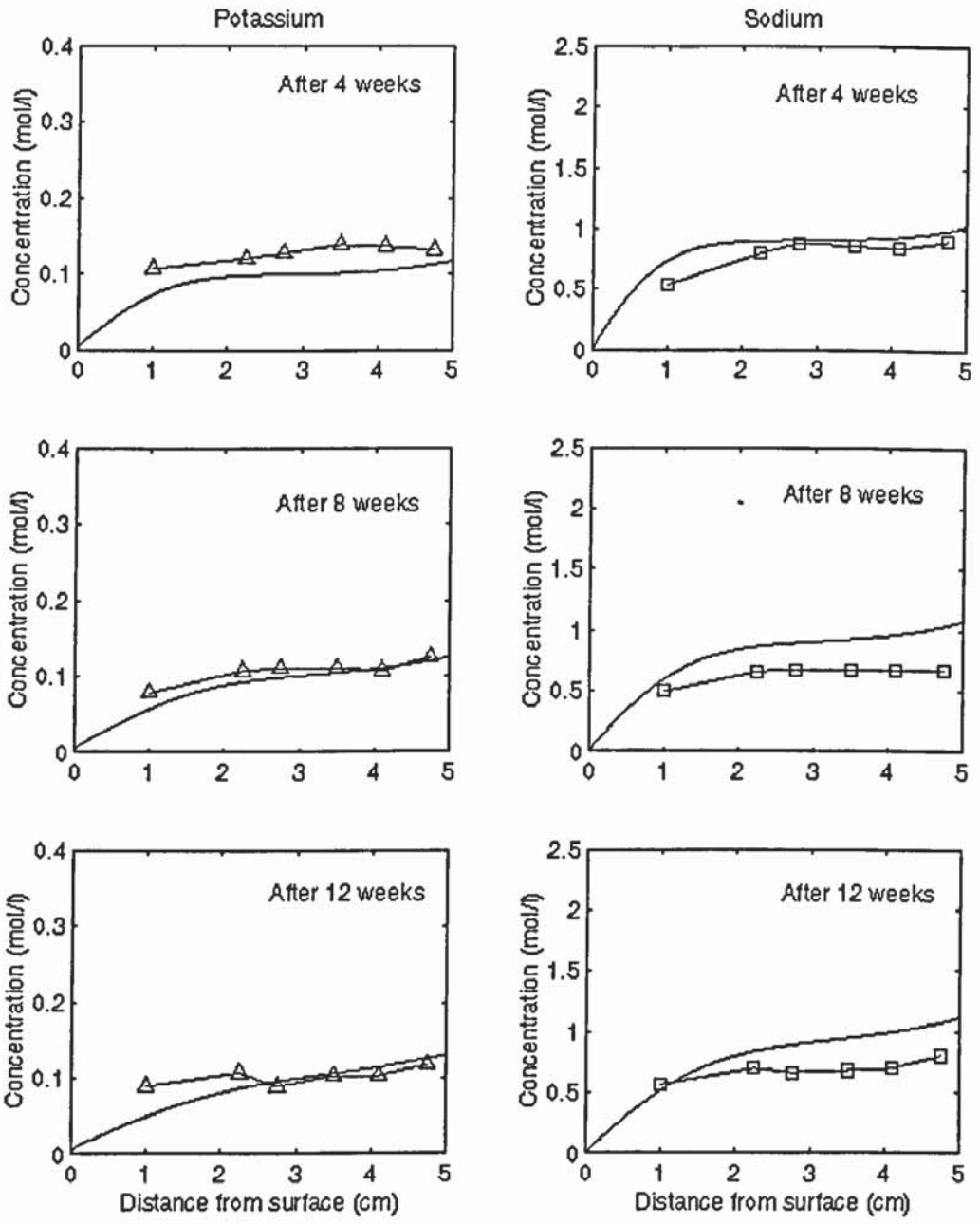

Fig. 5.3b Ionic concentration profiles in pore solution of cement paste with 1% chloride addition

($I = 1$ A/m^2)

–: numerical results, ∇ : experimental results

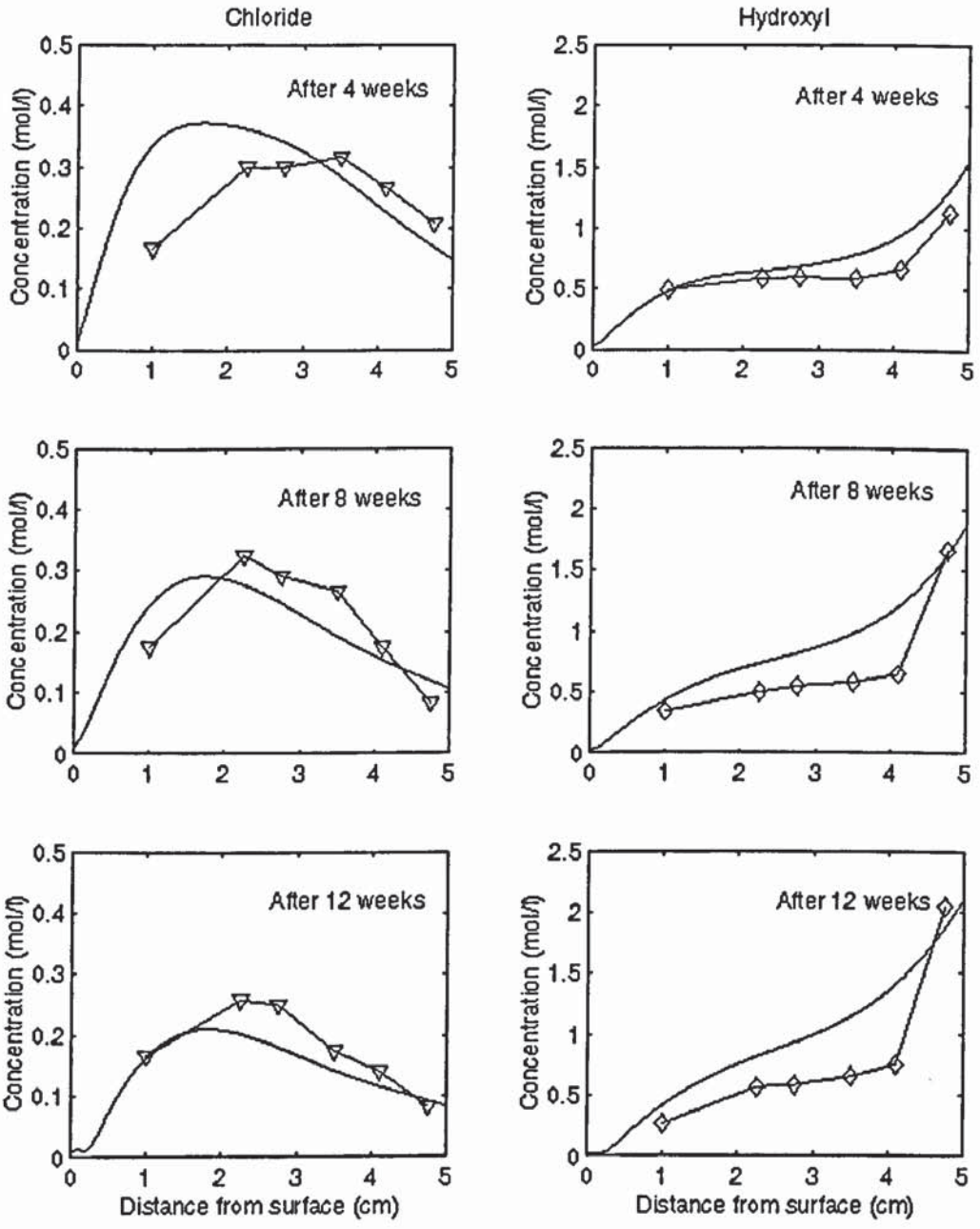

Fig. 5.4a Ionic concentration profiles in pore solution of cement paste with 1% chloride addition

($I = 5$ A/m^2)

–: numerical results, ∇: experimental results

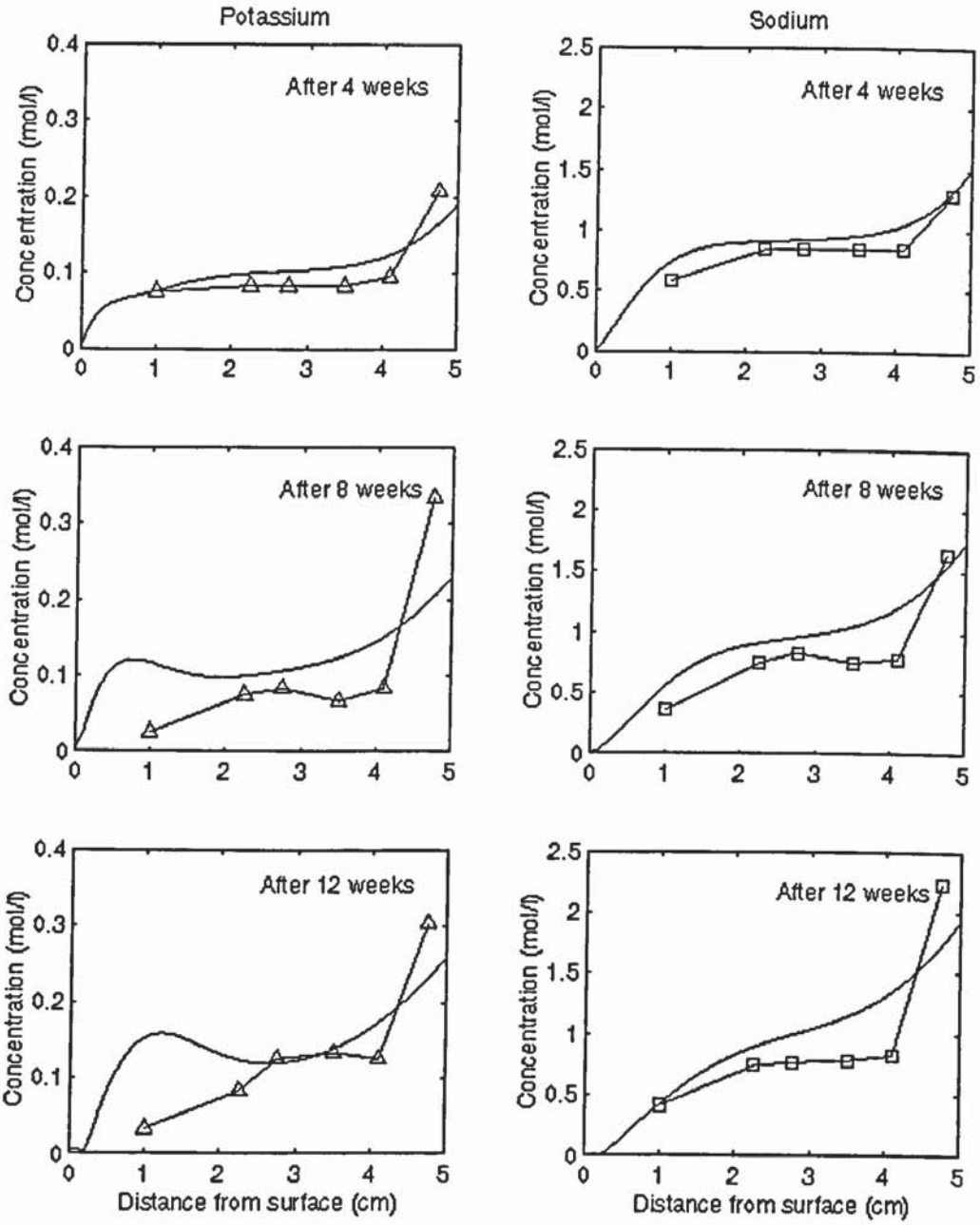

Fig. 5.4b Ionic concentration profiles in pore solution of cement paste with 1% chloride addition

($I = 5$ A/m^2)

–: numerical results, ∇ : experimental results

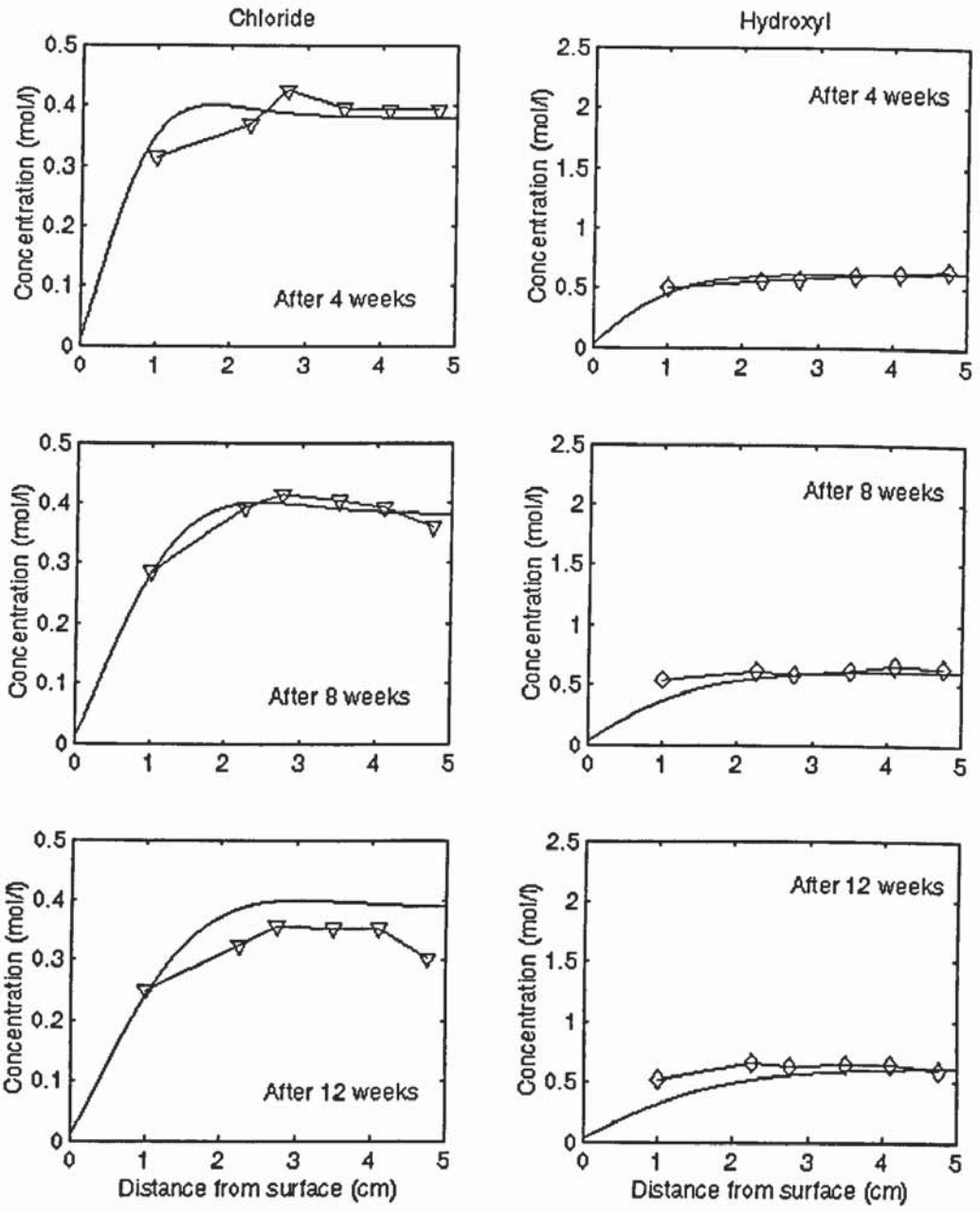

Fig. 5.5a Ionic concentration profiles without considering chloride binding ($I = 0.005$ A/m^2)

–: numerical results, ∇: experimental results

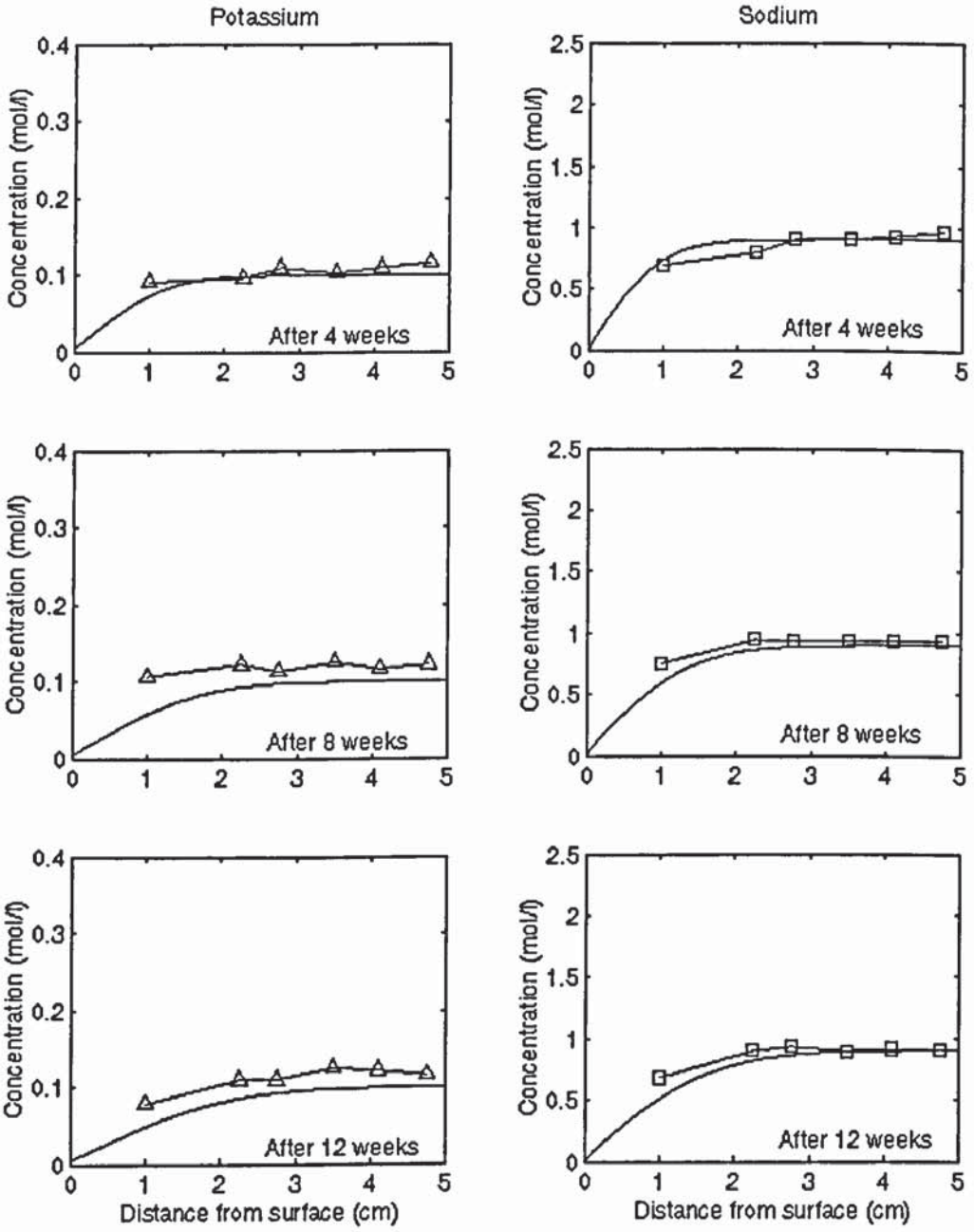

Fig. 5.5b Ionic concentration profiles without considering chloride binding ($I = 0.005$ A/m^2)

–: numerical results, ∇ : experimental results

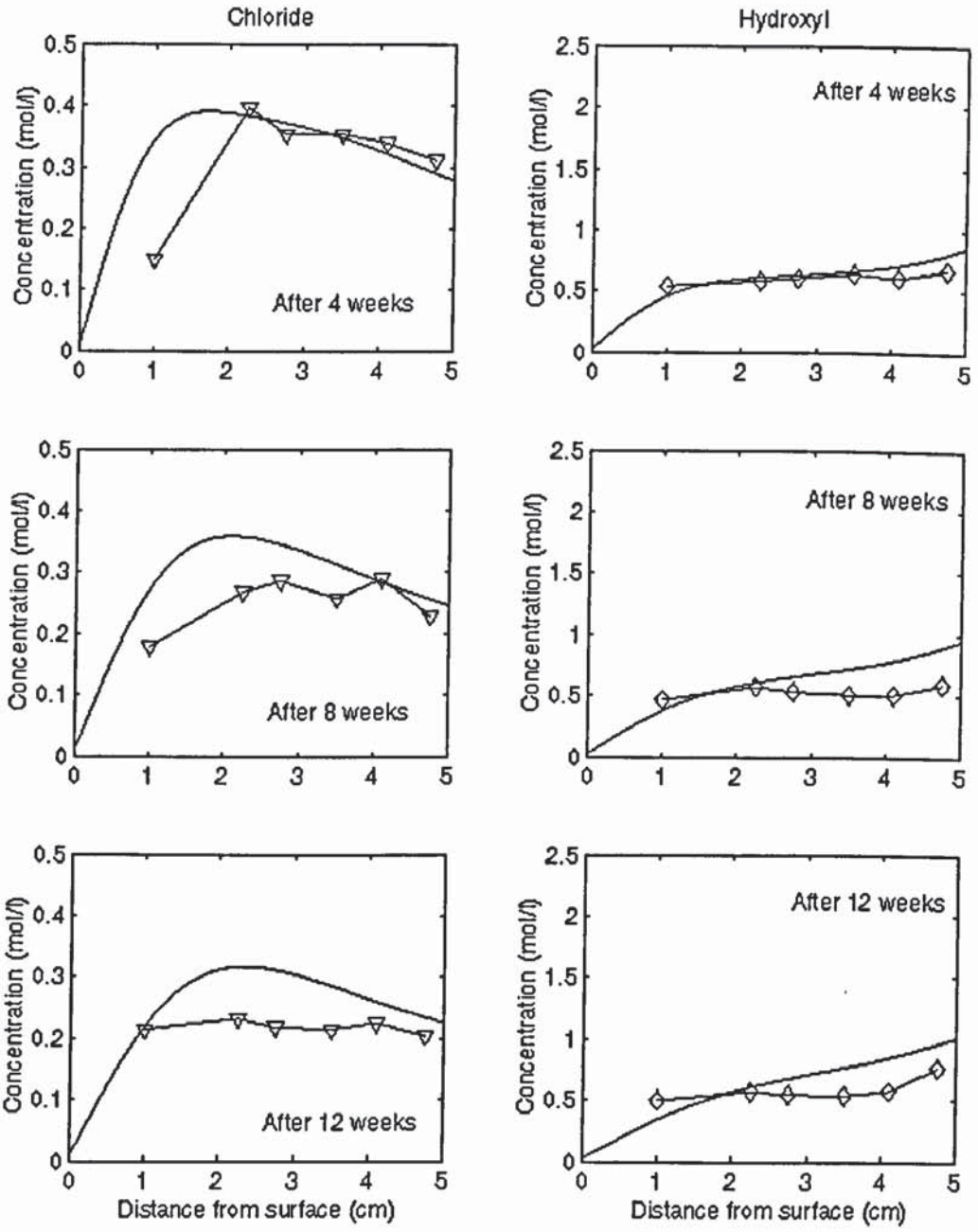

Fig. 5.6a Ionic concentration profiles without considering chloride binding

($I = 1$ A/m^2)

–: numerical results, ∇: experimental results

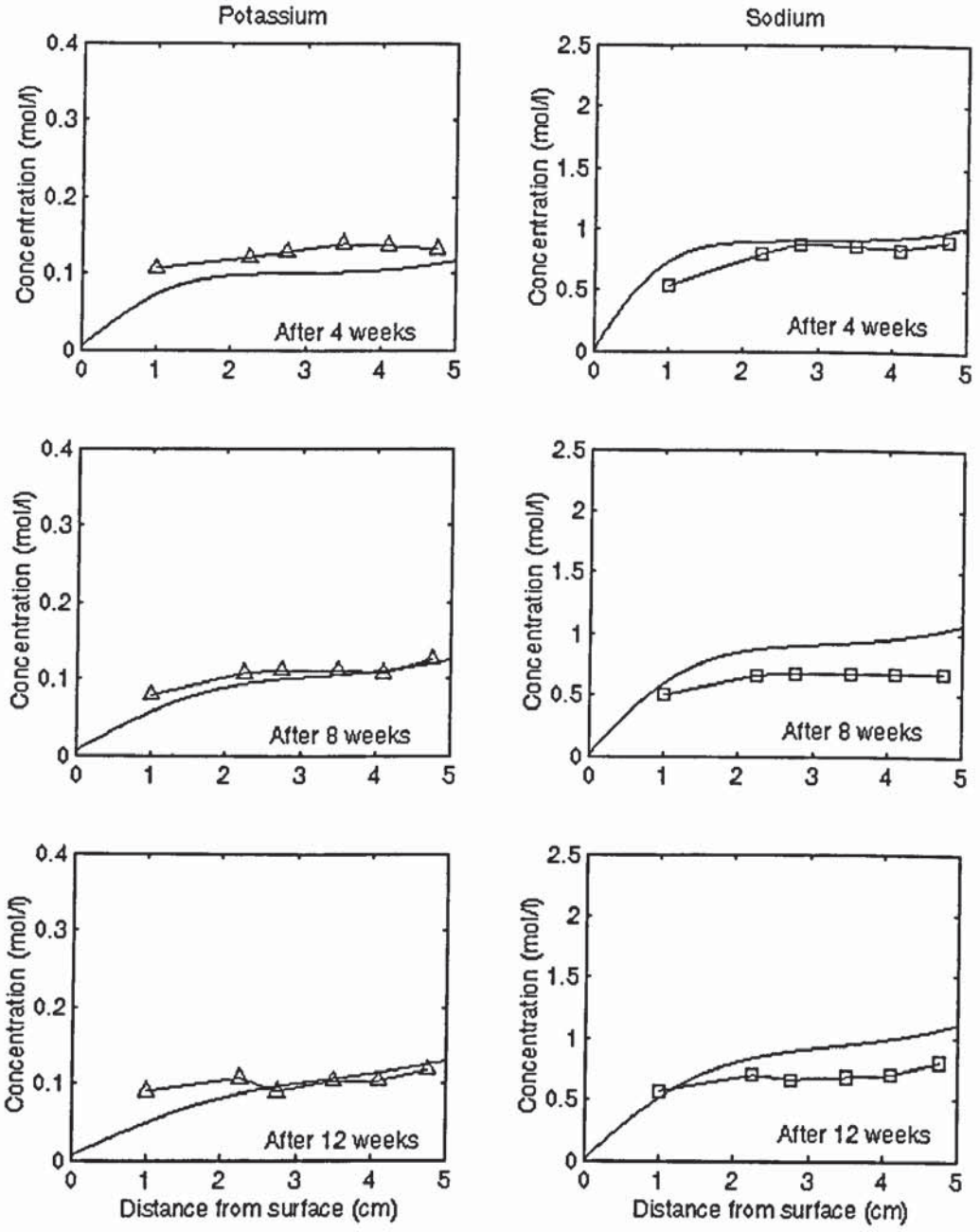

Fig. 5.6b Ionic concentration profiles without considering chloride binding ($I = 1$ A/m^2)

–: numerical results, ∇ : experimental results

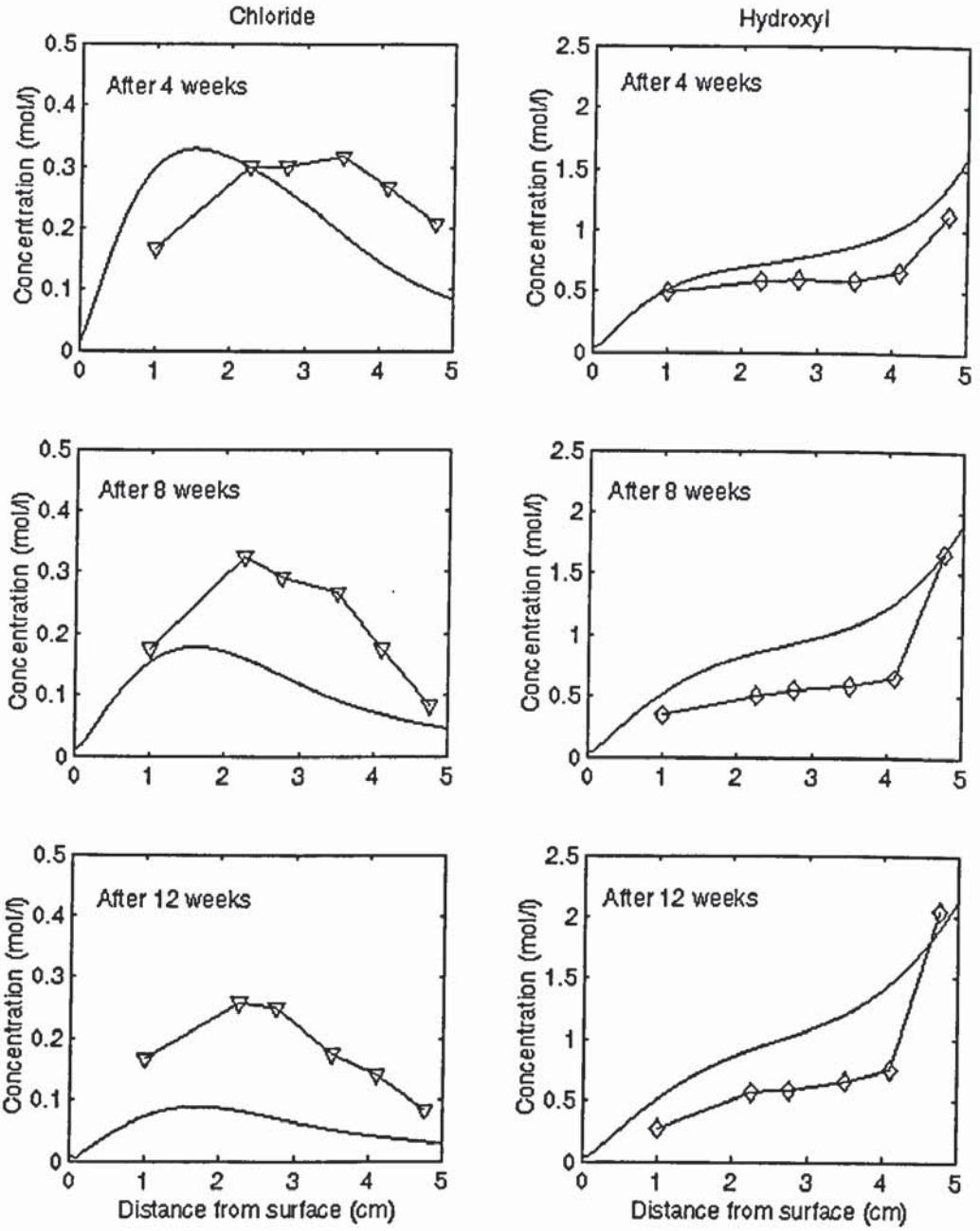

Fig. 5.7a Ionic concentration profiles without considering chloride binding ($I = 5$ A/m^2)

–: numerical results, ∇: experimental results

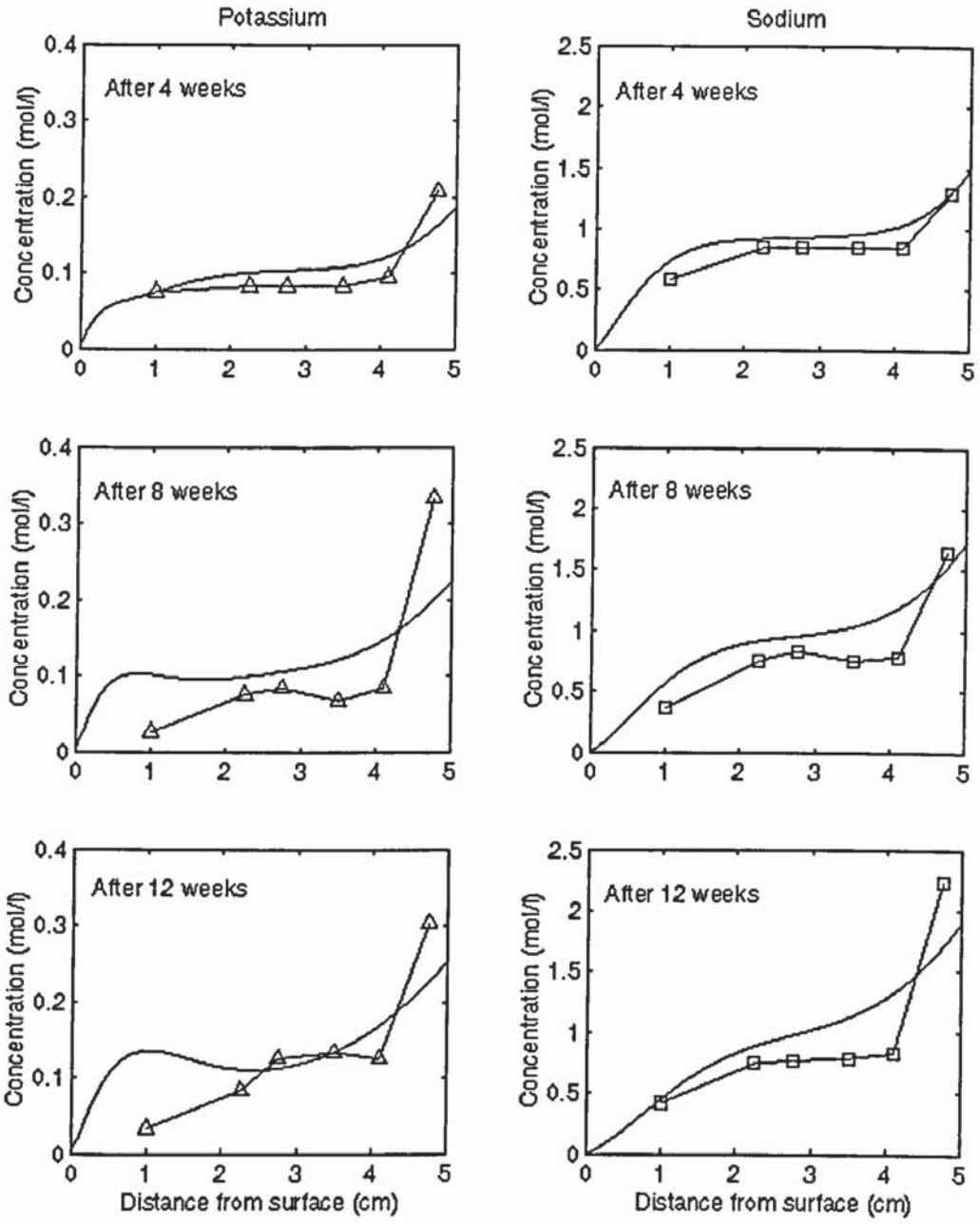

Fig. 5.7b Ionic concentration profiles without considering chloride binding ($I = 5$ A/m^2)

–: numerical results, ∇ : experimental results

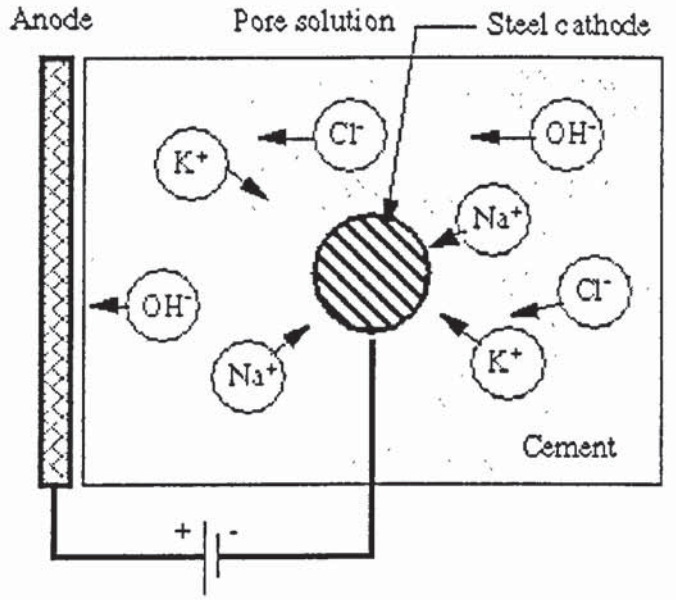

(a) Case one

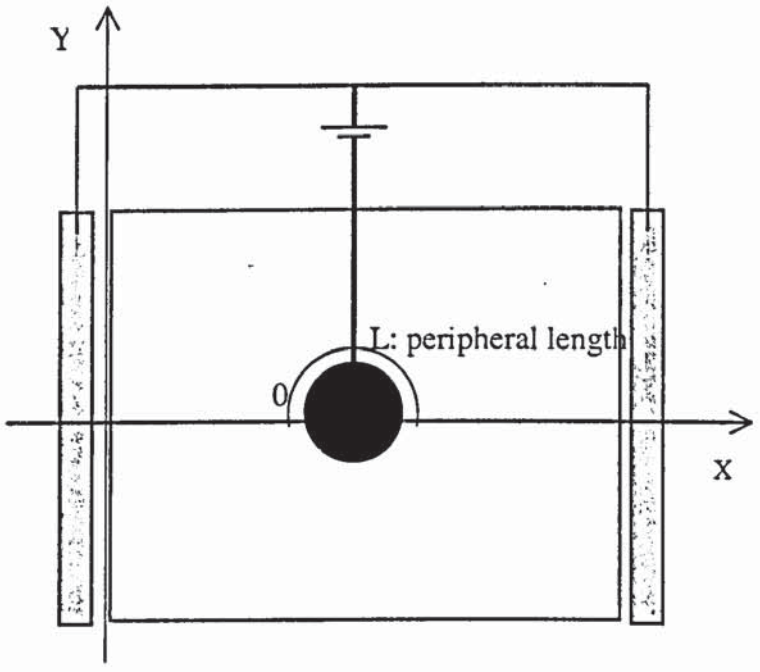

(b) Case two

Fig. 5.8 Two-dimensional cases studied

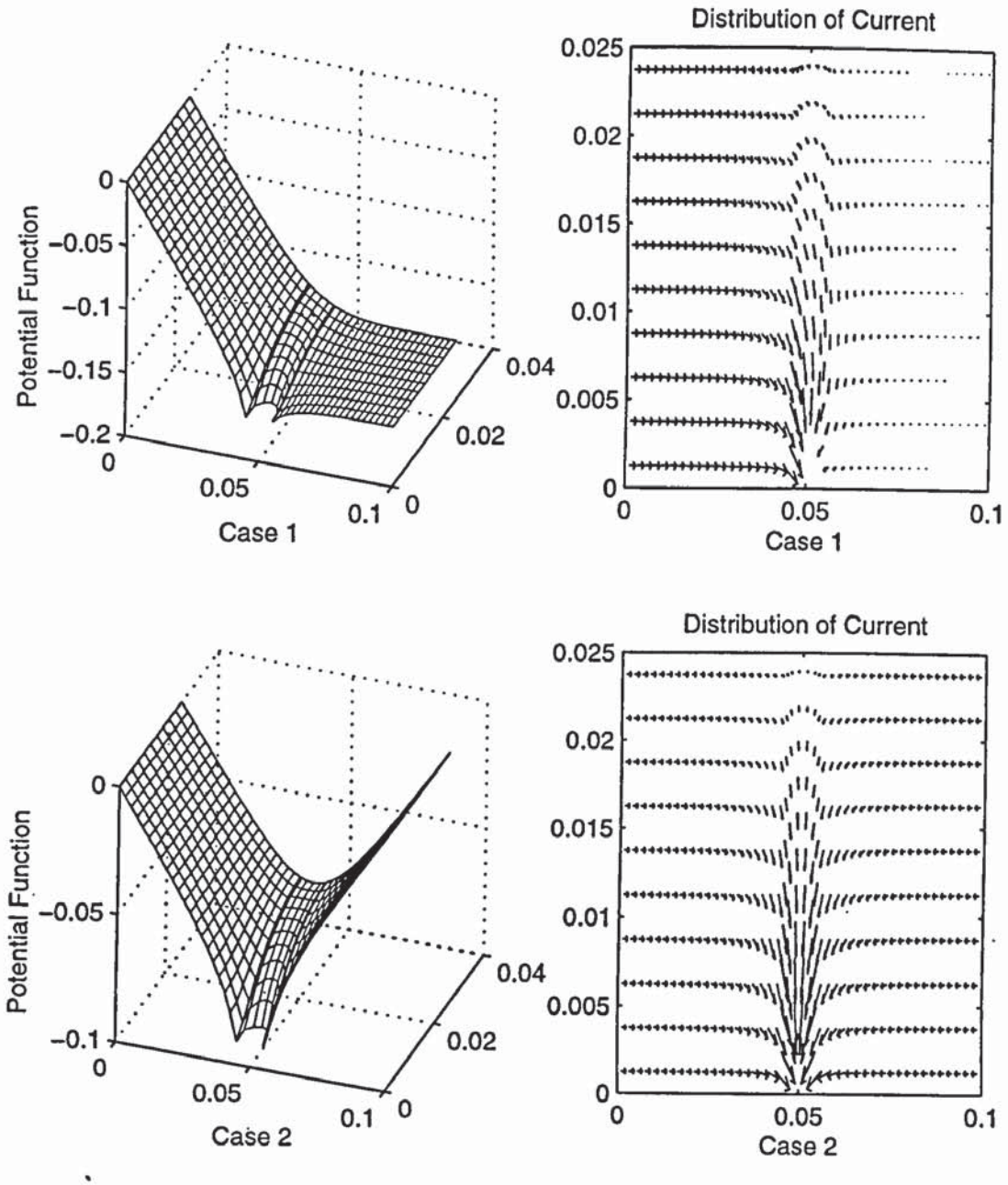

Fig. 5.9 Distributions of potential function φ and the distribution of their corresponding current densities in case 1 and case 2

(co-ordinate dimension is in m)

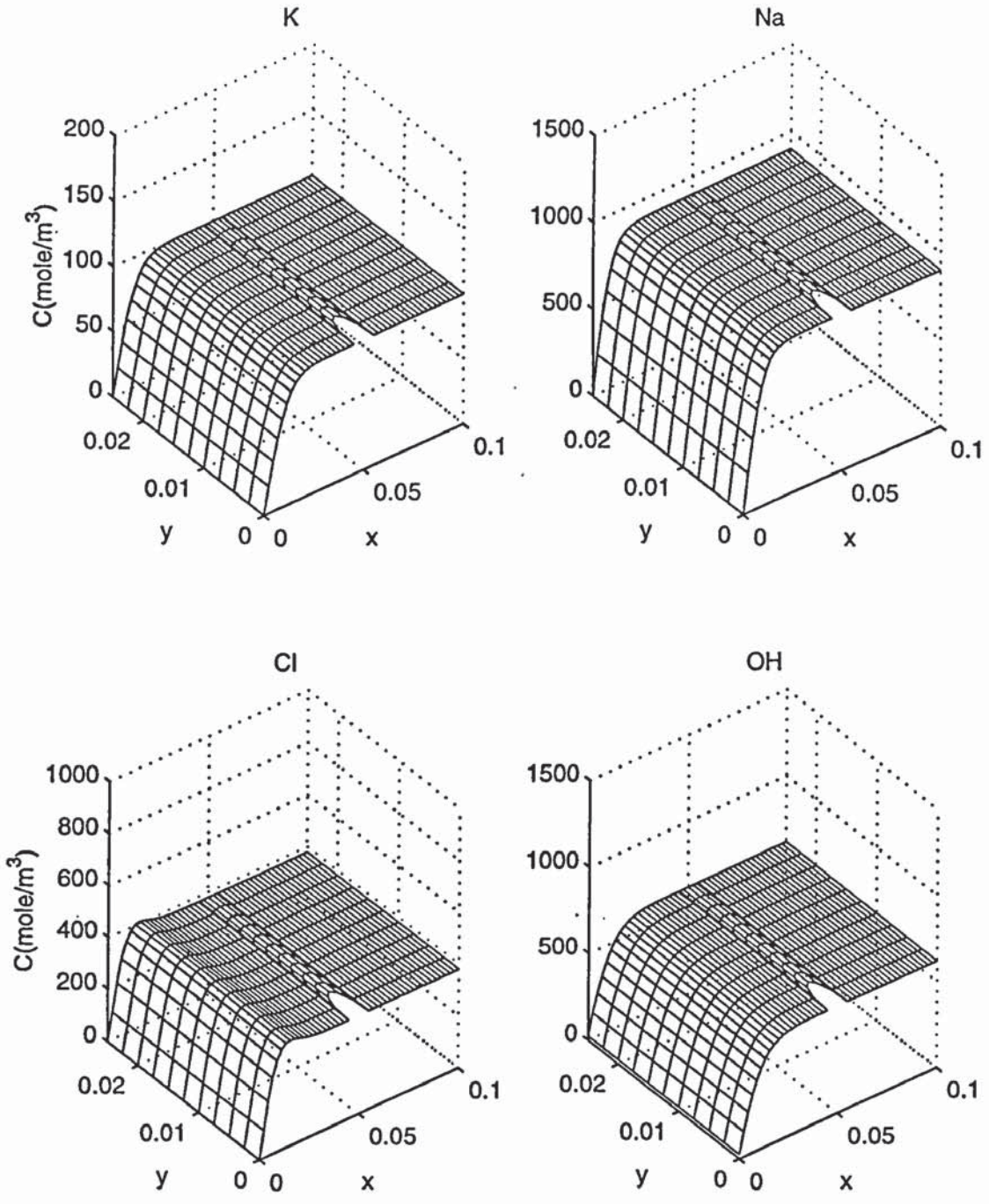

Fig. 5.10a Ionic concentration profiles after 4 weeks at $I = 0.001$ A/m^2 in case one (x: m, y: m)

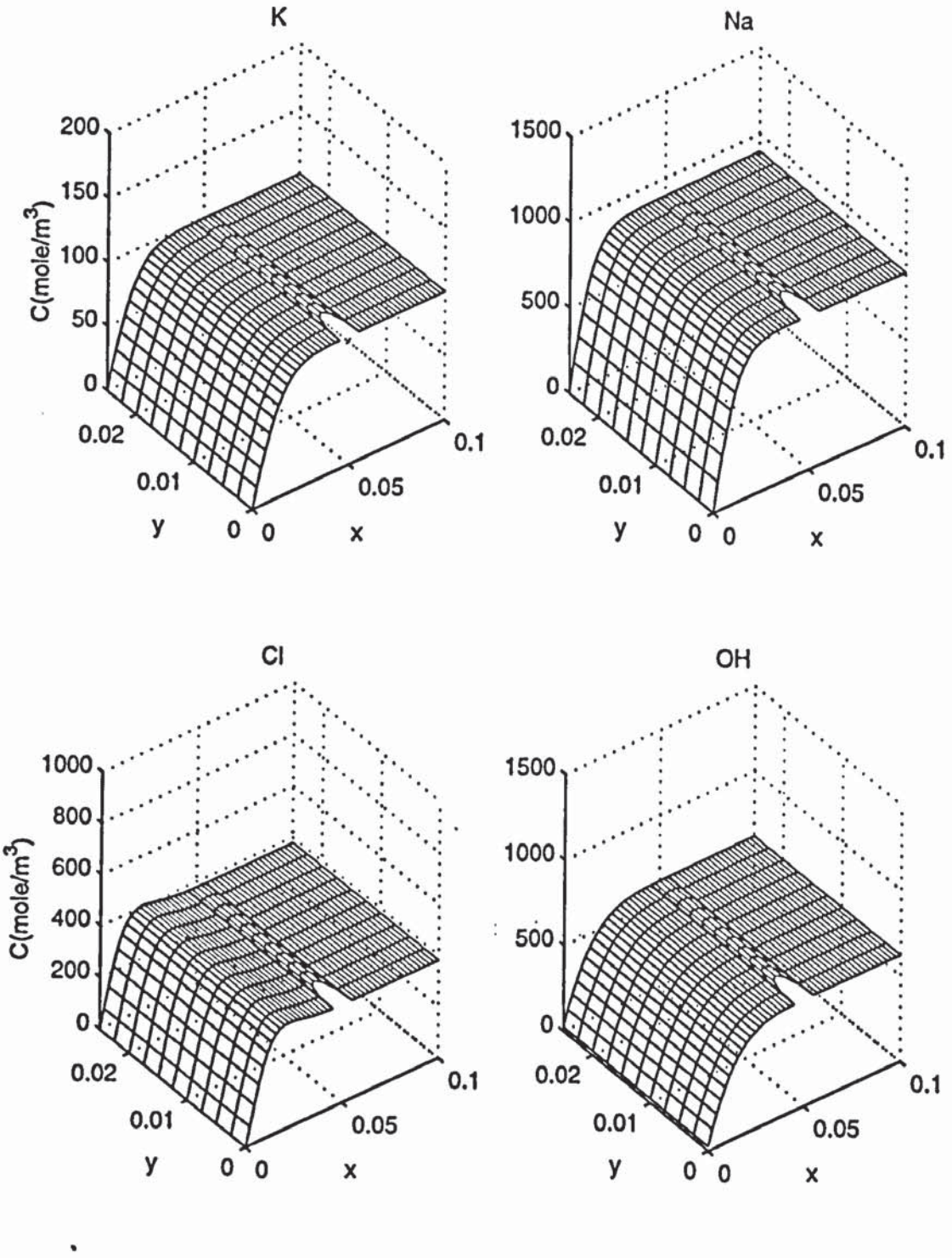

Fig. 5.10b Ionic concentration profiles after 8 weeks at $I = 0.001$ A/m^2 in case one (x: m, y: m)

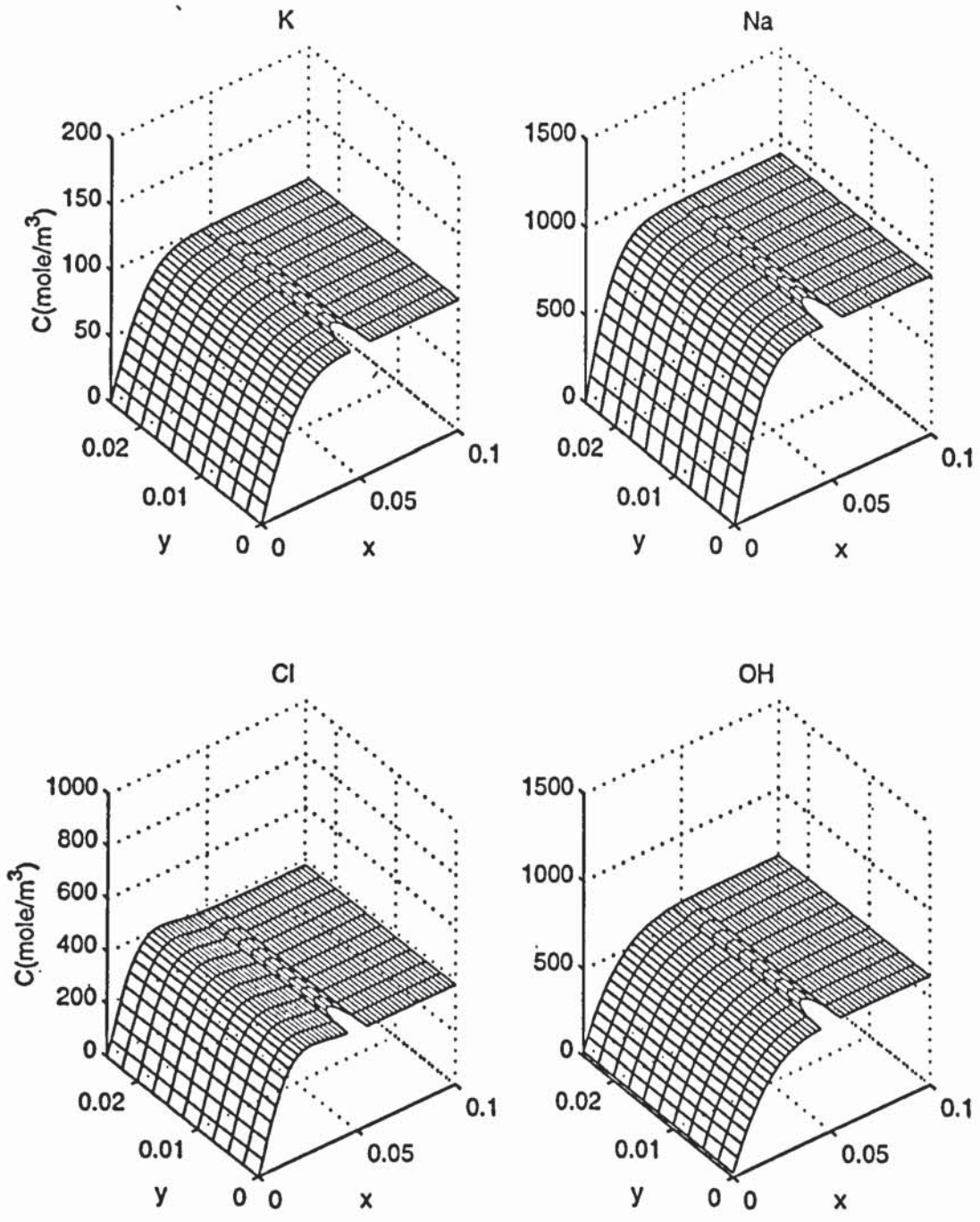

Fig. 5.10c Ionic concentration profiles after 12 weeks for $I = 0.001$ A/m^2 in case one (x: m, y: m)

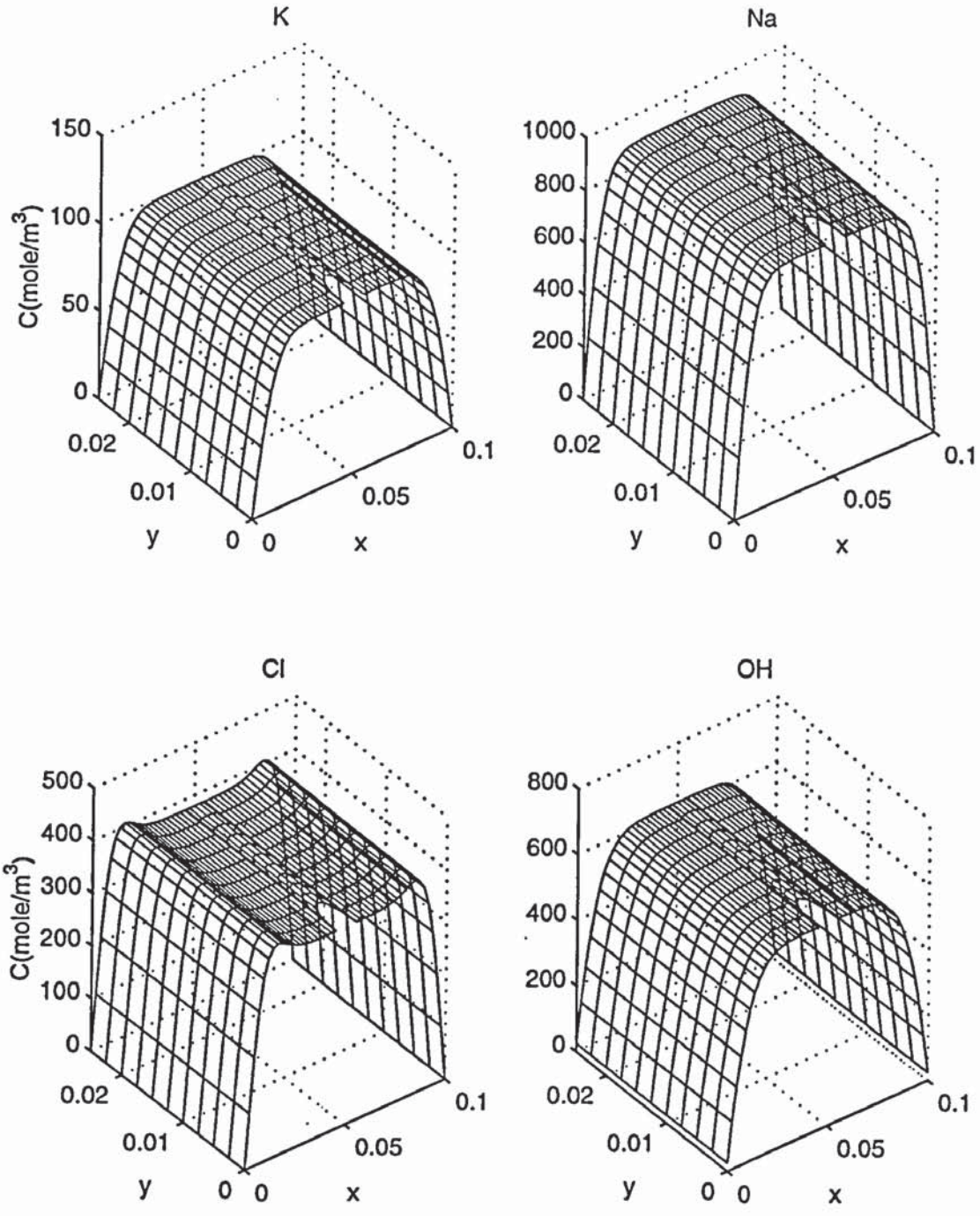

Fig. 5.11a Ionic concentration profiles after 4 weeks at $I = 0.001$ A/m^2 in case two (x: m, y: m)

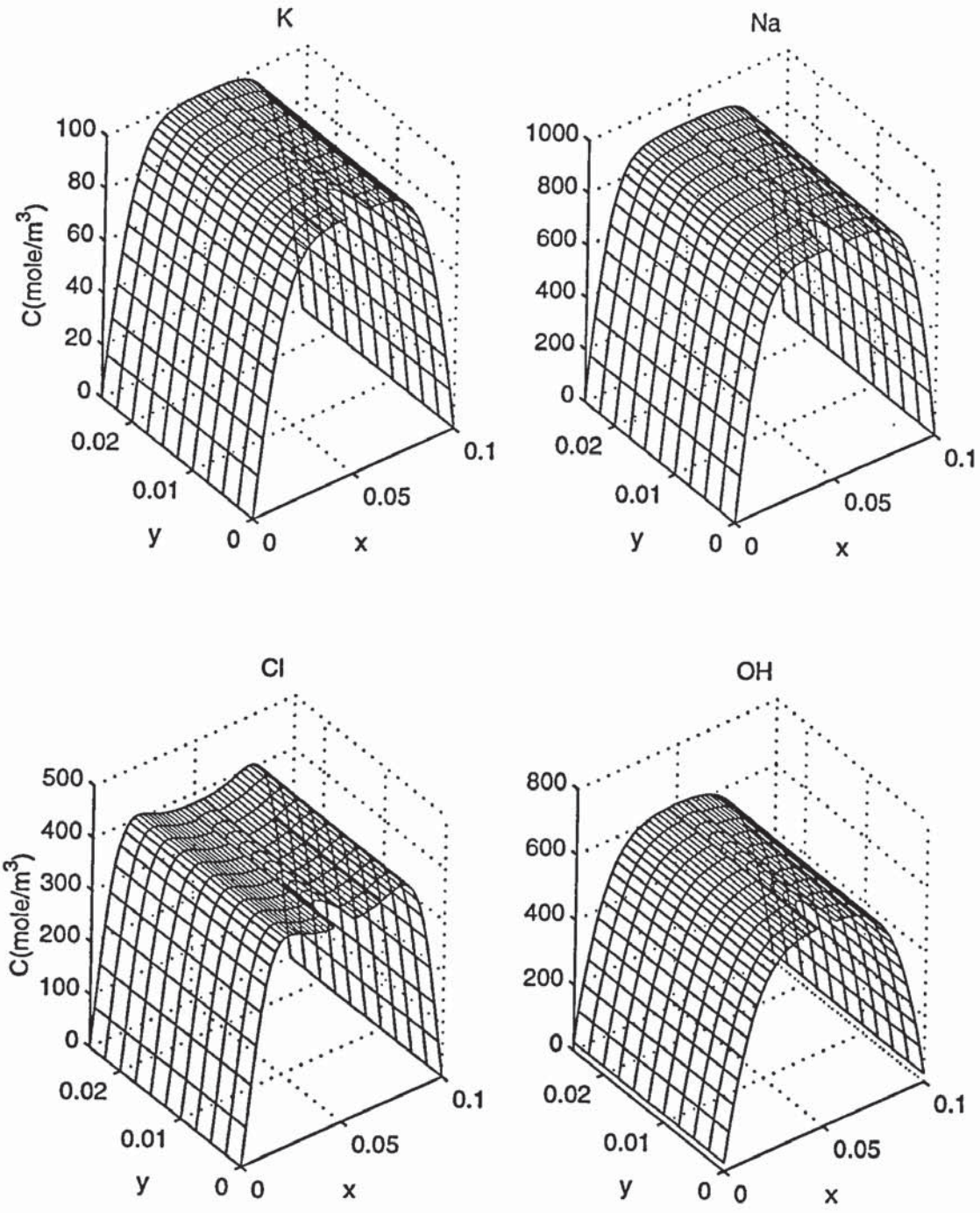

Fig. 5.11b Ionic concentration profiles after 8 weeks at $I = 0.001$ A/m^2 in case two (x: m, y: m)

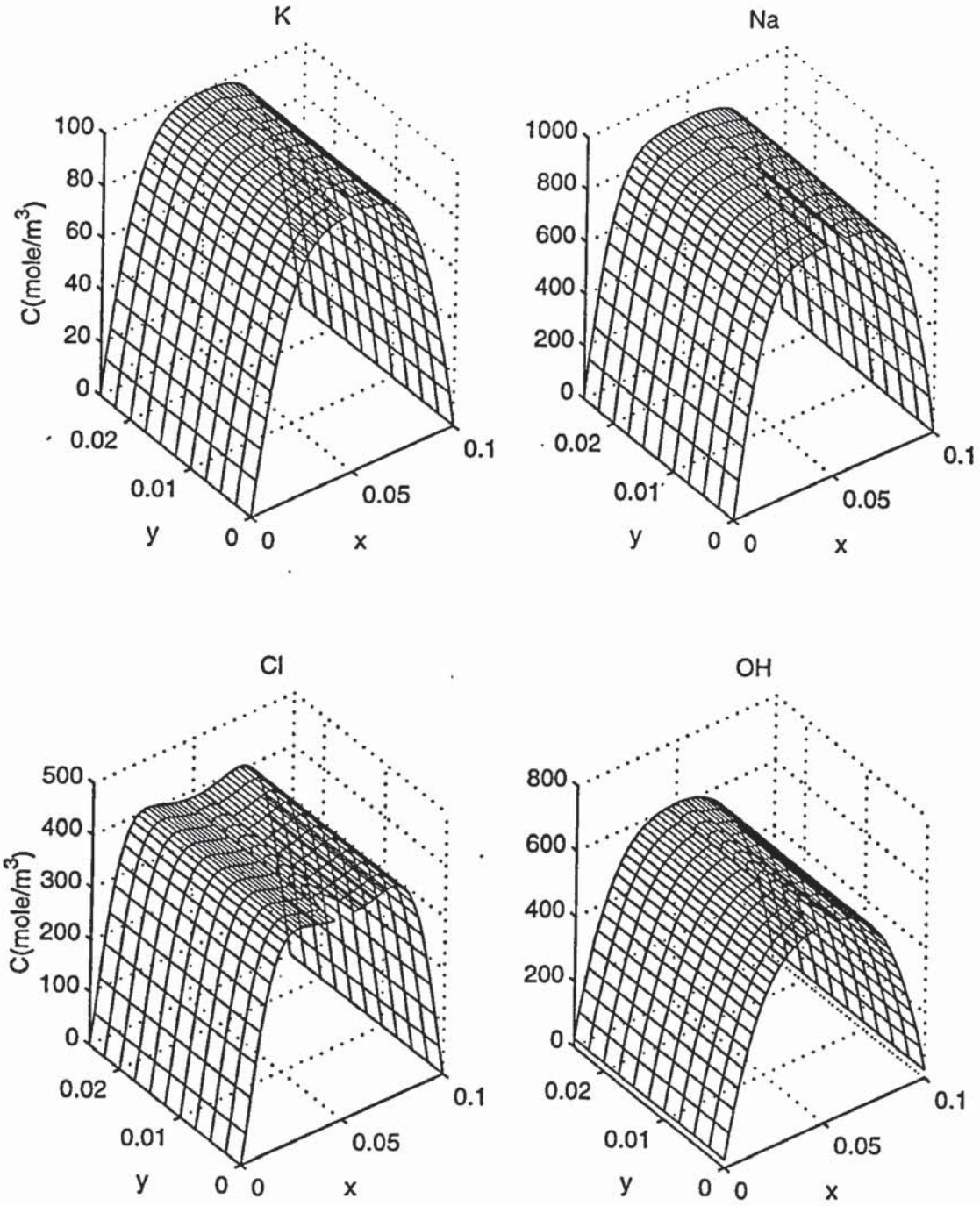

Fig. 5.11c Ionic concentration profiles after 12 weeks at $I = 0.001$ A/m^2 in case two (x: m, y: m)

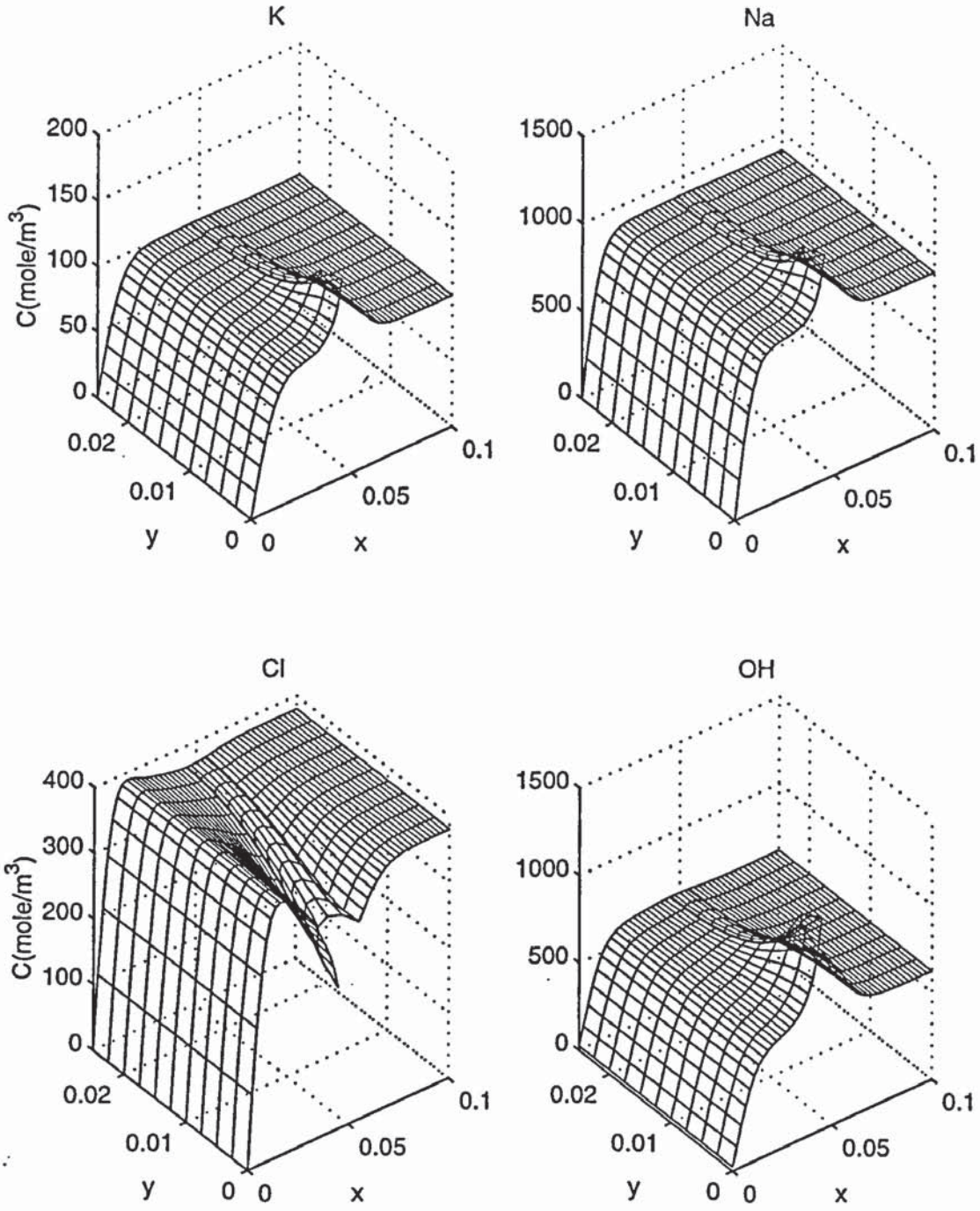

Fig. 5.12a Ionic concentration profiles after 4 weeks at $I = 3$ A/m^2 in case one (x: m, y: m)

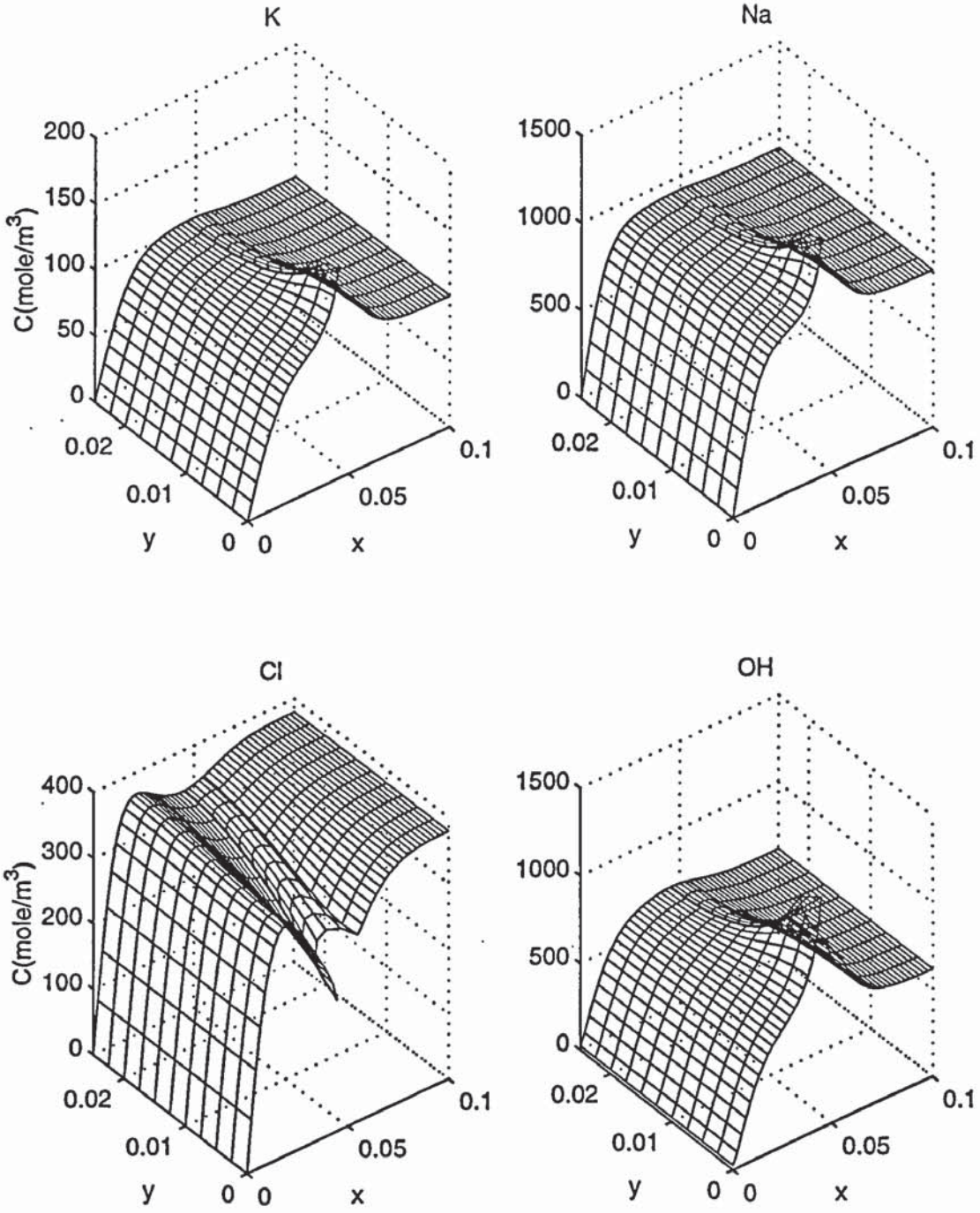

Fig. 5.12b Ionic concentration profiles after 8 weeks at $I = 3$ A/m^2 in case one (x: m, y: m)

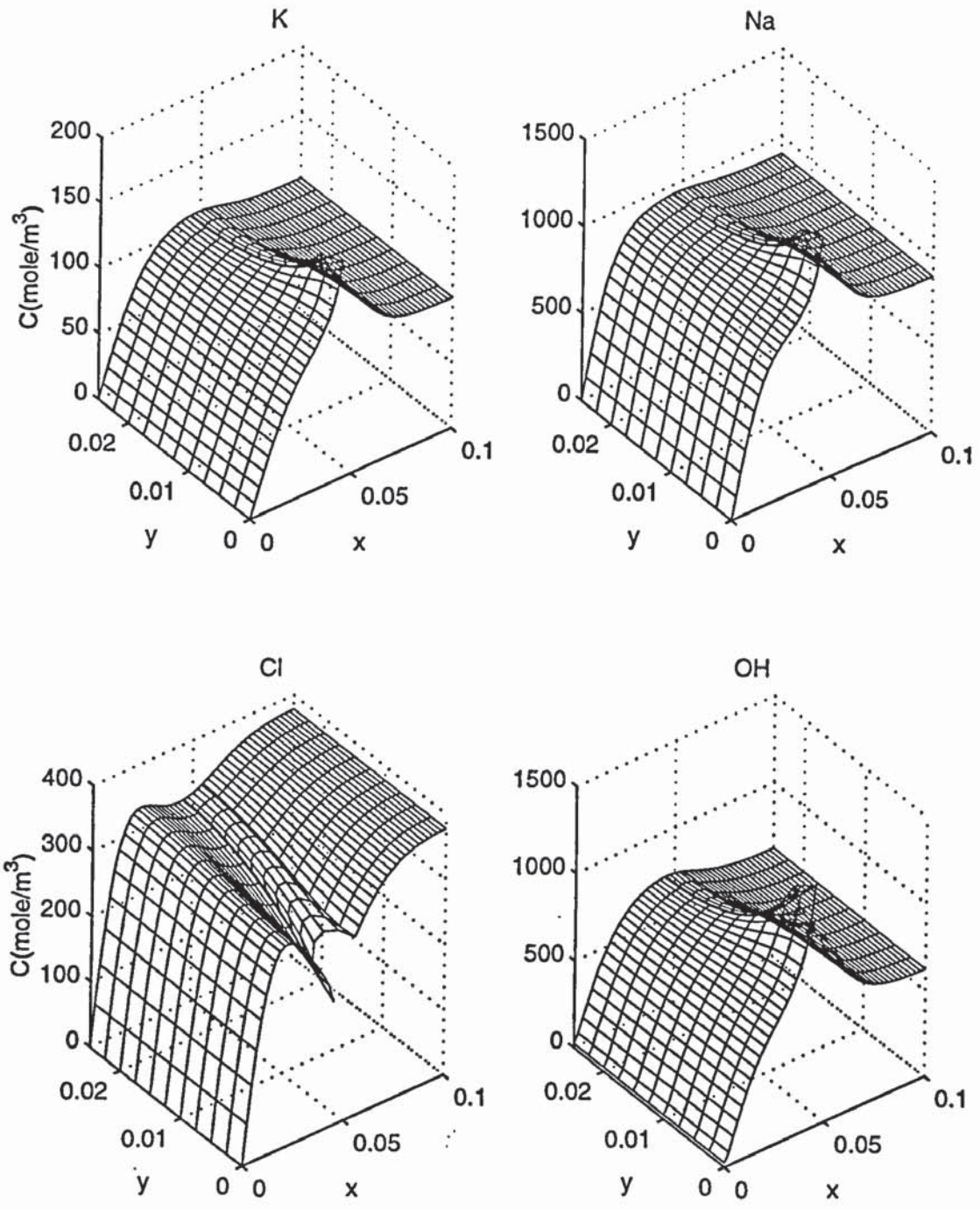

Fig. 5.12c Ionic concentration profiles after 12 weeks at $I = 3$ A/m^2 in case one (x: m, y: m)

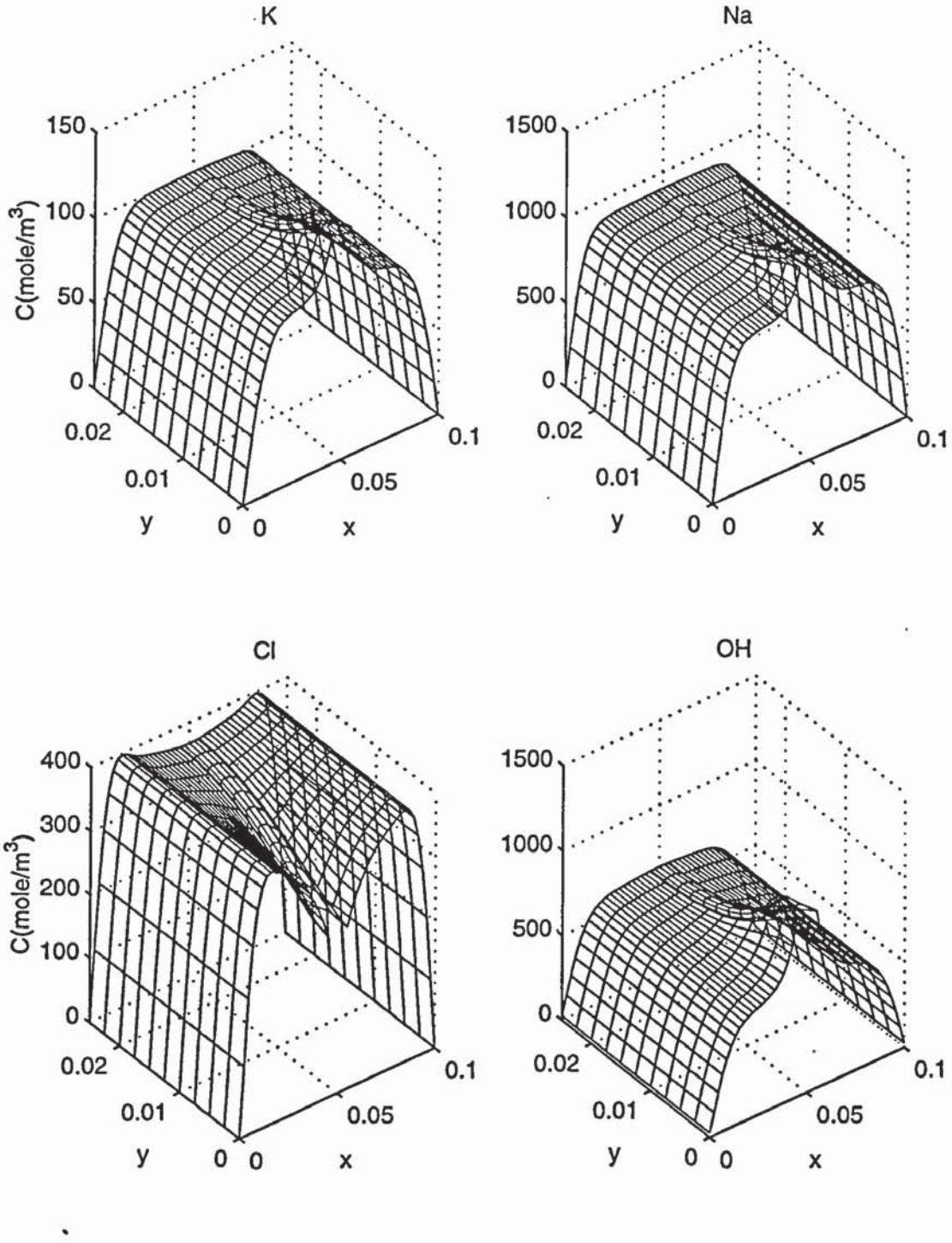

Fig. 5.13a Ionic concentration profiles after 4 weeks at $I = 3$ A/m^2 in case two (x: m, y: m)

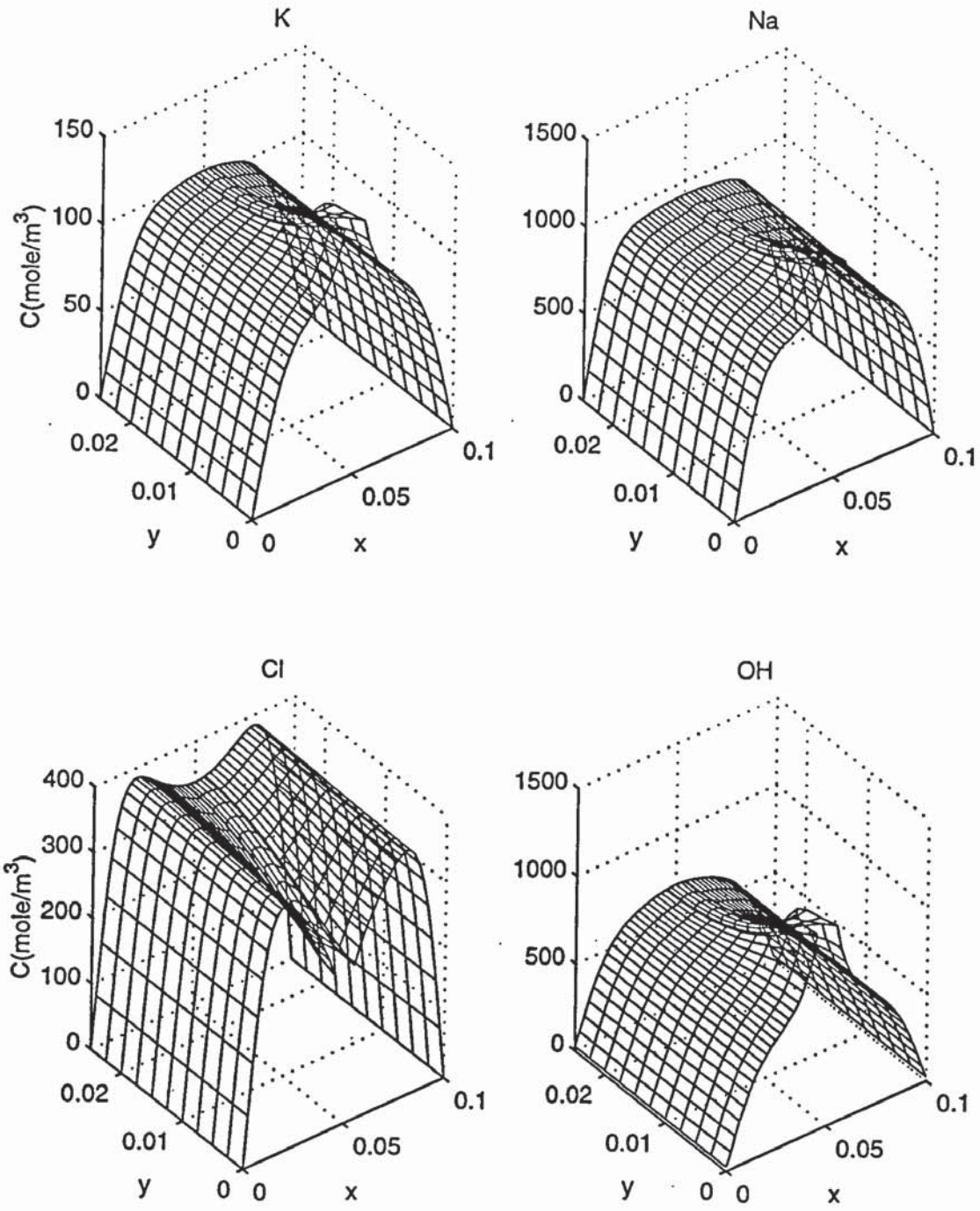

Fig. 5.13b Ionic concentration profiles after 8 weeks at $I = 3$ A/m^2 in case two (x: m, y: m)

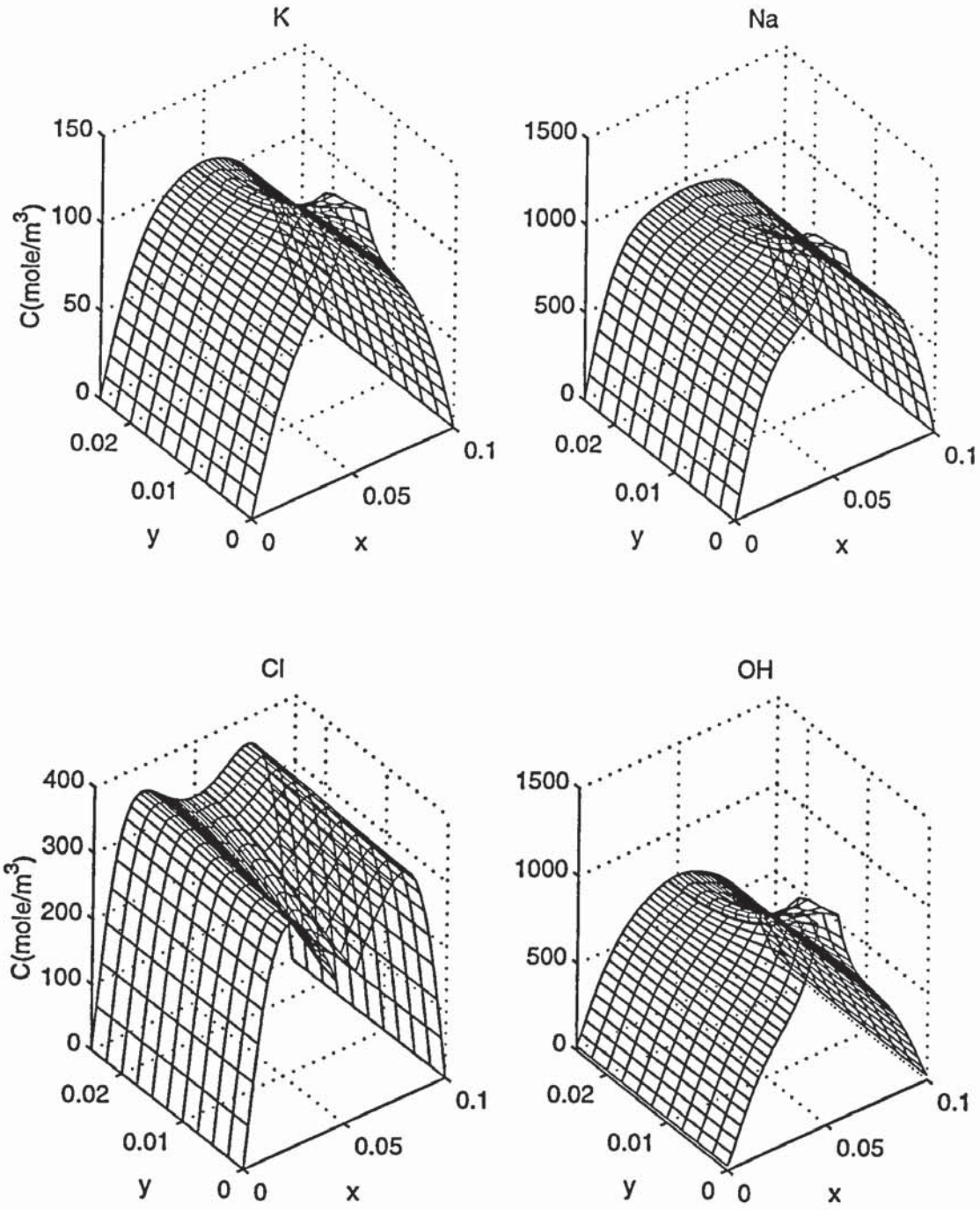

Fig. 5.13c Ionic concentration profiles after 12 weeks at $I = 3$ A/m^2 in case two (x: m, y: m)

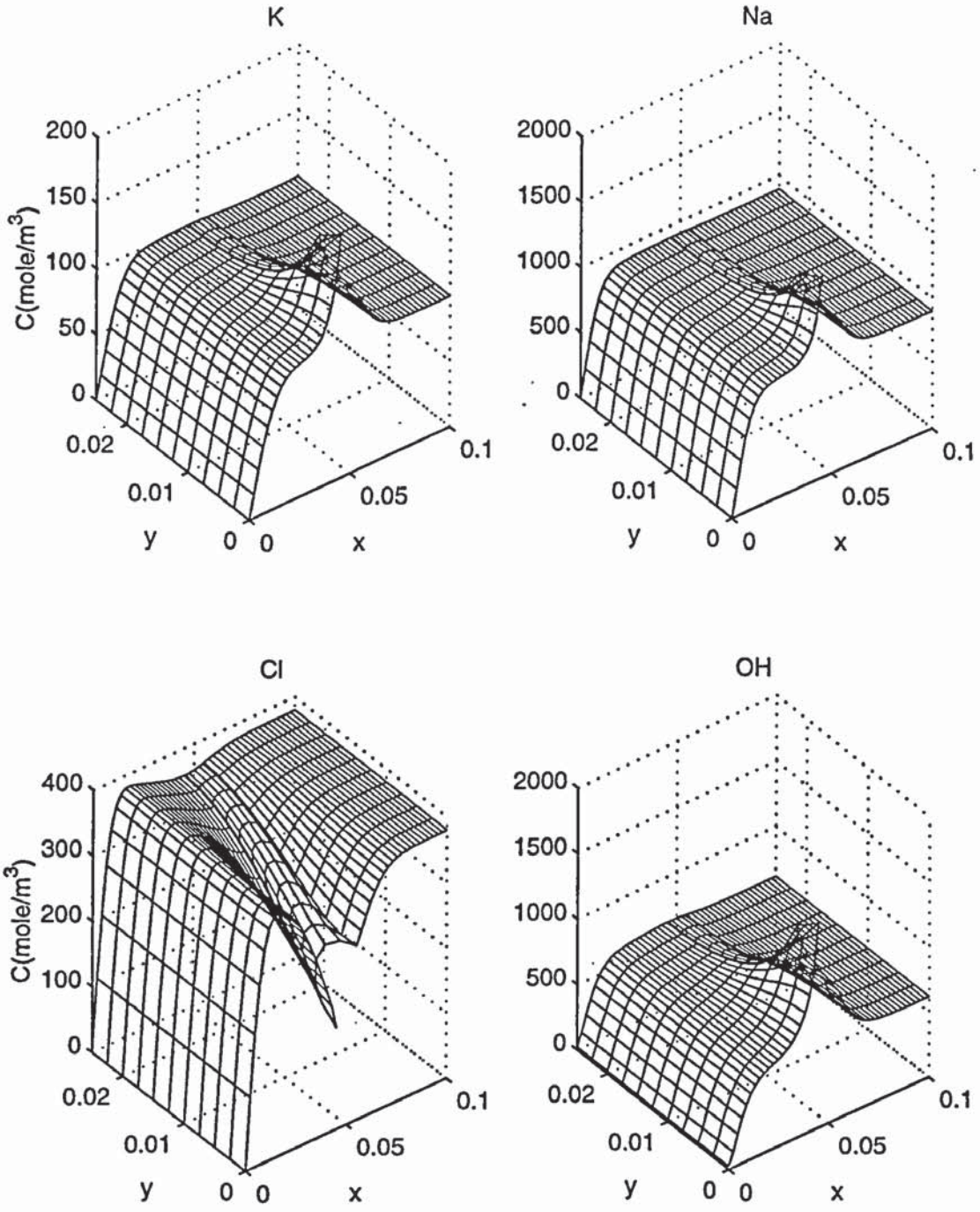

Fig. 5.14a Ionic concentration profiles after 4 weeks at $I = 5$ A/m^2 in case one (x: m, y: m)

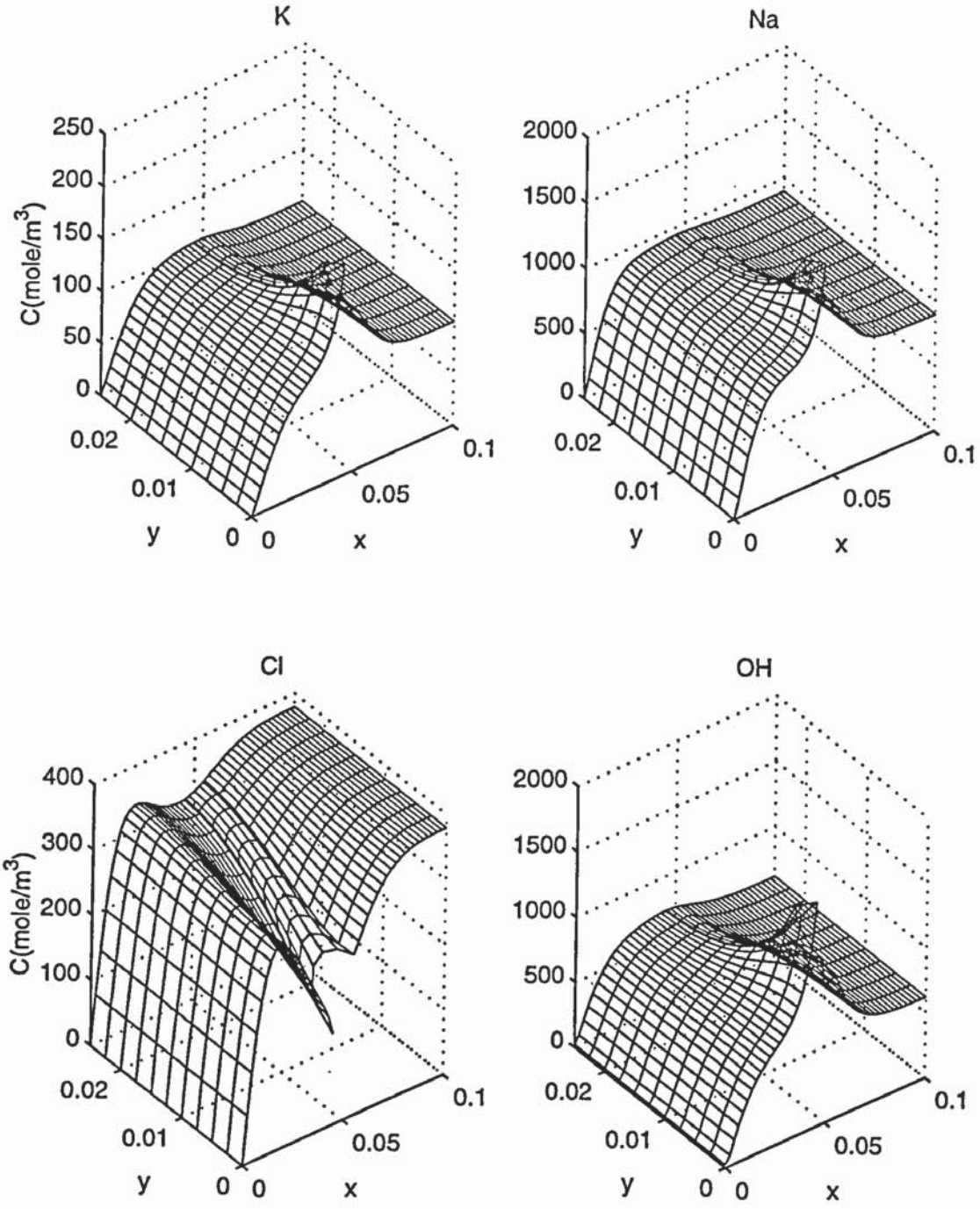

Fig. 5.14b Ionic concentration profiles after 8 weeks at $I = 5$ A/m^2 in case one (x: m, y: m)

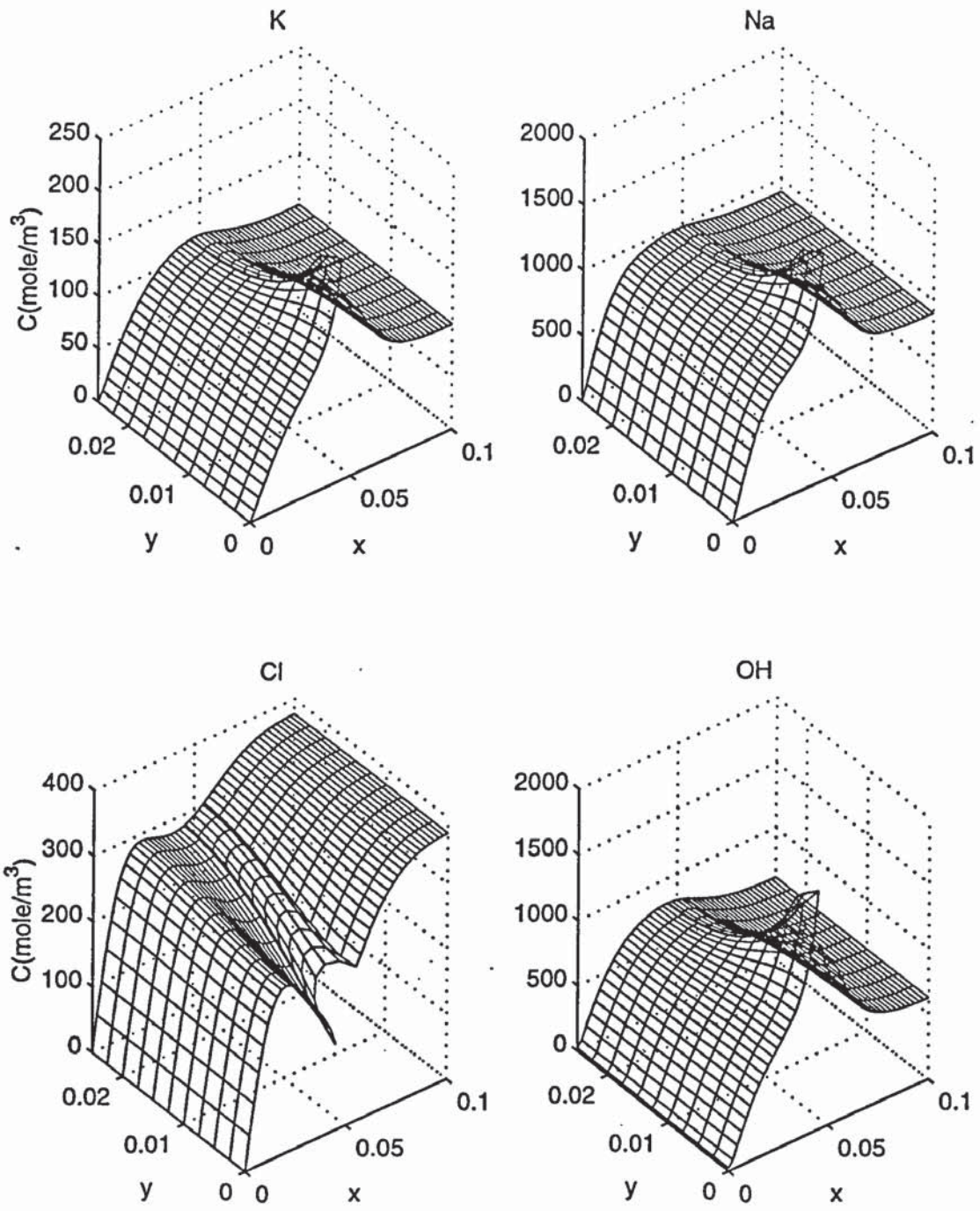

Fig. 5.14c Ionic concentration profiles after 12 weeks at $I = 5$ A/m^2 in case one (x: m, y: m)

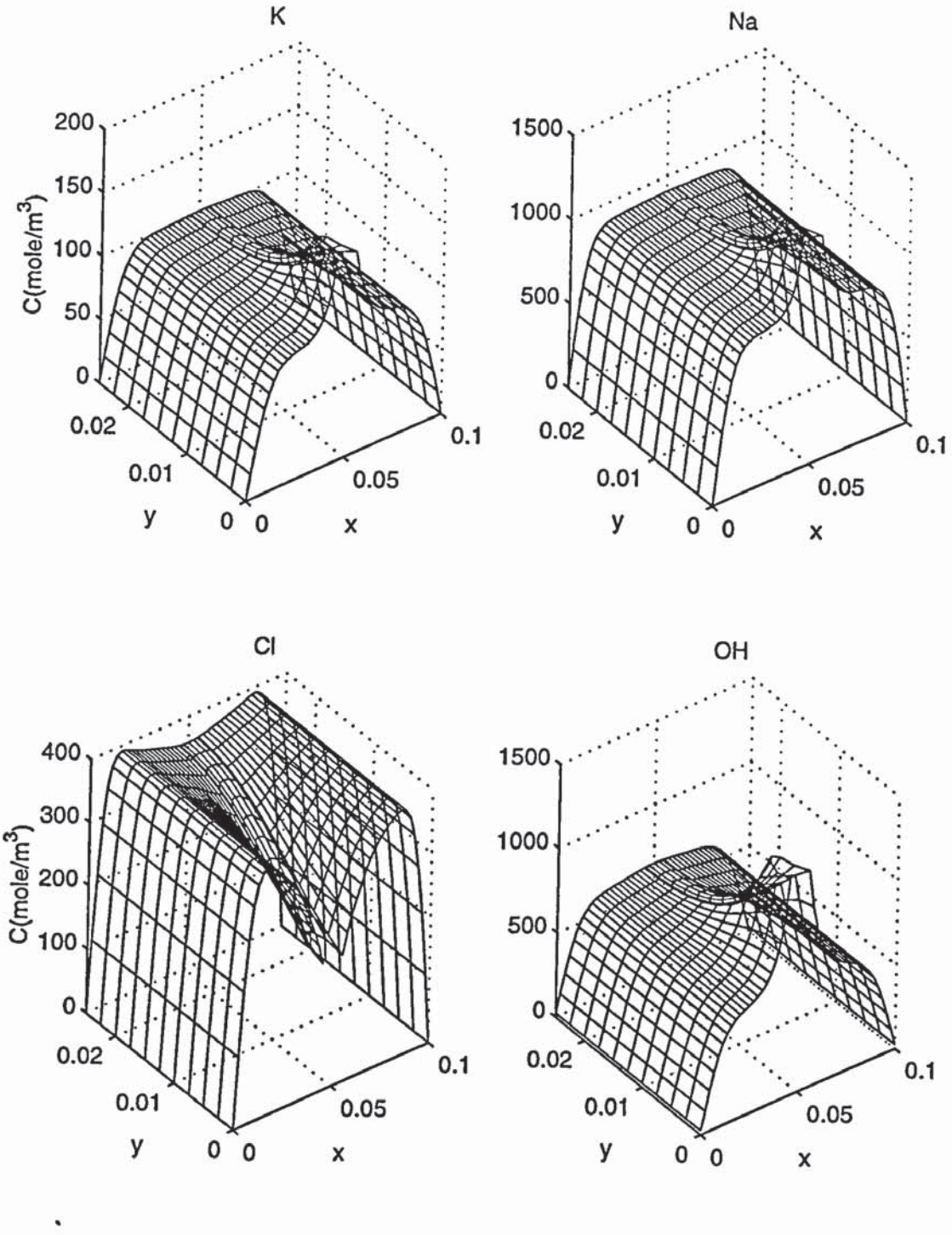

Fig. 5.15a Ionic concentration profiles after 4 weeks at $I = 5$ A/m^2 in case two (x: m, y: m)

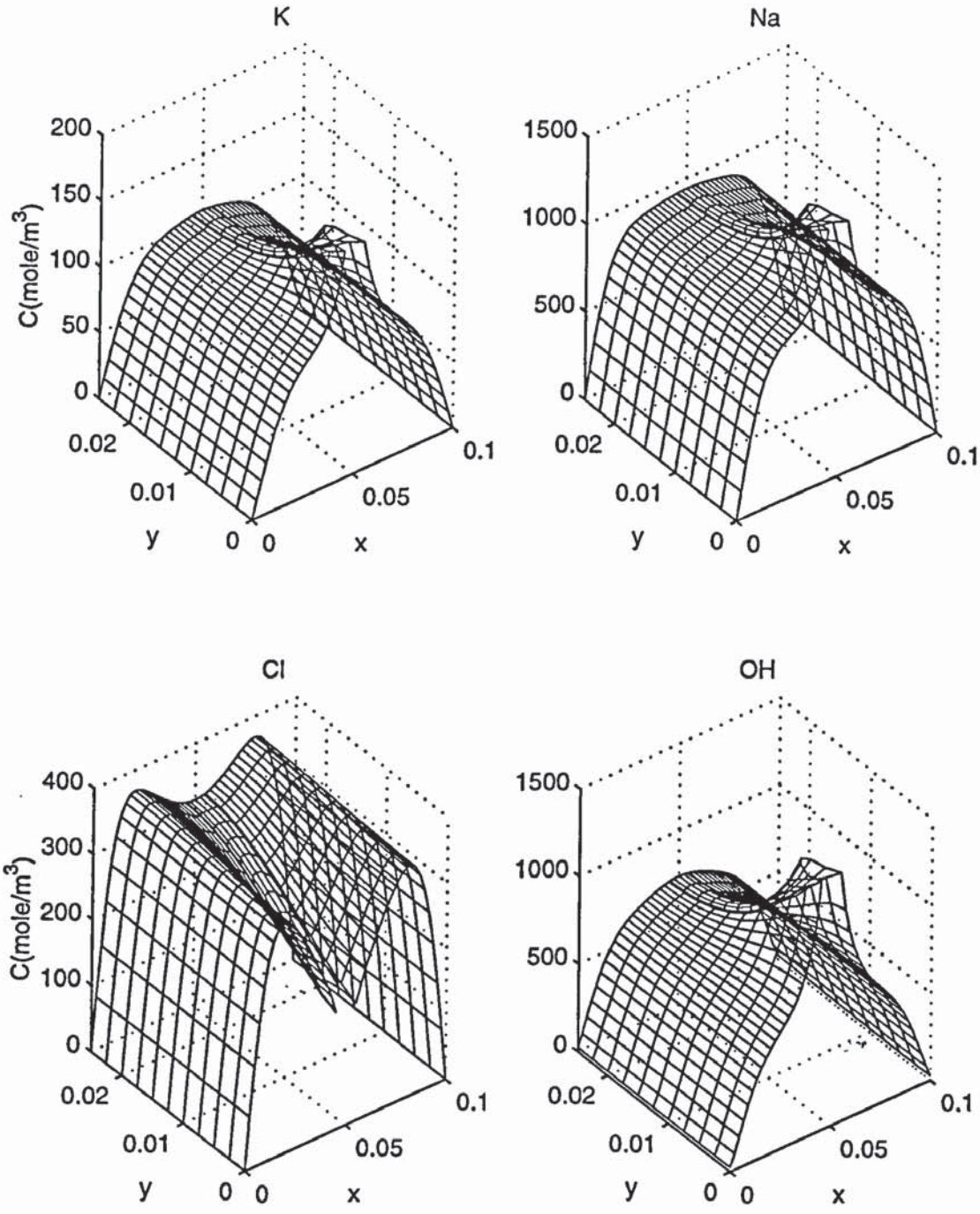

Fig. 5.15b Ionic concentration profiles after 8 weeks at $I = 5$ A/m^2 in case two (x: m, y: m)

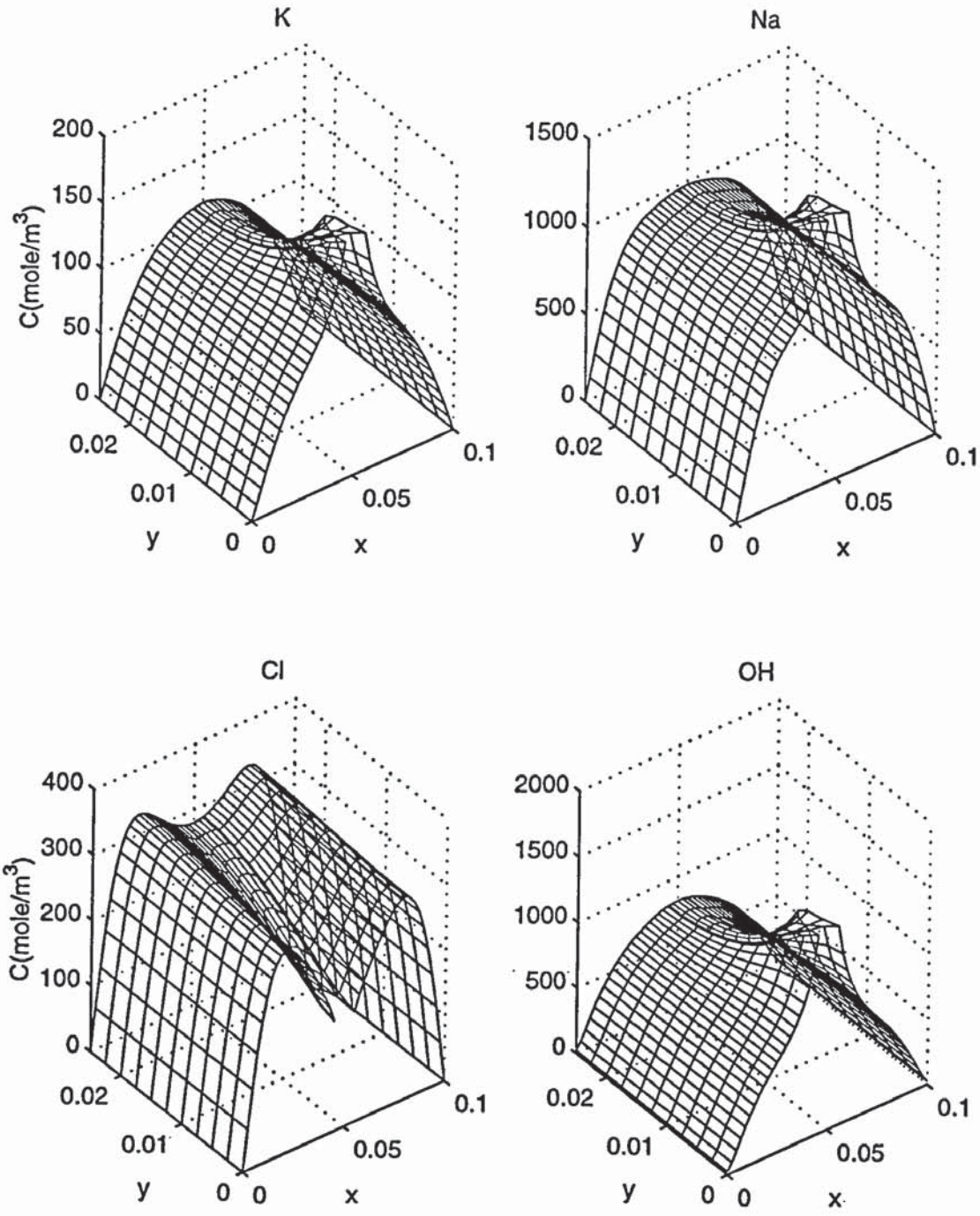

Fig. 5.15c Ionic concentration profiles after 12 weeks at $I = 5$ A/m^2 in case two (x: m, y: m)

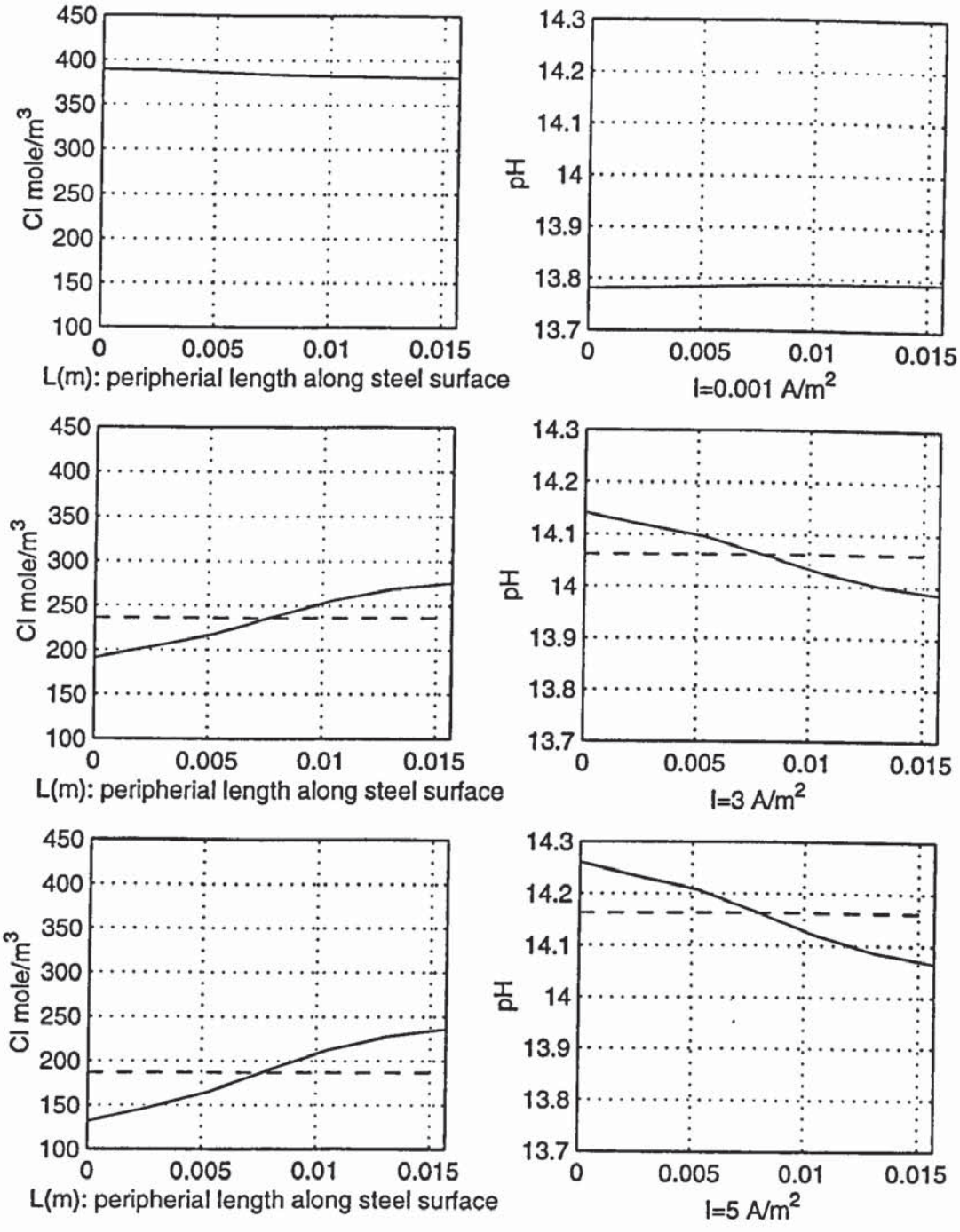

Fig. 5.16 Distributions of free chloride concentrations and pH values of pore solution at the surface of steel bar after 12 weeks treatment in case one

– –: average level

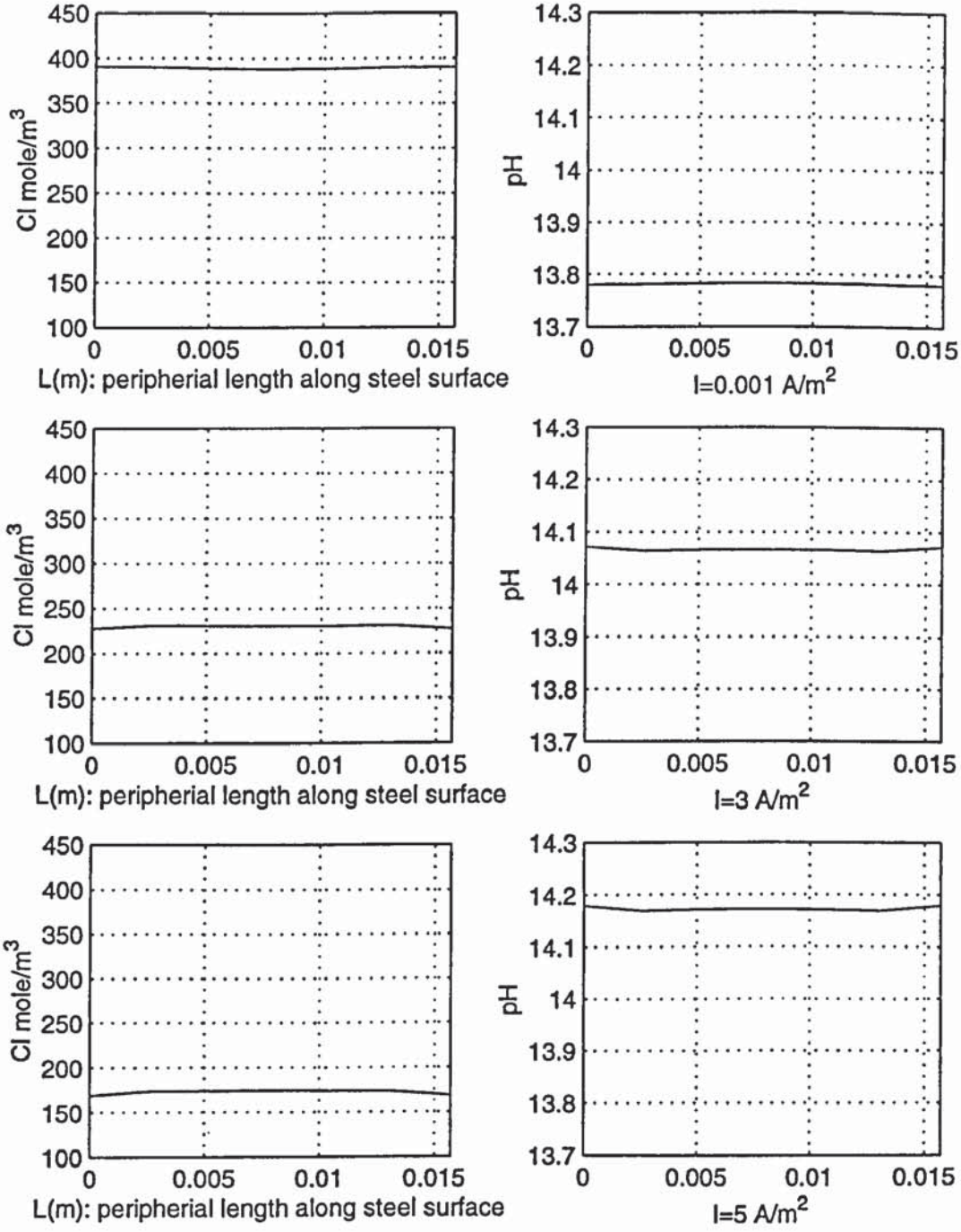

Fig. 5.17 Distributions of free chloride concentrations and pH values in pore solution at the steel surface after 12 weeks in case two

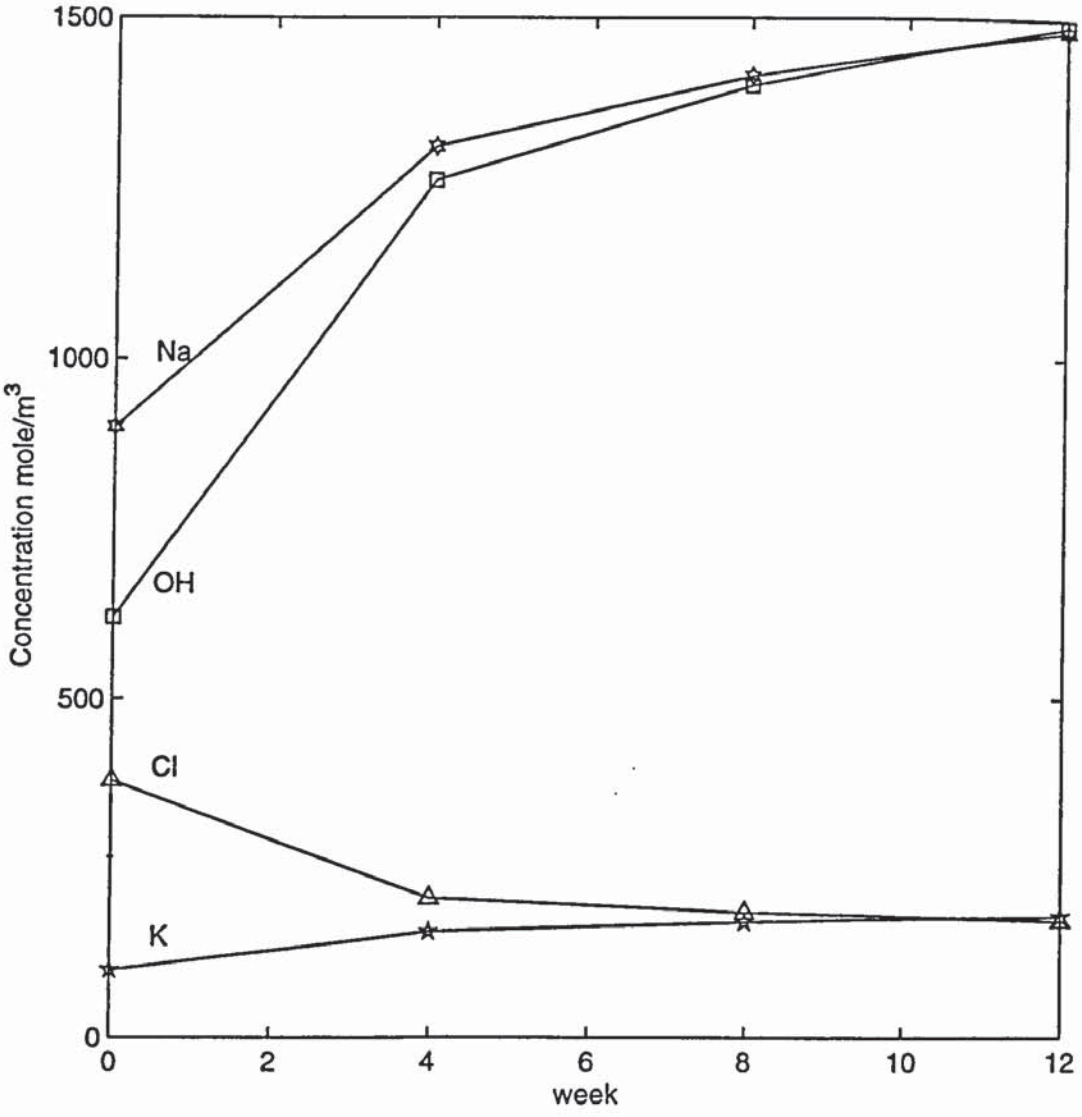

Fig. 5.18 The variation of average ionic concentrations at the surface of steel cathode in case two subjected to 5 A/m^2 current density

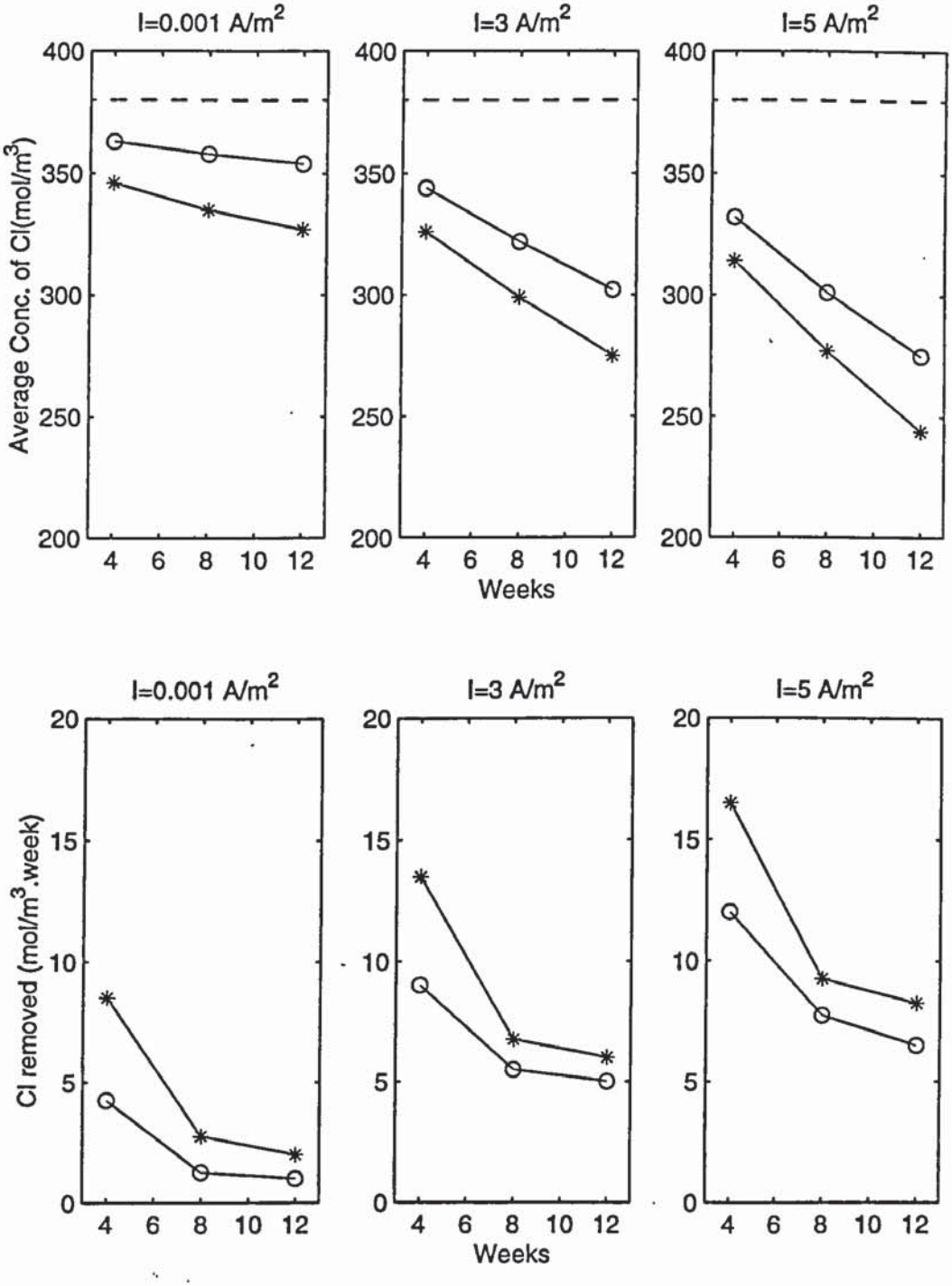

Fig. 5.19 The comparison of the chloride removal effectiveness and efficiency at different current densities in two cases

o-case 1, *-case 2, dash line - initial chloride concentration

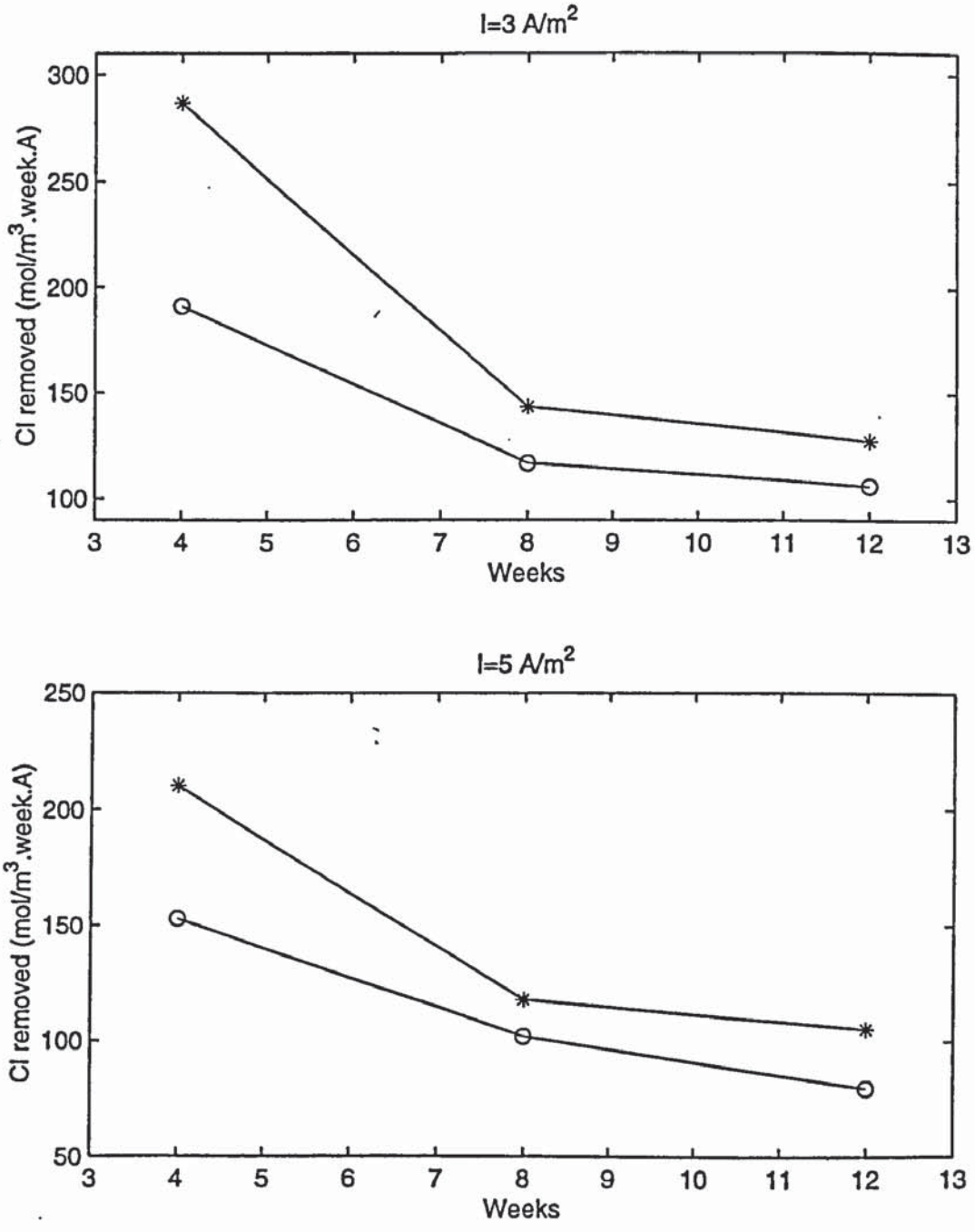

Fig. 5.20 The average chloride removed by a unit current per week

o-case 1, *-case 2

CHAPTER 6

EFFECTIVENESS AND EFFICIENCY INVESTIGATIONS OF ECR

6.1 INTRODUCTION

This chapter presents the results of case studies. Three different cases are investigated using the mathematical model developed in the preceding chapter, in which a specimen with six reinforcing steel bars is subjected to different treatment schemes. The aim of this study is to investigate the influence of configuration of reinforcements, which act as the cathodes during the treatment. Discussion is focused on the chloride removal effectiveness and efficiency. Effects of externally applied current density and treatment period on ionic concentration distributions are also discussed.

6.2 CASE STUDIES

A rectangular prism specimen of hydrated cement paste with six embedded steel reinforcing bars is studied. The distances from their central lines to the external anode are 0.15 and 0.25m, respectively (see Figs. 6.1-6.3). The current is galvanostatically controlled by an equivalent average current density of 3 A/m^2 on the surface of the steels. The initial concentrations of ionic species are assumed to be uniform, the values of which together with other parameters used in the numerical study are given in Table 6.1. Three different treatment cases are investigated here. The first case is that in which all of the reinforcements are linked together and the current is applied between the external anode and the six reinforcing bars (Fig. 6.1). In the second case, the six steel bars are separated and the current is applied between each of the steel bars and the external anode (see Fig. 6.2). The value of the current applied to each pair is a sixth of the total current applied in the first case. The third case is very much similar to the second one except that the current is applied to each of three rear bars (see Fig. 6.3). The specimen are divided into three regions, named as A, B and C for the convenience of

analysis and discussion. The tortuosity and porosity are assumed as $\tau = 2.0$ and $\varepsilon = 0.129$. The parameters used in the chloride binding model (Langmuir isotherm) are $\alpha = 1.67$, $\beta = 4.08$ (l/mol) and $w = 0.5$.

In this study, the ionic transports in specimen and in external solution are considered at the same time. The ionic diffusion coefficients are assumed different in the specimen and in the external solution (see Table 6.1). Because the concentrations of hydroxyl and calcium are determined according to charge balance and solubility equilibrium, it is only needed to solve Eq. (3.9) for potassium, sodium and chloride. The boundary conditions for the three ionic species are assumed as that except at the interface of the specimen and external solution there are no fluxes of them along the boundaries of the specimen and the external solution.

6.3 RESULTS AND DISCUSSIONS

Fig. 6.4 shows the distributions of current densities in the three cases. Because the structure is symmetrical, only half of it is presented. It is clear that the current flow in the first case is mainly located in the region A, which is between the anode and the front reinforcing bars which are close to the anode. When the current is separately applied between the anode and each of the reinforcing bars the current flow is found not only in the region A but also in the region B between the two sets of reinforcements although the current density in the region B is slightly lower than that in the region A. As expected, when the current is applied between the anode and the three rear reinforcing bars the current density is nearly uniform in the two regions. It can also be seen that the current flow in the y direction is mainly located in the narrow regions where reinforcements are placed. Compared to the current density in the x direction, the current density in the y direction is very small.

Fig. 6.5 shows the concentration distribution profiles of potassium, sodium, chloride and hydroxyl ions after four weeks (see Fig. 6.5a), eight weeks (see Fig. 6.5b) and twelve weeks (see Fig. 6.5c) for case one. Similar results for case two and three are shown in

Fig. 6.6 and Fig. 6.7, respectively. The concentration profiles of calcium ions are not presented since they are very low in the pore solution.

In case one, it can be seen that during the process potassium and sodium ions move from the anode towards the inside of the concrete, whereas the chloride ions move in the opposite direction. The highest concentrations of potassium and sodium ions are found at the edges of front steel bars where the chloride concentration is the lowest. In contrast, the increase of the concentrations of potassium and sodium ions and the decrease of the chloride concentration at the rear steel bars are very limited and insignificant. The concentration of hydroxyl ions near the steel bars is found to increase with the time. This is because of the cathodic electrochemical reactions taking place at the steel bars. However, because the current density at each of the steel bars is not equal (although they are linked together), the generation rate of hydroxyl ions at each of the steel bars is also different; the closer the steel bar is to the anode the faster the generation of hydroxyl ions. Since the steel bars near the anode carry most of the current, the removal of chloride ions is mainly in the regions between the anode and the front steel bars. The treatment has very little influence on the rear steel bars, which are far from the surface. For the region C, which is behind the rear steel bars, there is little current flow and thus the transport of ions in that region is almost purely due to diffusion. As is shown in Fig. 6.5 the removal of chloride due to diffusion is very slow.

Fig. 6.6 shows the ionic concentration distribution profiles at four, eight, and twelve weeks for case two. Unlike case one, the highest concentrations of potassium and sodium ions are found at the edges of the rear steel bars. The chloride concentration along the surface of each steel bar is not even, but the average level at the front steel bars is lower than that at the rear bars. Comparing with case one, chloride removal in region B is enhanced. Since the current density is equally applied for each of the steel bars the generation rate of hydroxyl ions is identical. However, because of the large concentration gradient between the anode and the front steel bars the hydroxyl ions move rather quick in region A. Consequently, the rear steel bars have higher hydroxyl concentrations than the front bars. Again, because there is little current flow in region C, no significant concentration variation is found there.

The global features of the ionic concentration distribution profiles in case three (Fig. 6.7) are found to be similar to those in case two except that in the local area close to the front steel bars where there is no significant localised concentration distribution. This is because no current applied on the front steel bar.

Fig. 6.8 shows the average chloride concentration remaining in the pore solution and Fig. 6.9 shows the amount of chloride removed by per unit current at different times. It can be seen that the most chloride was removed in case two and the least removed is in case one. However, as the current applied in the case two is larger than that in case three, the removal by per unit current is thus lower. The most efficient treatment is therefore represented by case three in which the current is the smallest, but the rate of removal per unit current is the highest.

Fig. 6.10 shows the average chloride concentration at the steel bar surfaces for case two. It can be seen that after 12 weeks, the chloride concentration at the surface of the front bars is lower than that of rear bars. It means that for the same current density applied to each steel bar, the effectiveness of the chloride removal at each steel bar is different. The present results show that, in order to achieve the same chloride level at the region near the steel bars, the current densities applied to the rear bars should be higher than that applied to front bars. In another words, the current density should be increased with the distance of the embedded steel bar from the surface or the thickness of concrete cover.

6.4 CONCLUSIONS

The selection of steel bars as cathodes on the current distribution has significant influence on chloride removal. The case studies show that, when the current is applied separately to each of the steel bars in concrete at the same time, the ECR process has the highest effectiveness. When the current is applied separately only to the deepest embedded steel bars, the highest efficiency will be achieved. When all of the steel bars in concrete are connected together and current applied, ECR has the lowest effectiveness and efficiency.

Table 6.1 Initial concentrations and diffusion coefficients

	Potassium	Sodium	Chloride	Hydroxyl	Calcium
External solution (mol/m^3)	0.0	0.0	0.0	25.2	12.6
Pore solution (mol/m^3)	100.0	900.0	380.0	620.0	0.0
Diffusion coefficient in external solution (10^{-9} m^2/s)	1.96	1.33	2.03	5.28	0.79
Diffusion coefficient in pore solution (10^{-9} m^2/s)	0.392	0.266	0.406	1.056	0.158

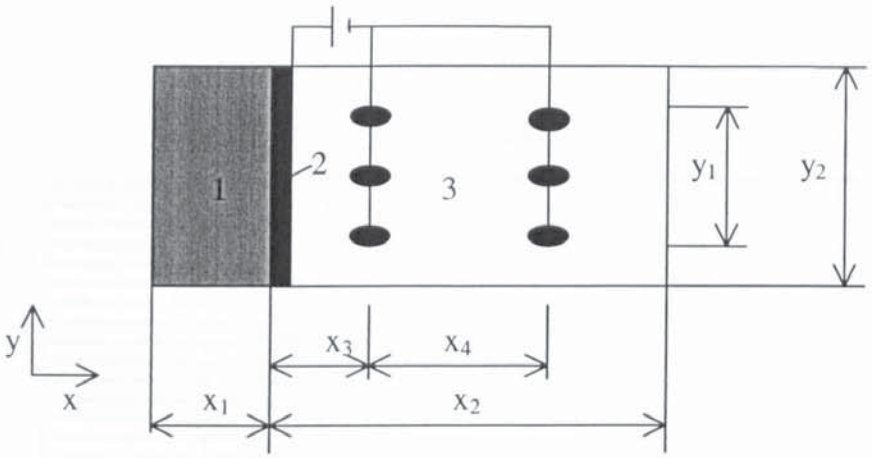

Fig. 6.1 Case one: all of the reinforcements are connected to a galvanostat

1 – external solution, 2 – external anode, 3 – reinforced concrete

$x_1 = 0.1$m, $x_2 = 0.2$m, x_3=0.05m, x_4= 0.1,

$y_1 = 0.06$m, $y_2 = 0.1$m, diameter of steels is 0.01m

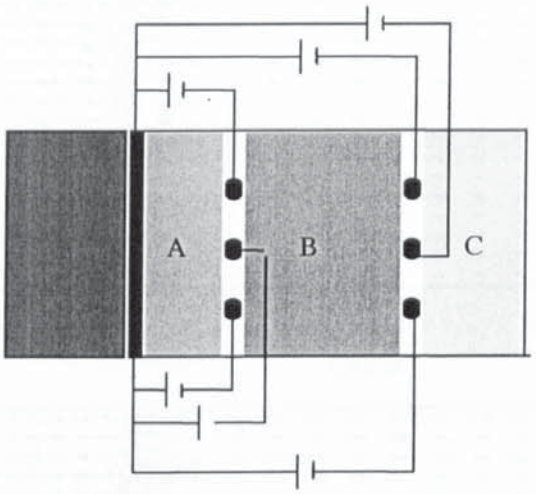

Fig. 6.2 Case two: every steel is connected to its own galvanostat

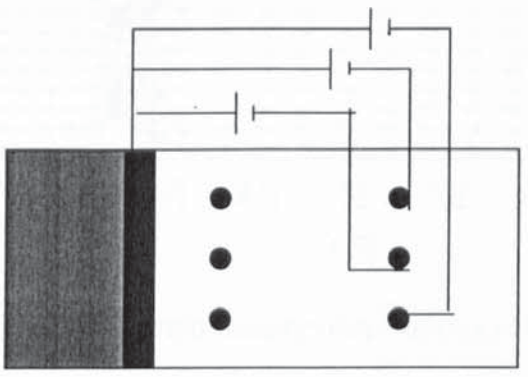

Fig. 6.3 Case three: each deepest embedded steel is connected to its own galvanostat

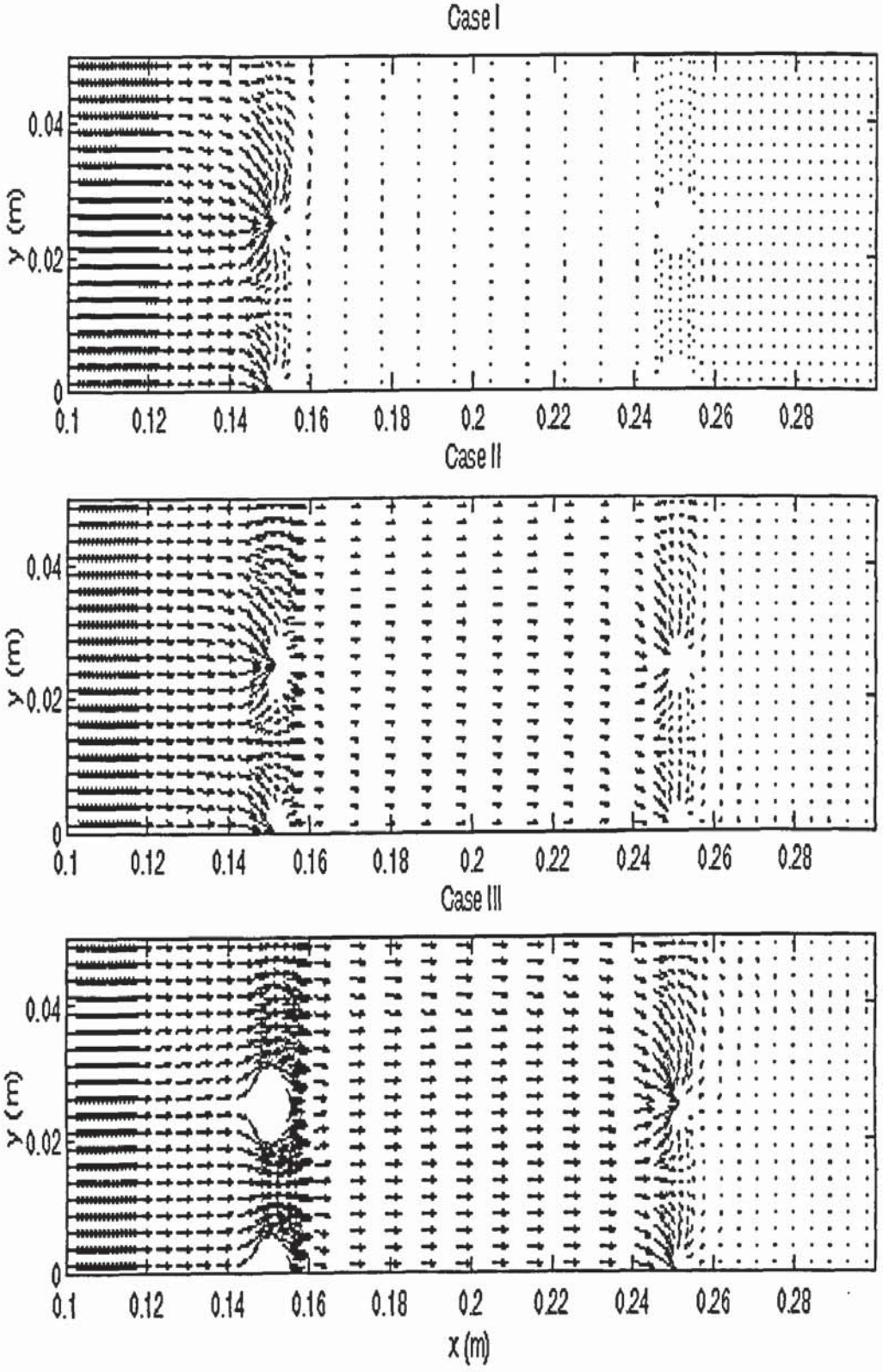

Fig. 6.4 Current density distributions in three cases

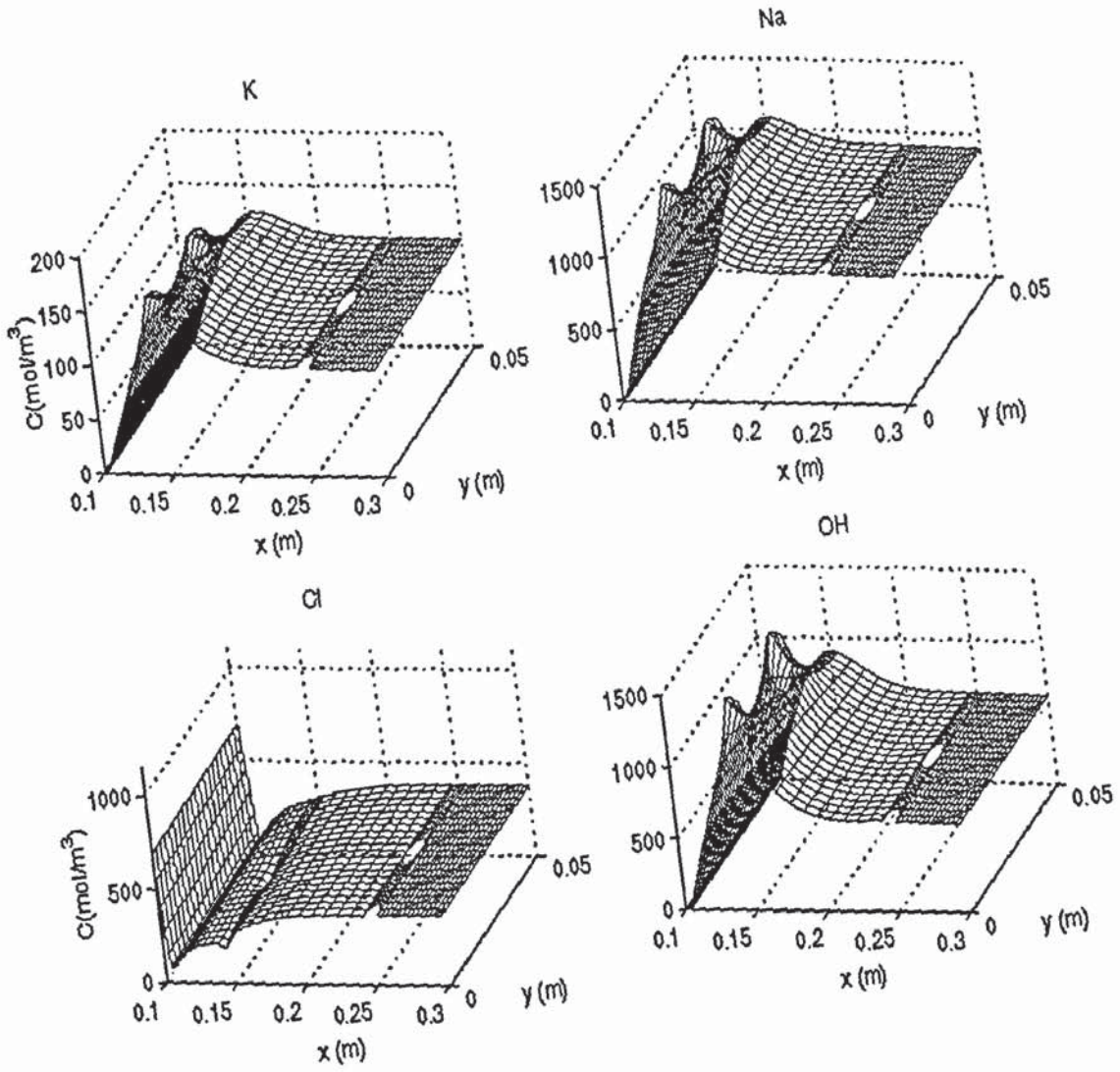

Fig. 6.5a Ionic concentration profiles after 4 weeks in case one

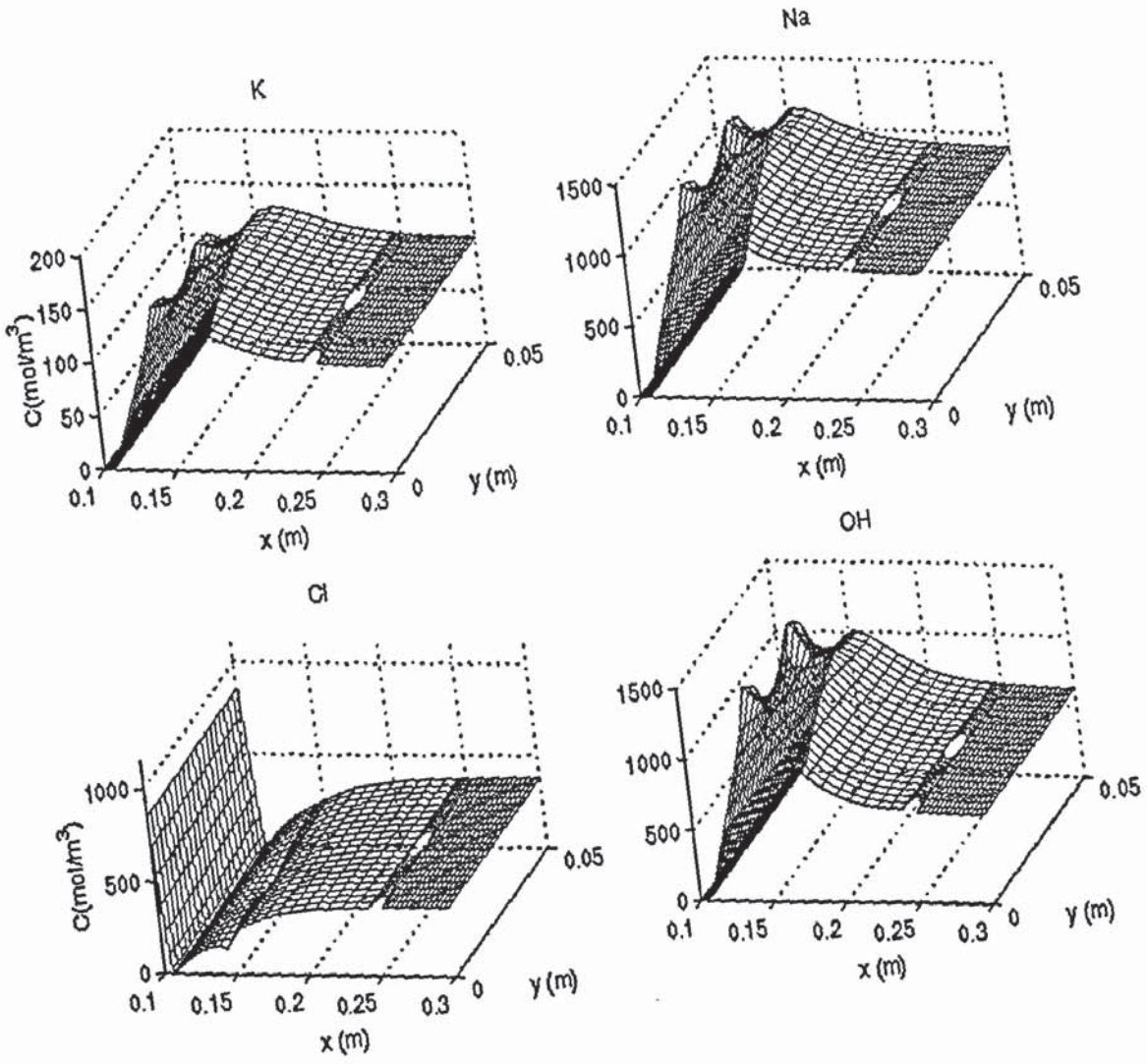

Fig. 6.5b Ionic concentration profiles after 8 weeks in case one.

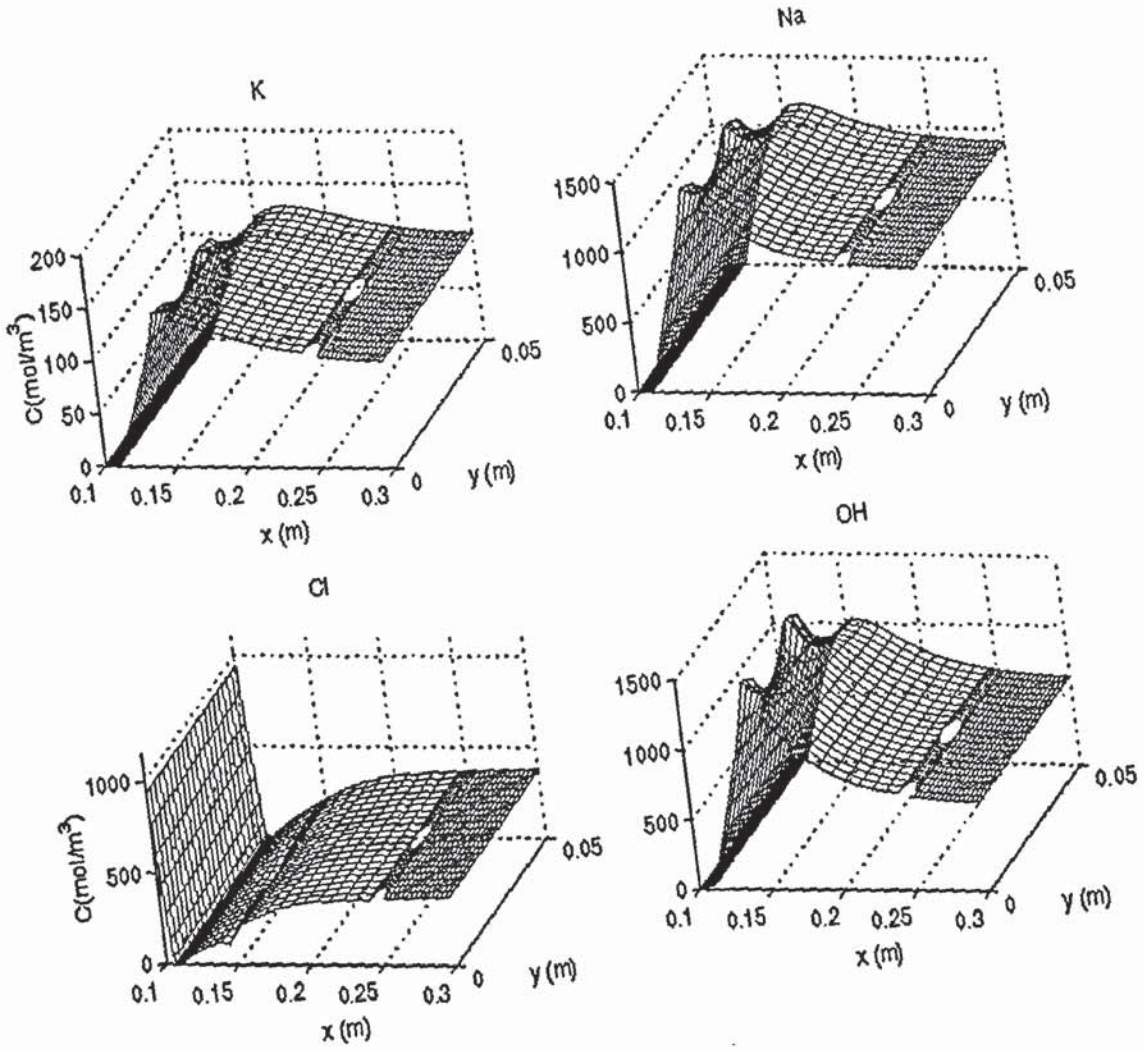

Fig. 6.5c Ionic concentration profiles after 12 weeks in case one.

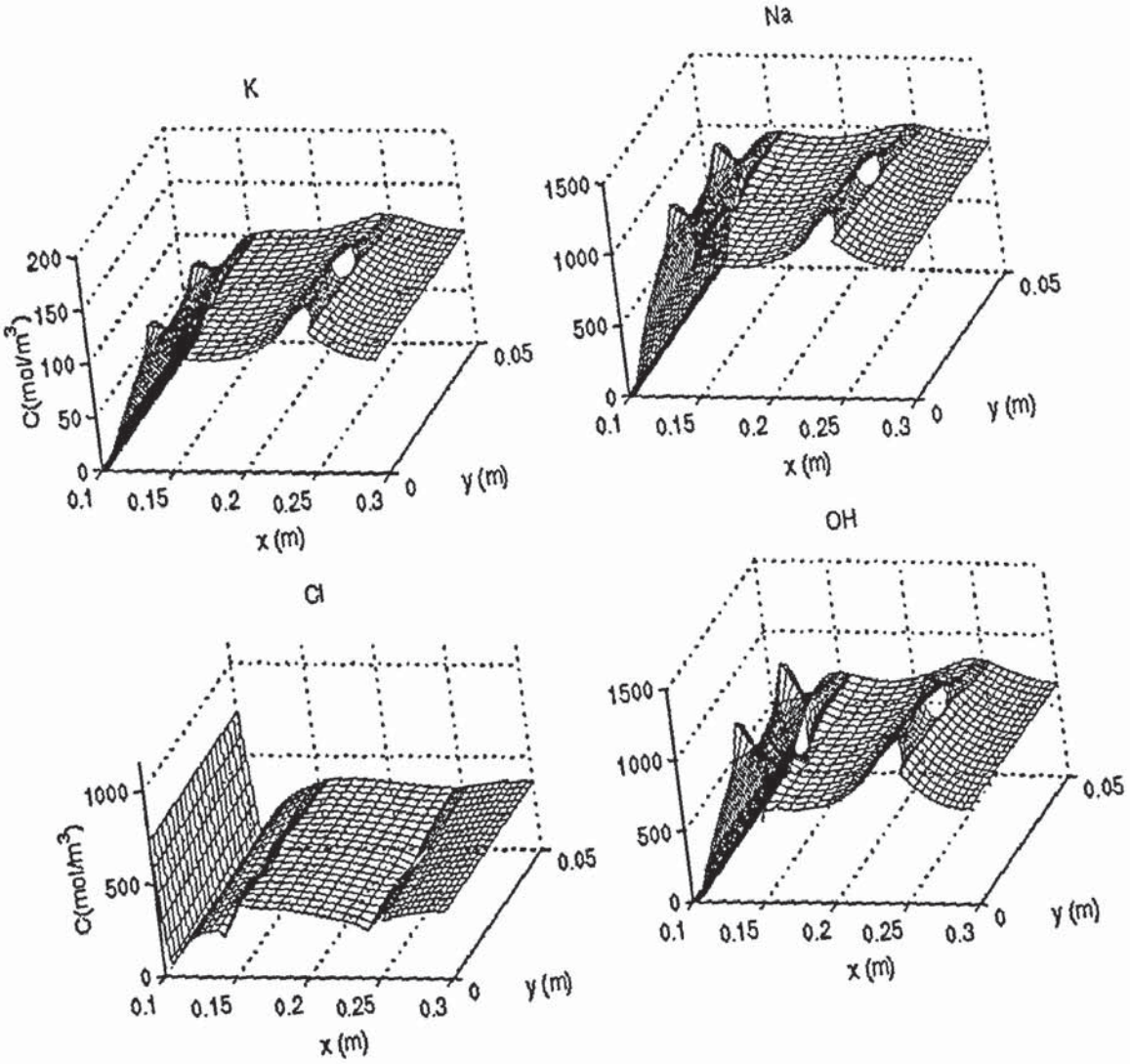

Fig. 6.6a Ionic concentration profiles after 4 weeks in case two.

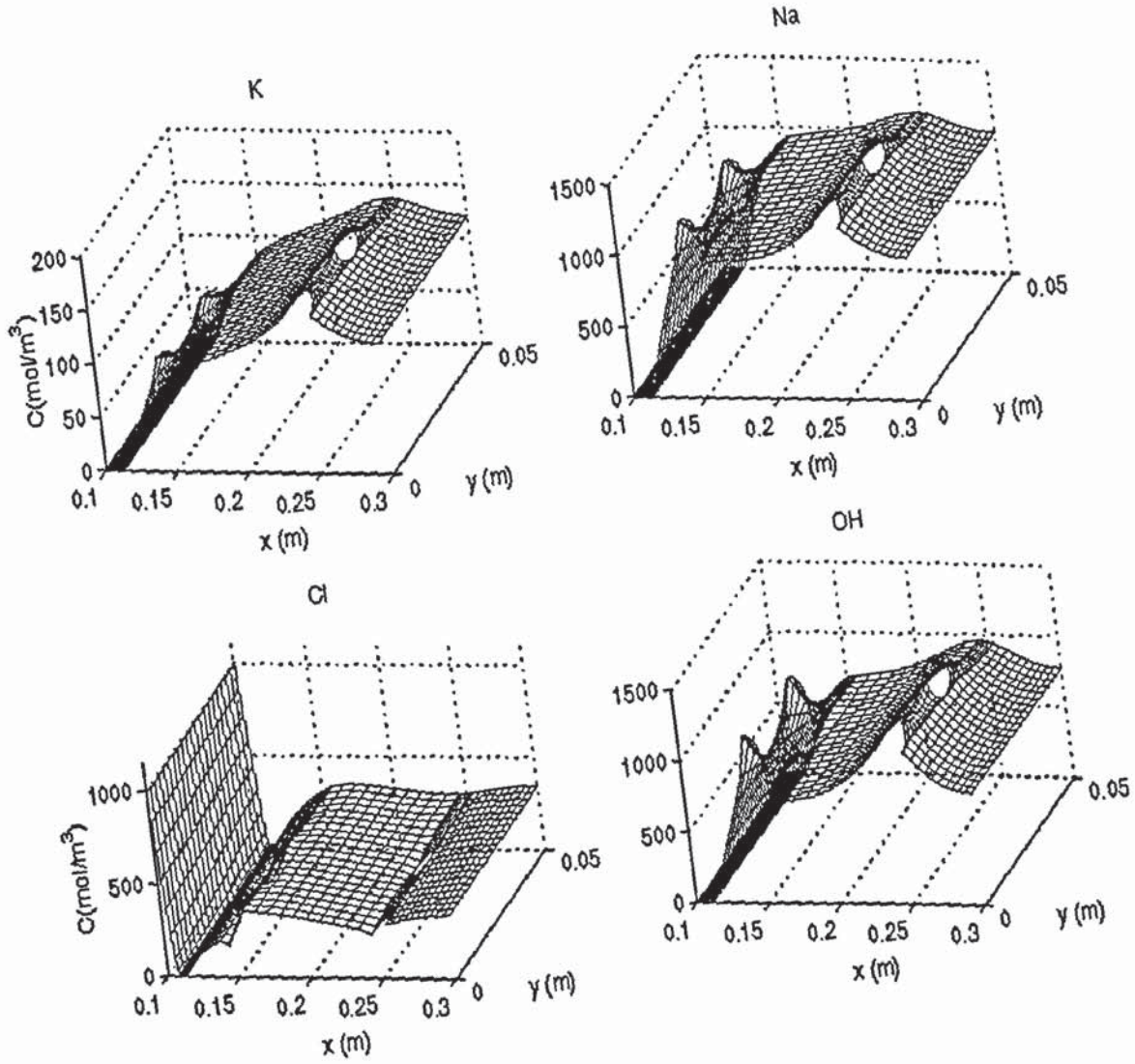

Fig. 6.6b Ionic concentration profiles after 8 weeks in case two.

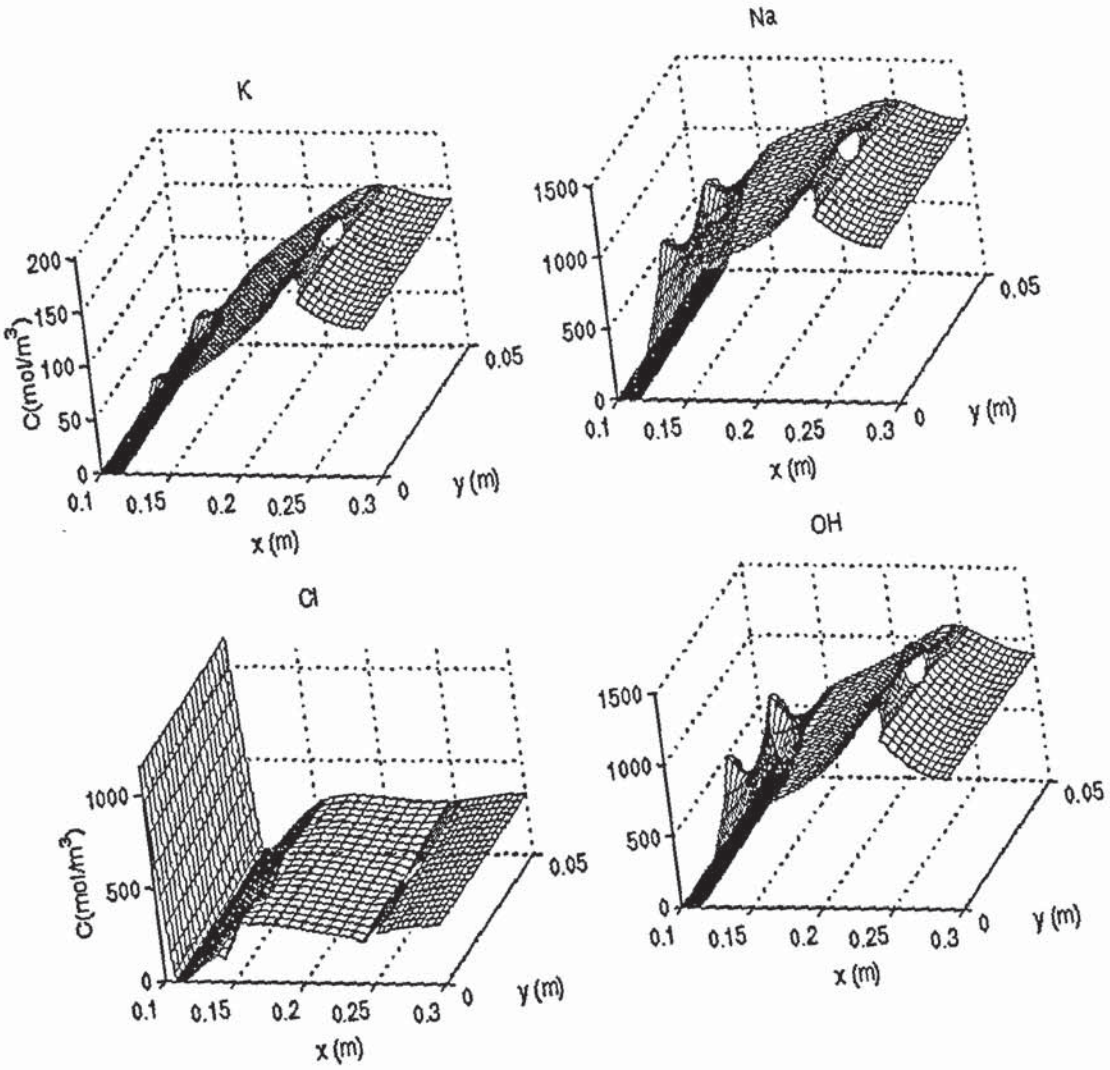

Fig. 6.6c Ionic concentration profiles after 12 weeks in case two.

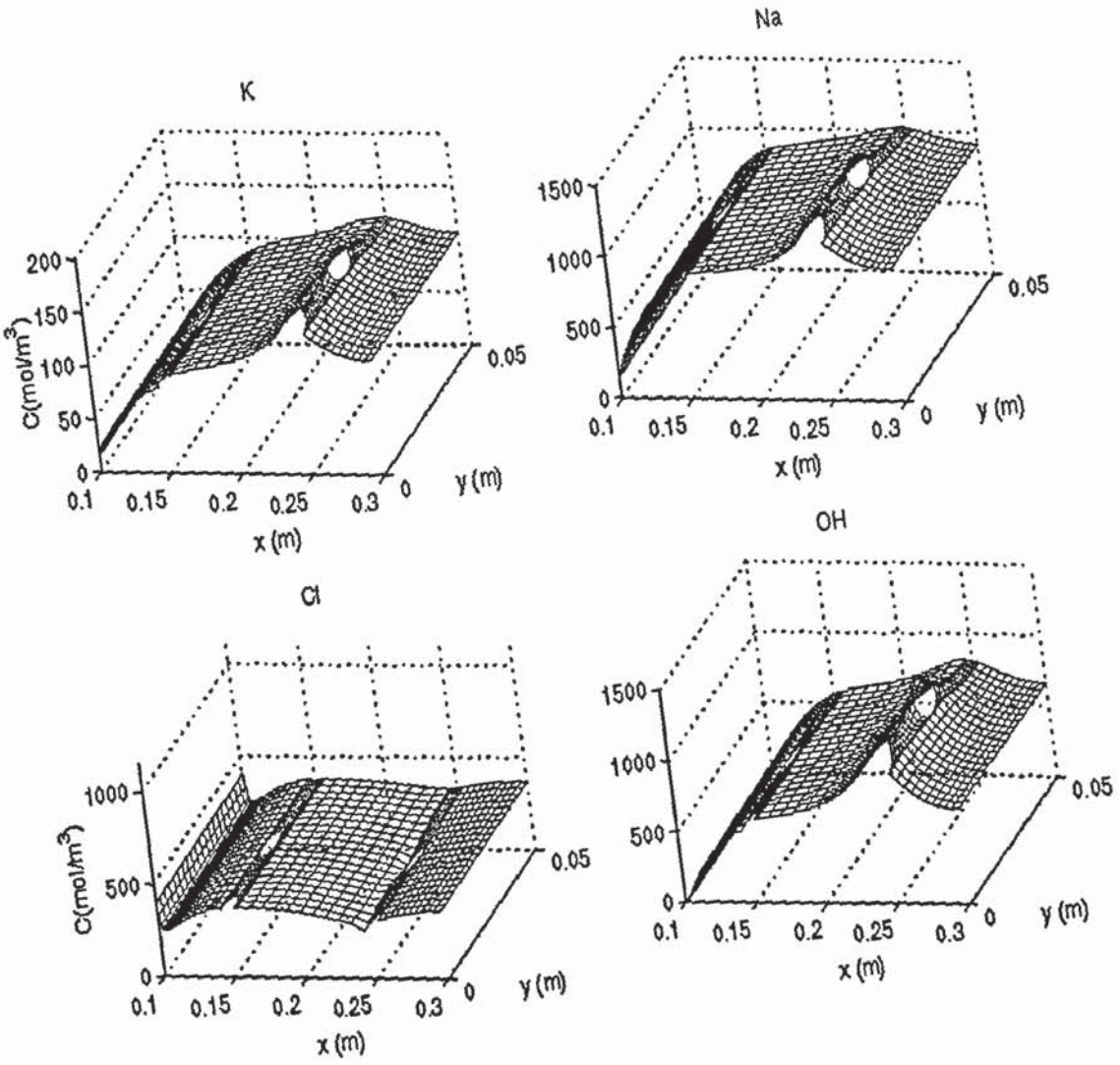

Fig. 6.7a Ionic concentration profiles after 4 weeks in case three

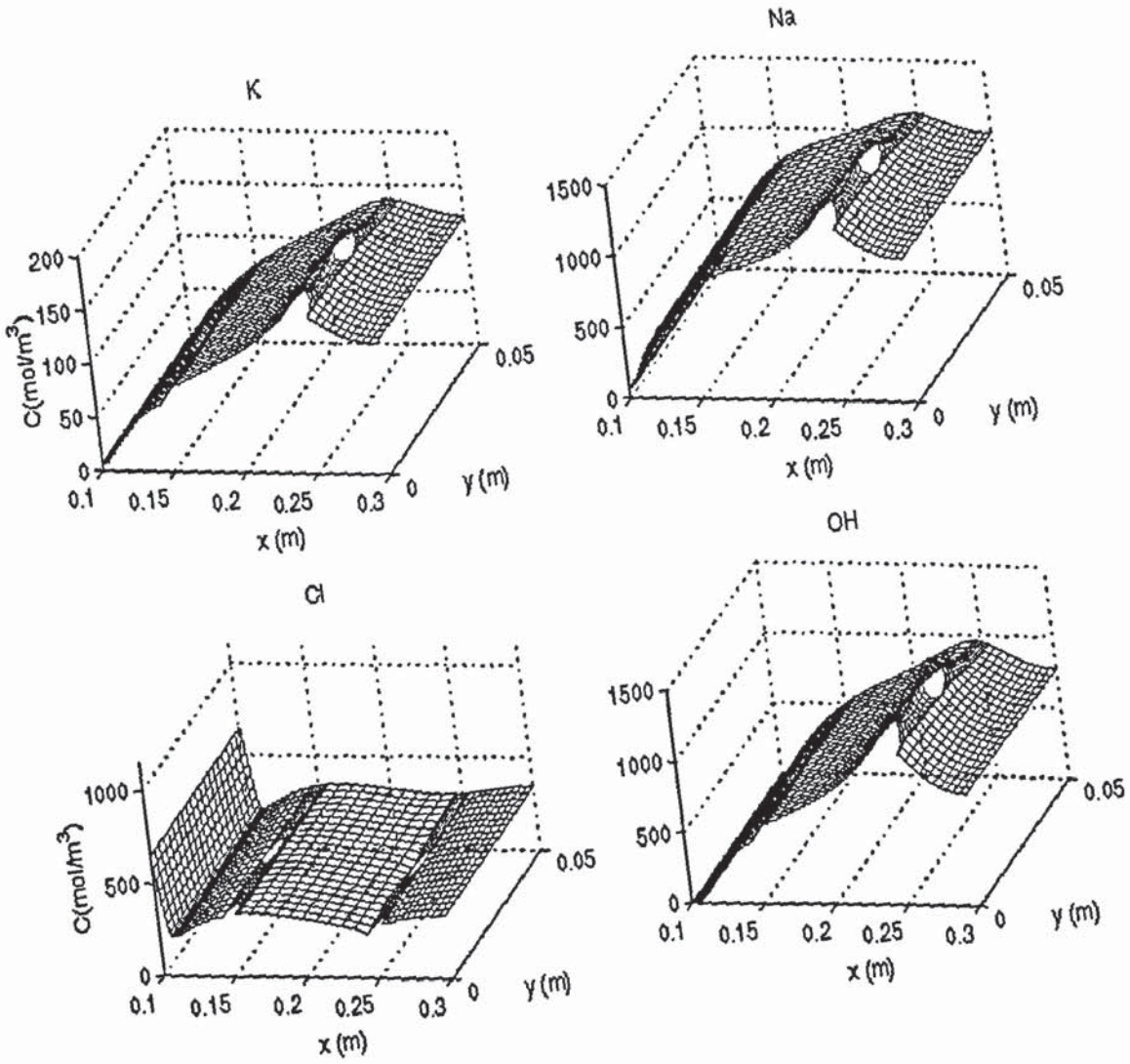

Fig. 6.7b Ionic concentration profiles after 8 weeks in case three

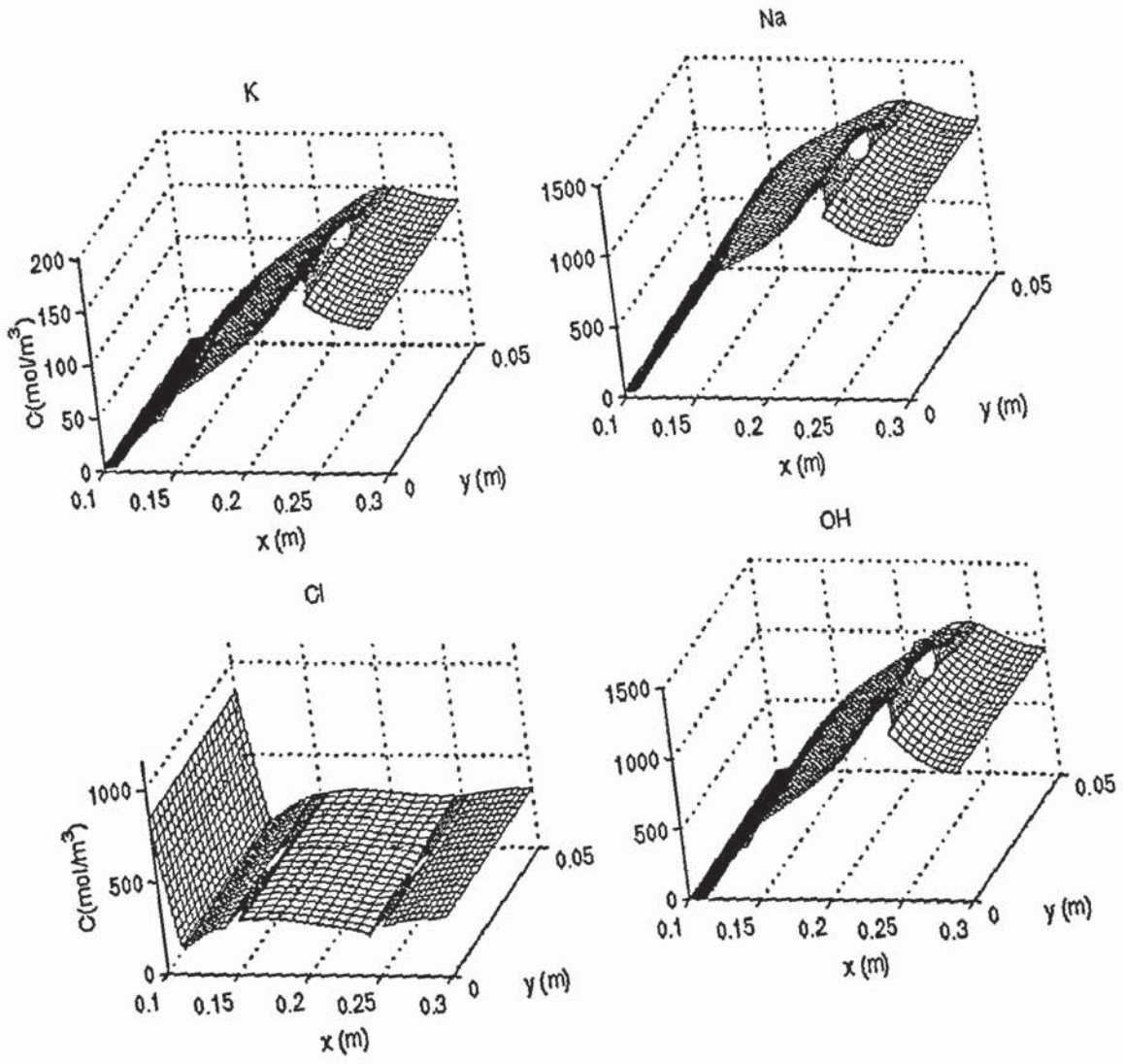

Fig. 6.7c Ionic concentration profiles after 12 weeks in case three

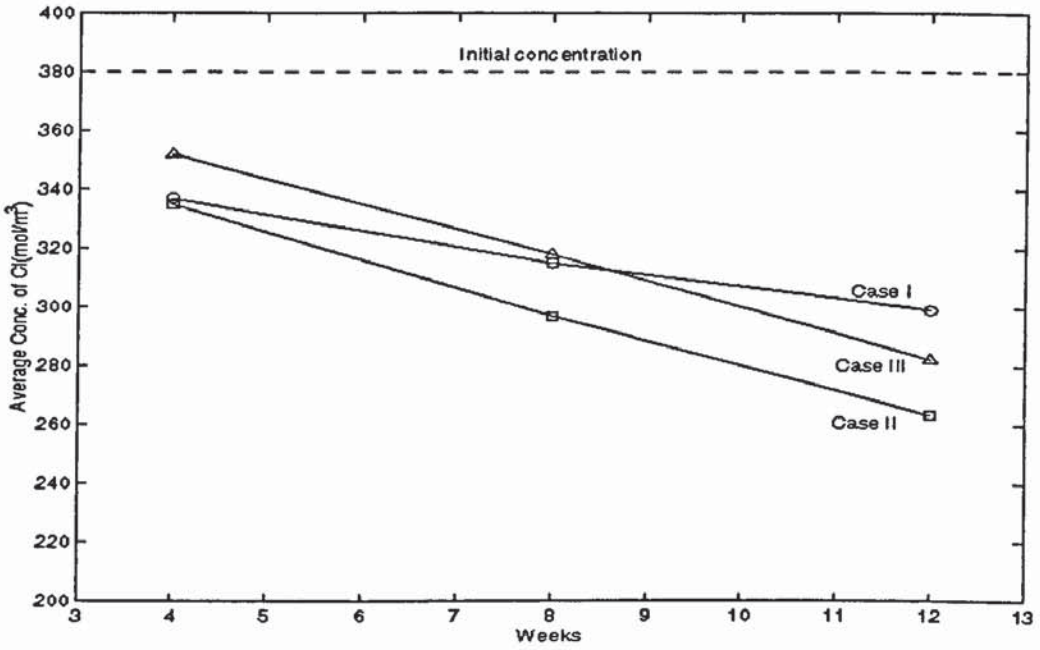

Fig. 6.8 Comparing of the effectivenesses of the ECR process

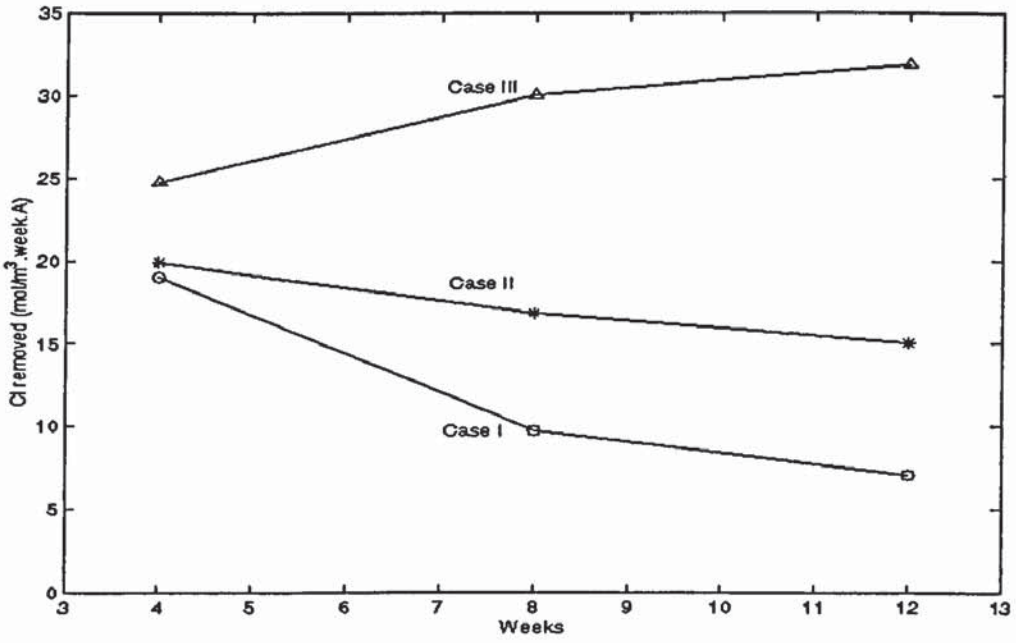

Fig. 6.9 Comparing the efficiencies of the ECR process

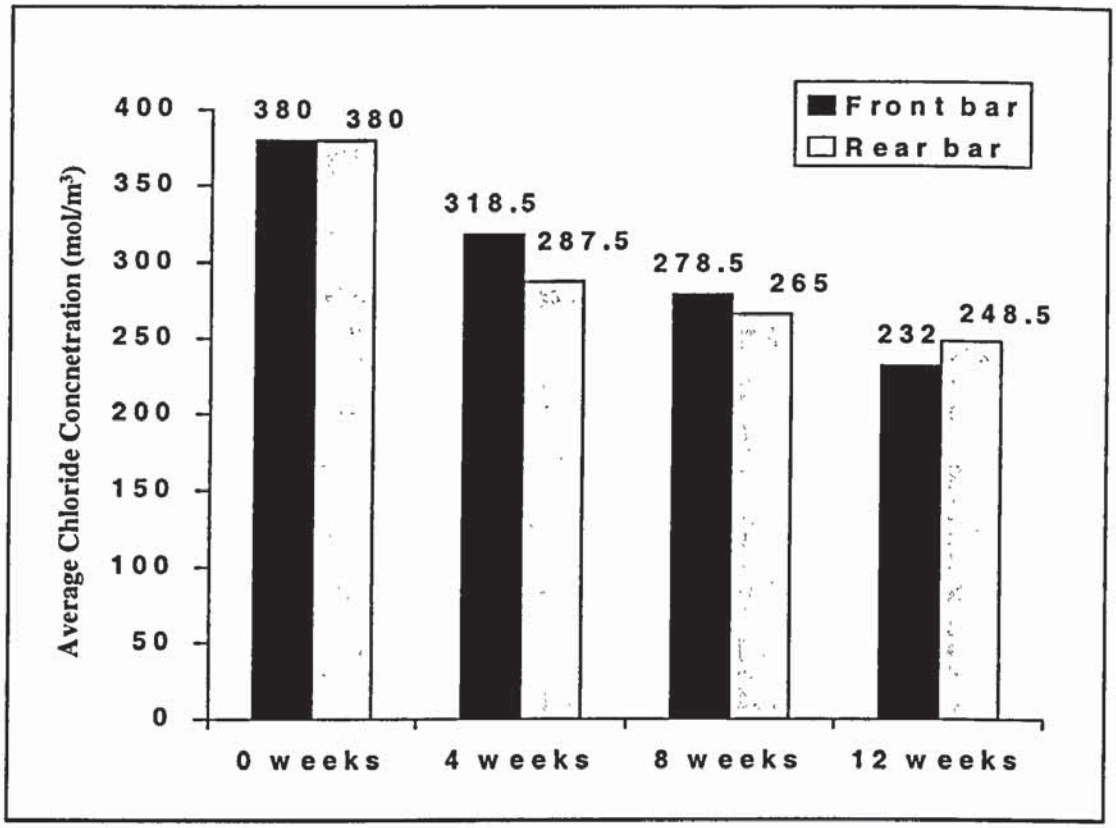

Fig. 6.10 Average chloride concentration at the steel surface for case two

CHAPTER 7

CHLORIDE BINDING RELATIONSHIPS

7.1 INTRODUCTION

In Chapter 4, it has been shown that when chloride ingresses into concrete from a saline environment, part of it is absorbed by solid phase of concrete. Although it is generally assumed that the bound chloride ions have no direct effects on the corrosion of reinforcement, it has been seen in Chapter 5 that when chloride ions in the pore solution are reduced by ECR, the bound chloride could release from the solid phase of concrete into the pore solution, which in turn reduces the removal process. The release of bound chloride during ECR has also been demonstrated by the experimental investigation of Bertolini et al. and Ismail, which showed that following the removal of free chloride ions the concentration of bound chloride ions reduces [Bertolini, et al., 1996; Ismail, 1998]. This indicates that the effect of chloride binding should be considered when studying chloride transport in concrete, in both chloride ingress into concrete and chloride removal from concrete.

The chloride binding capacity is a non-linear function of the total chloride content and this will be reflected in the rate of chloride ingress into concrete. The review of literature in Chapter 2 suggests that the binding capacity usually can be described by using a binding isotherm that may be defined as the equilibrium relationships between the total and free, or the free and bound chloride contents at a constant temperature [Glass, et al., 1998]. However, the detailed mathematical expressions vary from case to case.

Previous research has also suggested that for chloride ingress into concrete from a saline environment the chloride binding could be considered to be a relatively fast process compared with chloride diffusion and thus an instantaneous equilibrium between bound and free chlorides could be assumed [Sergi, et al., 1992]. Under this assumption Pereira

and Hegedus [1984] used a Langmuir isotherm to describe approximately the relationship between free and bound chlorides.

The Langmuir isotherm also was adopted in the mathematical model of ECR by some researchers [Li and Page, 1998a and 2000]. However, because the Langmuir isotherm is based on the assumption of the equilibrium state between free and bound chlorides, it could not be strictly maintained in the process of ECR. Some researchers proposed that when a relatively high current density is applied to a concrete structure in the process of ECR, the rate of release of bound chloride is likely to be slow in comparison to the rate of free chloride removal and, under such conditions, becomes rate limiting. In this case, the relationship between free and bound chloride may be far from equilibrium [Hassanein, et al., 1998]. Based on this assumption, Hassanein et al. [1998; 1999] suggested a simple first order chemical reaction Eq. (7.2) to approximate the bound chloride release in the process of ECR, in which the change of the bound chloride contend is given by the following equation:

$$\frac{\partial S}{\partial t} = -k_r S \tag{7.1}$$

where k_r is the rate constant for the release of bound chloride, S is the mass of bound chloride expressed relative to the mass of sample.

Obviously, the above equation regards that the bound chloride release rate is only linearly dependent on the content of bound chloride. Rigorously, however, the rate of bound chloride release should depend on the content of bound chloride as well as the content of free chloride in pore solution because any process of release or adsorption of ions at the interface depends on the concentration difference between the free and bound ions. In this chapter, a new chloride binding relationship is proposed. The new chloride binding relationship considers the possible non-equilibrium between the free and bound chlorides which is an extension of the previous instantaneous equilibrium model. The proposed relationship is used to simulate a one-dimensional case. The numerical results are compared with that of the Langmuir isotherm and the experimental data.

7.2 A NEW CHLORIDE BINDING RELATIONSHIP

According to the simplified formula described by Hassanein et al. [1998; 1999], the reaction of chloride binding may be expressed as the free chloride ions react with binding sites (b) to give bound chloride (bCl) as the following:

$$Cl^- + b \leftrightarrow bCl\,. \tag{7.2}$$

The above reaction can be assumed only taking place at the interface between bulk pore solution and the concrete solid phase. In literature, these kind of reactions, which take place at surfaces, are named as the heterogeneous reactions [Probstein, 1989].

Normally, a heterogeneous reaction involves several steps. The first is the transfer of reacting species to the surface on which the reaction occurs (reaction surface). The second is the heterogeneous reaction itself. This step is often composed of a series of substeps that may include diffusion of the reactants through the solid phase, adsorption on the surface, chemical reaction, desorption of products and diffusion of products out of the solid phase. The third is the transfer of the products away from the reaction surface into the bulk solution.

The overall rate of a heterogeneous reaction is mainly controlled by the rate of the slowest step in it. This step is then called the rate determining step or rate limiting step. If the rate limiting step is either step one or three, which involves the introduction or removal of reactants, then the reaction is said to be diffusion controlled, with the rate governed by the mass transport relations. On the other hand, if step two, involving the chemical, physical transformation, is the slowest step, then the rate is determined by the kinetics of the given process. As noted, within this step there may in turn be a distinction between diffusion and chemical, physical rates. Those cases where the rates of the diffusion and reaction steps are comparable are sometimes termed mixed heterogeneous reactions.

For heterogeneous reactions the molar rate of species production refers to a surface rather than a volume source, and can be written as:

$$R_i' = \frac{1}{A}\left(\frac{dn_i}{dt}\right)_{by\ reaction} \tag{7.3}$$

where R_i' is the molar rate of species production, A is the reaction surface area, n is the molar number of the species, t is the time.

A heterogeneous reaction can be thought of as being equivalent to a homogeneous reaction. Homogeneous reactions are the reactions taking place in bulk solution, for which the molar rate of species production is referred to per volume of solution:

$$R_i = \frac{1}{V}\left(\frac{dn_i}{dt}\right)_{by\ reaction} \tag{7.4}$$

where R_i is the molar rate of species production, V is the volume of bulk solution. It is only the constants of proportionality and dimensions that change when compared with Eq. (7.3). The relationship between R_i' and R_i can be expressed as that $R_iV=R_i'A$ [Probstain, 1998].

A simple homogeneous reaction is one for which the reaction rate at a given temperature is, according to the law of mass action, proportional to the active masses (concentrations) of the reacting substances:

$$R_1 = k\prod(C_i^{\nu_i})_{reactants} \qquad \text{and} \qquad \nu = \sum \nu_i \tag{7.5}$$

where R_1 is the reaction rate, k is the rate constant, C_i is concentration of species, and ν_i the stoichiometric coefficient of the species i. The coefficient ν_i is also called the order of the reaction with respect to the species i, and ν is called the overall order of the reaction. Most known reactions are of first or second order.

In a reversible reaction the net rate of the reaction R_1 is the difference between the forward and reverse reaction rates. At equilibrium there is no net rate of reaction, so the forward and reverse reaction rates are equal and this yields

$$\frac{k_f}{k_r} = K \tag{7.6}$$

where k_f and k_r are the rate constants for the forward and reverse reactions, respectively, and K is the thermodynamic equilibrium constant for the reaction.

Based on the above reaction kinetics, for the reaction of Eq. (7.2), a forward first order reaction is assumed as:

$$Cl^- + b \rightarrow bCl \tag{7.7}$$

for which the molar rate of production of bound chloride can be approximated as:

$$R_{S_{Cl}} = k_f C_{Cl^-} \tag{7.8}$$

where C_{Cl^-} is the free chloride concentration in solution.

On the other hand, a reverse first order reaction is assumed as:

$$bCl \rightarrow Cl^- + b \tag{7.9}$$

for which the molar rate of production of free chloride can be approximated as:

$$R_{Cl^-} = k_r S_{Cl} \tag{7.10}$$

where S_{Cl} is the bound chloride concentration.

It is obvious that the increase of bound chloride is equal to the decrease of the free chloride in solution. So we can get the following equations:

$$\frac{\partial S_{Cl}}{\partial t} = R_{s_{Cl}} - R_{Cl^-} = k_f C_{Cl^-} - k_r S_{Cl} = k_r (K C_{Cl^-} - S_{Cl}) \tag{7.11}$$

Because the stoichiometric coefficients of Cl^- and bCl in reaction (7.2) are unit, at an equilibrium state, the rate of bound chloride production equals to the rate of free chloride production. This will yield:

$$k_f C_{Cl^-} = k_r S_{Cl} \tag{7.12}$$

$$K = \frac{k_f}{k_r} = \frac{S_{Cl}}{C_{Cl^-}} \tag{7.13}$$

Assuming that the Langmuir isotherm holds at the equilibrium state, we have:

$$K = \frac{\alpha}{w(1+\beta C_{Cl^-})} \tag{7.14}$$

Substituting Eq. (7.14) into (7.11) yields:

$$\frac{\partial S_{Cl}}{\partial t} = -k_r \left(S_{Cl} - \frac{\alpha C_{Cl^-}}{w(1+\beta C_{Cl^-})} \right) \tag{7.15}$$

In the following sections, we will bring the above equation into the governing equation (3.9) to simulate the process of ECR.

7.3 MODELLING OF THE EXPERIMENT OF ECR

7.3.1 The Experiment

In order to test the proposed isotherm, the one-dimensional experiment of ECR described in Chapter 5, which was carried out by Bertolini et al. [1996], is simulated. The detail about the experiment can be found in section 5.2.1. In the experimental investigation, the specimens were prepared to have uniform initial ionic concentration distributions. The mathematical model developed in Chapter 3 is adopted, but the specimens are assumed to be saturated so that the ionic convection with the pore solution is neglected. The parameters used in the modelling are same as that in section 5.2.1. Only potassium, sodium, chloride, hydroxyl and calcium ions ade considered in the model. Because of its low concentration, results related to calcium are not presented in the result figures.

7.3.2 Results And Discussions

Because there are no available data for the rate constant k_r, we employ three constants, which are 4.0×10^{-6}, 4.0×10^{-7} and 4.0×10^{-8} (1/s), respectively. Fig. 7.1 shows the predicted ionic concentration profiles at 4, 8 and 12 weeks, for the specimen subjected to a current density of 5 mA/m^2. It can be seen that for chloride ions the three different rate constants yield very similar predictions; for hydroxyl and other two cations the predictions are almost the same. It can also be seen that when the rate constant, k_r, equals 4.0×10^{-6} (1/s), the prediction is almost same as that predicted by Langmuir isotherm. This means that when the current density is very small, free and bound chlorides are almost in equilibrium.

Fig. 7.2 shows the predicted ionic concentration profiles at 4, 8 and 12 weeks for the specimen subjected to a current density of 1.0 A/m^2. The results show that for chloride ions the predictions with the three different rate constants slightly different. The result with $k_r = 4.0\times10^{-6}$ (1/s) is almost the same as that of Langmuir isotherm. Differences

due to different rate constants in the hydroxyl profiles are found negligible. For the two cations, no difference is found. This indicates that at the current density of 1.0 A/m^2, the assumption of equilibrium between free and bound chlorides still holds.

Fig. 7.3 shows the predicted total chloride content expressed as per unit weight of concrete. It can be seen that the predictions from Langmuir isotherm and that from the proposed isotherm with three different rate constants are almost the same.

Fig. 7.4 shows the predicted ionic concentration profiles after the treatments for 4, 8 and 12 weeks when the specimen is subjected to a current density of 5.0 A/m^2. Compared with the previous results in the case where the specimen is subjected to a current density of 1.0 A/m^2, the results in this case show that the difference between the predictions of the three different rate constants increases. Compared with the experimental data, the chloride concentration in pore solution is significantly under-estimated by using the rate constant of 4.0×10^{-8} (1/s), but the results with the rate constant of 4.0×10^{-6} (1/s) presents a good prediction, especially at the region near the reinforcing steel. In addition to that, the constant of 4.0×10^{-6} (1/s) presents almost the same prediction as that of the Langmuir isotherm.

Fig. 7.5 shows the predicted total chloride content expressed as per unit weight of the specimen. It also can be seen that the difference between the predictions of the three rate constants increases when the specimen is subjected to the current density of 1.0 A/m^2. In agreement with the above results obtained from the analysis of pore solution, for total chloride content the rate constant 4.0×10^{-6} (1/s) presents a good approximation to the experimental data, especially in the region near the reinforcing steel. The comparison also shows that the predicted total chloride content by the rate constant of 4.0×10^{-6} (1/s) is the same as that by the Langmuir isotherm.

The above analysis shows that at a relatively high current density, such as 1.0 and 5.0 A/m^2, the proposed model provides different results for different rate constants. This indicates that the proposed model has the ability to reflect the possible non-equilibrium between free and bound chlorides. However, the comparison with experimental data shows that a good prediction is achieved when using a high rate constant, which also

presents the same results as that when using the Langmuir isotherm. This demonstrates that in the process of ECR, the equilibrium between free and bound chloride still holds and the Langmuir isotherm is likely to be acceptable in most ECR cases.

7.4 CONCLUSIONS

In this chapter, based on the chemical reaction kinetics, we have proposed a new chloride binding model, which not only considers the non-linear relationship between the free and bound chlorides but also is able to take account of possible non-equilibrium between the free and bound chlorides. The state of equilibrium between free and bound chloride depends on the local free chloride concentration in pore solution and the bound chloride concentration. Both influence the rate of bound chloride release in the process of ECR.

Through the comparison with the experimental data and the results of the Langmuir isotherm, it is shown that in the process of ECR, the bound and free chlorides seem to be still in a stste of equilibrium. This indicates that the release of bound chloride release is much faster than the transport of free chloride even under a high current density. This further confirms that in the process of ECR, the Langmuir isotherm may still be applicable and may provide reasonable results in the mathematical modelling.

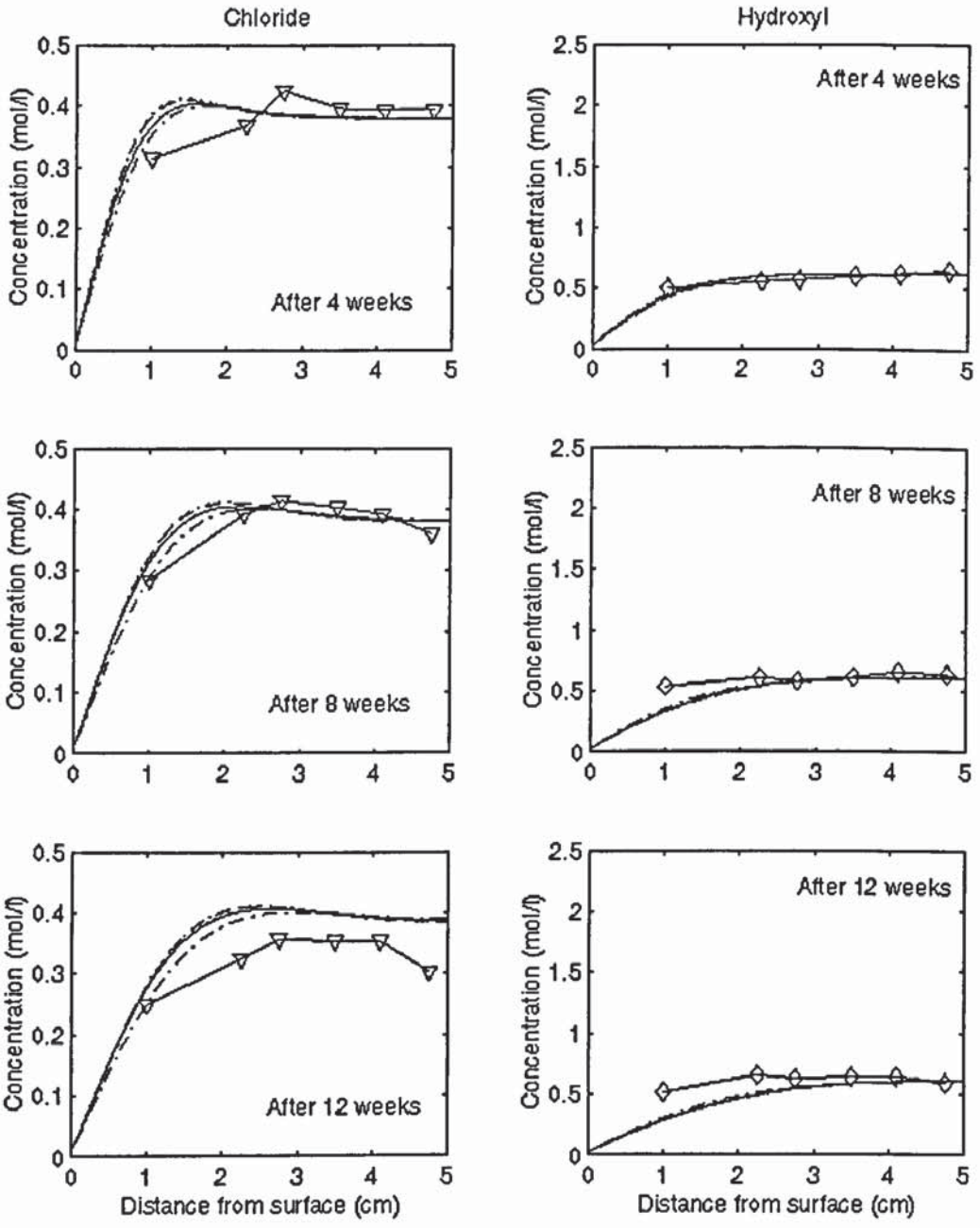

Fig. 7.1a Predicted ionic concentration profiles for the experiment of Bertolini et al. ($I = 0.005$ A/m^2)

.. Langmuir Isotherm, $--$ $k_r = 4.0\times10^{-6}$ (1/s), $-$ $k_r = 4.0\times10^{-7}$ (1/s), $-.$ $k_r = 4.0\times10^{-8}$ (1/s)

∇ experiment

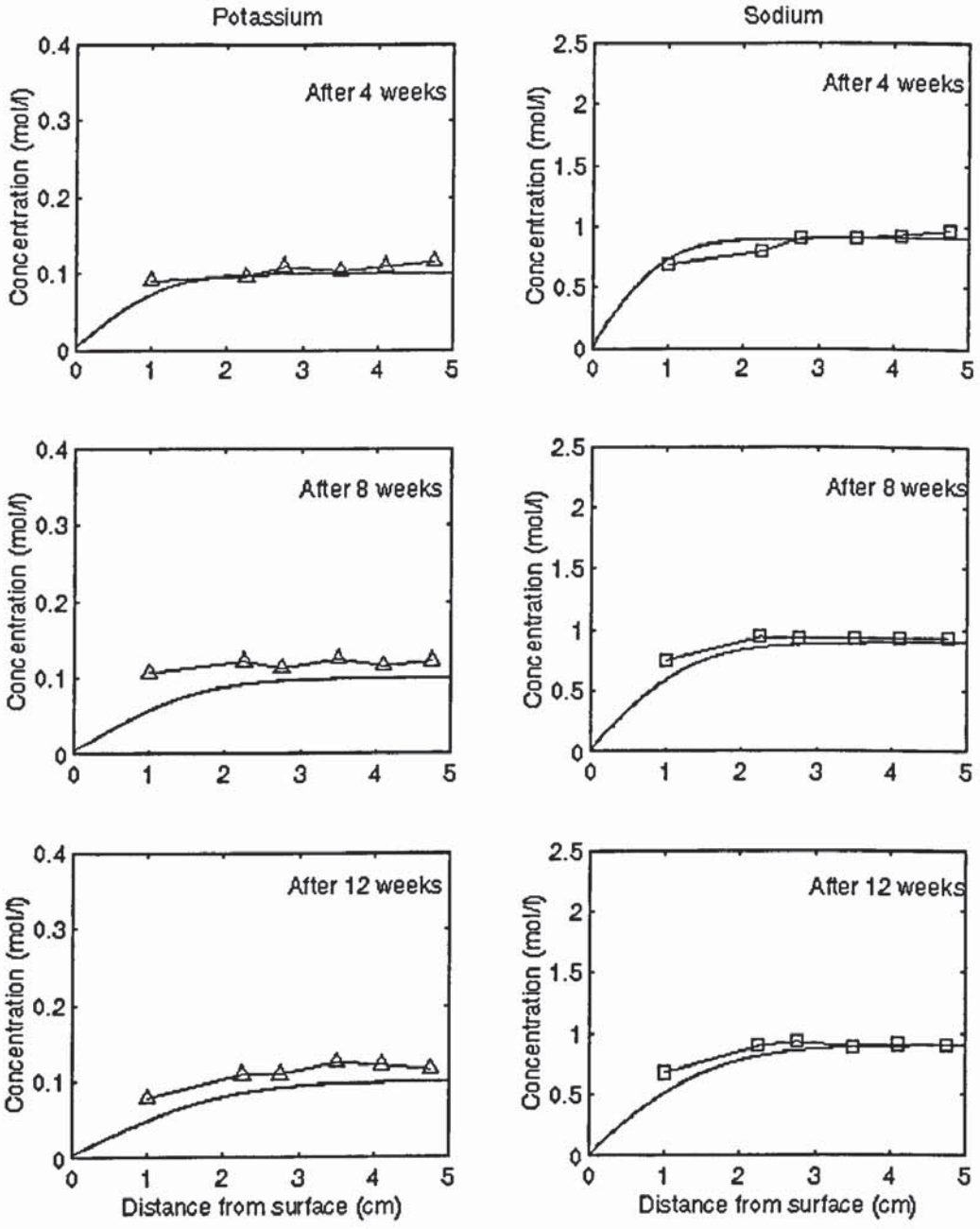

Fig. 7.1b Predicted ionic concentration profiles for the experiment of Bertolini et al. ($I = 0.005$ A/m^2)

.. Langmuir Isotherm, $--$ $k_r = 4.0\times10^{-6}$ (1/s), $-$ $k_r = 4.0\times10^{-7}$ (1/s), $-.$ $k_r = 4.0\times10^{-8}$ (1/s)

∇ experiment

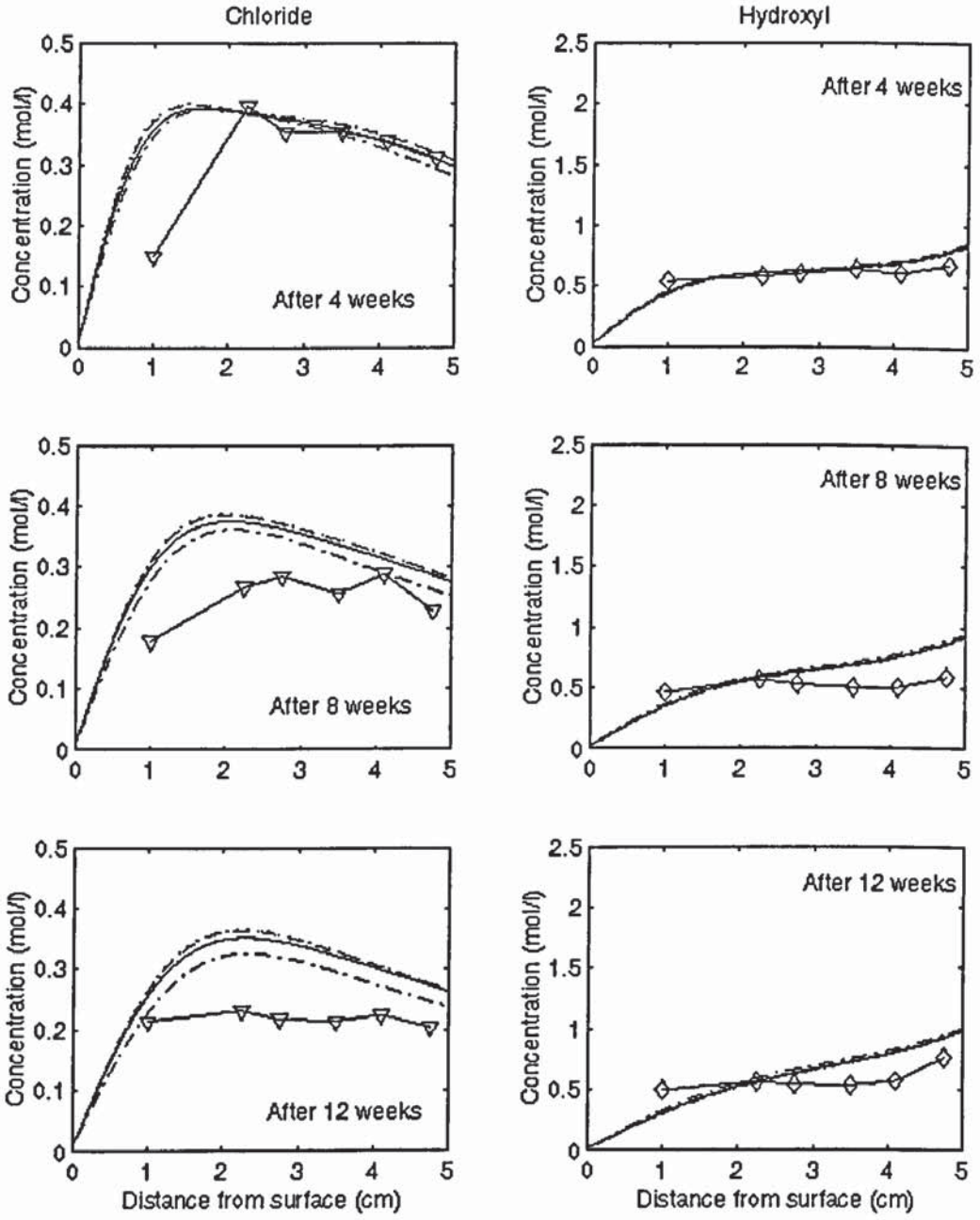

Fig. 7.2a Predicted ionic concentration profiles for the experiment of Bertolini et al. ($I = 1$ A/m^2)

.. Langmuir Isotherm, $--$ $k_r = 4.0\times10^{-6}$ (1/s), $-$ $k_r = 4.0\times10^{-7}$ (1/s), $-.$ $k_r = 4.0\times10^{-8}$ (1/s)

∇ experiment

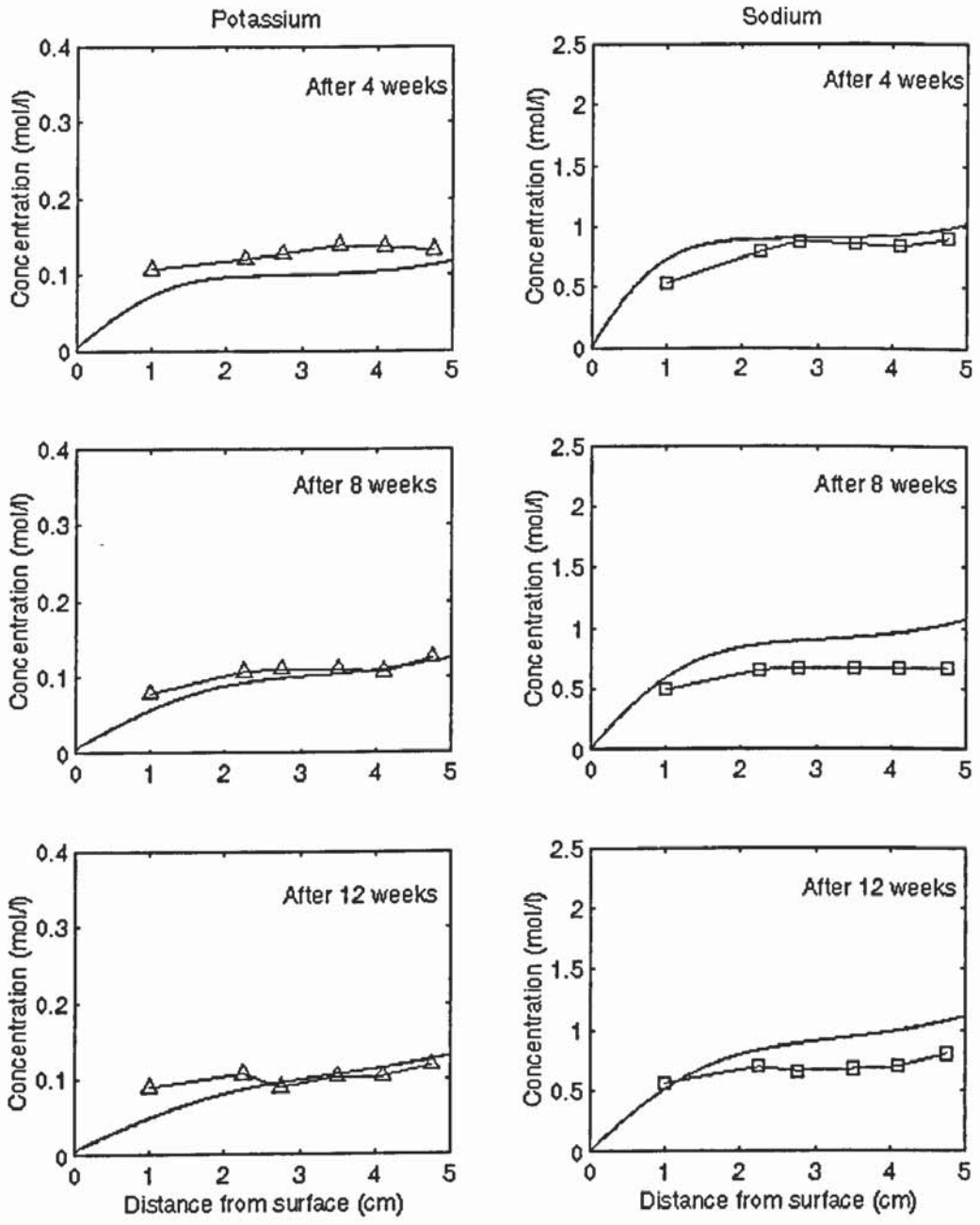

Fig. 7.2b Predicted ionic concentration profiles for the experiment of Bertolini et al. ($I = 1$ A/m^2)

.. Langmuir Isotherm, $--$ $k_r = 4.0\times10^{-6}$ (1/s), $-$ $k_r = 4.0\times10^{-7}$ (1/s), $-.$ $k_r = 4.0\times10^{-8}$ (1/s)

∇ experiment

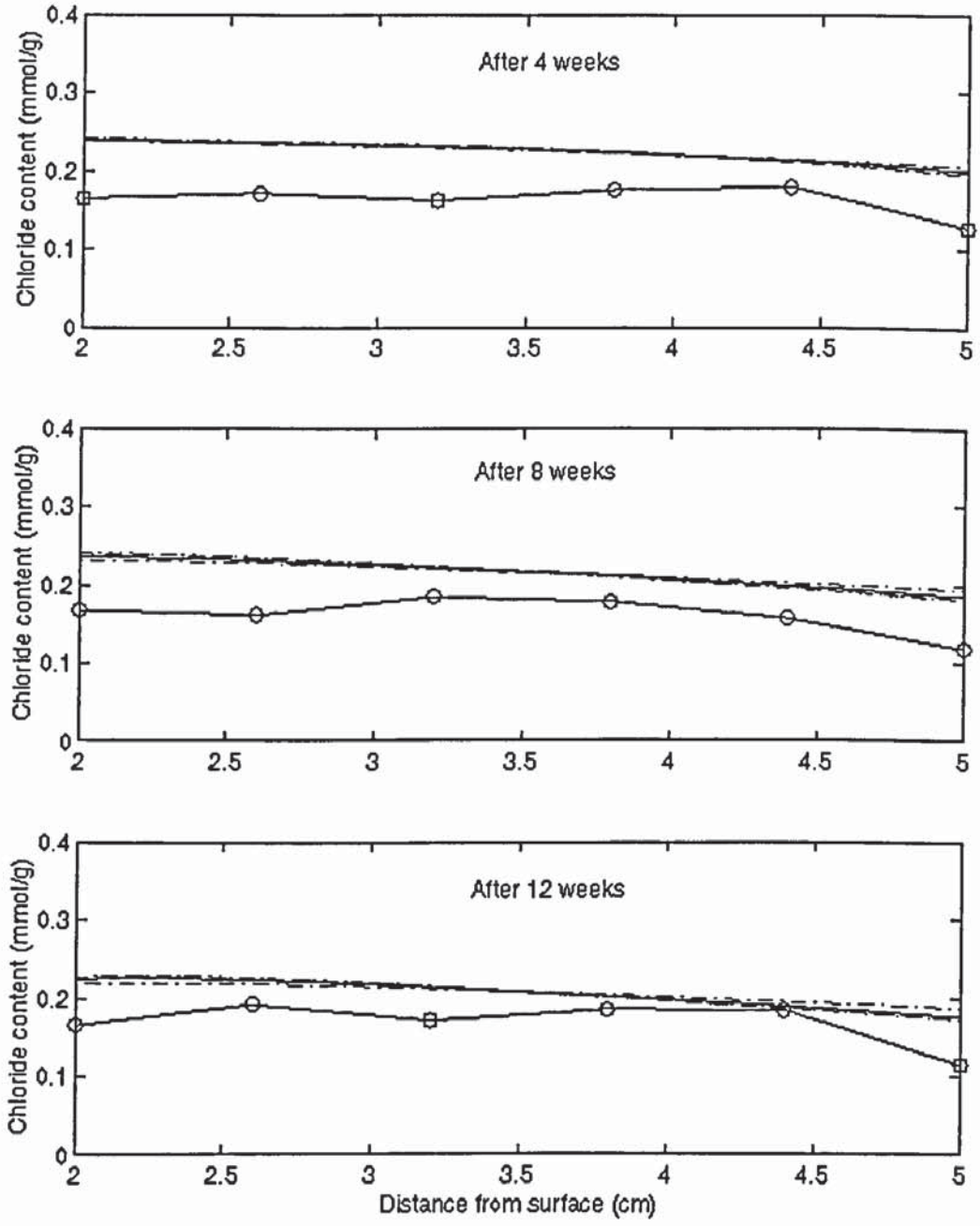

Fig. 7.3 Predicted total chloride content for the experiment of Bertilini et al. (I =1 A/m^2)

.. Langmuir Isotherm, – – $k_r = 4.0\times10^{-6}$ (1/s), – $k_r = 4.0\times10^{-7}$ (1/s), –. $k_r = 4.0\times10^{-8}$ (1/s)

∇ experiment

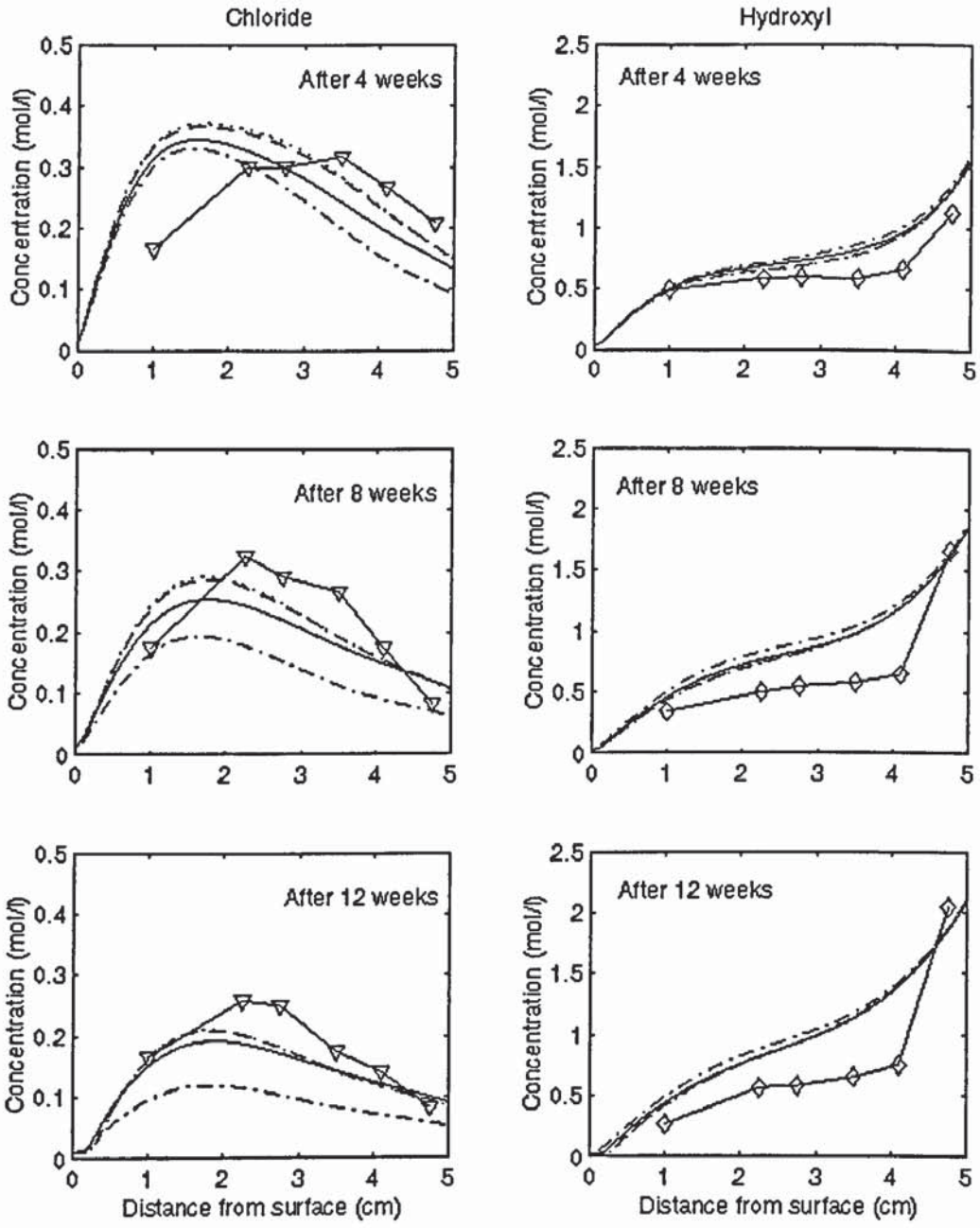

Fig. 7.4a Predicted ionic concentration profiles for the experiment of Bertolini et al. ($I = 5$ A/m^2)

.. Langmuir Isotherm, $--$ $k_r = 4.0\times10^{-6}$ (1/s), $-$ $k_r = 4.0\times10^{-7}$ (1/s), $-.$ $k_r = 4.0\times10^{-8}$ (1/s)

∇ experiment

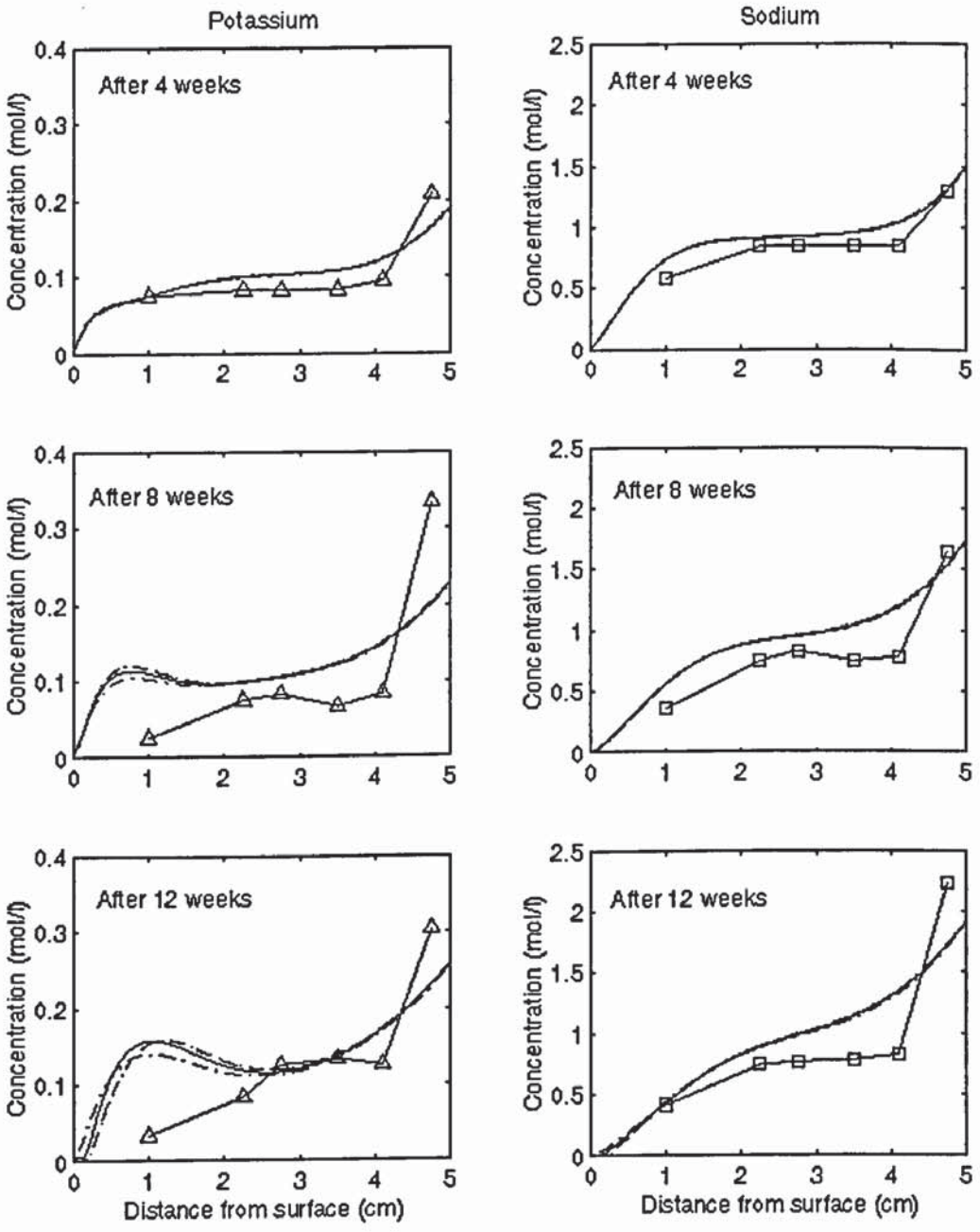

Fig. 7.4b Predicted ionic concentration profiles for the experiment of Bertolini et al. ($I = 5$ A/m^2)

.. Langmuir Isotherm, $--$ $k_r = 4.0\times10^{-6}$ (1/s), $-$ $k_r = 4.0\times10^{-7}$ (1/s), $-.$ $k_r = 4.0\times10^{-8}$ (1/s)

∇ experiment

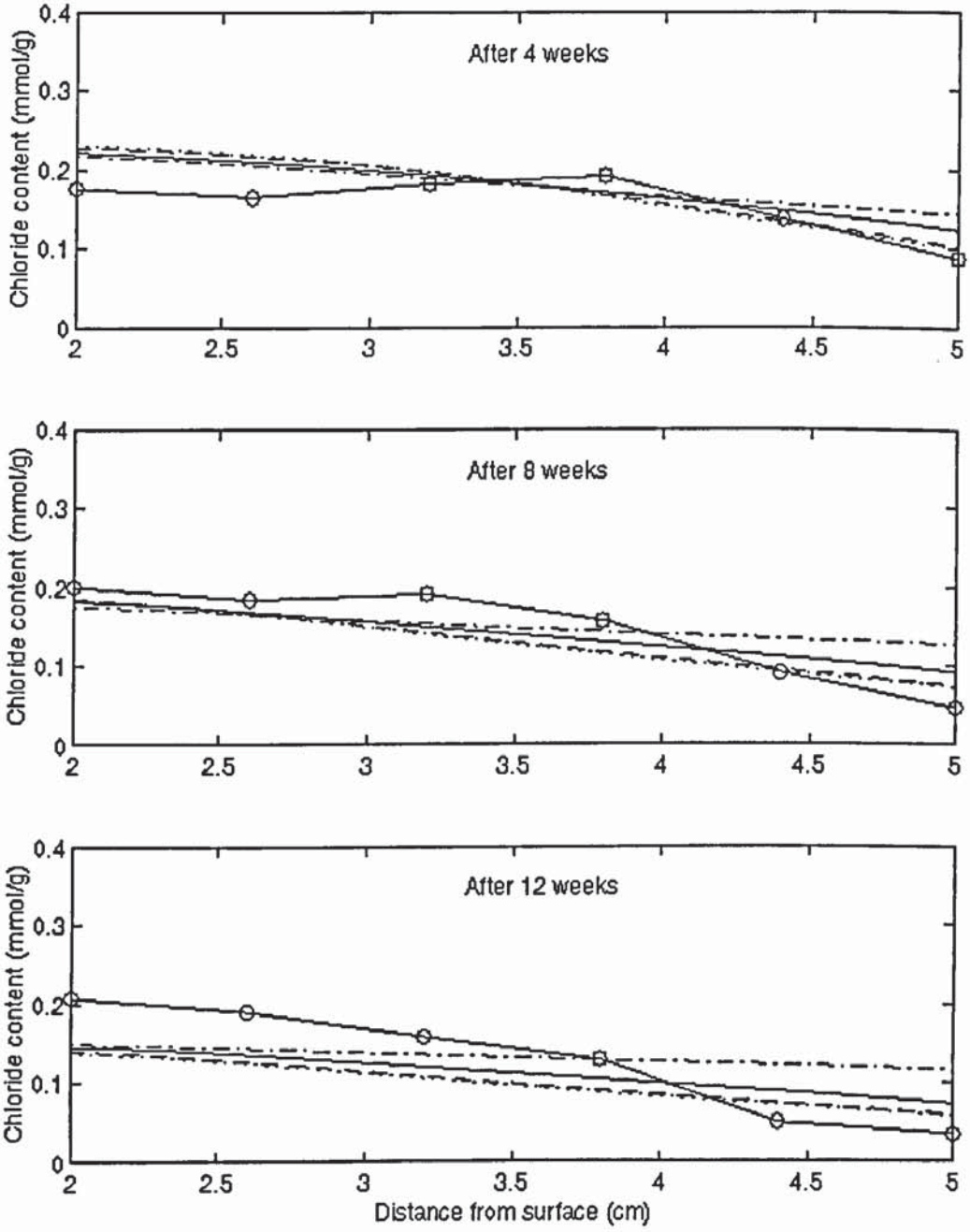

Fig. 7.5 Predicted total chloride content for the experiment of Bertilini et al. ($I = 5$ A/m^2)

.. Langmuir Isotherm, $--$ $k_r = 4.0\times10^{-6}$ (1/s), $-$ $k_r = 4.0\times10^{-7}$ (1/s), $-.$ $k_r = 4.0\times10^{-8}$ (1/s)

∇ experiment

CHAPTER 8

IONIC TRANSFERENCE NUMBERS IN THE PROCESS OF ECR

8.1 INTRODUCTION

The most important problems related to ECR are how much chloride can be removed during the process and how the chloride ions redistribute in concrete after the process. These two problems have been discussed though the Chapter 5 and Chapter 6. In addition to that, the efficiency of chloride removal is another issue to evaluate the process of ECR, which has also been discussed in Chapters 5 and 6. The efficiency of ECR is examined by calculating the amount of chloride that can be extracted by a certain charge quantity pass through the concrete. In literatures chloride transference number is a parameter that is often used to describe the efficiency [Mietz, 1999 and Castellote, et al., 1999] and is defined as the fraction of total current that is carried by the chloride ions.

In the experimental studies, the chloride transference number is calculated from the total decrease of chloride content in specimen, or simply from the total increase of chloride ions in the external electrolyte [Castellote, et al., 1999; 2000]. This method, however, cannot provide the information of the local variation of chloride distribution. In the process of ECR, the chloride transference number is related to the mobilities and concentrations of all ions in the pore solution. This is because each of the ions in pore solution carries part of the current, but with different values. In general, species with a higher concentration and a higher mobility can carry more current. As a result of this, the chloride transference number, and thus the efficiency of chloride removal, varies with both time and location. It is an unstable state, which is difficult to be determined with experimental measurements.

Comparing to the experimental investigation, however, computer modelling is able to give detailed information about the local variation of the ionic distribution and thus the ionic transference numbers. In this chapter the variation of ionic transference numbers

during the process of ECR is investigated. The mathematical model and chloride binding isotherm described in Chapter 3 and Chapter 7 are employed for this study. Effects of the external applied current density, treatment period and the releasing of bound chloride on the local ionic transference numbers especially are discussed.

8.2 THE FINITE ELEMENT ANALYSIS OF IONIC TRANSFERENCE NUMBERS

The transference number, in terms of its definition, can be expressed as:

$$t_i = \frac{z_i F J_i}{I} = \frac{z_i F J_i}{F \sum_i^n z_i J_i} \tag{8.1}$$

where t_i is transference number of species i. J_i is flux of species i, which is defined by Eq. (3.1). For a saturated pore structure if the convection of pore solution is ignored, the flux Eq. (3.1) can be simplified as Eq. (8.2) according to the finite element method.

$$J_i = -z_i D_i \left(\frac{F}{RT} \nabla \phi\right) [N] \{(C_i)^J\} - D_i \nabla [N] \{(C_i)^J\} \tag{8.2}$$

When the nodal ionic concentrations are determined by solving Eq. (3.9), the ionic flux and transference number at any position can be determined by Eqs. (8.2) and (8.1). Because $[N]$ is a piecewise linear function and $\nabla[N]$ is generally not continuous at nodes, the flux and thus the transference number is not continuous at nodes. To overcome this problem, the transference number is calculated at gauss points and is interpolated to element nodes. This is same as that done for stresses in the stress analysis.

In this study, the experiment of Bertolini, et al. [1996] is modelled. The parameters and initial conditions used in this study are the same as those used in Chapter 5 and the rate constant, k_f is 4.0×10^{-8} (1/s).

8.3 RESULTS AND DISCUSSIONS

The one-dimensional experimental investigation of ECR carried out by Bertolini el al. [1996] is simulated. Figs. 8.1-8.2 show the variation of the local ionic transference numbers within the pore solution at four different treating times for I = 1 and 5 A/m^2, respectively. It is observed from Figs. 8.1a and 8.2a that, at the start of the process, the cations have negative transference numbers in the region near the surface, where the anions have higher positive transference numbers. This means that at the beginning of the treatment, cations will move into the external solution because of the diffusion caused by concentration gradient at the surface, whereas the anions have higher fluxes flowing into the external solution under the combined influences of the concentration gradient and the electrical driving force. Because the transference numbers are computed according to Eq. (8.1) and there is no current in the external solution, the computed ionic transference numbers in the external solution is theoretically equal to ∞. This causes the ionic transference number discontinuous at the surface of concrete. This can be noticed that the ionic transference number has the absolute value greater than 1 near the surface.

It can be seen from Fig. 8.1a that, in the bulk solution, except near the concrete surface, the variation of the profiles of potassium and sodium transference numbers with the treating period is not very significant. But for chloride, the profile of chloride transference number in bulk solution has a significant change, especially in the first 4 weeks. In that period, the chloride transference number increases greatly at the side of concrete surface, but it decreases significantly at the side of steel cathode. After that time, it remains a similar profile with a little change. Comparing this result with the corresponding chloride concentration profiles in the process (shown in Fig. 7.2), we can see that in the early 4 weeks, the significant change of the profile of chloride transference number is corresponding to the significant change of chloride concentration profile in solution in the period. After 4 weeks, the change of chloride concentration profile in solution becomes less than that in the early 4 weeks. For hydroxyl ions, the numerical results show that it has the highest value in all of the four ions displayed, which is near to 1. That means most part of the treating current is carried by hydroxyl

ions in solution. The profile of hydroxyl transference number has little change with the treating time.

Fig. 8.1b shows the variations of the chloride transference number with the ionic concentration in pore solution at three different treating times. The numerical results show that the chloride transference number decreases as the concentrations of potassium, sodium and hydroxyl ions increase. That means that with the increase of other ionic concentration in solution the part of the current carried by chloride ions in total current will decrease. For chloride itself, the results show that the chloride transference number does not always increase with the increase of chloride concentration in solution. It has been shown that the highest chloride transference number occurs at the concrete surface, where chloride concentration is the lowest, which is nearly equal to zero. However, at steel cathode, where the chloride concentration is about 0.3 mole/l, the chloride transference number is almost equal to zero. Although it is difficult, from the numerical results, to determine a specific relationship between chloride transference number and chloride concentration in pore solution, Fig. 8.1b shows that the average level of chloride transference number decreases with the treating time. That is to say the average level of chloride transference number will decrease as the total chloride content in concrete decreases. From the above discussions, it can be seen that the distribution of chloride transference number depends on the distribution of all ionic species in the pore solution, but the average level of chloride transference number corresponds to the average level of chloride content in the pore solution.

Fig. 8.2a shows the local variation of ionic transference numbers within pore solution at four different times for $I = 5$ A/m^2. Similar results as that in Fig. 8.1a are presented for potassium, sodium and hydroxyl ions. For chloride ions, however, the variation of its transference number with the treating period is more significant than that in Fig. 8.1a. The results show that the average level of chloride transference number decreases significantly with the treating period. This is caused by the enhanced decrease of free chloride concentration in pore solution due to the high treating current density (shown in Fig. 7.4a).

Fig. 8.2b shows the variation of chloride transference number according to the ionic concentrations after different treating periods. Compared with Fig. 8.1b, it can be seen that with the increase of the treating current density, chloride transference number varies more significantly from time to time, this is caused by the significant change of ionic content distribution over time under a higher treating current. Another significant difference between Fig. 8.2b and Fig. 8.1b is that there is a swing of chloride transference number corresponding to the potassium concentration after a longer period of treatment (after 8 and 12 weeks). The reverse proportional relation between chloride transference number and the potassium concentration that has been observed in Fig. 8.1b does not exist any more. This is caused by the wave like distribution of potassium concentration in the process (shown in Fig. 7.4b). This result indicates that the chloride transference number does not certainly decrease as any other positive charged ion increases. The variation of chloride transference number corresponding to the chloride concentration indicates that its average level in the specimen will decrease as the average level of chloride concentration decreases, but its distribution in the specimen is not in agreement with this conclusion.

From the results discussed above, it can also be noticed that in the process of ECR, both cations have lower transference number because of their lower concentration (such as potassium) and lower mobility (such as sodium), while hydroxyl has the highest transference number due to its highest concentration and mobility. Fig. 8.3 shows the variation of chloride transference number corresponding to the ratio of chloride concentration and hydroxyl concentration, which presents a direct proportional relation except in the region near the surface.

Figs. 8.4 and 8.5 display the variation of ionic transference numbers according to the position and the treating period and variation of chloride transference number according to the ionic concentration without the consideration of chloride binding or releasing. The comparison of Figs. 8.4a and 8.5a with Figs. 8.1a and Fig. 8.2a indicates that chloride binding has much less influence on the transference numbers of other ions except that of itself. The average level of chloride transference number in the specimen decreases as the result of no chloride release into pore solution, the distribution of chloride transference number in the specimen, however, is similar as that having the consideration of the effect of chloride binding. The comparison of Fig. 8.1b and 8.2b

with Figs. 8.4b and 8.5b indicates that the effect of chloride binding reduces the influence of treating period on decrease of average level of the ionic transference numbers. In another word, the average level of ionic transference numbers will become less as the chloride content in the specimen decrease slowly.

8.4 CONCLUSIONS

From the results of the numerical analysis of ionic transference numbers in the process of ECR, the following conclusions can be drawn.

The ionic transference numbers vary from place to place and from time to time. They depend on concentrations of all ions in the pore solution. The potassium and sodium have lower transference number in comparison with the chloride and hydroxyl because of their low concentrations and low mobility. Hydroxyl has the highest transference number, especially near the cathode. The transference numbers of the other three species vary very little except at very early stage.

The chloride transference number is sensitive to the current density, treating time and its reaction with the solid phase of concrete. All of these have influence on the concentration of chloride in specimen, that has a direct effect on the chloride transference number. The lower the chloride concentration, the less the average level of chloride transference number. The local chloride transference distribution has the highest value at the surface and the lowest at cathode in a long term. A direct proportional relation exists between the chloride transference number and the *Cl/OH* ratio except for the region near the surface.

The chloride transference number at cathode decreases rapidly at very beginning because large quantity of hydroxyl is produced from the electrochemical reaction. The chloride in the region is reduced significantly at very beginning, but its concentration decreases very slowly in the later time.

The efficiency of chloride removal expressed by the chloride transference number will decrease with the increase of current density and treating period. The release of bound

chloride enhances the chloride content in pore solution that causes the average of chloride transference number remains at a higher level.

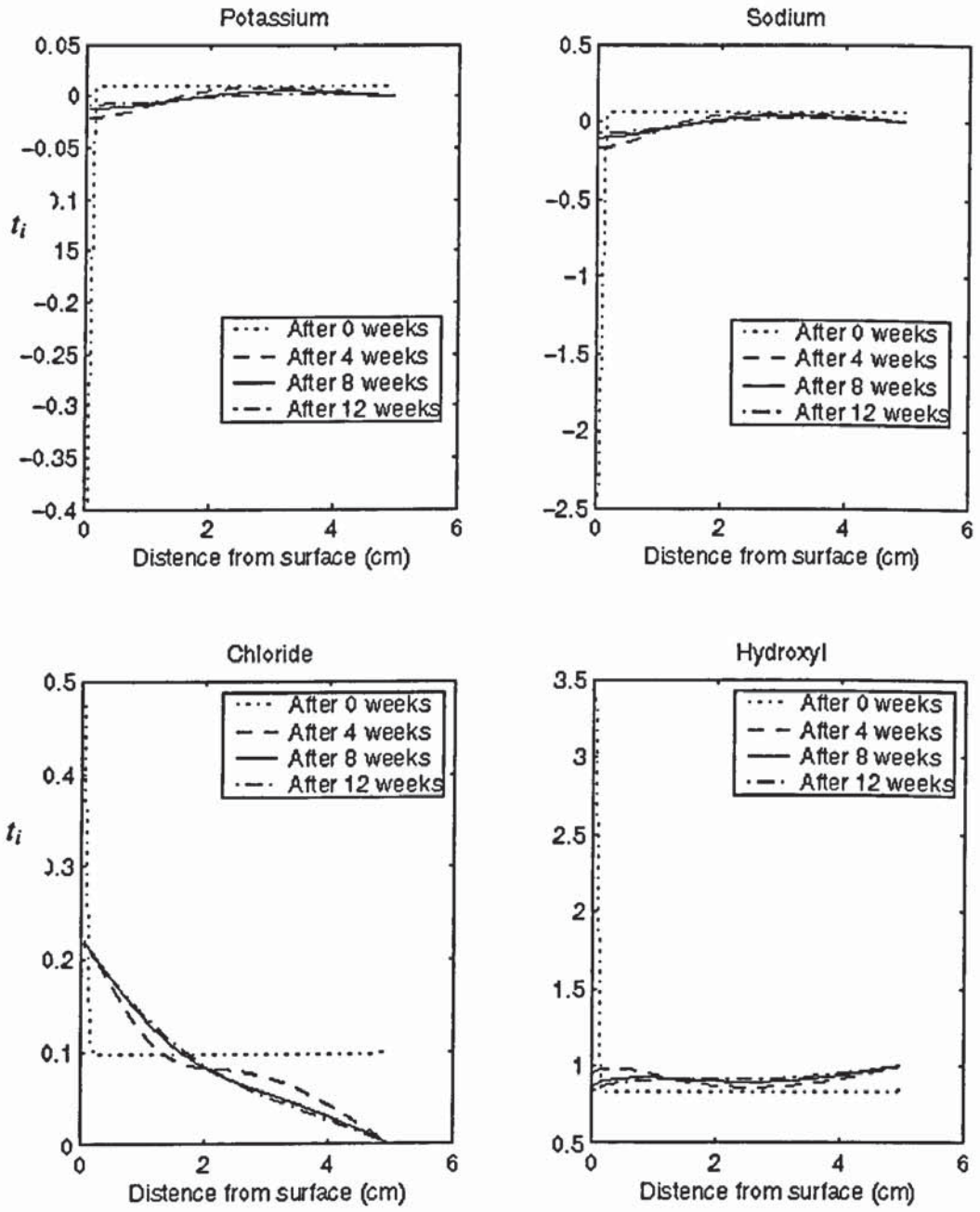

Fig. 8.1a. Distribution of ionic transference numbers with the effect of chloride binding ($I = 1$ A/m^2)

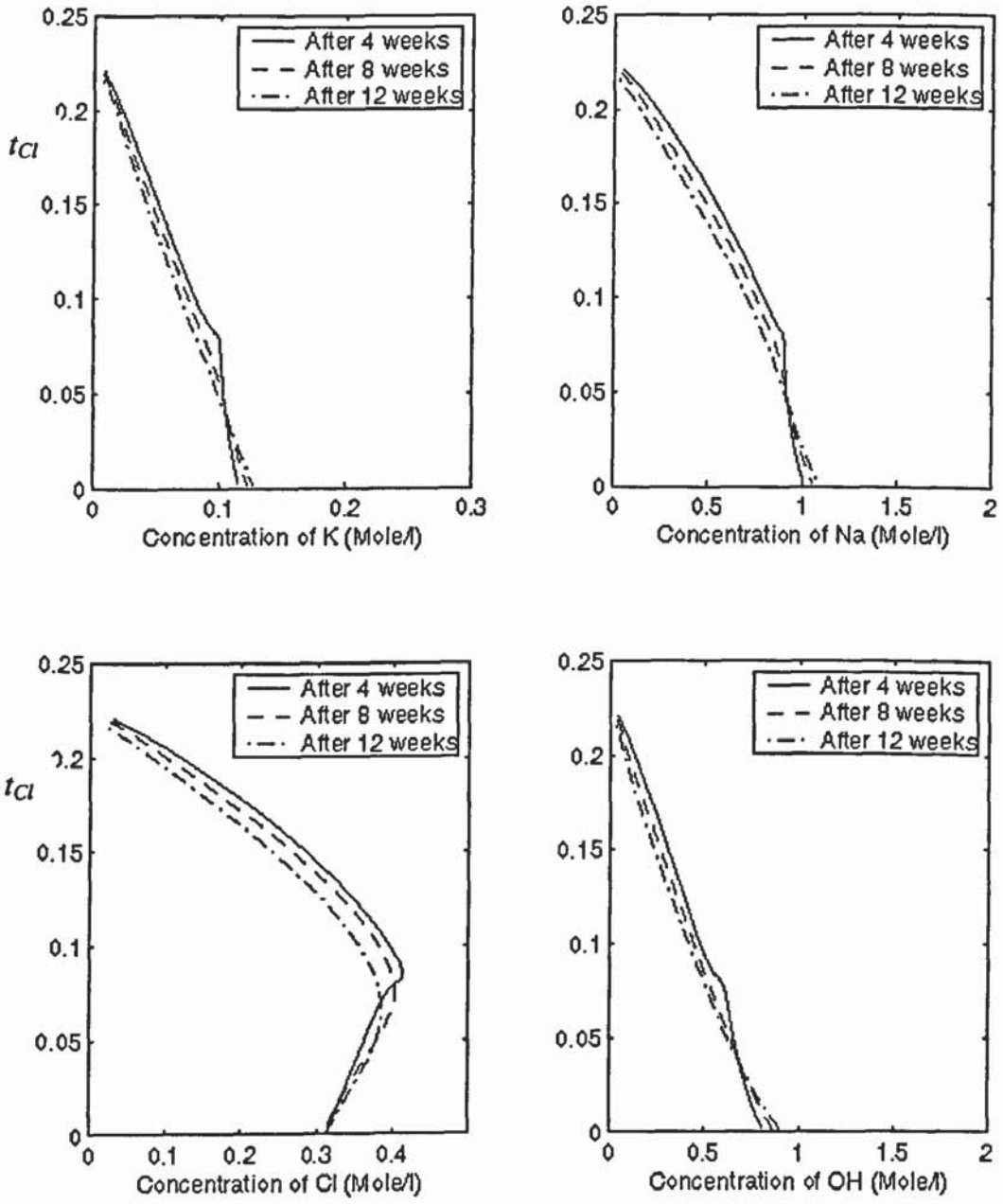

Fig. 8.1b. Variation of chloride transference number according to the ionic concentrations with the effect of chloride binding ($I = 1$ A/m^2)

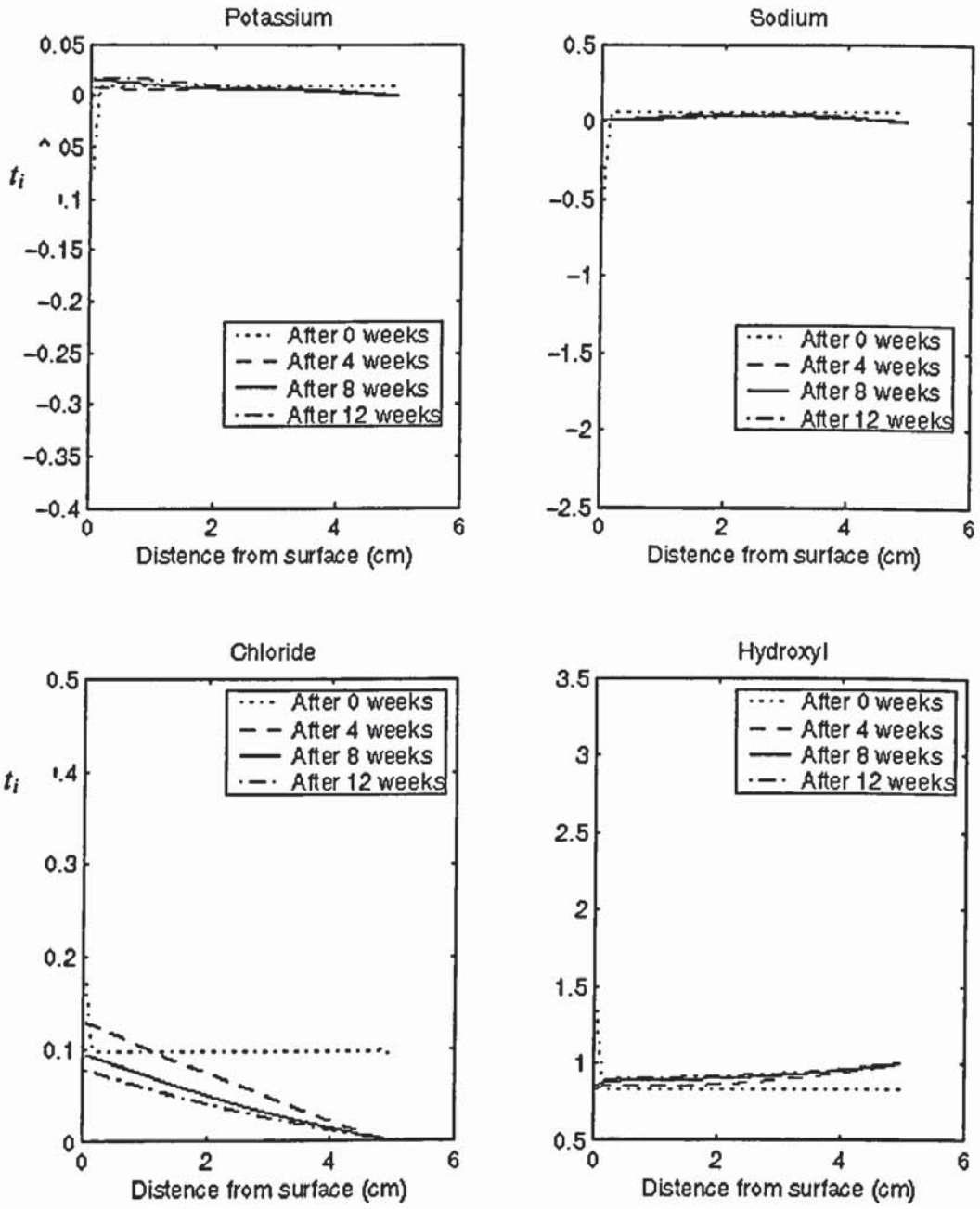

Fig. 8.2a. Distribution of ionic transference numbers with the effect of chloride binding ($I = 5$ A/m^2)

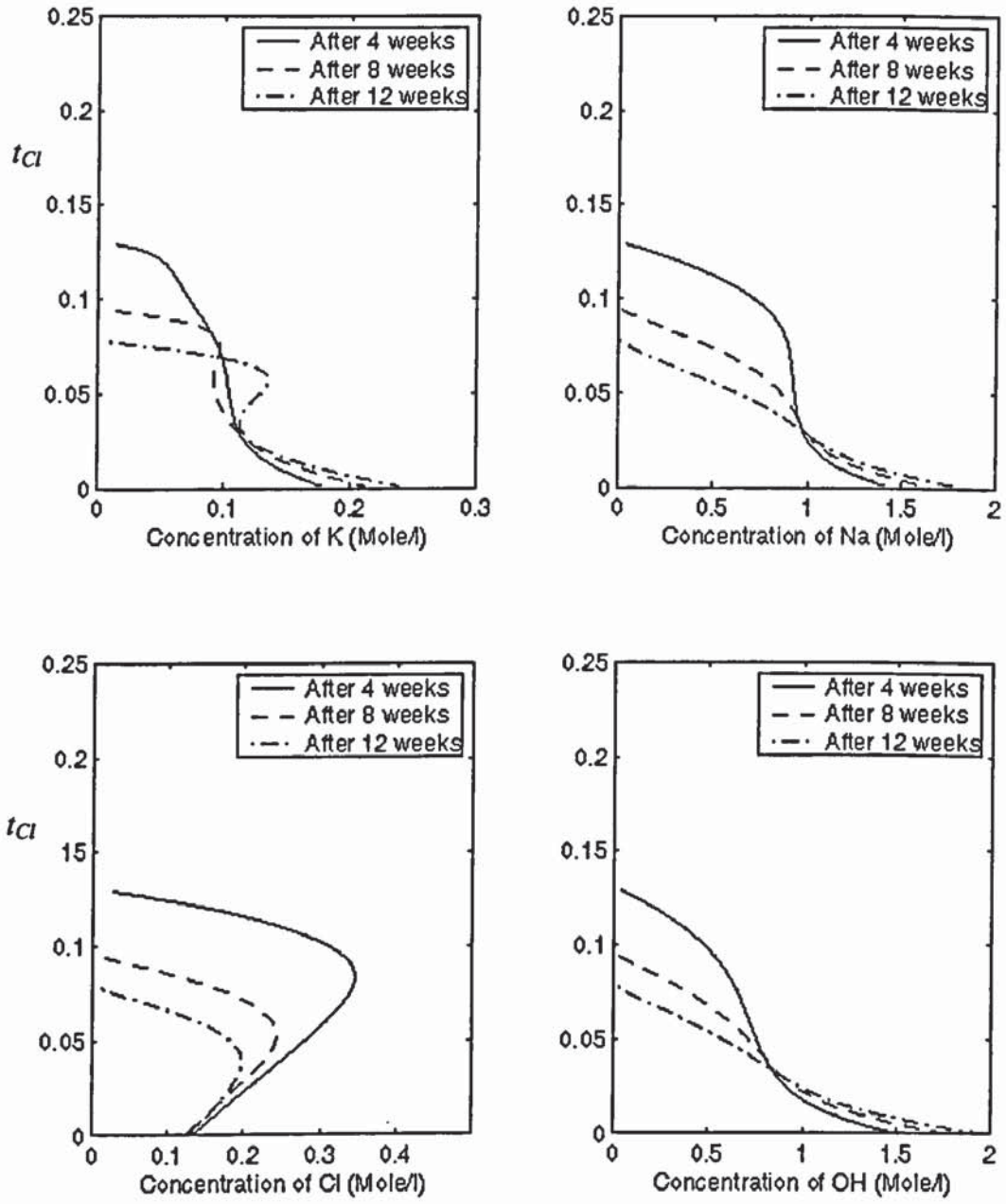

Fig. 8.2b. Variation of chloride transference number according to the ionic concentrations with the effect of chloride binding ($I = 5$ A/m^2)

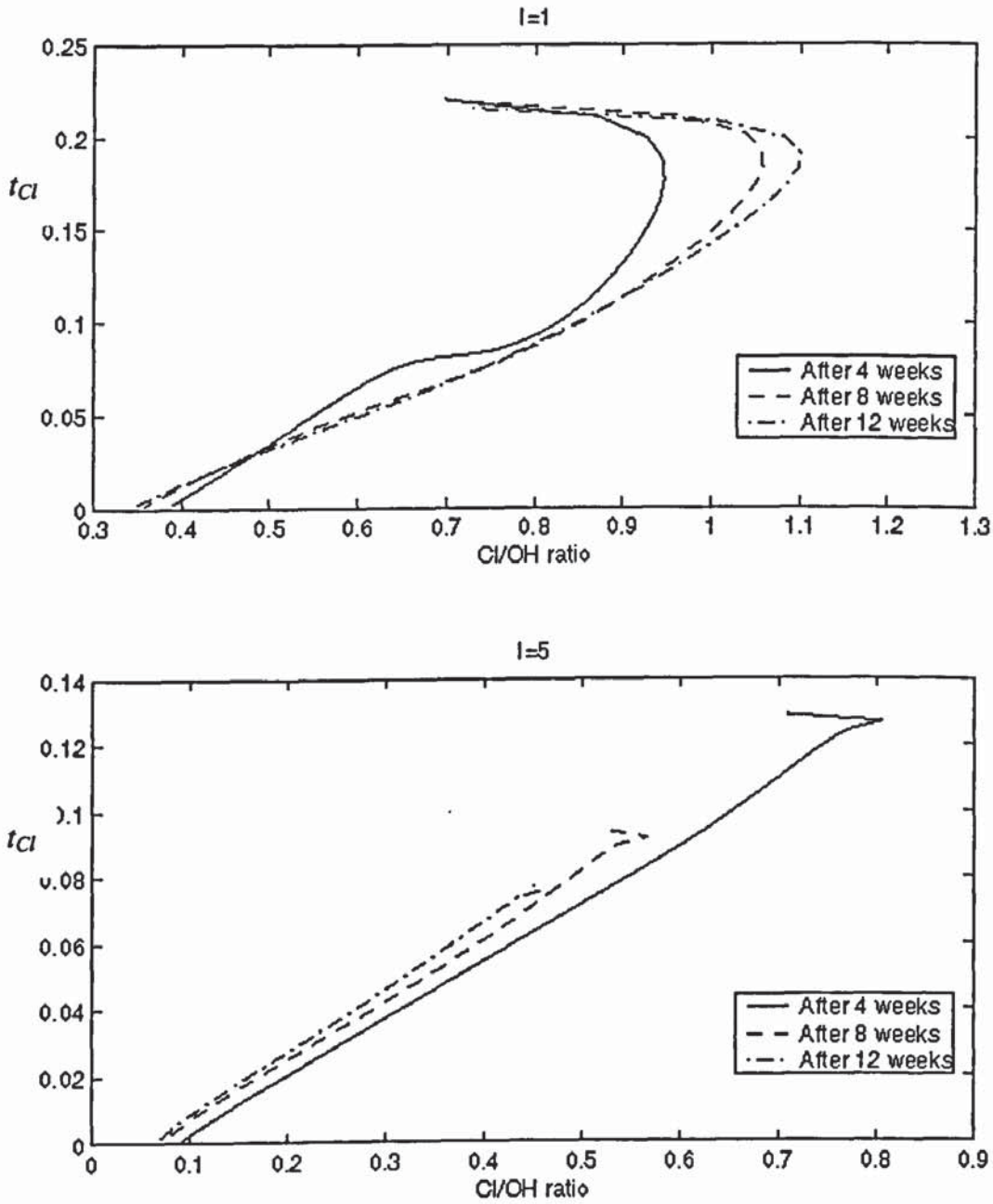

Fig. 8.3. Variation of chloride transference number according to the *Cl/OH* ratio

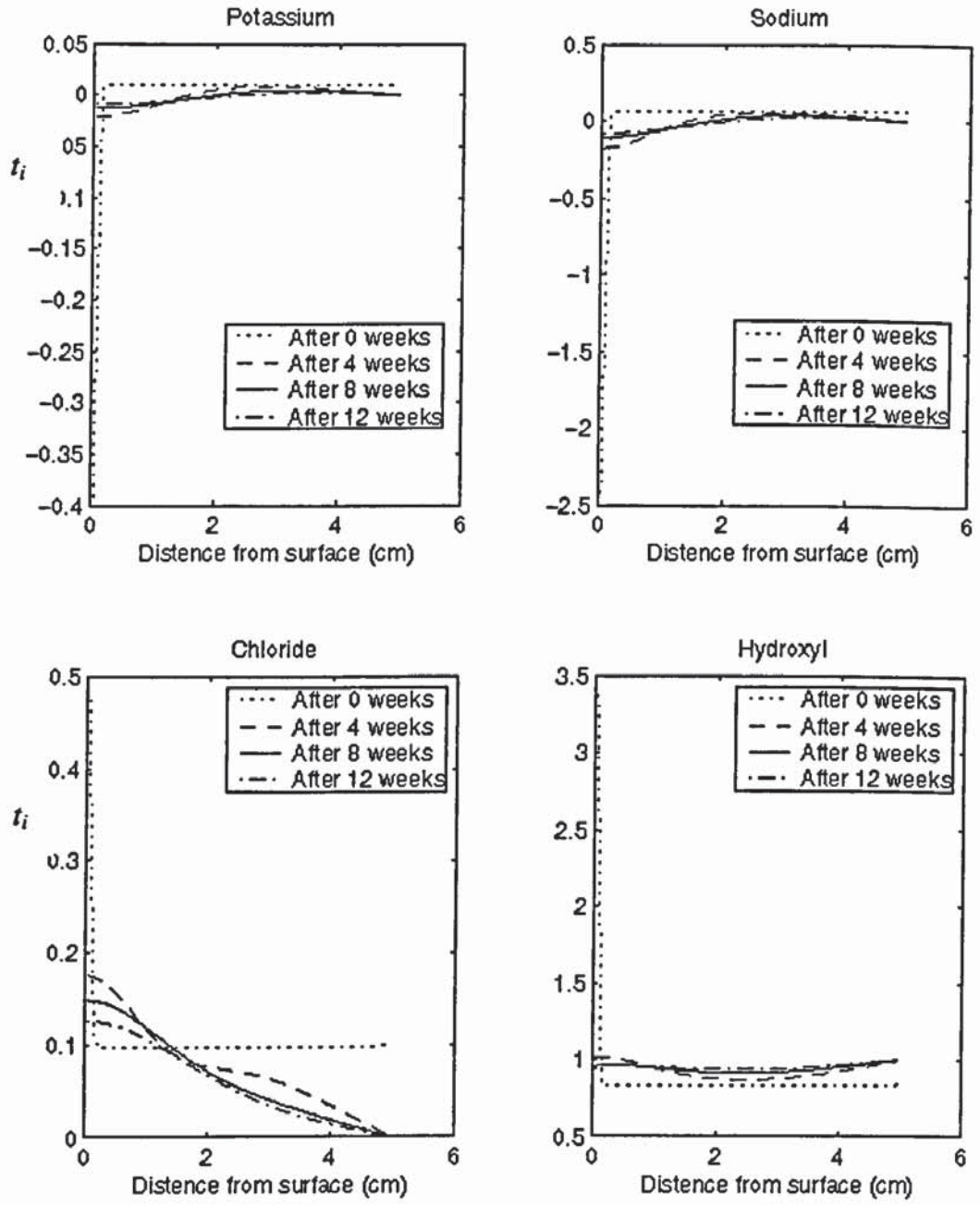

Fig. 8.4a. Distribution of ionic transference numbers without the effect of chloride binding

($I = 1$ A/m^2)

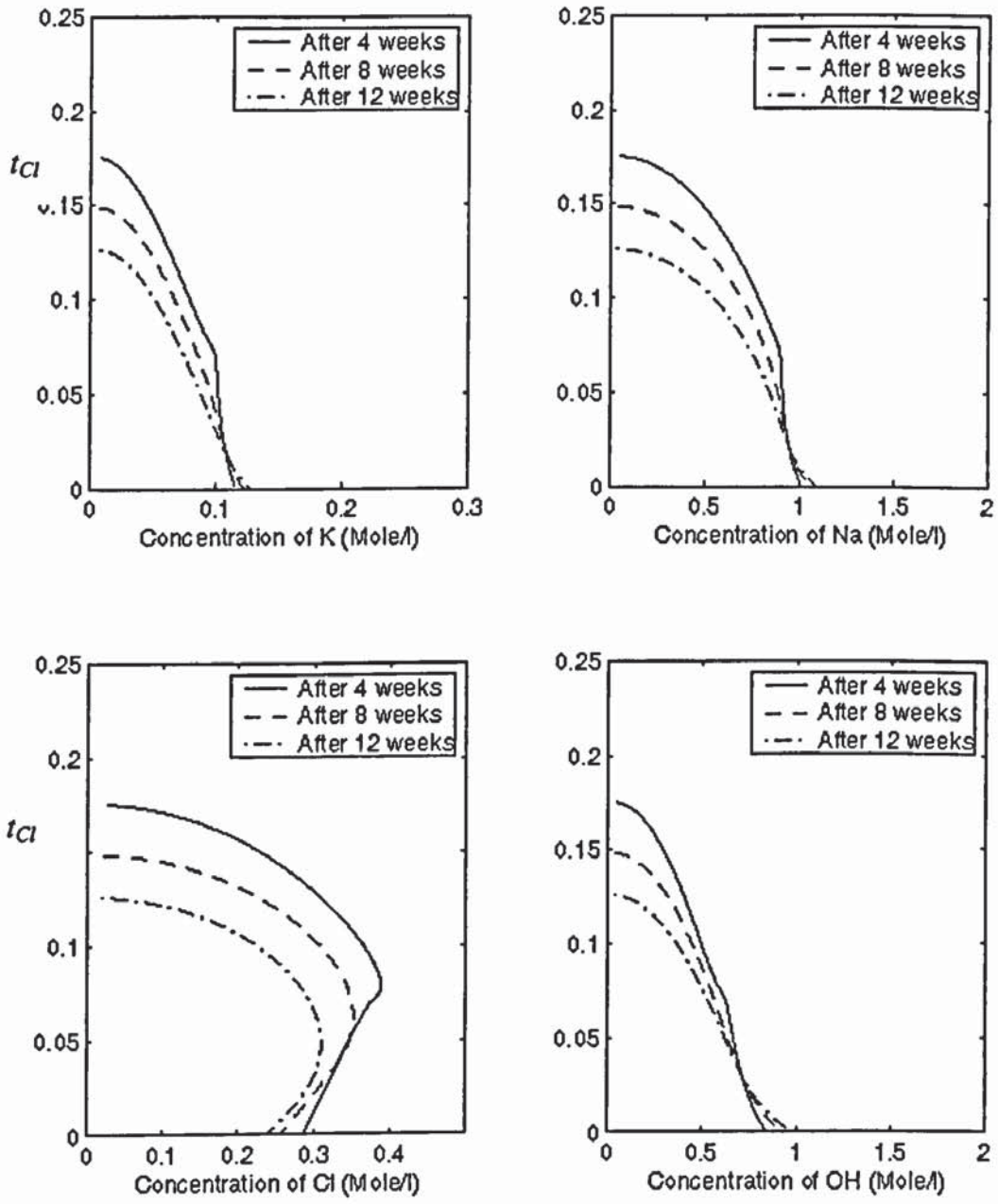

Fig. 8.4b. Variation of chloride transference number according to the ionic concentrations without the effect of chloride binding (I = 1 A/m^2)

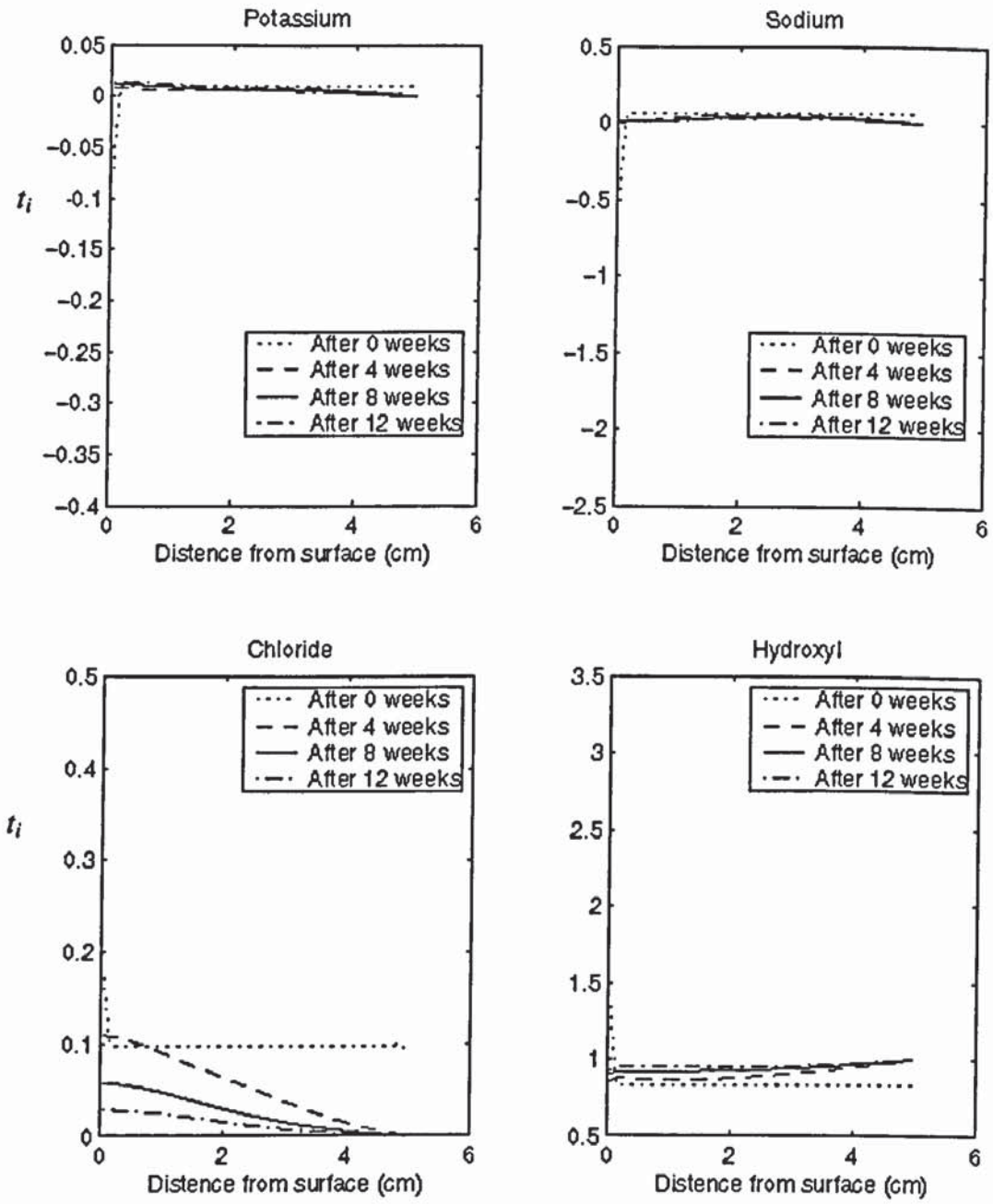

Fig. 8.5a. Distribution of ionic transference numbers without the effect of chloride binding

($I = 5$ A/m^2)

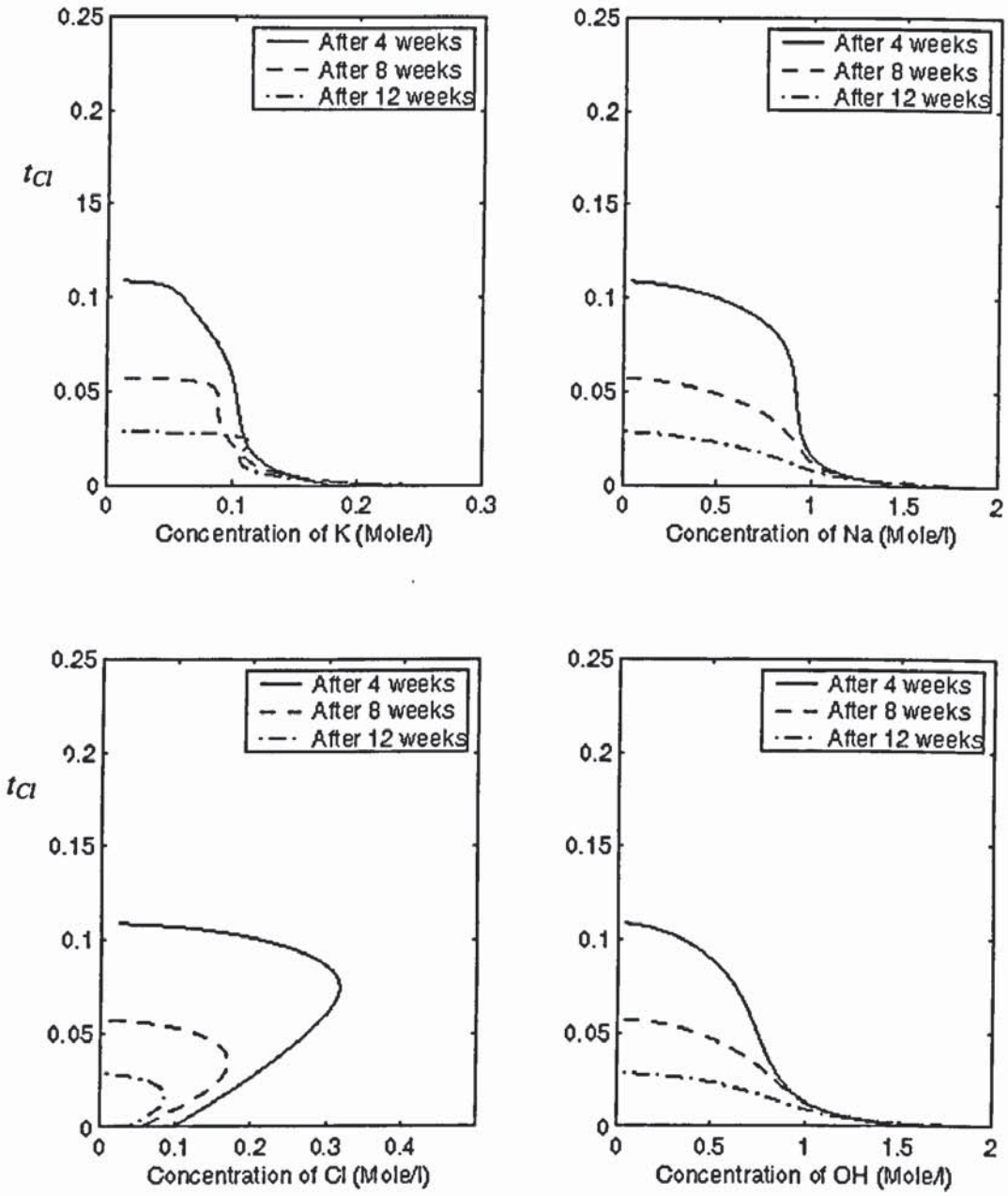

Fig. 8.5b. Variation of chloride transference number according to the ionic concentrations without the effect of chloride binding ($I = 5$ A/m^2)

CHAPTER 9

COMPUTER PROGRAM

9.1 INTRODUCTION

FEAECR (Finite Element Analysis of Electrochemical Chloride Removal) is a computer program developed to evaluate two-dimensional ionic concentration distribution during the process of ECR. The program was designed to solve the ECR governing equation (3.9) for ionic species in concrete. The solution technique used in FEAECR is the bilinear isoparametric finite element method coupled with a time step integration. This general approach has been described in Chapter 3. In fact, besides used to make modelling of ECR, the program also can be used to simulate the ionic transport process at other situations, such as the chloride diffusion into cemetitious materials exposed to a saline environment.

In an attempt to facilitate the use of FEM, activities have been taken to develop pre- and post-processors. An auto mesh generation pre-processor can easily generate node and element information for any complex geometrical model with a minimum amount of input from users, while a post-processor can produce clear and convincing graphical outputs which enable users to present the results of analysis in an effective manner for practical purpose.

Computer Graphical User Interfaces (GUIs) provide a means through which individuals can communicate with the computer without programming commands [Hou, et al., 1998; Marchand, 1999]. Matching GUIs with the designed finite element programme FEAECR can create an informative, intuitive and friendly interactive software package, that provides a useful tool, which can be easily handled by the users with little FEM knowledge. In this chapter an introduction to the structure of FEAECR is presented, while an interactive software package developed and a demonstration to use it are presented as well.

9.2 PROGRAM -- FEAECR

FEAECR contains the option of either solving directly or iteratively. In present study, the first one has been adopted because the convergence in the iterative processes is not easy to achieve for our complex problem. The structure of FEAECR and its main containing control subroutine, ECRPRO, are presented in Figs. 9.1 and 9.2, respectively.

As a general ECR analyser, the present version of FEAECR has limited use. These limitations stem from the fact that ECR process belongs to the convection dominated problems. For these problems the standard Garlerkin method applied solves a modified under-diffused equation [Lewis, et al., 1996]. Indeed as the parameter Peclet number (Pe) increases, such as the current density increases in the problem of ECR, the accuracy will deteriorate. When $Pe \rightarrow \infty$, the solution is purely oscillatory and bears no relation to the underlying problem [Zienkiewicz and Taylor, 1991]. This basic defficiency limits the scope of this program which only can be used to analyse the galvanostatically controlled situation, not for cases where the applied electric field having a constant potential gradient between the anode and the cathode, because, in the later case, caused by a very high electrical potential gradient near the anode and cathode, the Peclet number will be greater than 1 there and oscillation occurs in the solution.

The program was designed to solve governing equation (3.9) for concentration of ionic species. Because of the solubility equilibrium condition between the hydroxyl and calcium ions in pore solution and charge balance condition, the concentration of Ca^{2+} and OH^- can be determined in the terms of these conditions.

In order to enhance its adaptability, the program was designed to have the capability to cope with the inhomogeneous materials. For this inhomogeneous problem, the structure may be divided into several homogeneous substructures. In the program, a parameter, NMAT, was designed to define the number of the homogeneous material substructures. So it should be noticed that all of the medium property dependent parameters, such as w_e (water/cement ratio), D_i (diffusion coefficient), α and β (parameters of the binding models) and τ and ε (tortuosity and porosity), are defined in terms of the ionic transporting media. This function of the program was used in Chapters 6 and 7, in which

both of the treated specimen and the external alkaline solution were regarded as a wholly integrated structure.

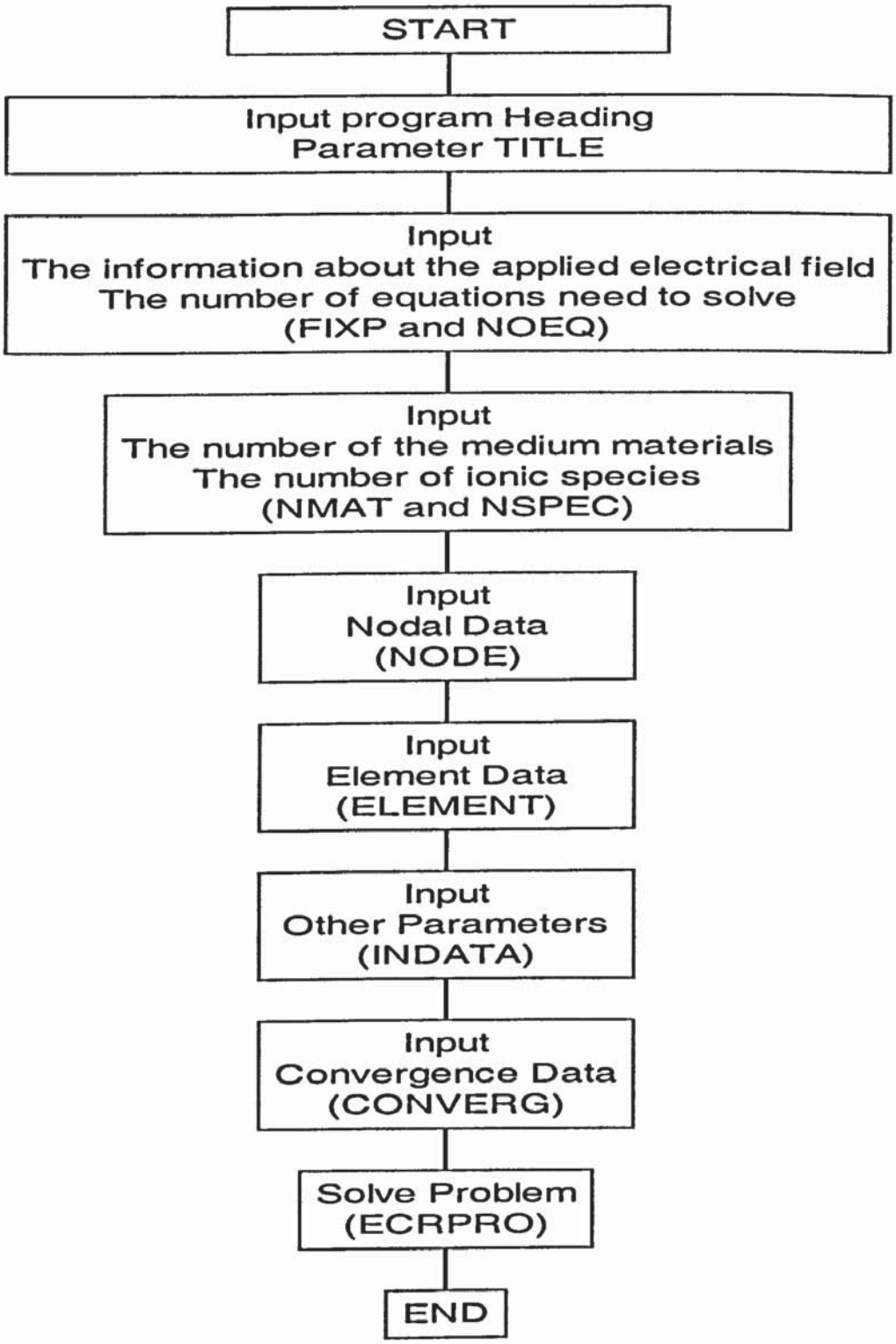

Fig.9.1 Structure and flow-chart of FEAECR

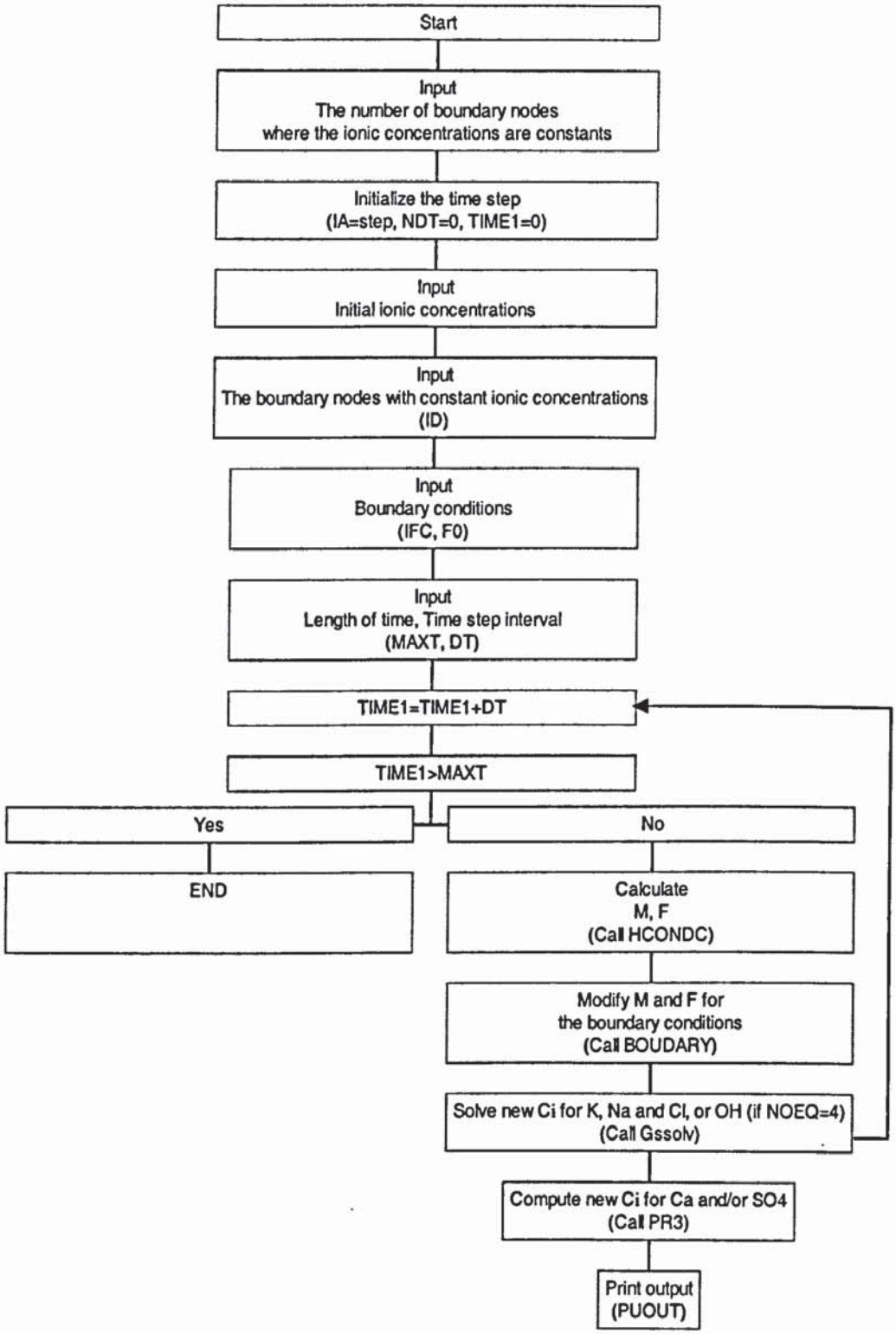

Fig. 9.2 Structure and flow-chart of ECRPRO

There are four input files and two output files are related to the main program. They are coopn.txt, INPUT.DAT, potent.txt, interfaceboundary.txt, result.m and RESULTW.DAT. The file coopn.txt records the node and element information produced by the mesh generation program. The file interfaceboundary.txt records boundary information. The file potent.txt records the nodal values of the potential function resulting from the solving Laplace's equation. INPUT.DAT records other input parameters, such as NMAT, ionic diffusion coefficients, constants for binding isotherm (k_f, α and β), time step and maximum time of computing, etc. RESULTW.DAT records the computation results; the file result.m was designed to record the computation results which are updated every two step interval that provides a convenient way to observe the process of the computation. If the initial ionic concentrations are not evenly distributed, they will be recorded in the file result.m which will be regarded as an input file by the program.

9.3 FUNCTIONS OF THE INTERACTIVE SOFTWARE

Matching GUIs with the designed finite element programme FEAECR and pre- and post-processors create an interactive software package (Fig. 9.3). The developed interactive software is designed to be applicable for both UNIX and PC windows systems. The core finite element analysis programme FEAECR was written in FORTRAN 77. The user interface, and corresponding pre- and post-processors, however, were written in MATLAB. The software is divided into four parts according to their functions. A flowchart of the structure of the software is presented in Fig. 9.4.

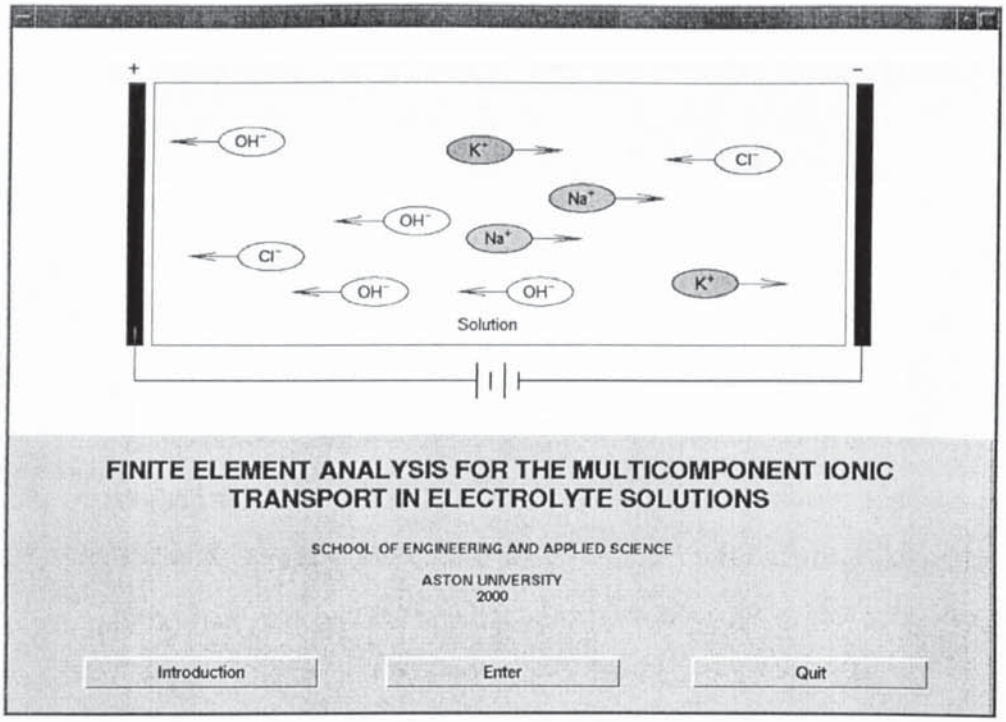

Fig. 9.3 FEA software for ionic transport in electrolyte solution

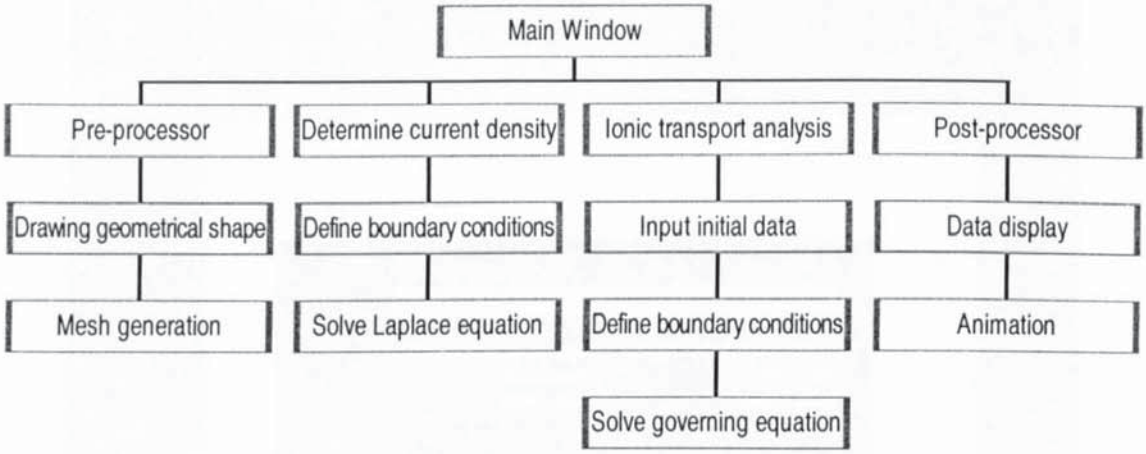

Fig. 9.4 Structure and flowchart of the software

The software starts with a main window, in which the main functions are listed in the menu bar, meanwhile a reminder which asks the user to define the axis is displayed first at the centre of the window (Fig. 9.5). Click the "OK" button and then click the icon marked with an up-left pointing arrow in the tool bar followed by double click of the presented axis, a sub-window with the name of "Edit Axes Properties" will appear (Fig. 9.6).

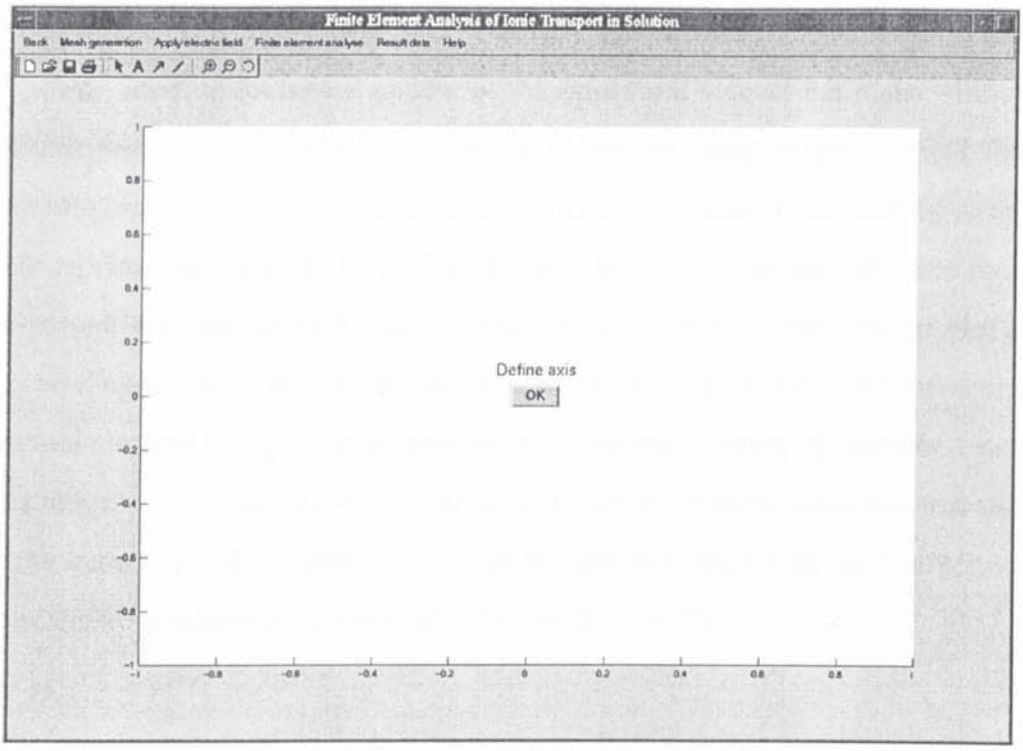

Fig. 9.5. Main window

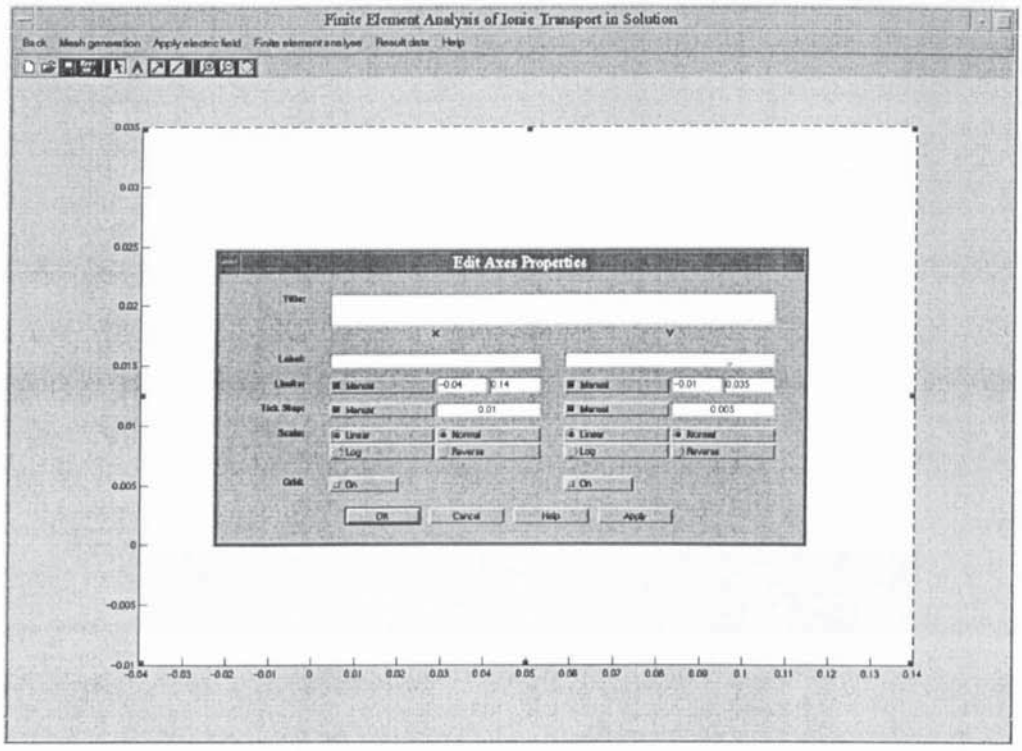

Fig. 9.6 Window for editing axes

After defining the axis, the next step is to build the geometrical model analysed and to generate the information of nodes and elements, a task undertaken by the pre-processor

which is linked to the menu named as "Mesh generation", under which there are two submenus (Fig. 9.7). When the user chooses the submenu, "Drawing geometrical shape", three drawing tools will appear at the upper left side of the main window, viz. Line, Curve and Arc, with which the user can draw any complex geometrical shapes of the structure analysed. After the completion of drawing, these lines, curves or arcs (the geometrical elements) need to be further defined. In order to do that, the user moves the mouse pointer into the defined area of these geometrical elements and presses the left button, causing a dialog box to appear, which presents the editable information of the geometrical element being defined, such as co-ordinates, number of elementst, boundary information, etc (see Figs. 9.8-9.11). After defining all of these elements, the user then clicks the submenu "Mesh generation" and the pre-processor will start to generate the node and element information automatically (see Fig. 9.12).

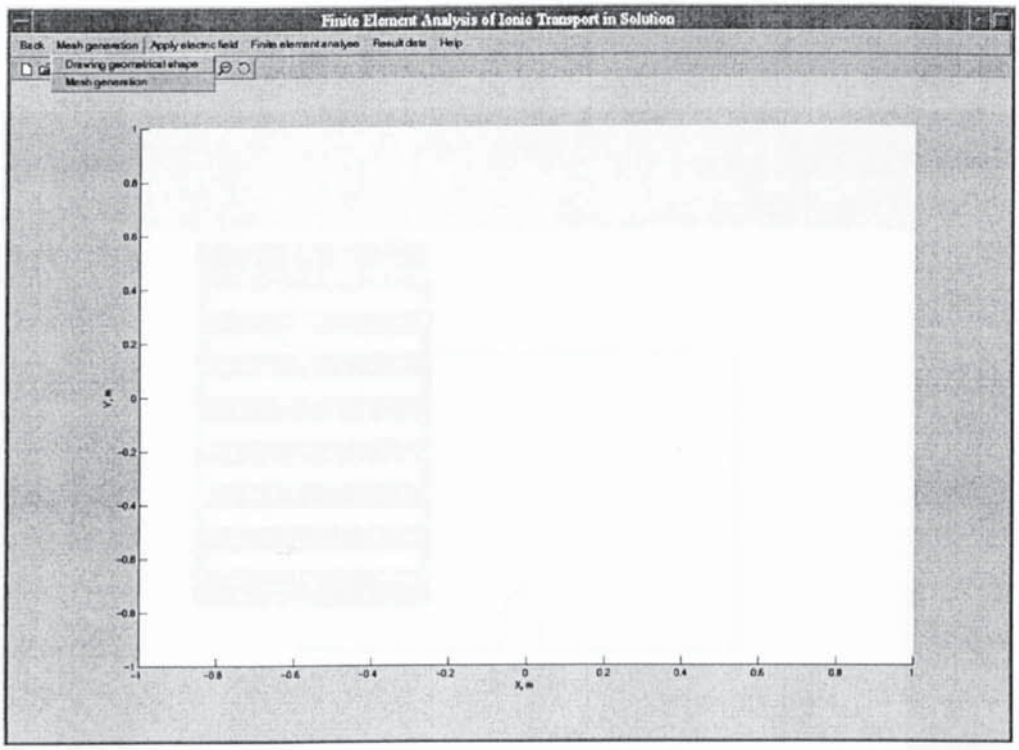

Fig. 9.7 Submenu under the menu of Mesh generation

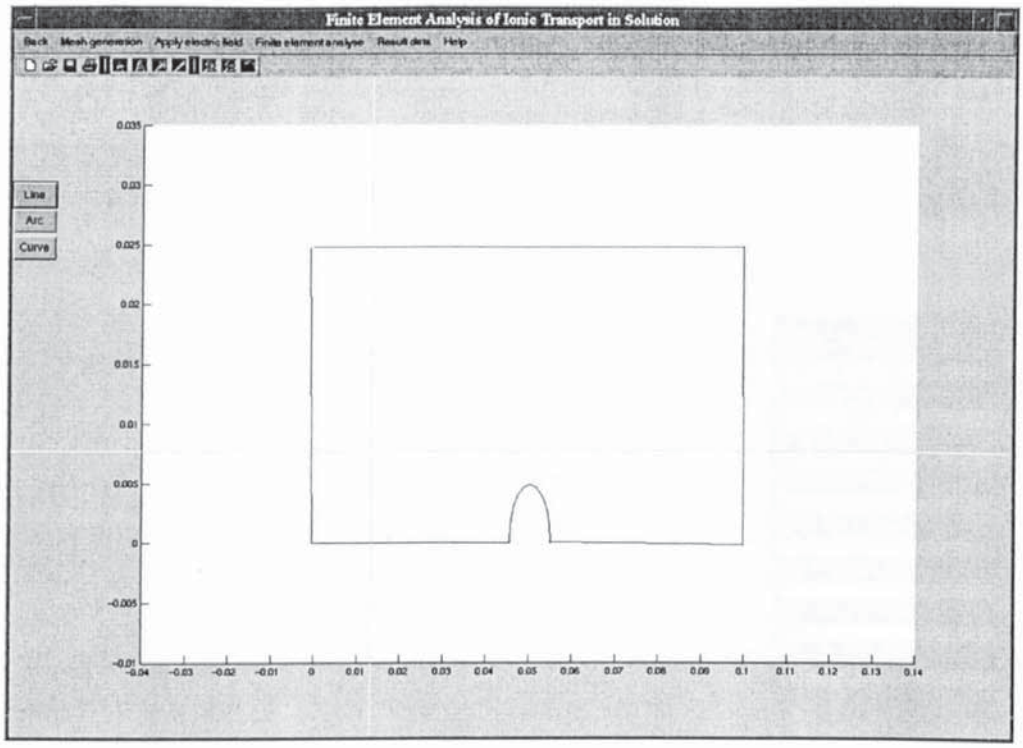

Fig. 9.8 Drawing structure

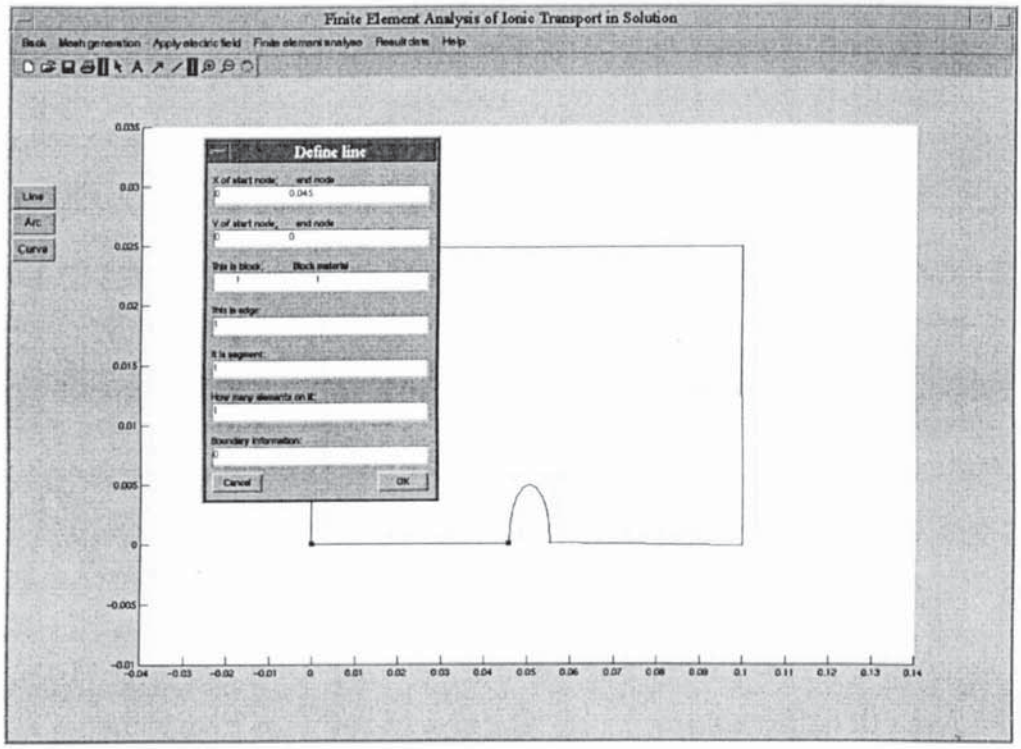

Fig. 9.9 The dialog box for defining line

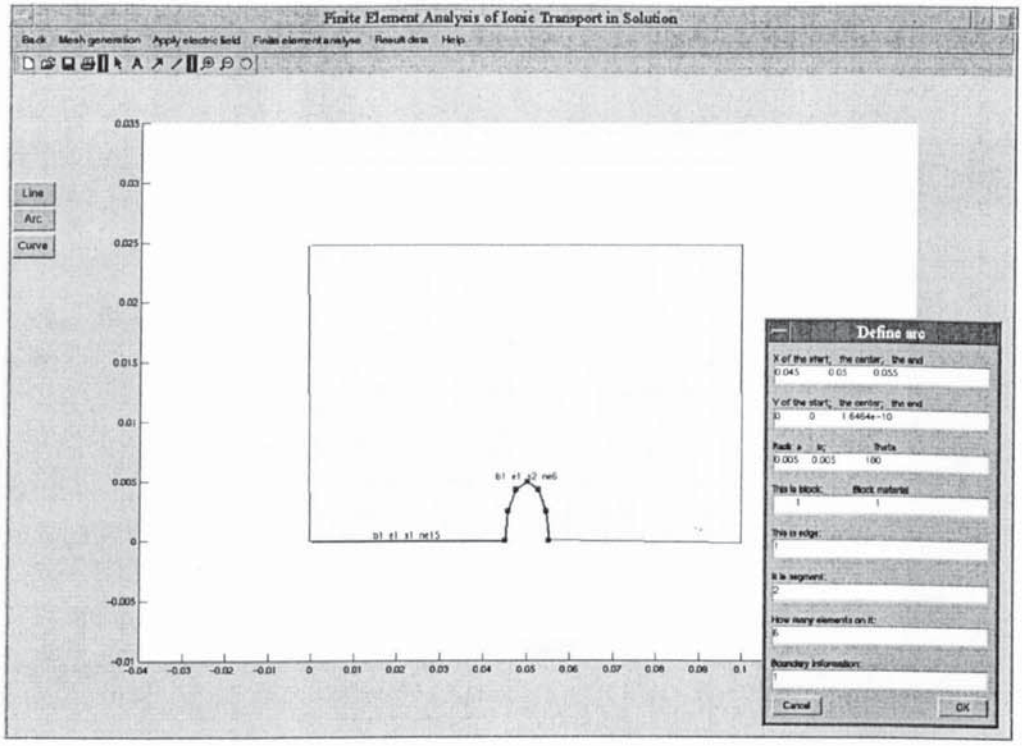

Fig. 9.10 Dialog box for defining arc

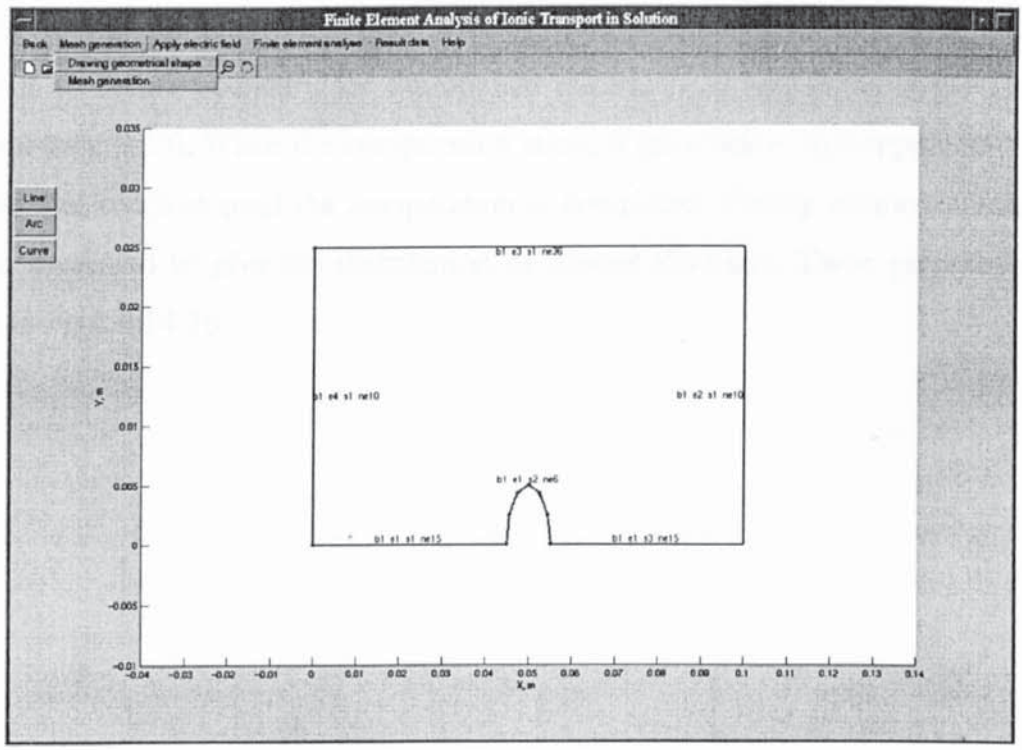

Fig. 9.11 Defined structure

(The line with marks is boundary associating with the boundary condition)

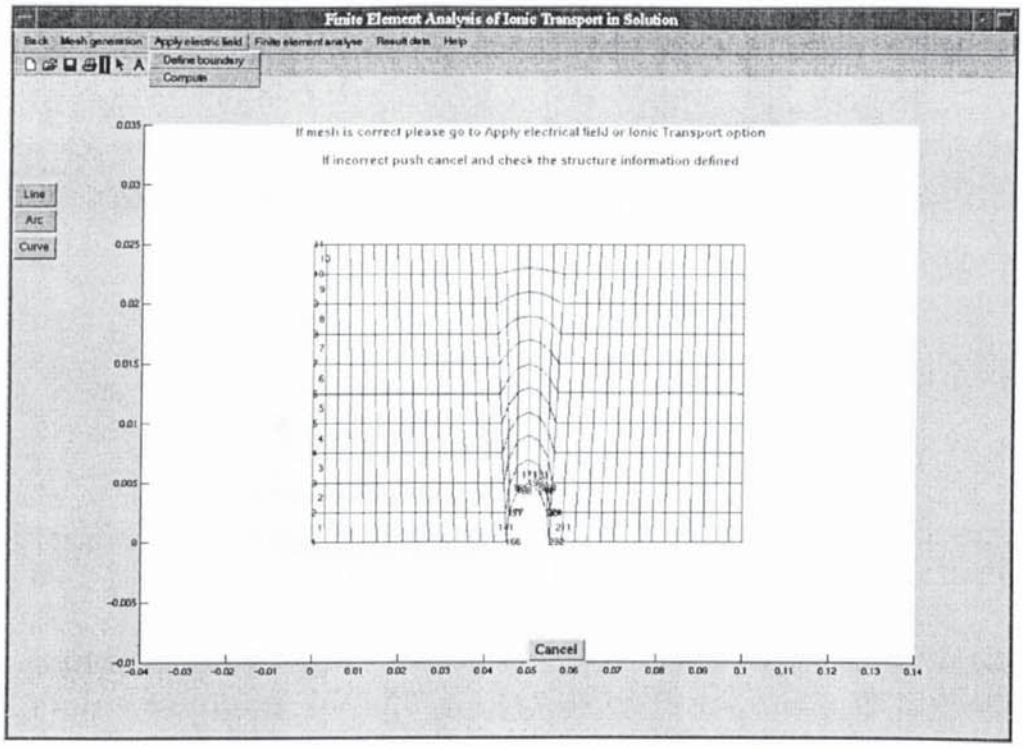

Fig. 9.12 Mesh generated

The menu with the name of 'Apply electric field' contains two submenus with the functions to define boundary for the applied electric field and to solve the Laplace equation (Fig. 9.13). When the computation starts, a subwindow will appear to display the potential function until the computation is completed. Finally another subwindow will be presented to give the distribution of current densities. These procedures are shown in Figs. 9.14-16.

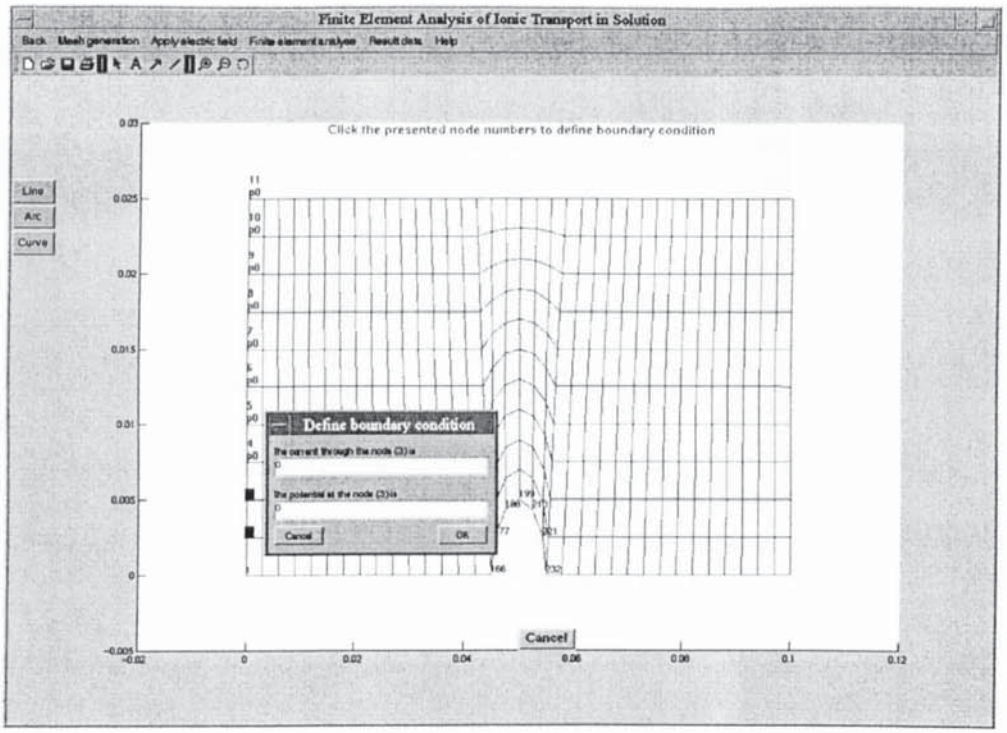

Fig. 9.13 Submenu under the menu of Apply electric field

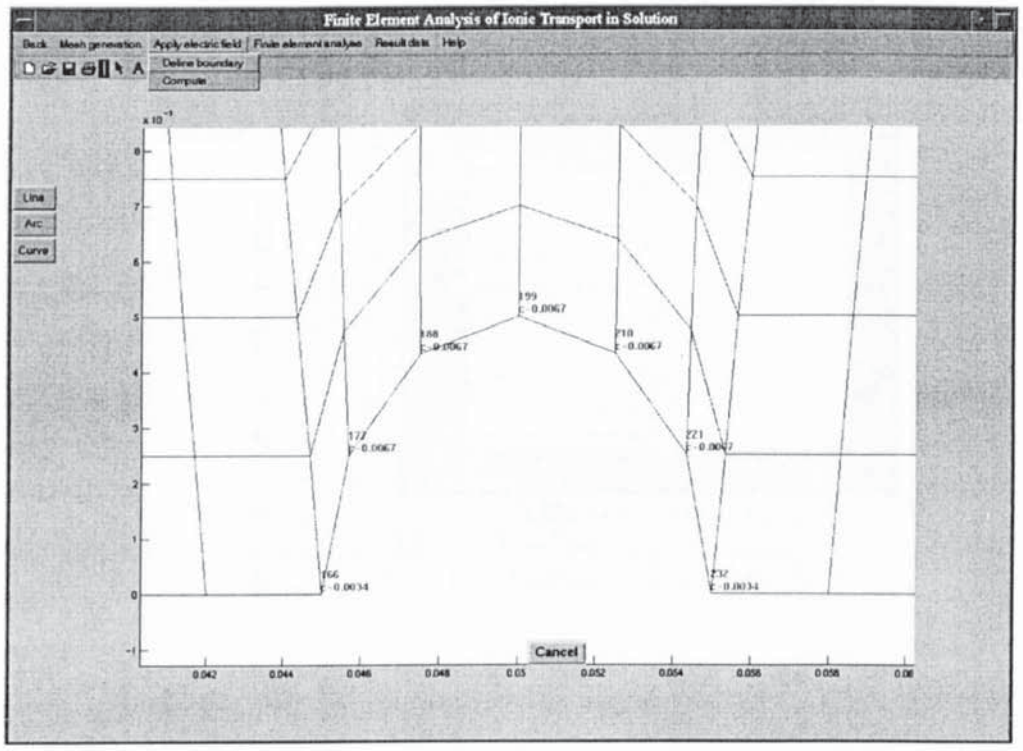

Fig. 9.14 Define boundary for solving Laplace equation

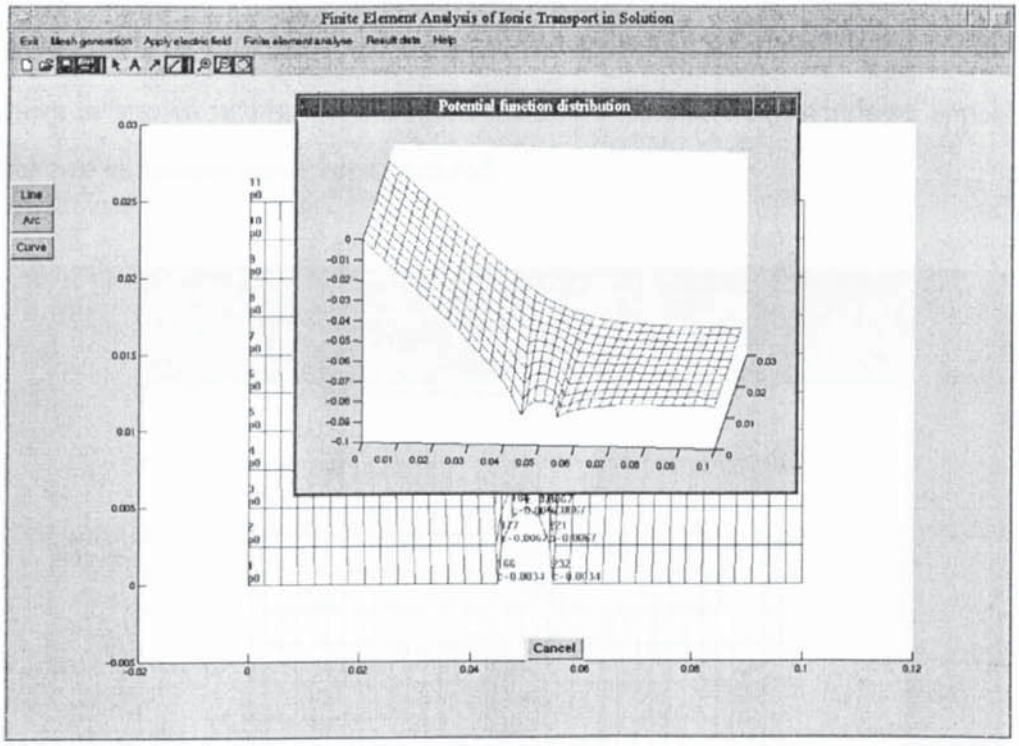

Fig. 9.15 Subwindow for displaying the potential function

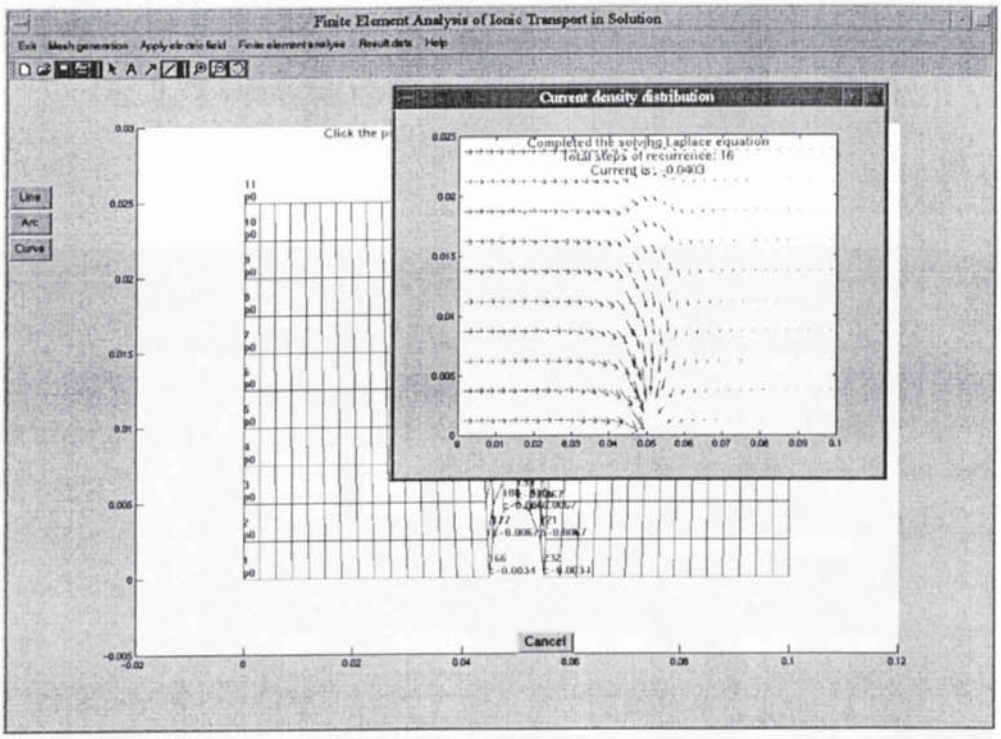

Fig. 9.16 Subwindow for displaying the current density distribution

A menu with the name of "Finite element analysis" connects with the programme designed to analyse the ionic transport in dilute solutes. Three submenus associate with

this function (Fig. 9.17). When the user selects the Input data, a dialog box will appear for editing as shown in Fig. 9.18. Figs. 9.19 and 9.20 show the windows appearing as the other two submenus have been selected.

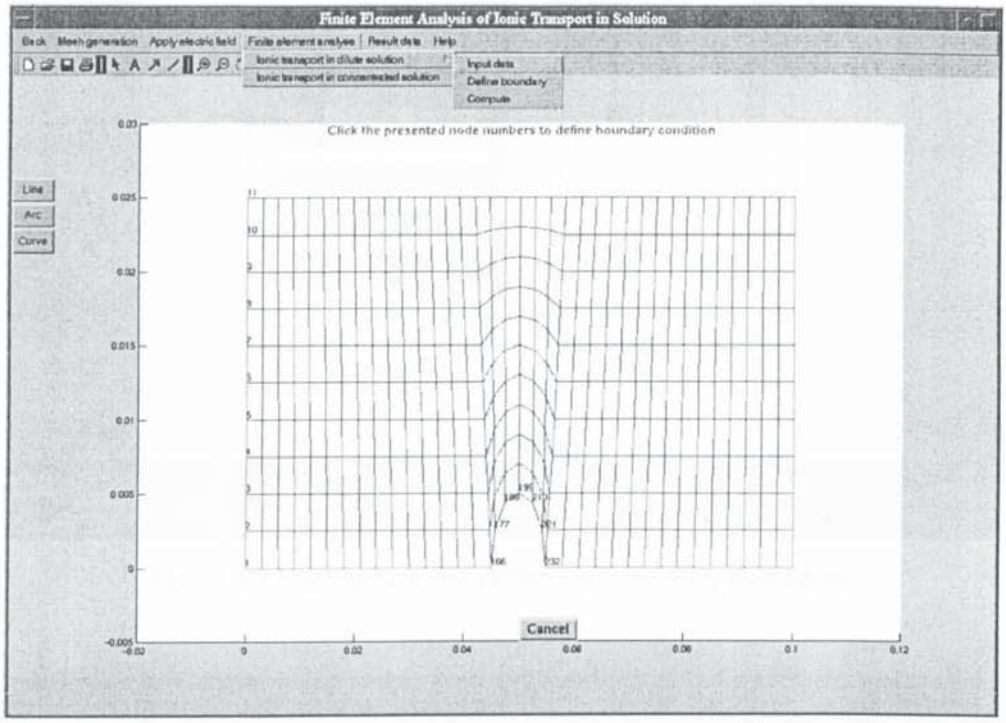

Fig. 9.17 Submenu under the menu of Finite element analysis

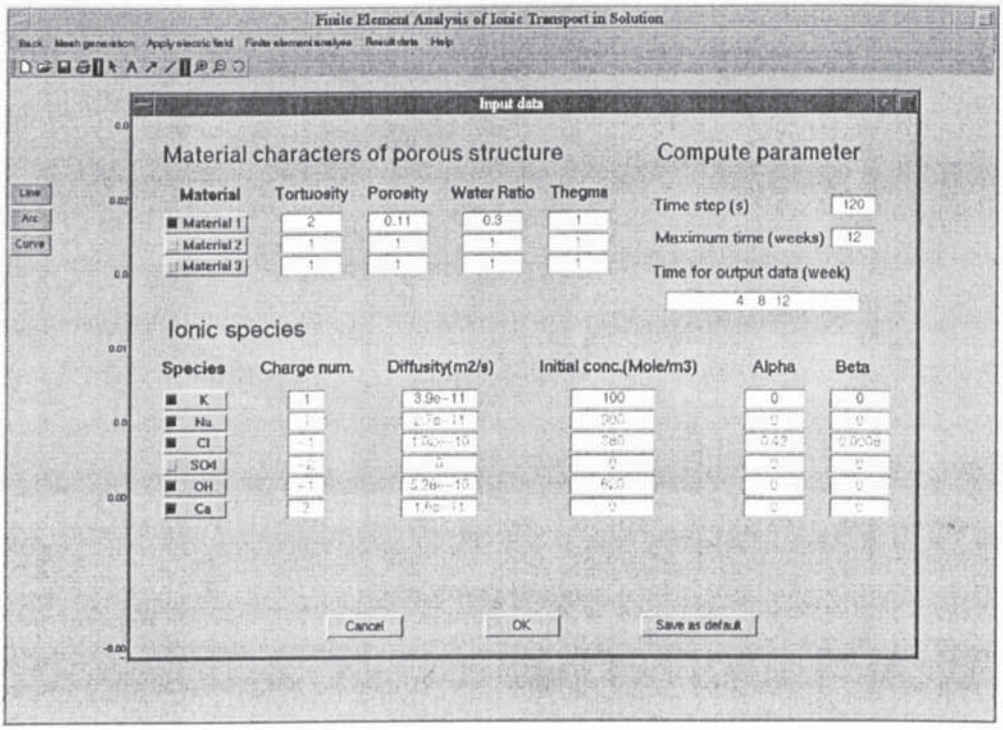

Fig. 9.18 Subwindow for data input

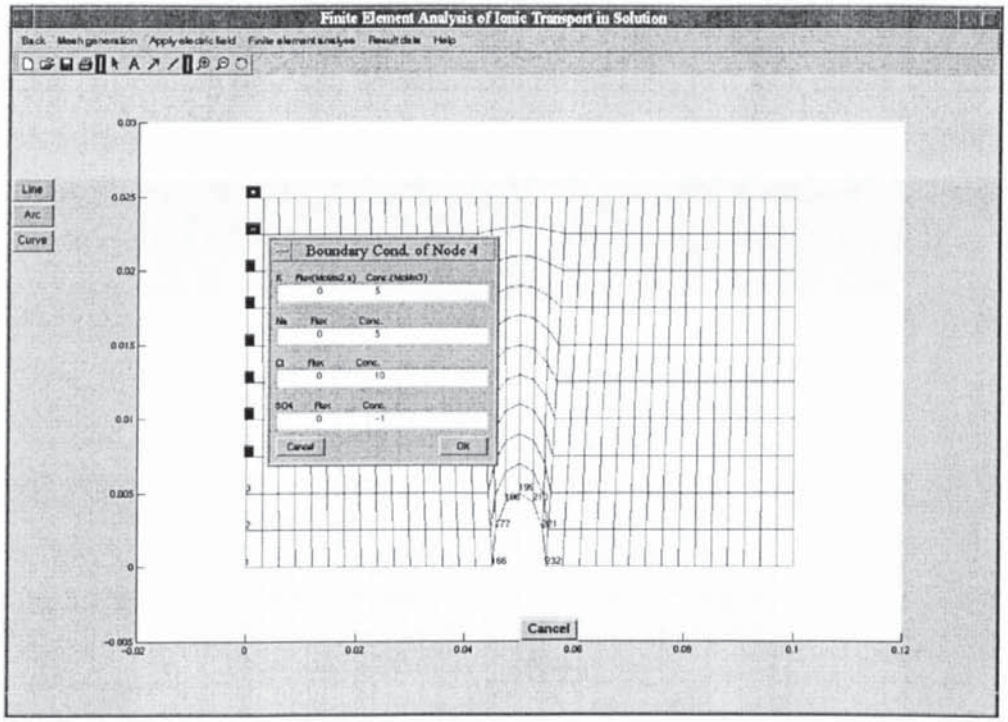

Fig. 9.19 Dialog box for defining boundary condition

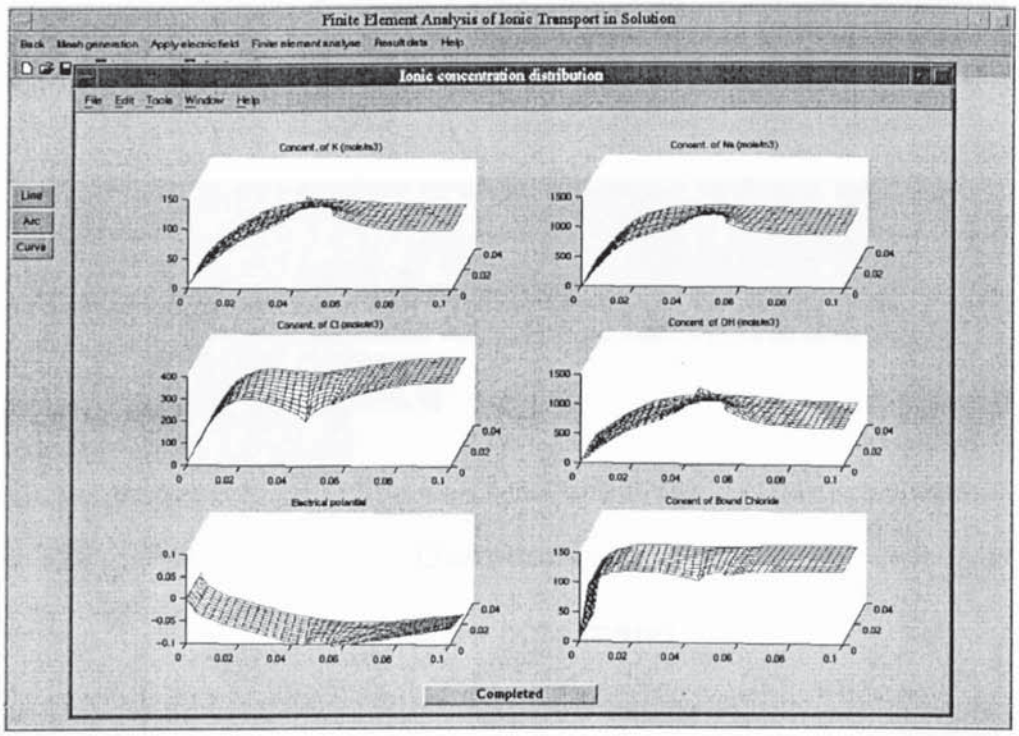

Fig. 9.20 Subwindow for displaying the results at a defined time interval in the process of computation

Figs. 9.21-24 show the windows associated with the selection of the submenus under the main menu item "Result data" which connects with the post-processor. The result at any node and at any chosen time can be obtained immediately just with mouse clicking.

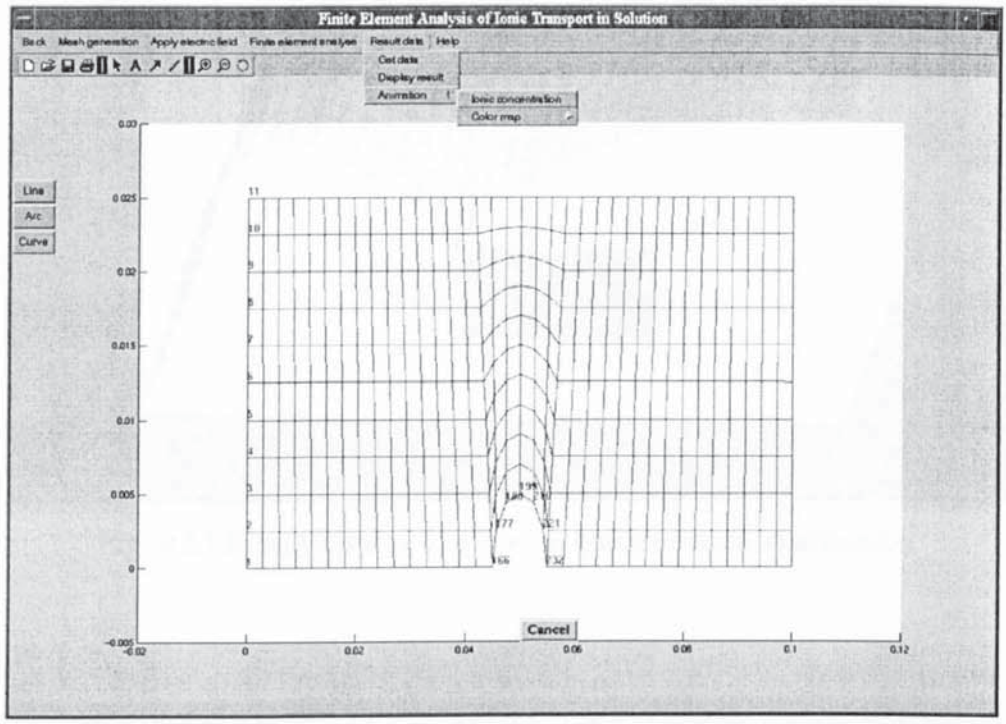

Fig. 9.21 Submenu under the menu of Result data

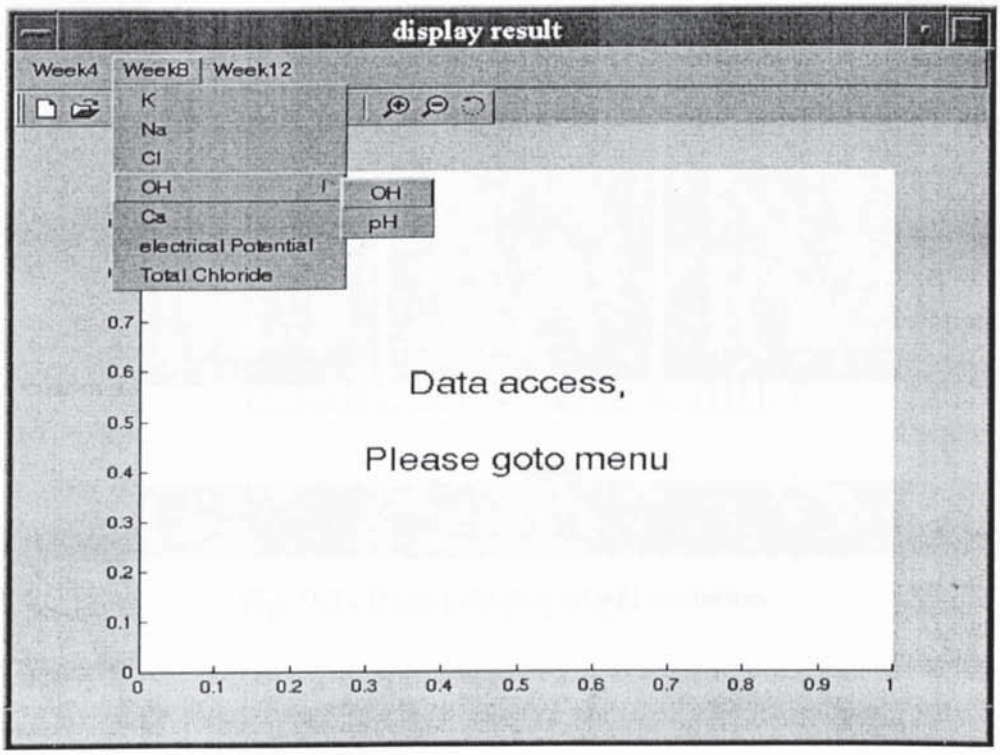

Fig. 9.22 Result displaying window

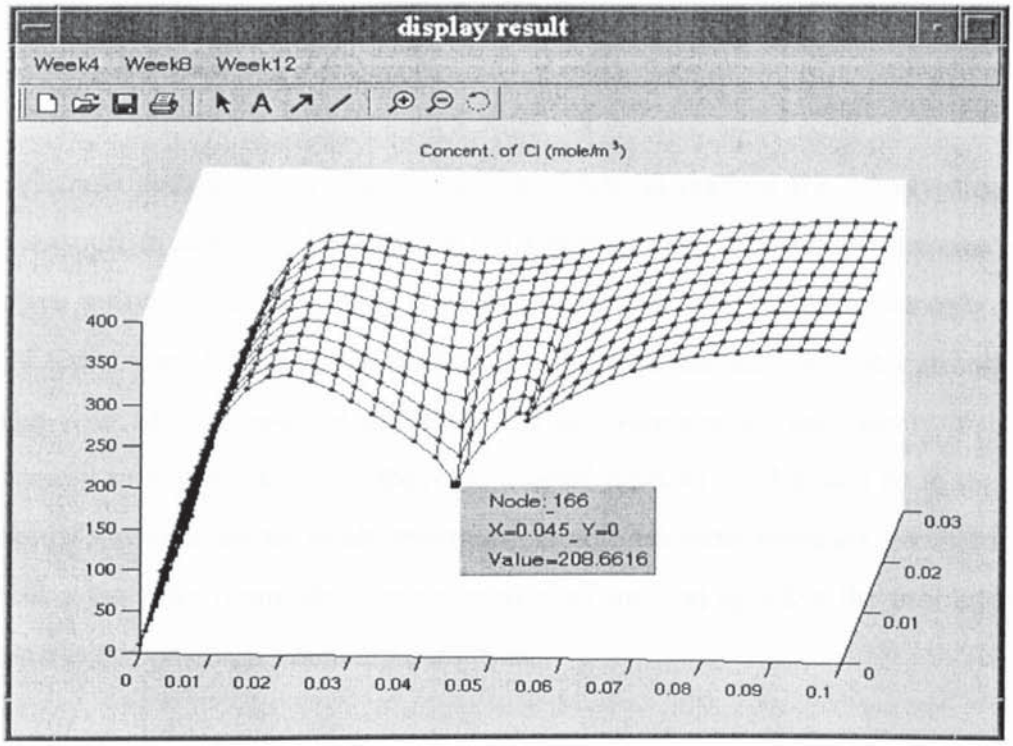

Fig. 9.23 Result display of chloride concentration distribution

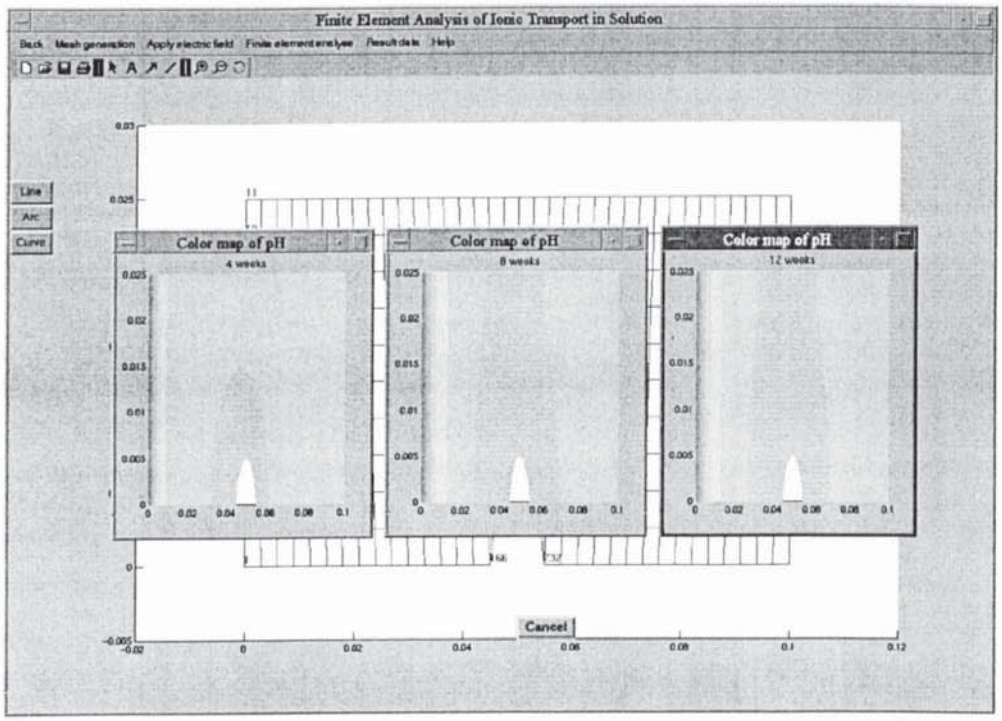

Fig. 9.24 Result display of pH variation

9.4 CONCLUSIONS

Finite element analysis is an effective and economical method for the investigation of ionic transport in solution. Developing the finite element analysis programme into an interactive software package with friendly graphical user interface, not only reduces some of tedious work required in preparing input data, but also provides simple access for users with little knowledge of FEM. The software can be used easily, but further development to expand its applicability is needed. Further work could be in the area of developing a more adaptive mesh generator suitable for more complex geometric shape and have a less user input, developing numerical method to solve the problem with a constant electric potential boundary condition.

CHAPTER 10

GENERAL CONCLUSIONS AND FURTHER WORK

10.1 GENERAL CONCLUSIONS

The present work has proposed a comprehensive mathematical model for ionic transport in pore solutions, which comprises of the main factors related to the ionic transport process. As applications, this model has been used to simulate the process of chloride ingress into concrete from a saline environment and the process of electrochemical chloride removal.

In the case of chloride ingress, this model shows that ionic interaction and capillary suction of solution in unsaturated concrete pore structures have significant influence on the ionic distributions. Compared with other mathematical models, this model presents a fairly good agreement with experimental results. In addition to that, the model also has made itself applicable to different cases with unified ionic diffusivities in dilute solution. This can make the model more practical because it considers the influence factors on the process specifically and the parameters introduced are directly related to the concrete quality and condition, which can be easily determined by standard experimental measurements.

In the case of electrochemical chloride removal, the one-dimensional modelling shows that this model presents a reasonable prediction for the ionic concentration profiles in the process. In agreement with the experimental data, numerical results show that ECR is capable of removing chloride from concrete quite effectively. In particular, the chloride concentration near the steel cathode decreases very significantly during ECR. In the mean time, the concentrations of hydroxyl and cations increase near the cathode. The higher the treating current density, the more chloride will be removed.

Two dimensional modelling of ECR shows that the position of external anode, the configuration of the reinforced concrete structure and the selection of steel cathode have

significant influence on the current distribution in concrete, a result that is directly related to the effectiveness and efficiency of ECR.

Chloride binding has a significant influence on the process of ECR. Based on the chemical reaction kinetics, a new chloride binding isotherm has been proposed. Compared with Langmuir isotherm, the proposed isotherm not only considers the non-linear relationship between the free and bound chlorides but also is not restricted by the pre-requirement of the equilibrium between free and bound chlorides. Numerical modelling results show that good prediction for ionic concentration profiles is provided by the proposed isotherm for different treating current densities and different treating times. However, the rate constant in the isotherm is likely to depend on the ionic concentration and current density. Further investigation is needed to find the quantitative relationship between the rate constant and the influencing factors.

Chloride transference number is a parameter that is often used to describe the efficiency of ECR in literatures. Compared with experimental investigation, computational model is able to give detailed information about the local variation of the ionic distribution and thus the ionic transference numbers. The numerical modelling in this study shows that the local chloride transference number is related to the concentrations of chloride and other ionic species in the solution. The ionic transference number varies from place to place and from time to time. A direct proportional relationship exists between the chloride transference number and the *Cl/OH* ratio except for the region near the surface of concrete. The chloride transference number at cathode decreases rapidly at the early stage, because large quantity of hydroxyl is produced from cathodic electrochemical reactions. As the result, the chloride in the region near cathode is reduced significantly at very beginning, but its concentration decrease becomes very slow in the later time. The efficiency of chloride removal expressed by the chloride transference number will decrease with the increase of current density and treating period.

Finite element analysis is a quick, effective and economical method for the investigation of ionic transport in solutions. The finite element analysis program developed in this study has an interactive, friendly graphical interface, which can be easily handled by the users with little FEM knowledge.

10.2 FURTHER WORK IN DEVELOPMENT

Developments made through the course of this thesis have directly or indirectly highlighted a number of research areas that would improve further our understanding of the processes of chloride ingress into concrete and electrochemical chloride removal. These research areas are related to ionic interaction, capillary suction and chloride binding studies. Further work for development in the areas is discussed in the follows.

In order to validate the proposed model, a large number of comparisons with experiments are needed. In this thesis, the model was compared only with tow available one-dimensional experiments [Bertolini, et al., 1996; Ismail, 1998]. For two-dimensional problems, however, there is no available experimental data. At this point, two-dimensional experiments are needed to test the model. As was suggested in Chapter 5, Two-dimensional experiments need to be carried out to examine the influence of anode positions on the ionic profiles in pore solution. In particularly, for the chloride ions, experiments are required to investigate how they are redistributed in the region near the steel bar and how the external anode affects the redistribution of chloride ions. The relationship between the chloride average concentration level along the steel bar surface and the position of external anode should be assessed. In addition to this, as was suggested in Chapter 6, two-dimensional experiments are also needed to study the effects of the configuration of reinforced concrete on ECR. The effect of the selection of cathodes in complex reinforced concrete structures on the effectiveness and efficiency needs to be investigated experimentally.

The precision of computer modelling mainly depends on the mathematical model adopted to describe the problem concerned. Chloride transport in concrete is a complex process, which involves three transport mechanisms. Because there are too many factors related to the three mechanisms, especially the role of some of them is uncertain in the process, it is impossible to consider all these factors in the mathematical model. The proposed model is based on the assumption of ideal dilute electrolyte with considering the electrostatic coupling of the dissolved ionic species. In some practical cases, electrolytes in pore structure tend to be highly concentrated, in which case ion/ion and ion/solvent interactions may be important and may need to be considered [Bockris and

Reddy, 1970; Adamson, 1990; Li and Page, 1998b; Climent, et al., 1998]. Numerous semi-empirical models have been developed to account for the influence of ionic strength on the thermodynamic properties of electrolytes [Pitzer, 1973; 1979]. For the mathematical modelling of ionic transport in saturated porous media, some simple models for calculating the chemical activity coefficients of ions in concentrated solutions have been reported [Li and Page, 1998b; Samson, et al., 1999]. Therefore, further work to incorporate these considerations into the current model will be useful.

As was mentioned through the thesis, chloride binding isotherm is one of the important factors having significant influence on chloride transport in concrete. The chloride binding isotherm proposed based on the chemical reaction kinetics gives an improvement on the numerical prediction of free and total chloride profiles compared with other models. The results of the proposed isotherm show that the rate constants of the reactions of the free chloride adsorption and bound chloride release depend on the contents of free and bound chlorides, the treating current densities and the treating periods. Further investigation is required in order to find the quantitative relationship between the rate constant and these factors. In particularly, experimental studies on this issue are needed.

Finally, in this study, only galvanostatic treatments, i.e. with constant current densities on the surfaces of cathode and anode, were modelled. Further work on the modelling for the treatments that are under the condition that a constant electrical potential gradient applied between reinforcement and the external anode is needed. Comparison of the results between the galvanostatic and the constant electrical potential gradient cases will be useful to evaluate the difference between the two treatments. Comparisons of ionic profiles in the process of ECR and the effectiveness and efficiency of chloride removal in the two cases will be helpful to further understand the process. Other issues such as the side effects in the two different treatments also need to be investigated.

REFERENCE

Adamson, A.W., [1990], *Physical Chemistry of Surfaces*, John Wiley & Sons, 5th ed.

Ahmad, S., Bahattacharjee, B. and Wason, R., [1997], 'Experimental Service Life Prediction of Rebar-Corroded Reinforced Concrete Structure', *ACI Materials Journal*, Vol. 94, pp. 311-316.

Al-Bahar, S., Attiogbe, E K., and Kamal, H., [1998], 'Investigation of Corrosion Damage in A Reinforced Concrete Structure in Kuwait', *ACI Materials Journal*, May-June, pp. 226-231.

Al-Amoudi, O.S.B., Maslehuddin, R.M. And Abduljauwad, S.N., [1994], 'Influence of Chloride Ions on Sulphate Deterioration in Plain and Blended Cements', *Magazine of Concrete Research*, Vol. 46, No. 167, pp. 113-123.

Al-Khaiat, H. and Hague, M.N., [1997], 'Carbonation of Some Coastal Concrete Structure in Kuwait', *ACI Materials Journal*, Vol. 97, No. 6, pp 602-607.

Allam, A.M., Ateya, B.G. and Pickering, H.W., [1997], 'Effect of Chloride Ions on Adsorption and Permeation of Hydrogen in Iron', *The Journal of Science and Engineering Corrosion*, Vol. 53, No. 4, pp. 284-289.

Andrade, C., [1993], 'Calculation of Chloride Diffusion Coefficients in Concrete from Ionic Migration Measurements', *Cement and Concrete Research*, Vol. 23, pp. 724-742.

Andrade, C., Sanjuan, M.A., Recuero, A. and Rio, O., [1994], 'Calculation of Chloride Diffusivity in Concrete from Migration Experiments in Non-steady-state Conditions', *Cement and Concrete Research*, Vol. 24, No. 7, pp. 1214-1228.

Andrade, C., Diez, J.M., Alaman, A. and Alonso, C., [1995], 'Mathematical Modelling of Electrochemical Chloride Extraction from Concrete', *Cement and Concrete Research*, Vol. 25, No. 4, pp. 727-740.

Arup, H., [1983], 'The Mechanisms of The protection of steel by Concrete', in *Corrosion of Reinforcement in Concrete Construction*, A.P. Crane (ed.), Ellis Horwood, Chichester, pp. 151-157.

Arya, C. and Newman, J.B., [1990], 'An Assessment of Four Methods of Determining the Free Chloride Content of Concrete', *Materials and Structures*, Vol. 23, pp. 319-330.

Atkinson, A, and Nickerson, A.K., [1984], 'The Diffusion of Ions Though Water-saturated Cement', *Journal of Materials Science*, Vol. 19, pp. 3068-3078.

Barneyback, R.S. and Diamond, S., [1981], 'Expression and Analysis of Pore Fluids from Hardened Cement Pastes and Mortars', *Cement and Concrete Research*, Vol. 11, No. 2, pp. 279-285.

Bentz, E.C., Evans, C.M. and Thomas, M.D.A., [1996], 'Chloride Diffusion Modelling for Marine Exposed Concretes', in *Corrosion of Reinforcement in Concrete Corrosion Construction*, C.L. Page, P.B. Bamforth and J.W. Figg, (ed.), Hartnolls Ltd, Cornwall, UK.

Berke, N.S. and Hicks, M.C., [1994], 'Predicting Chloride Profiles in Concrete', *Corrosion Engineering*, Vol. 50, No. 3, pp. 234-239.

Bertolini, L., Yu, S.W. and Page, C.L., [1996], 'Effects of Electrochemical Chloride Extraction on Chemical and Mechanical Properties of Hydrated Cement Paste', *Advances in Cement Research*, Vol. 8, No. 31, pp. 93-100.

Boam, K. [1989], 'Concrete Highway Structures-Current Experience of Investigation and Repair', Concrete Repair Conference, Tara Hotel, London, 16th Mar., Palladian Publication Ltd.

Bockris, J.O'M. and Reddy, A.K.N., [1970], *Modern Electrochemistry: An Introduction to An Interdisciplinary Area*, Plenum Press.

Bohris, A.J., Goerke, U., McDonald, P.J., Mulheron, M., Newling, B. and Page, Le.B., [1998], 'A Broad Line NMR and MRI Study of Water and Water Transport in Portland cement Pastes', *Magnetic Resonance Imaging*, Vol. 16, pp. 455-461

Broomfield, J.P., [1997], *Corrosion of Steel in Concrete: Understanding, Investigation and Repair*, E and F N Spon.

Brunauer, S., Skaluy, J., and Bodor, E. E., [1969], 'Adsorption on Non-porous Solids', *Journal of Colloid and Interface Science*, Vol. 30, pp. 549-552.

Brutsaert, W., [1979], 'Universal Constants for Scaling The Expotential Soil Water Diffusivity?', *Water Resource Research*, Vol. 15, pp. 481-483

Byfors, K., [1990], 'Chloride-Initiated Reinforcement Corrosion: Chloride Binding', Swedish Cement and Concrete Research Institute, Stockholm, Report 1.

Canham, I., Page, C.L. and Nixon, P.J., [1987], 'Aspects of The Pore Solution Chemistry of Blended Cements Related to The Control of Alkali Silica Reaction', *Cement and Concrete Research*, Vol. 17, pp. 839-844.

Castellote, M., Andrade, C. and Alonso, C., [1999], 'Modelling of The Process During Steady-State Migration Test: Quantification of Transference Numbers', *Materials and Structures/Materiaux et Constructions*, Vol. 32, pp. 180-186.

Castellote, M., Andrade, C. and Alonso, C., [2000], 'Chloride Transference Numbers in Steady-State Migration Tests', *Magazine of Concrete Research*, Vol. 52, No. 2, pp. 93-100.

Chatterji, S., [1995], 'On The Applicability of Fick's Second Law to Chloride Ion Migration Through Portland Cement Concrete', *Cement and Concrete Research*, Vol. 25, No. 2, pp. 299-303.

Climent, M.A., de Vera G., Hidalgp, A., Andrade, C. and Alonso, C., [1998], 'Chloride Ion Activities in Synthetic Concrete Pore Solutions: Theoretical Models and Potentiometric Measurements', Materials Science of Concrete – The Sydney Diamond Symposium, American Ceramic Society, pp. 285-294.

Collins, F.G. and Farinha, [1991], 'Repair of Concrete in the Marine Environment: Cathodic Protection vs Chloride Extraction', *Australian Civil Engineering Transaction*, 33, 1, Feb.

Crane, A.P., [1983], *Corrosion of Reinforcement in Concrete Construction*, Ellis Horwood, Chichester.

Damidot, D. and Glasser, F.P., [1993], 'Thermodynamic Investigation of The $CaO - Al_2 - O_3 - CaSO_4 - H_2O$ system at $25^{o}C$ and the influence of Na_2O', *Cement and Concrete Research*, Vol. 23, pp. 221-238.

Dhir, R.K. and Byars, E.A., [1993], 'PFA Concrete: Chloride Diffusion Rates', *Magazine of Concrete Research*, Vol. 45, No. 162, pp. 1-9.

Dhir, R.K., Jones, M.R. and Ng, S.L.D., [1998], 'Prediction of Total Chloride Content Profile and Concentration/Time-dependent Diffusion Coefficients for Concrete', *Magazine of Concrete Research*, Vol. 50, pp. 37-48.

Dhir, R.K., Jones, M.R., Ahmed, H.E.H. and Seneviratne, A.M.G., [1990], 'Rapid Estimation of Chloride Diffusion Coefficient in Concrete', *Magazine of Concrete Research*, Vol. 42, No. 152, pp. 177-185.

Elmiligy, A.A, Geana, D. and Lorenz, W.J., [1975], Electrochem. Acta. Vol. 20, pp. 273.

Fraczek, J., [1987], 'A Review of Electrochemical Principles as Applied to Corrosion of Steel in A Concrete or Grout Environment' in *Corrosion, Concrete and Chlorides, Steel Corrosion in Concrete: Cause and Restrains*, F.W. Gibson (ed.), pp. 13-14.

Ganda V.K., [1970], 'Corrosion and Corrosion Inhibition of Reinforcing Steel 1-Immersion in Alkaline Solution', *British Corrosion Journal*, Vol. 5, pp. 198-203.

Gibson, F.W. (ed.), [1987], *Corrosion, Concrete and Chlorides, Steel Corrosion in Concrete: Cause and Restrains*, American Concrete Institute, Detroit.

Gjorv, O.E., Tan, K. and Zhang, M., [1994], 'Diffusivity of Chlorides from Sea-water into High-strength Lightweight Concrete', *ACI Materials Journal*, Sept.-Oct., pp. 447-452.

Glass, G.K. and Buenfeld, N.R., [1997], 'The Presentation of The Chloride Threshold Level for Corrosion of Steel in Concrete', *Corrosion Science*, Vol. 39, No. 5, pp. 1001-1013.

Glass, G.K., Stevenson, G.M. and Buenfeld, N.R., [1998] 'Chloride-Binding Isotherms From The Diffusion Cell Test', *Cement and Concrete Research*, Vol. 28, No. 7, pp. 939-945.

Gonda, V.K., [1970], 'Corrosion and Corrosion Inhibition of Reinforcing Steel I, Immersed in alkaline Solutions', *British Corrosion Journal*, No. 5, pp. 198-203.

Gonzalez, J.A., Otero, E., Feliu, S., Bautista, A., Ramirez, E., Rodriguez, P. and Lopez, W., [1998], 'Some Considerations on Effect of Chloride Ions on The Corrosion of Steel Reinforcements Embedded in Concrete Structures', *Magazine of Concrete Research*, Vol. 50, No. 3, pp. 189-199.

Hall, C., [1989], 'Water Sorptivity of Mortars and Concretes: A Review', *Magazine of Concrete Research*, Vol. 41, No. 147, pp. 51-61

Hansson, I.L.H. and Hasson, C.M., [1993], 'Electrochemical Extraction of Chloride from Concrete Part 1, A Qualitative Model of The Process', *Cement and Concrete Research*, Vol. 23, pp. 1141-1152.

Hassanein, A.M, Glass, G.K. and Buenfeld, N.R., [1998], 'A Mathematical Model for The Electrochemical Removal of Chloride from Concrete Structures', *Corrosion*, Vol. 54, No. 4, pp. 323-332.

Hassanein, A.M., Glass, G.K. and Buenfeld, N.R., [1999], 'Chloride Removal by Intermittent Cathodic Protection Applied to Reinforced Concrete in Tidal Zone', *Corrosion*, Vol. 55, No. 9, pp. 840-850.

Hausmann, D.A., [1967], 'Steel Corrosion in Concrete: How Does It Occur?', *Materials Protection*, Vol. 6, No. 11, pp. 19-23.

Heinrich, J.C. and Pepper, D.W., [1999], *Intermediate Finite Element Method: Fluid Flow and Heat Transfer Application*, Printed by Hamilton Printing Co., Castleton, NY.

Hewlett, P.C. (ed.), [1988], *Cement Admixtures: Use and Applications*, Longman, Harlow, pp. 166.

Hewlett, P.C. (ed.), [1997], *Lea's chemistry of Cement and Concrete*, 4th ed., Arnold.

Hoar T.P., Mears R.B. and Rothwell G.P., [1965], 'The Relationships between Anodic Passivity, Bribhtening and Pitting', *Corrosion Science*, Vol. 5, pp. 279-289

Hoar, T.P. and Jacob, W.R., [1967], 'Breakdown of Passivity of Stainless Steel by Halide Ions', *Nature*, Vol. 216, pp. 1299-1301.

Hobbs, D.W., [1998], 'Expansion and Cracking in Concrete Associated with " Delayed Ettringite Formation', paper presented at 'Degradation of Reinforced Concrete:

Processes, Investigation and Control', 5 days post-experience course Master's level module in Dept of Civil Engineering, Aston University, 18-22 th, May.

Holden, W.R., Page, C.L. and Short, N.R., [1985], 'The Influence of Chlorides and Sulphates on Durability', in *Corrosion of Reinforcement in Concrete Construction*, A.P. Crane, pp. 79-89.

Hou, Q., Luo, Z. and Teng, L. (1998). 'A Software for The Calculation of Ion Transport in Solids', *Nuclear Instruments and Methods in Physics Research B*, Vol. 135, pp. 159-163.

Hussain, S.E., Al-Gahtani, A., and Rasheeduzzafar, [1996], 'Chloride Threshold for Corrosion of Reinforcement in Concrete', *ACI Materials Journal*, pp. 534-538.

Ismail, M.B., [1998], 'Electrochemical Chloride Extraction to Halt Corrosion of Reinforcement', PhD. Thesis, Aston University.

Jacobs, R.A. and Probstein, R.F., [1996], 'Two Dimensional Modelling of Electroremediation', *AICHE Journal*, Vol. 42, No. 6, pp. 1685-1696.

Jones, D.A., [1996], *Principles and Prevention of Corrosion*, 2th Ed., Prentice-Hall, Upper Saddle River, N.J.

Kayyali, O.A. and Haque, M.N., [1995], 'The Ratio in Cl^-/OH^- The Chloride-Contaminated Concrete -- A Most Important Criterion', *Magazine of Concrete Research*, Vol. 47, No. 172, pp. 235-242.

Kitowski, C.J. and Wheat H.G., [1997], 'Effect of Chlorides on Reinforcing Steel Exposed to Simulated Concrete Solutions', *The Journal of Science and Engineering Corrosion*, Vol. 53, No. 3, pp. 216-226.

Lewis, R.W., Morgan, K., Thomas, H.R. and Seetharamu, K.N., [1996], 'The Finite Element Method in Heat Transfer Analysis', J. Wiley & Sons, New York.

Li, L.Y. and Page, C.L., [1997a], 'Effect of Diffusion Coefficients on Ionic Distribution Profiles: Analytical Solutions in Steady State', Report, Dept of Civil Engineering, Aston University.

Li, L.Y. and Page, C.L., [1997b], 'Notes on The Application of Basic Equations of Ionic Transport for Chloride Extraction from Concrete by Using Electrochemical Method', Report, Aston University.

Li, L.Y. and Page, C.L., [1998a], 'Mathematical Modelling of Electrochemical Chloride Extraction from Concrete', *Computational Modelling of Concrete Structures*, Balkema, Rotterdam, pp. 497-503.

Li, L.Y. and Page, C.L., [1998b], 'Modelling of Electrochemical Chloride extraction from Concrete: Influence of Ionic Activity Coefficients', *Computational Materials Science*, Vol. 9, pp. 303-308.

Li, L.Y. and Page, C.L., [2000], 'Finite Element Modelling of Chloride Removal from Concrete by An Electrochemical Method', *Corrosion Science*, Vol. 42, pp. 2145-2165.

Longuet, P., Burglen, L. and Zelwer, A., [1973], 'The Liquid Phase of Hydrated Cement', *Revue des Materiaux de Construction*, Vol. 676, pp. 35-42.

Magnat, P.S. and Molloy, B.T., [1995], 'Chloride Binding in Concrete Contain PFA, GBS or Silica Fume Under Sea Water Exposure', *Magazine of Concrete Research*, Vol. 47, No. 171, pp. 129-141.

Mallet, G.P., [1994], 'Repair of Concrete Bridge-State of the Art Review', Thomas Telford, ISBN 0 7277 20074.

Manfore G.E. and Verbeck G.J., [1960], 'Corrosion of Pre-Stressed Wire in Concrete', *Journal of The ACI*, Vol. 32, No. 5, pp. 491-515.

Mangat, P.S. and Molloy, B.T., [1994a], 'Prediction of Long-Term Chloride Concentration in Concrete', *Materiala and Structures*, Vol. 27. 1994, pp. 338-346.

Mangat, P.S. and Molloy, B.T., [1994b], 'Prediction of Free Chloride Concentration in Concrete Using Routine Inspection Data', *Magazine of Concrete Research*, Vol. 46, No. 169, pp. 279-287.

Mangat, P.S. and Molloy, B.T., [1995], 'Chloride Binding in Concrete Containing PFA, GBS or Silica Fume Under Sea Water Exposure', *Magazine of Concrete Research*, Vol. 47, No. 171, pp. 129-141.

Marchand, P., [1999], 'Graphics and GUIs with MATLAB', 2th ed., CRC Press LLC.

Martin-Perez, B., Zibara, H., Hooton, R.D. and Thomas, M.D.A., [2000], 'A Study of The Effect of Chloride Binding on Service Life Predictions', *Cement and Concrete Research*, Vol. 30, pp. 1215-1223.

Martys, N.S. and Ferraris, C.F., [1997], 'Capillary Transport in Mortars and Concrete', *Cement and Concrete Research*, Vol.27, No. 5, pp. 747-760

McCarter, W., Ezirim, H. and Emerson, M., [1992], 'Absorption of water and chloride into concrete', *Magazine of Concrete research*, Vol. 44, No. 158, pp. 31-37.

Mietz, J., [1999], 'Electrochemical Rehabilitation Method for Reinforced Concrete Structure', Published for The European Federation of Corrosion by IOM Communications.

Miller, J.B., [1994], 'Structural Aspect of High Powered Electro-Chemical Treatment of Reinforced Concrete', in *Corrosion and Corrosion Protection of Steel in Concrete*, Prof. R.N. Swamy (ed.), Academic Press, Sheffield, ISBN 1 85075 723 2.

Nagesh, M. and Bishwajit, B., [1998], 'Modelling of Chloride Diffusion in Concrete and Determination of Diffusion Coefficients', *ACI Materials Journal*, Vol. 95, No. 2, pp. 113-120

Neville, A. M., [1995], *Properties of Concrete*, 4th ed., Longman, Harlow, pp. 844.

Newman, J., [1973], *Electrochemical System*, Prentice-Hall, Inc, Englewoods Cliffs.

Ngala, V.T., Page, C.L., Parrott, L.J. and Yu, S.W., [1995], 'Diffusion in Cementitious Materials: II. Further Investigations of Chloride and Oxygen Diffusion in Well-Cured OPC and OPC/30% pta Pastes', *Cement and Concrete Research*, Vol. 25, No. 4, pp. 819-826.

Nilsson, L.O., Poulsen, E., Sandberg, P. and Sorensen, H.E., [1996], 'Chloride Penetration into Concrete: State-of-the-art', HETEK Report, AEC-Chalmers-Cementa.

Nixon, P. and Page C.L., [1987], 'Pore Solution Chemistry and Alkali Aggregate Reaction', in *ACI SP-100 Concrete Durability*, J.M. Scanlon (ed.), American Concrete Institute, Detroit, pp. 1833-1862.

Ogura K and Ohama T., [1981], 'Pit Formation in The Cathodic Polarization of Passive Iron: II--Effects of Anious', *Corrosion-NACE*, Vol. 37, No. 10, pp. 572.

Onyejekwe, O.O. and Reddy, N., [2000], 'A Numerical Approach to The Study of Chloride Ion Penetration into Concrete', *Magazine of Concrete Research*, Vol. 52, No. 4, pp 243-250.

Page, C.L. [1992], 'Interfacial Effects of Electrochemical Protection Methods Applied to Steel in Chloride_Containing Concrete', in *Proc. Int. Conf. Rehabilitation of Concrete Structures*, D.W.S. Ho and F. Collins (ed.), RILEM, Melbourne, pp. 179-187

Page, C.L. and Ngala, V.T., [1995], 'Steady-state Diffusion Characteristics of Cementitious Materials' International RILEM Workshop, 'Chloride Penetration into Concrete', pp. 15-18.

Page, C.L. and Treadanay, K.W.J., [1982], 'Aspect of electrochemistry of Steel in Concrete', *Nature*, 297, No. 5862, pp. 109-116.

Page, C.L. and Vennesland, O., [1983], 'Pore Solution Composition and Chloride Binding Capacity of Silica Fume Cement Pastes', *Materials and Structures*, Vol. 16, pp. 19-25.

Page, C.L. and Yu, S.W., [1995], 'Potential Effects of Electrochemical Desalination of Concrete on Alkaki-Ailica', *Magazine of Concrete Research*, Vol. 47, No. 170, pp. 23-31.

Page, C.L., [1975], 'Mechanism of Corrosion Protection in reinforced Concrete Marine Structures', *Nature*, 258, No. 5535, pp. 514-515.

Page, C.L., [1998a], 'Concrete Materials', paper presented at 'Degradation of Reinforced Concrete: Processes, Investigation and Control', 5 days post-experience course Master's level module in Dept of Civil Engineering, Aston University, 18-22th, May.

Page, C.L., [1998b], 'Corrosion and Its Control in Reinforced Concrete', in the paper to be presented at the 26th Annual Convention of The Institute of Concrete Technology, at the Bosworth Holl Hotel, UK, 6-8th, April.

Page, C.L., [1998c], 'Corrosion Principles and Their Application to Steel in Concrete', paper presented at 'Degradation of Reinforced Concrete: Processes, Investigation and Control', 5 days post-experience course Master's level module in Dept of Civil Engineering, Aston University, 18-22th, May.

Page, C.L., Bamforth, P.B. and Figg, J.W. (ed.), [1996], *Corrosion of Reinforcement in Concrete Construction*, Hartnolls, UK.

Page, C.L., Lambert, P. and Vassie, P.R.W., [1991], 'Investigations of Reinforcement Corrosion 1: The Pore Electrolyte Phase in Chloride-Contaminated Concrete' *Materials and Structures*, Vol. 24, No. 142, pp. 243-252.

Page, C.L., Short, N.R. and Tarras, A.E.I., [1981], 'Diffusion of Chloride Ions in Hardened Cement Pastes' *Cement and Concrete Research*, Vol. 11, No. 3, pp. 395-406.

Pereira, C.J. and Hegedus, L.L. [1984]. 'Diffusion and Reaction of Chloride Ions in Porous Concrete. European Federation of Chemical Engineering', EFCE publication series No. 37, ISCRE 8, Proc. 8th International Symposium on Chemical reaction Engineering, pp. 427-483.

Philip, J.R., [1969], 'Theory of infiltration', *Advance Hydroscience*, Vol. 5, pp. 215-296

Pitzer, K.S., [1973], 'Thermodynamics of Electrolytes – Part 1: Theoretical Basis and General Equations', *Journal of Physical Chemistry*, Vol. 77, pp. 268-277.

Pitzer, K.S., [1979], 'Theory: Ion Interaction Approach', in *Activity Coefficients in Electrolyte Solutions*, Vol. 1, R.M. Pytkowicz (ed.), CRC Press Inc., pp157-208.

Polder, R.B. and Hondel, A.J. Van Den., [1992], 'Electrochemical Re-alkalisation and Chloride Removal of Concrete-State of the Art, Laboratory and Field Experience', in *Rehabilitation of Concrete Structure*, D.W.S. Ho and F. Collins, (ed.), Melbourne, Australia, 31th Aug.-2th Sept., pp. 135-148.

Power, T.C., Copeland, L.E., Hayes,J.C. and Mann, H.M., [1954], 'Permeability of Portland Cement Paste', *J. Amer. Concr. Inst.*, Vol. 51, pp. 285-298.

Probstein, R F. [1989]. *Physicochemical Hydrodynamics*, Butterworth Publishers, USA.

Probstein, R.F. and Hicks, R.E., [1993], 'Removal of Contaminant from Soils by Electric Field', *Science*, Vol. 260, 23, pp. 498-503.

Puyate, T.Y. and Lawrence, C.J., [1999], 'Effect of Solute Parameters on Wick Action in Concrete', *Chemical Engineering Science*, Vol. 54, pp. 4257-4265

Ritter, J.J. and Rodriguez M.J., [1982], 'Corrosion Phenomena for Iron Covered with A Cellulose Nitrate Coating', *Corrosion-NACE*, Vol. 38, No. 4, pp. 223-226.

Rixom, M.R. and Mailvaganam, N.P., [1986], *Chemical Admixtures for Concrete*, 2nd. ed., Spon, London, pp. 306.

Sa'id-Shawqi, Q., Arya, C., and Vassie, P.R., [1998], 'Numerical Modelling of Electrochemical Chloride Removal from Concrete', *Cement and Concrete Research*, Vol. 28, No. 3, pp. 391-400.

Samson, E., Marchand, L.J. and Beaudoin, J.J., [1999], 'Modelling Chemical Activity Effects in Strong Ionic Solutions', paper submitted to *Computational Materials Science.*

Society for the Cathodic Protection of Reinforced Concrete [1995], 'Cathodic Protection of Reinforced Concrete', Status Report, SCPRC/001.95, ISBN 0952190 0 3.

Sergi, G., Yu, S.W. and Page, C.L., [1992], 'Diffusion of Chloride and Hydroxyl Ions in Cementitious Materials Exposed to A Saline Environment', *Magazine of Concrete Research* 44 pp. 63-69.

Shapiro, A P., Renaud, P C. and Probstein, R F., [1989]. 'Preliminary Studies on The Removal of Chemical Species from Saturated Porous Media by Electroosmosis', *PCH PhysicoChemical Hydrodynamics*, Vol. 11, pp. 785-802.

Sharif, A., Loughlin, K.F., Azad, A.K. and Navaz, C.M., [1997], 'Determination of The effective Chloride Diffusion Coefficient in Concrete via A Gas Diffusion Technique', *ACI Materials Journal*, May.-Jun., pp. 227-233.

Sharland, S.M., [1987], 'A Review of The Theoretical Modelling of Crevice and Pitting Corrosion', *Corrosion Science*, Vol. 27, No. 3, pp. 289-323

Shaw, J.D.N., [1993] 'Concrete Decay: Causes and Remedies' in the paper printed from *Construction Repair*, January/February.

Smith, L.L., Kessler, R.J. And Powers, R.G., [1993], 'Corrosion of Epoxy Coated Rebar in a Marine Environment', Transportation Research Circular No. 403, Transportation Research Board, National Research Council, pp. 36-45.

Stoop, B.T.J. and Polder, R.B., [1996], 'Redistribution of Chloride after Electrochemical Chloride Removal from Reinforced Concrete Prisms', in *Corrosion of Reinforcement in Concrete Constructure*, C.L. Page, P.B. Bamforth, and J.W. Figg (ed.), Hartnolls Ltd, Cornwall, UK.

Stratful, R.F., [1974], 'Experimental Cathodic Protection of a Bridge Deck', Transportation Research Record, No. 500.

Strecker, P.P., [1987], 'Corrosion Damaged Concrete, Assessment and Repair', CIRIA, ISBN 0-408-02556-5.

Streicher, P.E. and Alexander, M.G., [1995], 'A Chloride Conduction Test for Concrete', *Cement and Concrete Research*, Vol. 25, No. 6, pp. 1284-1294.

Subramanian, E.V. and Wheat, H.G., [1989], 'Depassivation Time of Steel Reinforcement in a Chloride Environment -- A One Dimensional Solution', *Corrosion*, Vol. 45, No. 1, pp. 43-48.

Tang, L. and Nilsson, L.O., [1992], 'Rapid Determination of The Chloride Diffusivity in Concrete by Applying an electrical Field', *ACI Materials Journal*, Jan.-Feb., pp. 49-53.

Tang, L. and Nilsson, L.O., [1993], 'Chloride Binding Capacity and Binding Isotherms of OPC Pastes and Mortors', *Cement and Concrete Research*, Vol. 23, pp. 247-253.

Tang, L. and Nilsson, L.O., [1996a], 'Chloride Binding Isotherms: An approach by Applying The Modified BET Equation' in *Chloride Transport in Concrete: Measurement and Predictio*', L. Tang, PhD Thesis, Chalmers University of Technology, Goteborg.

Tang, L. and Nilsson, L.O., [1996b], 'A Numerical Method for Prediction of Chloride Penetration into Concrete Structures', in *Chloride Transport in Concrete: Measurement and Prediction*, L. Tang, PhD Thesis, Chalmers University of Technology, Goteborg.

Tang, L., [1996a], 'Chloride Transport in Concrete: Measurement and Prediction', PhD Thesis, Chalmers University of Technology, Goteborg.

Tang, L., [1996b], 'Electrical Accelerated Methods for Determining Chloride diffusivity in Concrete: Current Development', *Magazine of Concrete Research*, Vol. 48, No. 176, pp. 173-179.

Taylor, H.F.W., [1990], *Cement Chemistry*, Academic Press, London, pp. 475.

Tritthart, J., [1989], 'Chloride Binding in Concrete: II The Influence of the Hydroxide Concenration in The Pore Solution of Hardened Cement Paste on Chloride Binding', *Cement and Concrete Research*, Vol. 19, No. 5, pp. 683-691.

Tritthart, J., [1990], 'Pore Solution Composition and Other Factors Influencing The Corrosion Risk of Reinforcement in Concrete', *Corrosion of Reinforcement in Concrete*, Elsevier, London, pp. 96-106

Tritthart, J., [1996], 'Electrochemical Chloride Removal: A Case Study and Laboratory Tests', in *Corrosion of Reinforcement in Concrete Constructure*, C.L. Page, P.B. Bamforth and J.W. Figg (ed.), Hartnolls Ltd, Cornwall, UK, pp. 443-447.

Tuutti, K., [1982], *Corrosion of Steel in Concrete*, Swedish Cement and Concrete Research Institute, Slockholm.

Uhlig, H.H., [1971], *Corrosion and Corrosion Control*, 2nd ed., John Wiley & Sons Inc., pp. 419.

Walker, H.C., [1997], 'Parking Structure Durability', *Concrete International*, July, pp. 53-55.

Wang, H.F. and Anderson, M.P., [1982], *Introduction to Groundwater Modelling: Finite Difference and Finite Element Methods*, W. H. Freeman and Company

Wang, Y., Li, L.Y. and Page, C.L., [2000], 'Efficiency Investigation of Chloride Removal from Concrete by Using an Electrochemical Method', Concrete Communication Conference 2000, The 10th BCA Annual Conference on High Education and The Concrete Industry, 29-30th, June, Birmingham University, pp. 223-235.

Wang, Y., Li, L.Y. and Page, C.L. [2001]. 'A Two-Dimensional Model of Electrochemical Chloride Removal from Concrete', *Computational Materials Science*, Vol. 20, No. 2, pp. 196-212..

Wee, T.H., Wong, S.F., Swaddiwudhiping, S. and Lee, S.L., [1997], 'A Prediction Method for Long-term Chloride Concentration Profiles in Hardened Cement Matrix Materials', *ACI Materials Journal*, Nov.-Dec., pp. 565-576.

Yu, S.W. and Page, C.L., [1991], 'Diffusion in Cementitious Materials: I Comparative Study of Chloride and Oxygen Diffusion in Hydrated cement Pastes', *Cement and Concrete Research*, Vol. 21, pp. 581-588.

Yu, S.W. and Page, C.L., [1996], 'Computer Simulation of Ionic Migration during electrochemical Chloride Extraction from Hardened Concrete', *British Corrosion Journal*, Vol. 31, No. 1, pp. 73-75.

Zhang, T. and Gjorv, O.E., [1994], 'An Electrochemical Method for Accelerated Testing of Chloride Diffusivity in Concrete', *Cement and Concrete Research*, Vol. 24, No. 8, pp. 1534-1548.

Zhang, T. and Gjorv, O.E., [1995], 'Effect of Ionic Interaction in Migration Testing of Chloride Diffusivity in Concrete', *Cement and Concrete Research*, Vol. 25, No. 7, pp. 1535-1542.

Zienkiewicz, O.C. and Taylor, R.L., [1991], *The Finite Element Method*, 4th ed., Volume 2, McGraw-Hill Publ., New York.